University of Neuchâtel (Switzerland)
Faculty of Sciences

Geological Institute
Hydrogeology Centre

Botanical Institute
Microbiology Laboratory

Virus transport and attenuation in perialpine gravel aquifers

PhD thesis presented to the faculty of Sciences of the University of Neuchâtel to satisfy the requirements of the degree of Doctor of Philosophy in Science.

By

Raymond Matthew Flynn
Geologist graduated from Trinity College Dublin, Ireland

Thesis Jury Defence Date: 11 September 2003
Public Presentation Date: 14 November 2003

Prof F. Zwahlen	University of Neuchâtel	Thesis Director
Dr. D. Hunkeler	University of Neuchâtel	Thesis Co-director
Prof. M Aragno	University of Neuchâtel	Jury Member
Dr. P.Huggenberger	University of Basel	Jury Member
Dr. T. Hofmann	University of Mainz, D	Jury Member

IMPRIMATUR POUR LA THESE

Virus transport and attenuation in Perialpine Gravel Aquifers

M. Raymond Matthew FLYNN

UNIVERSITE DE NEUCHATEL

FACULTE DES SCIENCES

La Faculté des sciences de l'Université de Neuchâtel, sur le rapport des membres du jury

MM. F. Zwahlen (directeur de thèse), M. Aragno, D. Hunkeler, T. Hoffmann (Mainz D) et P. Huggenberger (Bâle)

autorise l'impression de la présente thèse.

Neuchâtel, le 31 octobre 2003

La doyenne:

Martine Rahier

Abstract

Pollution of groundwater by microbiological contaminants (bacteria, viruses and protozoa) is a widespread problem in the United States and Europe. Gravel aquifers, which form an important drinking water resource in many parts of Central Europe, may be highly vulnerable to this type of contamination. Due to the smaller size and perceived greater mobility, studies of microbiological contaminant migration have focused on viruses. However, virus behaviour in porous media remains poorly understood, particularly in aquifers. This thesis investigates virus transport and attenuation with particular emphasis on perialpine gravel aquifers, at the centimetre (lab-based) to Decametre (field-based) scale.

Column tests investigating the role of different grain surfaces on virus attenuation showed that natural fluvioglacial sands from the Kappelen, BE had a significant attenuation capacity. SEM imagery and associated XRF analysis revealed that the sands had fine-grained coatings of minerals with a composition similar to the bulk mineralogy of the sands. Removal of this coating reduced attenuation capacity demonstrating the potential importance of microtextural phenomena in attenuating viruses. Desorption of adsorbed viruses after three hour experiments showed that all adsorbed viruses remained virulent, demonstrating that inactivation was not an important process over the duration of the experiments. In contrast, desorption experiments carried out after 36 hours demonstrated that adsorbed viruses were inactivated faster than those in suspension. Field-based studies had similar rates to those in the lab, but indicated that the variable redox conditions observed at Kappelen did not influence inactivation of adsorbed viruses.

Despite these similarities, breakthrough curves (BTCs) observed in the field and the lab differed significantly from one another. This is believed, in part to be due to the effect of features such as sedimentary structures. Column studies using concentric layers of progressively coarser porous media investigated the effect of virus transport through a fining-upward sequence. The resulting BTCs bore a strong resemblance to those generated in the field. Simulations of transport though a fining-upward sequence demonstrated the sensitivity of viruses to both grain size and collision efficiency. Additional simulations demonstrated the potential errors in travel time encountered using average hydraulic conductivities and grain sizes. These results highlighted the importance of good site investigation data in permitting preferential flow zone detection.

A mobile downhole fluorometer used to detect zones of tracer arrival in an observation well at the Dornach Field Site further illustrated the importance of preferential flow zones in mass transport. The meter showed that tracers reached the well via zone that may be no thicker than 0.5m, even though the well was screened against 12 metres of gravel. Numerical modelling of tracer responses suggested that groundwater entered the well at other levels at comparable flow rates but no tracer was observed, indicating that the groundwater flow vector varied with depth.

Further tracer testing at Dornach using two observation wells corroborated the conclusions of the downhole fluorometer tests. High recoveries of both viral and bacterial tracers demonstrated the horizons supplying tracer to the observation wells had a low capacity to attenuate the microbiological tracers used. BTCs showed that both bacteria and viruses were transported faster than solutes due to size exclusion effects. In accordance with filtration theory, bacterial tracers were less attenuated than viral tracers despite being 50 to 100 times larger.

The results of this study highlight the importance of preferential flow zones in transporting microbiological contaminants through perialpine gravel aquifers. The presence of such zones may explain the non-linear manner in which bacteria and viruses are often attenuated. Microbiological contaminants entering fine-grained deposits can be more rapidly attenuated than those in coarse-grained units due to lower groundwater velocities and a greater number of collisions with grain surfaces. In contrast contaminants in coarse-grained horizons can flow more rapidly and collide less frequently with grain surfaces. This mechanism can explain initial high rates of viral attenuation observed close to injection points, which may decline rapidly with distance. Compositional heterogeneity may result in positive or negative feedback effects depending on the nature of the minerals at the solid-water interface.

Résumé

La pollution de l'eau souterraine par les contaminants microbiologiques (bactéries, virus, protozoaires) est un problème largement répandu en Europe et aux Etats-Unis. Les aquifères graveleux, qui constituent une importante ressource en eau potable pour de vastes régions d'Europe, sont susceptibles d'être très vulnérables à ce type de contaminants. Les études sur la migration des contaminants microbiologiques se sont essentiellement concentrées sur les virus car ils sont de plus petite taille et de fait a priori plus mobiles. Cependant, le comportement des virus en milieu poreux reste un domaine mal compris, particulièrement dans les aquifères. Cette thèse se concentre sur l'étude du transport et de l'atténuation des virus essentiellement dans les aquifères graveleux périalpins en allant de l'échelle centimétrique (expériences en laboratoire) à l'échelle décamétrique (expériences de terrain).

Des tests en colonnes ont permis d'investiguer le rôle des différentes surfaces de grain sur l'atténuation des virus. Les résultats ont montré que les sables fluvio-glaciaires de Kappelen (canton de Berne, Suisse) ont une capacité d'atténuation significative. Des analyses en microscopie électronique et rayons-X ont montré que les sables ont une fine pellicule de recouvrement ayant la même minéralogie que les grains. La suppression de cette pellicule réduit fortement la capacité d'atténuation, illustrant le rôle de ces micro-textures pelliculaires dans l'atténuation des virus. La désorption de virus adsorbés pendant trois heures a montré que ceux-ci restent virulents, l'inactivation est donc un phénomène non significatif sur la durée des expériences. A contrario, des expériences de désorption menées après 36 heures ont montré que les virus adsorbés se désactivaient plus vite que les virus en suspension. Les expériences de terrain ont résulté en des taux d'inactivation comparables à ceux obtenus au laboratoire ; la variabilité des conditions redox à Kappelen n'a montré aucune influence sur l'inactivation des virus adsorbés.

Malgré ces similitudes, les courbes de restitution (CR) obtenues au laboratoire et sur le terrain différent significativement. Il est proposé que ces différences sont au moins en partie dues à l'effet des structures sédimentaires. Des études en colonne utilisant des couches de matériel poreux progressivement plus grossier a permis d'investiguer le transport de virus dans une séquence sédimentaire (fining upward). La CR obtenue est très ressemblante à celle observée sur le terrain. Une simulation du transport des virus dans une telle séquence sédimentaire a démontré l'importance de la taille des grains et de l'efficacité des collisions. Des simulations additionnelles ont illustré les erreurs potentielles sur les vitesses de transit obtenues par la conductivité hydraulique et la taille des grains. Ces résultats ont souligné l'importance d'une investigation de terrain détaillée afin de détecter les zones d'écoulement préférentiel.

Un fluorimètre de forage a été utilisé pour déterminer les zones d'arrivée du traceur dans un puits d'observation sur le site de Dornach (Bavière, Allemagne). Cette expérience permit de détailler le rôle primordial des zones d'écoulement préférentiel pour le transport de masse. Le fluorimètre a montré que le traceur pouvait arriver par des zones de 0.5 m d'épaisseur, même si le puits était crépiné sur 12 m de graviers. La simulation numérique des réponses du traceur suggère que l'eau souterraine pénètre également dans le puits à d'autres niveaux avec des débits comparables. Cependant, comme aucun traceur n'est observé, il faut que le vecteur d'écoulement varie avec la profondeur.

D'autres expériences de traçage sur le site de Dornach avec deux puits d'observation appuient les conclusions tirées des tests réalisés avec le fluorimètre. Les taux de restitution pour les traceurs viraux et bactériens sont élevés ; de fait les horizons parcourus par les traceurs ont une faible capacité à atténuer les microbes. Les CR ont montré que les bactéries et les virus sont transportés plus rapidement que les solutés à cause de l'effet d'exclusion par la taille. Conformément à la théorie de filtration, les traceurs bactériens sont moins atténués que les virus bien qu'étant 50 à 100 fois plus larges.

Les résultats de cette étude soulignent l'importance des zones d'écoulement préférentiel pour le transport de contaminants microbiologiques dans les aquifères graveleux périalpins. L'existence de ces zones peut expliquer la non linéarité de l'atténuation des bactéries et des virus qui est souvent observée. Les contaminants microbiologiques pénétrant dans des sédiments fins sont plus rapidement atténués que ceux arrivant dans des niveaux grossiers étant donné des vitesses d'écoulement plus faibles et un plus grand nombre de collisions avec la surface des grains. Au contraire, les contaminants transportés dans des horizons plus grossiers se déplacent plus vite et subissent de moins nombreuses collisions. Ce mécanisme peut expliquer le taux élevé d'atténuation des virus dans les piézomètres proches du puits d'injection, puis un taux qui diminue significativement avec la distance de transport. L'hétérogénéité de la composition des sédiments peut jouer un effet positif ou négatif sur l'atténuation selon la nature des minéraux à l'interface solide – liquide.

Acknowledgments

This project was funded by Swiss National Science Foundation (Grant Number: FN-20-061370.00). Additional financial assistance for this study was provided by the Swiss Federal Office for Water and Geology, and by the Swiss Agency for Environment, Forest and Landscape. In the framework of this thesis, I wish to gratefully acknowledge the assistance of the following people and institutes:

From the Centre d'Hydrogeologie de l'Université de Neuchâtel, I wish to thank the students and staff for their assistance and encouragement over the past four years. In particular I wish to thank the following:
François Zwahlen for directing this thesis and providing additional financial and logistical assistance in the later parts of its preparation.
Daniel Hunkeler for being co-director of this thesis and for his valuable advice on technical issues, reviewing the five articles contained in this thesis and advising on publication procedure in the scientific literature.
Heinz Surbeck for his in-house review of the articles contained in this thesis.
Jerôme Perrin for translating the abstract of this thesis.
Imre Müller for initiating this project and providing me with many useful contacts.
Nedi Noseda, Karim Diomande and Christine Guerin also deserve special mention for their assistance in acquiring data during the four years of this thesis

From the Laboratoire de Microbiologie de l'Université de Neuchâtel, the following deserve special mention :
Pierre Rossi for his technical advice and comments on the biological details of the publications contained in this thesis.
Michel Aragno for his assistance and comments throughout this project.
Magali Grob for carrying out the innumerable analyses completed during this thesis and for her invaluable advice on tracer testing with phages.
Nicole Jeanneret for her assistance in procuring materials and her moral support.
Christine Burn for her assistance in acquiring valuable field hydrochemical data.

At the GSF in Munich, I wish to express my gratitude to German Mallèn, Michael Stökl, Marrion Engel and Klaus-Peter Seiler for their assistance with experiments at the Dornach test site. It is no coincidence that two of the five publications in this thesis concern Dornach.

The assistance of Pierre Schnegg and Roberto Costa of the Geomagnetism group at deserve special mention for their assistance in the development of the mobile downhole flourometer, modification of sampling apparatus and comments concerning the fluoroesence measurements, to mention amongst other things. The help and comments of Martin Burkhardt, Thierry Adatte and Alexi Ulanyanov concerning the mineralogy of sands used in column testing are also gratefully acknowledged. Geophysical assistance from Hendrik Pasch of ETH-Zürich and Youcef Hacini of the University Lausanne at the Kappelen Test Site is also gratefully acknowledged.

On a more personal level I wish to thank the friends I have made over the past four years, my family and Laura for the moral support that they have provided to me over the past four years. Without them, this thesis would not have been completed – Go raibh mile maith agaibh!

Table of Contents Page

Chapter 1 : Introduction

1.1 Background

> *"The inhabitants used water from a particular pump well. This well had been repaired, and a sewer which passes within nine inches of the edge of it became accidentally stopped up, and leaked into the well. The inhabitants of thirty houses used the water from this well; among them there occurred nineteen cases of diarrhoea, twenty-six cases of cholera, and twenty-five deaths "*

So wrote Dr. John Snow, M.D. in his monograph "On the mode of communication of Cholera" concerning an incidence of cholera related to contaminated groundwater in the industrial slums of Manchester during the middle of the 19th century (Snow, 1854). Since that time, water-borne epidemics such as those involving pathogens like cholera and typhoid, which regularly occurred world wide up until the end of the 19th century, have been all but eradicated from the developed world due to improved hygiene and the implementation of more effective water treatment and waste disposal practises. However, these developments have not occurred universally. Unicef's World Water Assessment Program estimated that 19% of all deaths due to infectious diseases in 1999 were water related (WHO, 1999). Indeed, Gleick (2002) argued that the failure to provide safe drinking water and sanitation services to all people is perhaps the greatest development failure of the 20th century, and could result in additional 135 million deaths by 2020 if no action is taken to address this issue.

The general perception of microbiological contamination of water supplies is that it is a problem largely restricted to the developing world. Incidences such as the Cholera epidemic that occurred in Latin America in the early 1990s tend to confirm this view. However, the complacency of many people in the developed world about the safety of their drinking water can be ill-founded. This is illustrated by occasional large-scale outbreaks of waterborne disease, such as the cryptosporidiosis epidemic that affected the city of Milwaukee, USA in 1992. This outbreak resulted in more than 400,000 people becoming ill, of which 102 died.

In general, however disease outbreaks related to microbiological contamination of water supplies tend to be more mundane and the source of illness may often remain unidentified or unreported, particularly when related to groundwater supplies (National Small Flows Clearing House (USA), 1996). Nonetheless, the United States centre for disease control registered 318 waterborne disease outbreaks associated with groundwater systems between 1971 and 1996 in the US (Macler and Merkle, 2000). Similarly, the United States Environmental protection Agency (USEPA) Science Advisory Board concluded that microbiological contaminants (bacteria, viruses and protozoa) were likely the greatest remaining health risk management challenge for drinking water suppliers. This later information has prompted the USEPA to propose the

Groundwater Rule which requires consumers of groundwater from supplies with at least 15 connections, or serving more than 25 people at least 60 days per year, to be protected against bacterial and viral contamination.

The Groundwater Rule recognises that the capacity for aquifers to remove microbiological contaminants from groundwater may not be adequate to protect public health, and requires groundwater supplies to achieve a 99.99% inactivation (loss of virulence) or removal of viruses, if groundwater is to be supplied without treatment.

Information concerning microbiological contamination of groundwater in Europe is less widely available than in North America. This does not imply an absence of microbiological contamination, rather a lack of widely available data and an absence of coherent systematic monitoring strategies. Indeed, data presented by Powell and others (2003) demonstrated that groundwater contamination by faecal bacteria and viruses was widespread in the Nottingham Aquifer, UK. Such microbiological contamination may not pose a problem to public health provided the water is not used for human consumption, or it is treated beforehand. However, groundwater is the main source of drinking water in many European countries (European Commission, 1996). Furthermore, in many areas groundwater is not treated prior to entry into distribution systems, under the assumption that the water is pathogen-free. Clearly, the entry of pathogenic micro-organisms into non-treating systems could pose a substantial threat to public health. This issue is of particular concern with respect to aquifers classified as sensitive to microbial contamination. Karst, fractured bedrock and gravel aquifers fall into this category of sensitive aquifers (USEPA, 1996).

In central Europe, coarse fluvioglacial and alluvial gravel aquifers in peri alpine areas can constitute a significant groundwater resource that may be used to supply drinking water to a large proportion of the population. In Switzerland, where groundwater makes up 80% of all drinking water, these aquifers supply approximately 40% of all potable water consumed (SAEFL, 2003). However, coarse sand and gravel aquifers frequently lack necessary protective cover, such as a thick unsaturated zone, to attenuate microbiological contaminants percolating from the surface. Indeed, in many cases, where recharge is induced from adjacent surface water by pumping the thickness of the unsaturated zone becomes irrelevant and attenuation processes in the aquifer along the flow path between surface water and the groundwater abstraction point become all the more critical.

Natural groundwater flow rates within saturated fluvioglacial deposits in Switzerland have often been shown to be extremely rapid (Rossi and others, 1994, Kennedy and others, 2001a). Consequently, once contaminants enter these aquifers, they can travel over large distances in short periods of time. As a result, perialpine sand and gravel aquifers can be particularly vulnerable to microbiological contamination. An example of the potential impact of such

contaminants on water quality is provided by the groundwater contamination event that occurred at La Neuveville, Switzerland, in 1998. A spill of sewage reaching the sand and gravel aquifer supplying the town resulted in pathogenic bacteria and viruses entering the municipal water supply well. Consumption of the well water caused gastro-enteritis in an estimated 84% of the town's population (Maurer and Sturchler, 2000).

Implementation of aquifer protection programs, particularly around well /spring capture zones, can reduce the risk associated with groundwater contamination. However, many fluvioglacial sand and gravel aquifers are located in areas of intensive land use. In these areas, compensation for restrictions on particular economic activities in well capture zones may become unnecessarily excessive, should the protection area be too large due to over-conservative estimates of travel distances necessary to attenuate contaminants. In terms of pathogens, an understanding of the transport mechanisms and attenuation processes operating to reduce overall contaminant concentrations can assist considerably in the designation of appropriate well catchment zones.

Unfortunately, both transport and attenuation processes affecting microbiological contaminants in porous media are not fully understood. Viral transport in particular has been an area of concern, due both to the inability of conventional water disinfection systems to fully remove viruses (Rose and others, 1996) and to virus' small size relative to bacteria and protozoa. Indeed, the reduced size of viruses is suspected to allow them to move more freely through both saturated and unsaturated media (Macler and Merkle, 2000). Moreover, studies by Rossi (1994) at the Wilerwald test site in Switzerland demonstrated that viruses could travel 14 metres through fluvioglacial sands and gravels in less than 40 minutes under natural gradient conditions. Further research at the same site noted that attenuation varied with the different virus types used, but also depended on whether monitoring wells were located within or outside a coarse-grained former fluvioglacial channel identified by geophysical methods (Kennedy and others, 2001a). Studies such as those by Harvey and others (1991) and Ryan and others (1999) have further highlighted the importance of spatial variations in composition and texture in virus transport in sand and gravel aquifers. To date, most work published on geological influences on virus transport and attenuation in perialpine sands and gravels to date in Switzerland has consisted of field-based tests comparing different virus responses to one another and to solutes (Cavalho-Dill, 1993, Rossi, 1994, Kennedy, 2001). However, Regli and others (2003) have recently presented a series of stochastic simulations in these deposits which begin to provide an understanding of the role of heterogeneity in contaminant transport processes. Nonetheless it is noteworthy that the study required data concerning contaminant-aquifer interactions. Such data at the time of writing were not widely available.

In order to develop a coherent groundwater protection strategy for heterogeneous fluvioglacial aquifers such as those present in Switzerland, a deeper understanding of microbiological contaminant transport and attenuation processes is necessary. This thesis aims to investigate the mechanisms of virus transport and attenuation in coarse-grained perialpine fluvioglacial sand and gravel aquifers. Within this investigation framework, a number of studies have been carried out at a range of scales of investigation in an attempt to further understand the influence of geology on the transport of microbiological tracers, with particular emphasis on the behaviour of viruses. The results have been incorporated into existing theories dealing with the transport of microbiological particles in the subsurface, with a view to understanding the effects of heterogeneity due to geological conditions. The following sections review the basis for these theories, current knowledge of this subject and the rationale for the research approach undertaken.

1.2 Particle Mass Transport in Porous Media - Theory

Many microbiological particles (viruses, bacteria and protozoa) have at least one dimension between 1nm (10^{-9}m) and 1μm(10^{-6}m). This size definition corresponds to a group of particles known as colloids (Lyklema, 1991). (Protozoa found in groundwater are usually a little larger than the upper end of this scale and usually have one dimension in the range of 1μm to 10μm, e.g. Cryptosporidium.) These microbiological particles can be referred to as biocolloids (Bales and others, 1997). As a consequence of their size, colloids tend to settle very slowly in water (provided they do not form clusters, also known as aggregation). This is often the case for biocolloids in aquifers, and consequently they can remain suspended in groundwater where they are exposed to additional forces that permit them to be transported. Biocolloid mass transport has been demonstrated in a number of porous hydrogeological environments, ranging from coarse montane gravels (Woessner and others, 2002) to fine-grained sands (Schijven and others, 1999). This section reviews the fundamental laws influencing biocolloid mass transport in porous media.

1.2.1 Advection and Dispersion

It is a natural tendency for dissolved and suspended substances to move from areas of greater concentration to those of lesser concentration by diffusion. The rate of change in concentration is described for groundwater systems by Fick's first and second laws (Freeze and Cherry, 1979). Diffusive processes are a direct result of random particle movement (Brownian motion), associated with the translational kinetic energy of particles. In general, particle velocity increases with decreasing particle mass, resulting in higher diffusion rates for smaller particles. Shaw (1998) summarised studies showing that rates of diffusion for colloidal particles 1nm in diameter are three orders of magnitude higher than those that are 1μm in diameter (2.1 x10^{-10}m^2/sec vs 2.1 x10^{-13}m^2/sec). Moreover, displacements calculated for each particle size in 20°C water showed that

smaller colloids travelled over 30 times further (1.23mm) than larger ones (39μm) after 1 hour.

Biocolloid transport rates due to diffusion are typically much lower than those observed in groundwater systems, due to groundwater flow (advective transport, Fetter, 1993). In advective transport, suspended particles are carried along through an aquifer with flowing groundwater. The mass transported depends on the quantity of particles in the water and the groundwater flow rate. Groundwater flow rate for a unit cross section area in one dimension (specific discharge) is the interstitial velocity v, times the effective porosity, ϕ_e. The interstitial velocity is defined as follows:

$$v = \frac{K}{\phi_e}\frac{dh}{dl} \qquad (1)$$

, where K is the hydraulic conductivity of the porous medium, and dh/dl is the hydraulic gradient. Both hydraulic gradient and hydraulic conductivity may vary over several orders of magnitude. Domenico and Schwartz (1992) summarised hydraulic conductivity measurements for a range of unconsolidated porous deposits and noted that this variation is strongly dependant on grain size. Reported hydraulic conductivities ranged from $3x10^{-2}$ m/s for gravels to $1x10^{-12}$ m/s for some glacial tills. The same authors note that the porosity of these materials may vary typically between 24% and 60%, but that effective porosity (the porosity through which groundwater flow may occur) is less. As a consequence of these variations the value of v can vary widely in natural porous deposits.

The value of v expresses an average linear velocity. However, groundwater will move at rates that are both greater than and less than those of the interstitial velocity. Bear (1972) observed that this phenomenon occurs because of (1) fluid will move faster in the centre of pores than at the pore margins; (2) some fluid will follow longer flow paths than others; (3) some pores are larger than others, permitting water to flow faster. The net result of these processes is that a population of suspended particles can be transported at different rates, resulting in a gradual change in concentration at a particular observation point. This process is known as mechanical dispersion. Moreover, the physical size of biocolloidal particles may mean that biocolloids are unable to enter a fraction of the porosity of a porous unit. This phenomenon has been referred to by a number of different terms, including pore exclusion and size exclusion (Ginn and others, 2003), depending on the precise nature of the exclusion mechanism. One result of this phenomenon is that colloids may flow with a faster average velocity than solutes in groundwater since solute might access smaller pores where groundwater flows more slowly (Grindrod and others, 1993).

When considering mass transport in actively flowing groundwater systems, mechanical dispersion may not be separated from molecular diffusion, and both processes are combined into a single term, known as hydrodynamic

dispersion, D. Contaminant concentrations may be significantly reduced by hydrodynamic processes, which can spread contaminant mass out both along the direction of flow (longitudinal dispersion), and normal to the flow direction (transverse and vertical dispersion).

For a one dimensional system (longitudinal dispersion only), advective transport can be coupled with hydrodynamic dispersion to allow the rate of change in concentration of a conservative substance with time to be determined using the following differential equation:

$$\frac{\partial C}{\partial t} = D_l \frac{\partial^2 C}{\partial x^2} - v\frac{\partial C}{\partial x} \qquad (2)$$

The reader is referred to Freeze and Cherry (1979) for the derivation of this equation, commonly known as the advective-dispersive transport equation. It is noteworthy that Equation (2) assumes a steady-state groundwater flow regime and that the substance in question does not react with the host aquifer material. Consequently, the mass of material that enters the system must be equivalent to that leaving. Non-reactive conditions rarely apply in the case of colloidal systems in the field, where material is often lost through physical, chemical and biological reactions (Schijven and Hassanizedeh, 2000).

1.2.2 Reactive Processes

In a review of particle transport through porous media, Mc.Dowell-Boyer and others (1986) subdivided conceptual models for suspended matter attenuation in porous media into the following three categories (Figure 1.1):

(1) Caking, where particles are of comparable size/larger than the pores of the medium, and accumulate at, or near the surface of the medium.
(2) Straining filtration, where particles are small enough to enter porous medium, but are mechanically removed in smaller pore spaces.
(3) Physico-chemical filtration, where particles are very small relative to pore sizes and are removed by physical and chemical forces between the particles and the media.

Due to their sizes, bacterial and protozoan transport through porous media can be controlled by both straining and physical-chemical filtration. However, because they are substantially smaller, transport of viruses through porous media is believed to be limited by predominantly physico-chemical filtration.

Although providing a conceptual basis for understanding colloidal attenuation, the above mechanisms do not quantitatively describe the rates at which matter is removed in porous media. By injecting easily detectable materials (tracers) into water flowing through a porous medium, and monitoring concentration changes at the outflow, concentration plots with time (breakthrough curves) can be constructed. Comparison of reactive tracer breakthrough curves with those generated for a conservative tracer can permit attenuation

mechanisms to be identified. Depending on tracer responses, it is possible to determine whether a reaction is reversible or irreversible, and whether kinetic or equilibrium processes influence a reactants transport.

Figure 1.1: Schematic illustration of colloid attenuation mechanisms. (After Mc Dowell-Boyer and others, 1986)

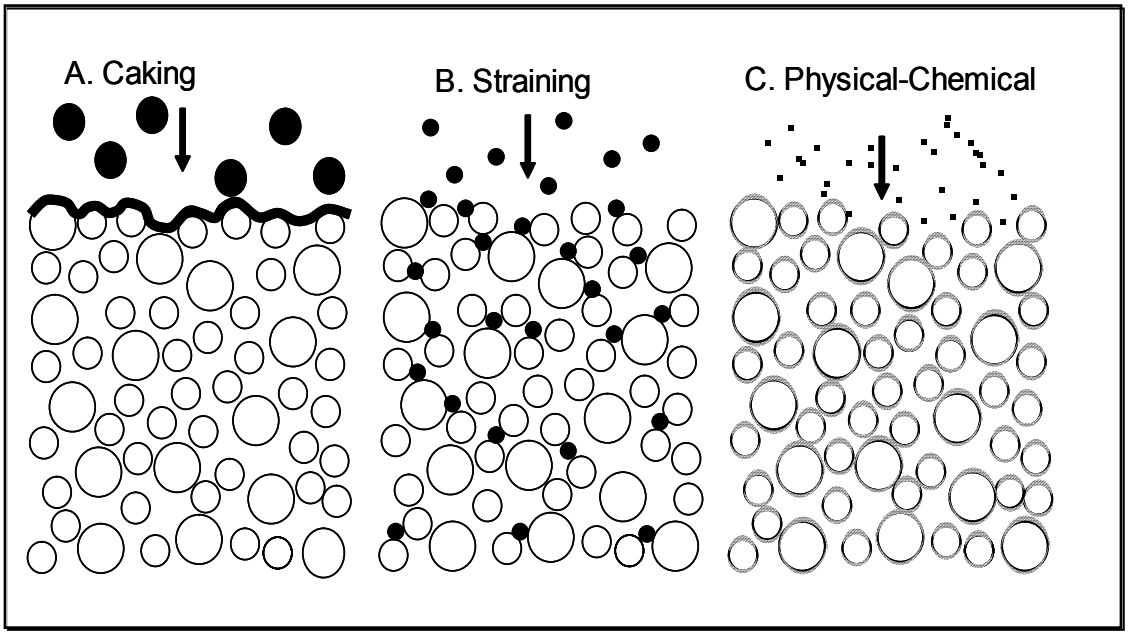

De Marsily (1986) noted that colloidal transport through porous media can be described by the advective-dispersive transport equation (Equation (4)) by incorporating a first order kinetic deposition constant (k_d) and a first order release constant (k_r) as follows:

$$\frac{\partial C}{\partial t} = D_l \frac{\partial^2 C}{\partial x^2} - v\frac{\partial C}{\partial x} - \frac{\rho_b}{\phi}\frac{\partial S}{\partial t} \qquad (3)$$

$$\frac{\rho_b}{\phi}\frac{\partial S}{\partial t} = k_d C - \frac{\rho_b}{\phi} k_r S \qquad (4)$$

where ρ_b is the bulk density of the medium and S is the number of colloidal particles deposited per unit mass. In this equation D_l and v refer to the hydrodynamic dispersion and interstitial velocity of the colloidal particles. Schijven and others (1999) also used the above model, with additional modifications to model virus transport through sandy deposits (see below).

1.2.2.1 Particle Deposition

In their filtration theory, developed to predict suspended particulate filtration rates in waste water filtration systems, Yao and others (1971) proposed that the colloidal deposition term, k_d, could be subdivided to reflect a two stage

process. An initial step involves transport of a particle to a collector (grain) surface, and is expressed by single collector efficiency, η. The single collector efficiency is the proportion of particles that collide with a collector surface divided by the number of particles approaching it.

A subsequent attachment step describes the probability that colliding particles may or may not stick to the matrix surface. The term describing this later process is known as the collision efficiency, α. Mathematically collision efficiency and single collector efficiency are related to the deposition constant by the following equation:

$$k_d = \frac{3}{2}\frac{(1-\phi)}{d_c}\alpha\eta v \qquad (5)$$

where d_c is the effective grain size of the collector influencing colloidal attenuation (L). The physical and chemical controls on particle deposition are discussed in more detail below.

Physical Controls on Particle Deposition. Mc.Dowell-Boyer and others (1986) noted that the kinetics of the transport step in colloid deposition depend primarily on physical factors, including colloidal particle size and density, pore structure, grain size and flow velocity. Yao and others (1971) argued that the three dominant mechanisms transporting particles to collector surfaces were sedimentation due to gravitational settling, collision of particles with the grain surface as they pass along their flow path, and Brownian motion (Figure 1.2). The influence of each mechanism on the transport step can be quantified by summing expressions employing particle and grain (collector) size, particle density, matrix porosity and water flow velocity to give the single collector efficiency. Rajagopalan and Tien(1976) provide details of the calculation of η.

The calculation of the value of the single collector efficiency involves a number of important assumptions including the concepts that both the suspended particle and collector surface are spherical, the flow field is uniform, and that the grains making up collector bed have a uniform size. These assumptions may have important implications for natural systems (see below).

In a review of the potential applications of the filtration theory in aquifers, Elimelech and others (1995) presented the results of a number of simulations, in which selected parameters were changed while all other variables remained constant. Using this approach, the authors determined the distance particles could penetrate into porous media, before 99.9% were removed. Simulation results demonstrated a strong dependence on the hydrogeological parameters, (collector) grain size and water velocity. For example, a four-fold increase in the collector diameter resulted particles being transported over an order of magnitude further into a formation. Similarly, a ten-fold increase in groundwater flow rate resulted in a corresponding increase in transport distance.

Figure 1.2: Illustration of the three dominant transport mechanisms of suspended particle transport to a collector surface. (After O'Melia and Tiler, 1993)

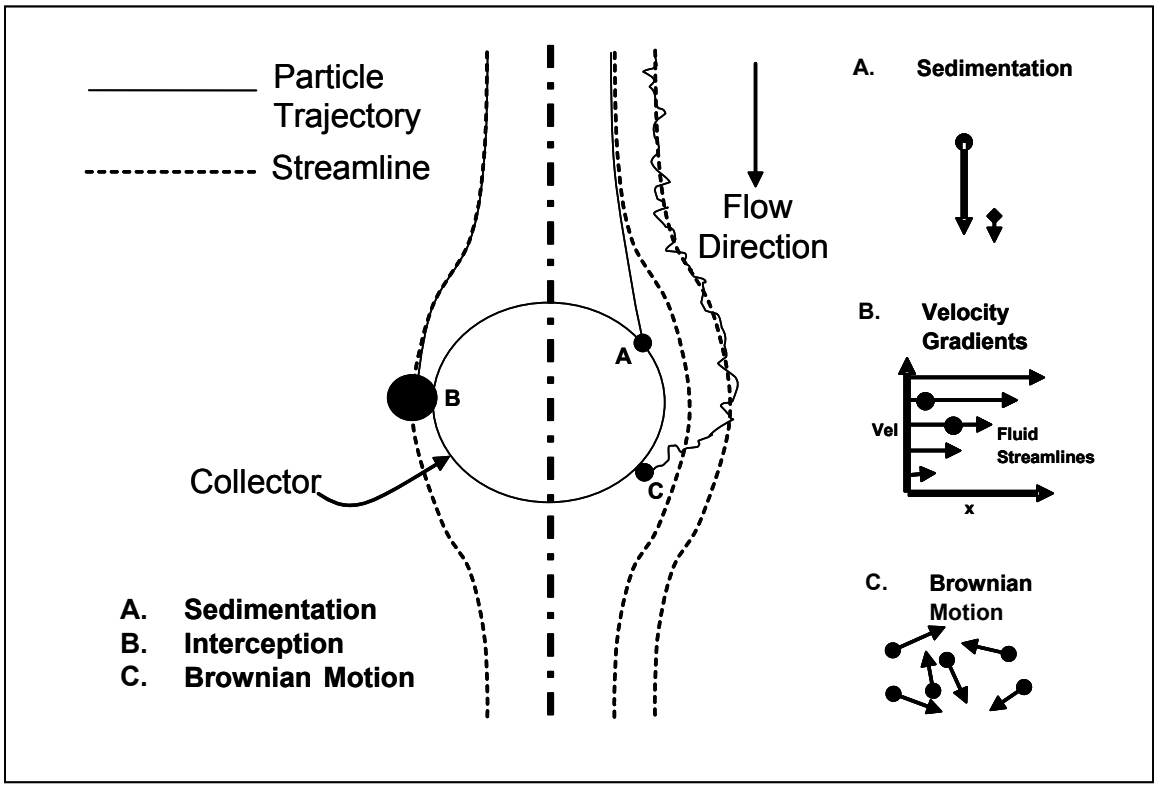

Chemical Controls on Particle Deposition : The simulations carried out by Elimelech and others (1995- discussed above) assumed constant collision efficiency between particles and collector surfaces. A separate set of simulations demonstrated that the distance penetrated by particles is directly proportional to α. However, the value of collision efficiency can be highly variable, and is largely a function of the chemistry of the system, and particularly of the surface charges of the collectors and particles of interest.

Solids can acquire surface charges when they come into contact with water in three main ways (Elimelech and others, 1995).

(1) A difference in affinity of different ions making up a crystal for the solid or liquid phase: Many surfaces contain ions that may have different tendencies to dissolve in the adjacent solution. Changes in concentration of particular ions in the solution, known as potential determining ions, determine the charge of the solid surface. For example, in natural systems the concentration of Ca^{2+} and HCO_3^- are potential determining ions for the calcite system (Thompson and Pownall, 1989). The relative abundance of each of these ions in solution will thus determine the surface charge of calcite. Consequently, when stating the surface charge of calcite, the

chemistry of the measuring solution should also be stated (Stumm and Morgan, 1996).

(2) Ionisation of surface groups: Many solids have ionisable functional groups on their surfaces. These groups include carboxyl and amino groups on the surfaces of many biological particles, and hydroxyl groups on metal oxides. These ionisable functional groups may be positively or negatively charged, depending on the pH of the system. This may be illustrated hydroxyl functional groups exposed on surfaces which may undergo the following reactions: $S\text{-}OH_2^+ \Leftrightarrow S\text{-}OH \Leftrightarrow S\text{-}O^-$
,where S denotes the solid surface. Consequently, as pH increases the surface moves from positively charged to negatively charged. The point at which there is no net surface charge is the point of zero charge PZC.

Table 1.1 provides the PZC of some common rock forming minerals. Based on these data, common rock forming silicates should be negatively charged at neutral pH. Moreover, the composition of the surfaces of most biological particles generally result in them also having net negative surface charges at neutral pH. (Ryan and Elimelech, 1996).

(3) Isomorphous replacements: Such replacements of one ion in a crystal lattice by another with a different charge results in charge imbalance, and an inherent excess charge. For example, the substitution of silicon with aluminium in clay minerals results in clay surfaces having a net negative charge. (Elimelech and others, 1995).

Table 1.1: Point of zero net proton charge of some common rock forming minerals.

Mineral	pH_{pznpc}
Fe_3O_4(Haemitite)	6.5
FeO(OH) (Amorph)	8.5
SiO_2(Quartz)	2.0
Feldspars	2-2.4
Montmorillonite	2.5

Note: Data summarised from Stumm (1992).

According to the principal of electroneutrality, the presence of a charge accumulated on a surface is exactly balanced by an equal but opposite charge in solution. This results in a cloud of oppositely charged ions (counter ions) immediately around the solid surface, and a corresponding deficit in similarly charged ions. This ionic imbalance declines with distance from the surface as a function of the overall ionic strength of the system, as described by the Stern-Grahame model, which envisages a fixed layer of counter ions adjacent to the surface and a more mobile “diffuse” layer further away (Grahame, 1947). Overall, the rate of decline of counterion excess is proportional to the ionic strength of the system, although it is noteworthy that the charge profile can be considerably modified by the presence of specifically adsorbing counterions that

may cause charge reversal (Elimelech and others, 1995). Consequently, the charge of a surface is dependant not only on the properties of the surface but also on the chemistry of the surrounding solution.

Measurements of surface charge are usually carried out using electrokinetic techniques, where the relative movement of the charged interface and the adjacent electrolyte are measured in an electric field (electrophoretic mobility). More specifically, the potential between fixed and mobile parts of the double layer are calculated based on these measurements (assuming that this corresponds fairly closely to the interface between the fixed and diffuse layers). This parameter is known as the zeta potential and is used to approximate the potential on a surface during theoretical calculations to determine the degree of attraction/repulsion between a suspended particle and a collector surface.

The Derjaguin-Landau-Verwey-Overbeek (DLVO) theory calculates electrostatic interaction potential between colloids and surfaces with distance while accounting for the ionic strength of the solution (Verwey and Overbeek, 1948). The DLVO theory sums the relative contributions of electrostatic forces with the van der Waals attraction. According to this theory, it is possible, for particle deposition to occur under electrostatically repulsive conditions, should van der Waals forces exceed those of repulsion. Based on theoretical predictions, overall energy profiles with distance indicate that net attractive or repulsive forces may exist in a system at different separation distances. Repulsive forces can occur as a consequence of the overlap of similarly charged particle and collector counterion layers. These forces may produce an energy barrier between the particle and collector, thereby inhibiting particle deposition. A zone of mutual particle-collector attraction may exist closer to the collector surface due to van der Waals forces, but the energy barrier must be breached by particles if deposition is to occur. The magnitude of this energy barrier is strongly controlled by ionic strength. In general, higher ionic strengths of a given solution will reduce the magnitude of the energy barrier and permit more particles to be deposited, i.e suppression of particle and collector double layer thickness will allow particles to be deposited more easily. Because of the barriers presence, only a fraction of collisions between particles and collectors are effective. The fraction of effective collisions is the collision efficiency. Where this barrier is absent, all collisions result in sticking and the collision efficiency is unity (Kretzschmar and others, 1997).

Figure 1.3 presents different types of energy profiles which may occur according the DLVO theory. The actual interaction energy of particles and collectors is normally approximated with zeta potentials using the approach of Rutter and Vincent (1980). The DLVO theory thus provides a theoretical means of predicting the degree of particle/collector attraction/repulsion due to electrostatic, van der Waals and acid base forces under particular hydrochemical conditions.

Despite its apparent rigorous treatment of colloidal-collector interactions, the DLVO theory has a number of shortcomings, the most notable of which is its failure to consider a number of additional forces which may influence deposition. These forces include shear forces due to fluid flow in dynamic systems, short range forces due to electon orbital overlap (Born repulsion) and structural forces (Elimelech and others, 1995). The later term applies to phenomena such as hydration forces, steric forces and hydrophobic forces. Bales and others (1991) have demonstrated that hydrophobic forces can be of particular importance in virus adsorption onto organic surfaces, while Zhuang and Jin(2003) argued they may be important, even in systems where there is no organic matter present on collector surfaces.

Notwithstanding its shortcomings, the DLVO theory provides a means of understanding the adsorption process in terms of the influences of electrostatic and van der Waals forces. It has been widely used both to understand deposition of inorganic colloids (Rodier and Dodds, 1993), bacteria (Jucker and others, 1996) and viruses (Penrod and others, 1999). Moreover, Redman and others (1999) used the theory to demonstrate the dominance of electrostatic forces in attenuation processes operating in a virus-silicate sand system. Furthermore, the inability to explain adsorption phenomena in purely electrostatic terms has also provided a means of more fully understanding the influence of non-DLVO forces (e.g. Jucker and others, 1997).

The DLVO theory has proved particularly useful in advancing our understanding of colloidal interactions in terms of deposition kinetics (Spielman and Friedlander, 1974), and especially with respect to the influence of collision efficiency on kinetic deposition constant (Kretzschmar and others, 1999). This theory thus provides a means of understanding the relative contributions of the chemical and physical conditions in a system to the overall interaction of colloids with collector surfaces.

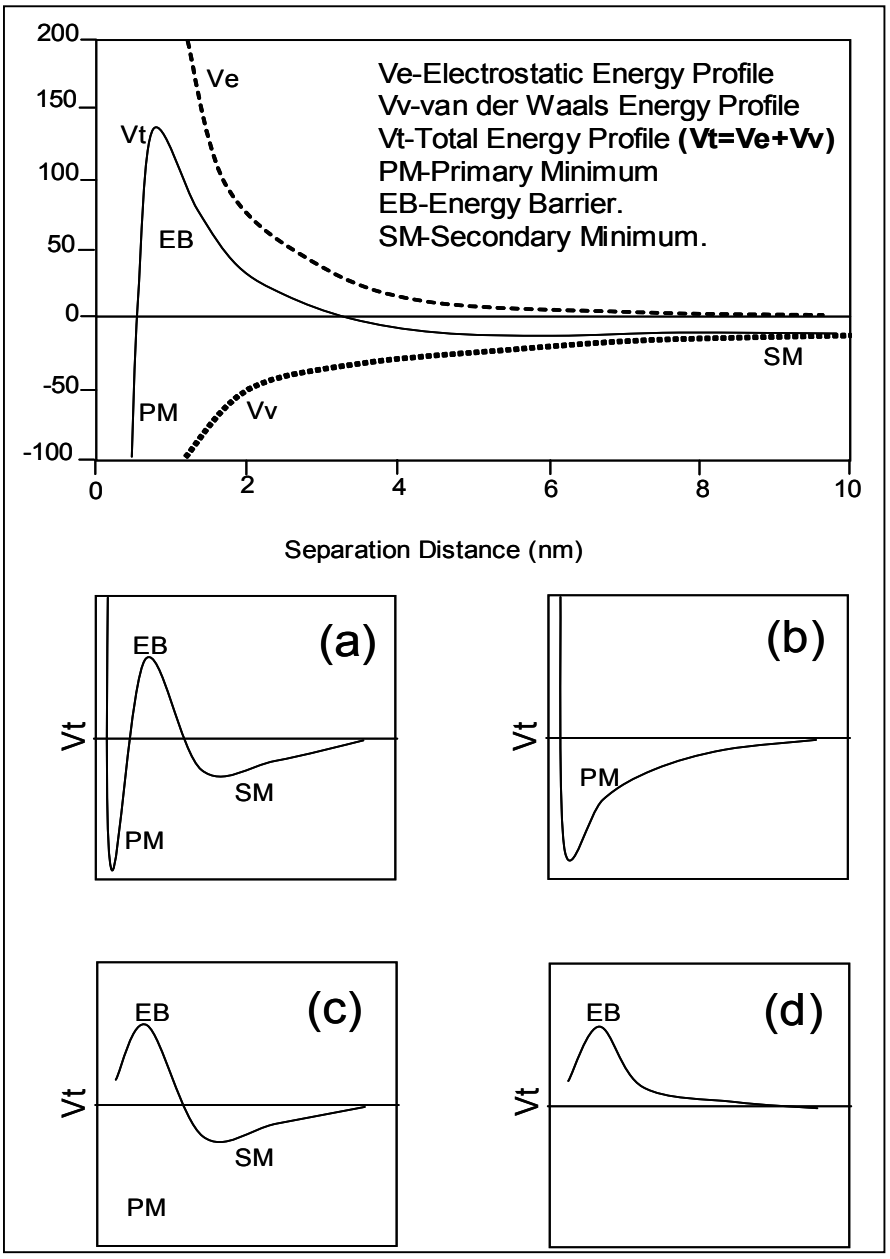

Figure 1.3: Schematic illustration of typical DLVO interaction energy profiles. Total interaction energy is the sum of electrostatic energy and van der Waals energy (Repulsive Energy-Positive. Acid-base forces are not shown). (a) Mutual particle-surface repulsion with net attraction at the collector surface, giving a primary energy minimum, and after energy barrier, giving a shallower secondary energy minimum. (b) Mutual particle-collector attraction giving a primary minimum and no energy barrier. (c) Mutual particle-collector repulsion resulting in a shallow secondary minimum, but no primary minimum. (d) Mutual particle-collector repulsion with no attractive forces. (Modified from Elimelech and others, 1995)

1.2.2.2 Particle Release

In contrast to the deposition of colloidal particles, the release of colloids is less clearly understood, and no quantitative theory exists (Kretzschmar and others, 1999). As with attachment, colloid release is generally perceived to be a two step process in which particles may diffuse across an energy barrier, followed by transport through the stationary water film surrounding aquifer grains. Alternatively, chemical conditions in the system may change, resulting in previously attractive surfaces becoming repulsive, thereby resulting in a significant release of previously-attached colloids into the system (Loveland and others, 1996). However, despite numerous phenomenological observations, to date no comprehensive theory exists to relate colloid release to potentially influential chemical and physical parameters in the host system, e.g. flow velocity, attractive/repulsive forces, particle/collector size. This is in part due to a lack of knowledge concerning short range interactions between particles and colloids (Isrealachvili, 1992).

1.2.2.3 Biocolloids-special considerations

Thus far the issue of microbiological particle transport and attenuation has been addressed, largely from the point of view of treating these microbiological particles as colloids. In terms of their size and surface properties, this approach is valid. However, additional processes influence the transport and attenuation of bacteria, viruses and protozoa. The transport and attenuation of bacteria in particular is complicated by phenomena such as chemotaxis and changing surface adhesion characteristics in response to changes in their surroundings. Moreover, bacterial survival may depend on the presence of particular substances that permit their metabolism to function and thus survive in aquifers for extended periods. These issues will not be considered further here. The reader is referred to Ginn and others (2002) for further details of these processes.

In contrast to bacteria, viruses cannot actively respond to conditions in groundwater, provided the host cells necessary for viral reproduction are absent from the system of interest (Schijven and Hassanizedeh, 2000). Nonetheless, additional processes influence viral transport in groundwater systems, compared to inorganic colloids. Most notable amongst these is the phenomenon of inactivation, where viruses loose their capacity to infect their host cells with time. Schijven and Hassanizedah (2000) suggested that the pathogenic protozoan cysts were believed to behave similarly to viruses in this respect.

Viral inactivation occurs when the protein coatings of viruses are disrupted and the enclosed nucleic acids may be degraded (Gerba and Bitton, 1984). This process may occur in suspension, or while viruses are adsorbed to surfaces. Grant and others (1993) showed that the rate of viral inactivation is not

necessarily the same for free and attached viruses, and identified three different states for reversible virus attachment, where the inactivation rate of adsorbed viruses may be enhanced, reduced or equal to that of suspended viruses. Consequently, Schijven and others (1999) proposed a form of the advective-dispersive transport equation, incorporating first order kinetic inactivation of adsorbed and free viruses as follows:

$$\frac{\partial C}{\partial t} = D_l \frac{\partial^2 C}{\partial x^2} - v\frac{\partial C}{\partial x} - \frac{\rho_b}{\phi}\frac{\partial S}{\partial t} - \mu_l C \qquad (6)$$

$$\frac{\rho_b}{\phi}\frac{\partial S}{\partial t} = k_d C - \frac{\rho_b}{\phi} k_r S - \mu_s \frac{\rho_b}{\phi} S \qquad (7)$$

where μ_s and μ_l are the inactivation rates of adsorbed and free viruses respectively. In the case of non-aggregating viral particles, inactivation is regarded as an irreversible process. Grant (1994) has argued that viral aggregates probably occur intercellularly, and their occurrence outside the cell is unlikely. Consequently, viral inactivation in groundwater systems can generally be regarded as irreversible, provided host cells are absent.

1.3 Colloidal transport in natural systems

The previous sections have outlined the theoretical basis for understanding virus transport and attenuation in groundwater environments. However, the correspondence between theoretical predictions and experimental data has met with varying degrees of success (Elimelech and O'Melia, 1990; Litton and Olson, 1993). Many investigations have been carried out in recent years to verify and, where necessary, modify existing theories with respect to both inorganic colloid and biocolloid transport and attenuation (Elimelech and O'Melia, 1990, Penrod and others ,1996; Behrens and others, 1998). Model systems, with idealised shapes and surfaces have often been used to this end. Model systems have the benefit of being relatively easy to analyze, and thus permitting the relative influences of various parameters to be easily ascertained. These systems typically employ columns packed with spherical beads (glass or steel), or more realistically, uniform cleaned sand grains that use compositionally simple solutions as particle suspension media. (Kuo and Matijevic, 1980; Bales and others, 1991; Rodier and Dodds, 1993; Penrod, 1996). Moreover, the colloidal particles under investigation often have regular geometries and surface chemistry characteristics, such as silica spheres, or fluorescent microspheres (e.g. Saiers and others, 1999, Niehren and Kinzelbach, 1999).

In contrast to idealised model systems, natural aquifers are characterised by varying degrees of heterogeneity which complicate the investigation of colloid transport processes. Aquifer heterogeneity may be a consequence of differences in aquifer texture (variations in grain size/shape and their distribution) and/or aquifer composition (variations in mineralogy, hydrochemistry). Both types

heterogeneities may occur on scales ranging from individual pores to entire basins (Huggenberger and Aigner,1999). Field-based and laboratory-based studies have demonstrated the potential importance of both compositional and textural heterogeneity of aquifer materials in the attenuation of microbiological contaminants (Harvey and others 1991; Ryan and others, 1999).

Huggenberger and Aigner (1999) argued that aquifer facies heterogeneity could be organised into a hierarchical system of scales ranging from entire basins to individual pores, as follows:

(1) Giga scale facies related to basin fill dynamics.
(2) Mega scale facies related to depositional systems.
(3) Macroscale architectural elements related to facies dynamics.
(4) Mesoscale sedimentary structures related to sedimentary dynamics.
(5) Microscale differences in petrology, porosity and hydraulic conductivity.

Field-scale investigations of virus transport are normally carried out at the scale of 10s of metres to 100s of m (Ryan and others, 2001; Kennedy and others, 2001a; Schijven and others, 2002). This scale corresponds to dimensions of many macroscale architectural elements. In contrast laboratory-scale investigations are often influenced by microscale heterogeneities (Lawrence and Hendry, 1998; Ryan and others, 1999). Studies investigating the influence of meso-scale heterogeneities on biocolloid transport in aquifers are much less common in the literature (e.g. Harvey and others , 1993). However, Harvey and others (1993) noted the importance of such structures in controlling biocolloid transport in a sand and gravel aquifers. Indeed, development of an understanding of virus migration through such features offers considerable potential for resolving discrepancies observed between the results of laboratory-scale studies with those obtained in field-based investigations, as well as providing a means of further understanding the relative importance of deviations from the idealised conditions assumed in theoretical models.

1.3.1 Textural Influences

From a textural perspective, irregular grain shapes can complicate predictions of single collector efficiency made using the filtration theory (Ryan and Elimelech, 1996). The various versions of the filtration theory assume regular geometries and smooth surfaces (Yao and others, 1971; Rajopalan and Tien, 1979; O'Melia 1989). In natural systems, departures from this assumed shape can be considerable. Grains may have may have highly variable degrees of roughness and sphericty both from one deposit to another and within a formation (Tucker, 1980). Grain roughness may also influence collision predictions, since the DLVO theory also assumes a smooth collector surface. However, Ross and Olivier (1964) note that surface charge heterogeneities may arise due to cracks and edge effects. These surface charge heterogeneities may in turn reduce repulsive conditions on otherwise smooth surfaces, and are suspected to be in part responsible for deposition rates in excess of those predicted by the DLVO theory,

even in model systems (Ryan and Elimelech, 1996). Moreover Elimelech and O'Melia (1990) have demonstrated that textural protrusions may significantly reduce repulsion between similarly charged particles even on surfaces with uniform charge density.

In general, laboratory scale investigations of virus migration through (natural and synthetic) porous media tend to use granular material with a uniform diameter (Bales and others, 1991; Loveland and others, 1996; Penrod and others, 1999). Texturally these deposits may differ significantly from those encountered in natural sediments, where a range of grain sizes and pore distributions may be encountered (Allen, 1985). Indeed, grain size analyses of fluvioglacial sediments by Ashworth and Ferguson (1986) demonstrated that individual samples of these deposits can have a wide range of grain sizes. The filtration theory does not account for this range of different grain sizes, where a uniform collector diameter is assumed (Yao and others, 1971). Martin and others (1996) investigated the influence of materials with non-uniform grain size distributions on bacterial transport using laboratory-scale columns packed with a homogeneous mixture of glass beads with different diameters. The authors found the finest 10% of the beads (by volume) could be used with filtration theory to best explain bacterial transport.

Approaches such as that used by Martin and others (1996) may significantly improve our understanding of biocolloid transport through porous media with non-uniform grain size distributions, but this approach must be applied with reservation. Grains and pores may not be distributed uniformly. Smith and others (1985) investigated bacterial migration through undisturbed natural deposits using laboratory-based column studies. The authors noted a significant decline in bacterial concentrations in the column effluent once the material had subsequently been homogenised and repacked, thus illustrating the importance of bacterial transport through preferential flow paths. Indeed, such types of physical heterogeneity can give rise to differences in behaviour between micro-organisms and conservative solute tracers (Harvey, 1997). Studies by Pieper and others (1997) demonstrated that viruses and solutes move at the same velocity in relatively homogeneous sands. In contrast, investigations of bacterial transport in soil by Abu-Ashour and others (1994) demonstrated that bacteria tend to move more rapidly than solutes due to the presence of macropores such as roots and cracks. Harvey (1997) argued that this was a consequence of solutes diffusing into pores that were inaccessible to biocolloids. Bales and others (1989) demonstrated that this behaviour can give rise to apparent differences in solute and virus breakthrough curves.

McDowell-Boyer and others (1986) argued that irregular pore size distributions that could not be reproduced in the laboratory necessitated field studies into biocolloid transport if their transport in groundwater was to be thoroughly understood. Indeed, studies by Harvey and others (1993) noted that considerable discrepancies may exist between the results of colloidal transport

investigations carried out at different investigation scales. This study attributed these differences to geological heterogeneity that influenced investigations at different scales in different ways. Campbell-Rehmann and others (1999) recently attempted to investigate the effects of field scale heterogeneity on virus transport using stochastic modelling and argued that increased heterogeneity will enhance virus transport relative to conservative solute tracers. However, to date the approach used remains controversial (Ginn, 2000) and consensus has yet to be reached concerning an appropriate means of dealing with this issue.

1.3.2 Compositional Influences

Pore scale compositional heterogeneities such as lattice defects and chemical impurities are also believed to play an important role in both inorganic colloid and virus attenuation (Johnson and others 1996; Ryan and others , 1999). Patches of iron and manganese oxide on grain surfaces are frequently cited as reasons for higher than anticipated viral attenuation in natural materials (Jin and others, 1997; Ryan and others, 1999). Moreover, Yates and Yates (1987) also noted the importance of compositional heterogeneities for influencing viral inactivation rates.

Few studies are available concerning virus migration through natural polymineralic sands (Ryan and others, 1999; Schulze-Makuch and others, 2003). Moreover, these studies have tended to deal with silicate systems, where carbonates were not detected in significant quantities. Nonetheless, carbonates are abundant in many perialpine fluvioglacial aquifers, where sediments are derived from limestone-bearing areas. Indeed in some areas, the aquifer mineralogy may be dominated by calcite, (e.g. the Munich fluvioglacial gravel plain. Mallèn, pers comm.). Consequently, the influence of carbonates requires attention when considering virus attenuation in these aquifer types.

In polymineralic aquifers such as those that may be encountered in perialpine fluvioglacial deposits, compositional heterogeneity can manifest itself on the grain scale, where different grains may have different compositions due to different mineralogies. Grains may consist of individual minerals or aggregates (rock fragments). Once again this results in departures from the simplified conditions assumed in the DLVO theory, since the different electrostatic properties of different grains may result in differing surface charges. This in turn results in variable degrees of attraction/repulsion of viruses to various collector surfaces. Schulze-Makuch and others (2003) noted such phenomena in laboratory-scale virus migration experiments where viruses were more attracted to feldspar surface than those of quartz under acidic pH conditions. Johnson and others (1996) dealt with the problem of such heterogeneity by treating the collision efficiencies of the different surfaces as a deposit with a single equivalent uniform value of α. This approach is appropriate for aquifers should the various minerals making up the deposit be homogeneously distributed throughout the formation. However, difference in mineral density and shape often result in

separation of different mineral fractions during deposition processes (Allen, 1985). Moreover, these differences may extend to larger scales, should depositional dynamics or the nature of the source sediments that were deposited to form an aquifer vary. Studies by Allen-King and others (1997) demonstrated the importance of such petrographic differences associated with depositional processes with perchlorethene distribution in the Borden aquifer. To date, however, similar studies have not been published for colloid transport.

It is notable that mineralogy can influence the composition of the groundwater in an aquifer due to processes such as dissolution and ion exchange (Appello and Potsma, 1993). Moreover, precipitation processes can result in materials being deposited on aquifer surfaces that differ from those of the underlying substrate and thus can influence the degree of viral attraction/repulsion. Similarly, in aquifers which contain waters with short residence times, water composition will be dominated by interactions with more reactive minerals. The presence of calcite in aquifers, in particular, can have important implications for virus transport and attenuation processes, due to its high reactivity relative to silicate minerals and it's ability to significantly alter hydrochemical conditions (Stumm and Morgan, 1992). Calcite dissolution introduces bivalent Ca^{2+} into groundwater. Redman and others (1999) demonstrated that the introduction of polyvalent ions can considerably increase the virus adsorption capacity of otherwise repulsive mineral surfaces. On the other hand, carbonate dissolution has a strong tendency to buffer groundwater, and generally increases the pH of infiltrating precipitation from acidic pHs to neutral conditions (Lloyd and Heathcote, 1985). Numerous studies have shown that increasing the pH of water can increase repulsive forces between viruses and the negatively charged conditions present on many silicate minerals at near neutral pHs (Bales and others ,1991, Loveland and others 1996, Schulze-Makuch and others, 2003).

Finally, it must be noted that experiments carried out using laboratory-based systems often use particle-free analytical grade water. However, Degueldre and others (1996) noted that colloids are ubiquitous in groundwaters. These colloids may enhance contaminant transport processes. A study by Jin and others (2000) demonstrated that the presence of suspended clay particles enhanced the transport of viruses through porous media. Consequently, the presence of inorganic particles may facilitate the transport of viruses through porous aquifers that may otherwise be attenuated.

Despite the numerous deviations from the theoretical assumptions of the DLVO model and the filtration theory, laboratory-scale investigations have demonstrated these theories to be valid, and thus applicable to field situations, provided compositional and textural heterogeneity are taken into account. Indeed, Harvey and Garabedian (1991) have used the filtration theory in a heterogeneous sand and gravel aquifer to obtain rough estimates of the relative influence of physical and chemical influences on biocolloid attenuation. However, studies such as those by Ryan and others (1999, 2001) demonstrate the

continued need for laboratory-scale investigations if virus responses obtained during field investigations are to be appropriately characterised and relevant attenuation mechanisms identified.

1.3 Data Gaps

Based on a literature review, the following gaps in the understanding of virus transport in perialpine fluvioglacial aquifers were identified:

- A dearth of published studies dealing with laboratory scale migration through natural sands was noted at the start of this study (1999)(e.g. Dowd and others, 1998). During the period in which this research was carried out, additional studies have been published (Ryan and others, 1999; Schulze-Makuch and others, 2003). However, it is noteworthy that none of the deposits investigated contained notable quantities of carbonate, which as previously noted may complicate predictions of virus interactions with aquifer material.
- Despite an increase in the number of field-based studies that investigated the transport of micro-organisms in porous aquifers in recent years, (Harvey and others, 1991; Harvey and others 1993; Bales and others, 1995), investigations that examined mass transport in coarse-grained gravel aquifers with rapid groundwater flow regimes were rare (Rossi and others, 1992; Carvalho-Dill, 1993) and tended to focus on virus response relative to conservative solutes without specifying the causes for differences in the responses of the two tracer types. More recently published studies have addressed this issue to some degree (DeBorde and others, 1998; Woessner and others, 2001) but have tended to focus on alluvial deposits in riparian settings. The depositional characteristics of these deposits may differ from some of the sediments laid down in fluvioglacial environments, e.g. deposition of sediments generated by large-scale catstrophic events that may no longer be possible under current climatic conditions. Moreover, the source materials for these aquifers were silicate-dominated igneous and metamorphic rocks. In contrast, many central European fluvioglacial deposits have derived their sediments from catchments containing significant quantities of sediments and limestone in particular. Potential complications introduced by the presence of carbonate in contact with groundwater on virus transport have already been highlighted.
- No study could be found in the literature that examined the potential influence of heterogeneous mineral distributions on viral transport in natural systems, despite the fact that numerical simulations by Sun and others (2001) demonstrated the potential importance of such phenomena on colloidal breakthrough curves. Moreover, this same study highlighted how compositional and textural heterogeneities may interact by assigning different attenuation capacities to the grains in beds with different textures. Both these differences were suspected to influence microbiological transport and attenuation processes. Consequently, studies examining

virus and bacterial transport and attenuation mechanisms in fluvioglacial aquifers with rapidly flowing groundwater were believed to require additional attention, especially in terms of the role of preferential flow zones in overall mass transport processes.

- Inactivation on grain surfaces has been demonstrated to be an important viral attenuation mechanism in influencing virus concentrations in groundwater (Yates and Yates, 1988; Grant and others, 1994). However, publications investigating this phenomenon were carried out at the laboratory scale using either batch techniques (Yates and others, 1988), or column testing (Jin and others, 1997). Published field studies dealing with inactivation in aquifers were rare at the start of this project (e.g. Bales and others, 1997). Subsequent investigations dealing with viral inactivation in fine-grained sands (Schijven and others, 1999), and in coarser sand and gravels (Ryan and others , 2002) have subsequently been published. However, as noted above, the texture and/or composition of these deposits differs from those commonly encountered in perialpine fluvioglacial aquifers, thus once again emphasising the importance of further research in this area.
- Finally, as previously noted, tracer responses in experiments carried out at field scales and those completed at laboratory scales can differ significantly. Harvey and others (1993) noted that small scale heterogeneities due to sedimentary structures can have a significant impact on both solute and particle responses. However, little systematic work is available in the literature that investigates the role of these features in mass transport processes.

1.4 Research Approach

The goal of the investigations carried out in the framework of this thesis was to address the research needs identified in the previous discussion in order to better understand the transport of biocolloids, with particular emphasis on virus transport in peralpine fluvioglacial aquifers. The importance of studying biocolloid transport through natural porous media at a range of different scales has already been highlighted. As a consequence of the issues raised, field-based research investigating biocolloid transport has been complimented by laboratory scale studies to identify appropriate viral attenuation mechanisms, and assess their relative importance in the transport and removal in natural deposits. The benefits of intensive sampling and analysis in constructing detailed breakthrough curves were believed to be sufficient to justify the refinement and/or development of monitoring techniques to permit frequent samples to be collected regularly over prolonged periods, where necessary.

The materials used for these investigations were conventional solute and particle tracers. Uranine has been used as the main solute tracer due to its proven efficiency in tracer tests in porous media, its widespread availability, and the ease at which it may be analysed on-line in the field down to levels as low as

0.1ppb (Schnegg and Bossy, 2001). Similarly, bacteriophages (bacterial viruses, or phages) acted as viral tracers for the similar reasons (Ease of preparation, ease of analysis and low detection limit). The University of Neuchâtel has considerable experience with the use of bacteriophages in laboratory-based batch studies (Rossi, 1994) and field-based tracer tests (Cavarhlo-Dill, 1993; Kennedy, 2001). During the course of the current research, the use of phages has been extended to one-dimensional and pseudo one-dimensional laboratory-scale column testing. Moreover, sampling strategies developed by Kennedy (2001) for field-based sampling have been further modified for more detailed sample collection over prolonged time periods.

Due to the absence of a comprehensive theoretical basis for predicting virus transport, investigations have focused on virus transport under natural conditions or conditions resembling those observed in the field as closely as possible. More specifically, research focused on the following aspects:

- Column-scale studies investigated the viral attenuation capacity of the sand size fraction of samples collected from a natural polymineralic sand and gravel aquifer. Mineralogical analysis and column studies using subsets of the minerals present in the gravel allowed the role of different materials in the attenuation process and the influence of surface heterogeneities to be better defined. Moreover, this study permitted the relative contributions of short term inactivation and adsorption in the attenuation process to be assessed.

- Virus transport through a meso-scale sedimentary structure was simulated under controlled laboratory conditions, by reconstructing a fining-upward sedimentary structure based on the grain size distributions observed in natural deposits exposed in a fluvioglacial sand and gravel outcrop. Solute and tracer responses were compared to the results observed in field-based tracer tests, and the relative responses of solute and particle tracers compared in simulations with different degrees of grain size variation.
- The results of tests using simulated sedimentary structures highlighted the importance of preferential flow paths in virus transport through porous media. In order to evaluate the influence of preferential flow zones on solute and biocolloid transport in the field, a mobile downhole fluorometer has been developed to identify zones of tracer arrival in monitoring wells. Multiple-level low flow sampling in subsequent tests, permitted the relative behaviour of solute and virus tracers at different levels in the monitoring well to be assessed. Moreover, modifications to the fluorometer setup permitted the well water flow regime to be assessed and the groundwater flow regime in the aquifer to be identified.
- Field scale comparative tracer tests permitted in situ virus transport and attenuation mechanisms in a perialpine fluvioglacial sand and gravel aquifer to be assessed and compared to the responses of solute, and

bacterial tracers. Detailed monitoring at observation points permitted solute and microbiological tracer transport mechanisms to be more confidently identified. Moreover, the use of multiple microbiological tracers permitted the relative mobility of bacteria and viruses in fast flowing coarse-grained fluvioglacial deposits to be evaluated, and the disinfection capacity of the aquifer for different bacteria and viruses to be more confidently characterised.

- Column-scale studies investigated the role of inactivation of viruses adsorbed to aquifer sands and gravels in disinfection processes operating in aquifers by comparing bacteriophage inactivation rates calculated for suspended viruses with those adsorbed on grain surfaces. Field-based tracer testing along with a program of hydrochemical and mineralogical characterisation of a fluvioglacial glacial aquifer permitted the influence of geochemical heterogeneity on virus survival in a real aquifer to be evaluated.

1.6 Thesis Structure

The research presented in this thesis is provided as a series of stand-alone papers that have been submitted to relevant scientific journals for publication. As a consequence of this format, a certain degree of repetition occurs from one article to the next. Nonetheless, in the interests of minimising unnecessary duplication, sections that have been repeated verbatim in two or more chapters have been modified from the original text of the submitted articles, such that modified chapters refer to relevant sections presented earlier on, where the passage was first written. Overall however, the focus of each article in this thesis differs from the others, while providing relevant results to allow a fuller understanding of virus transport and attenuation mechanisms in coarse grained perialpine aquifers to be developed.

Chapter 2 . Investigation of Virus Attenuation in a Fluvioglacial Sand using Column Experiments

2.1 Abstract

Virus inactivation and virus adsorption, resulting from interactions with minerals, constitute important aspects of an aquifers disinfection capacity. Investigations using a 20cm long column filled with medium-grained natural sands demonstrated that the sands can attenuate up to 62% of a pulse of viruses injected. Experiments using repeatedly-washed sands had significantly lower attenuation capacity than fresh sands, due to removal of fine-grained (silt and clay-sized) coatings on the sand surface. X-ray diffraction analysis of the sand, and of the fine-grained coating indicated that no significant mineralogical differences existed between these two materials. The experimental data suggested grain coatings reduced repulsive forces between viruses and the sands permitting greater virus adsorption to the column matrix. Soaking the sands with Tryptone solution after testing released adsorbed viruses and indicated that short-term viral inactivation due to interactions with the column matrix was a negligible part of the attenuation process.

2.2 Introduction

Microbiological contamination of water by bacterial, viral and protozoan pathogens constitutes a significant threat to public health. An idea of the extent of the problem is provided in 1987 United Nations Development Programme study that estimated that between three and five billon water-borne diarrhoeas occurred world wide annually, of which five million to ten million result in death (van der Leeden and others, 1990). In developed countries, strict controls on surface water quality have reduced the threat of infection from river and lake water. However, less stringent controls on groundwater quality have meant that contaminated groundwater may now constitute a greater threat to public health. Recently Macler & Merkle (2000) estimated that between 750,000 and 5.9 million diseases related to microbiologically contaminated groundwater occur in the US every year. Of these contaminants, viruses have caused the most concern in terms of public health, largely a result of their smaller size, which is suspected to result in enhanced mobility relative to larger micro-organisms (Macler & Merkle, 2000), but also because viruses, unlike bacteria, do not require metabolites to survive. Nonetheless, despite the prevalence of viral contamination in groundwater Macler and Merkle (2000) also noted that the physical and chemical controls governing its fate and transport in natural media are far from thoroughly understood.

Part of the reason for the lack of knowledge concerning the fate and transport of viruses in groundwater is that particle (including virus) transport in aquifers is a complex problem. Harvey and others (1993) recognised that much of the complexity associated with the transport of microbiological contaminants is a result of aquifer heterogeneity. This heterogeneity may be textural or compositional and occurs at different scales (Ryan & Elimelech, 1996) Textural heterogeneity may consist of variations in grain size and grain roughness, through to variations in the properties of different formations (Klingbeil and others, 1999, Anderson and others, 1999). Similarly, scales of interest relating to compositional heterogeneity may range from variations in the chemical content of individual grains to geochemical variations on the geological formation scale (Kleinedam and others, 1999).

Since media with different grain sizes and different compositions interact with viruses differently (Redman and others, 1999, Lukasic and others, 1999), it follows that compositional and textural heterogeneity can influence an aquifers natural disinfection capacity. The United States Environmental Protection Agency (1992) defined natural disinfection as “Source water treatment via virus attenuation by natural subsurface processes such as virus inactivation, dispersion (dilution) and irreversible sorption to aquifer framework solid surfaces”. Field studies such as those by Deborde and others (1999) have shown that even coarse-grained aquifers with fast flowing groundwater had a significant capacity to attenuate viruses. However, the results of studies such as this have been rarely able to determine the relative contributions of inactivation (loss of

virulence) and adsorption to viral attenuation. Recently however, a viral radioisotope labelling technique was used to demonstrate inactivation due to interactions with grain surfaces could occur in the field (Ryan and others, 2002). Nonetheless, this same study used laboratory-based studies to further characterise the inactivation process.

The principal benefit of laboratory-based investigations is that the imposition of closely controlled conditions using laboratory methods permits more confident determination of attenuation mechanisms (Harvey, 1991). Jin and others (1997) used column studies, where flow dynamics, water chemistry and column matrix composition were controlled, to demonstrate that although the bacteriophage (bacterial virus, or phage) ϕX-174 had been removed during column testing, they retained their virulence. In the same study, the authors demonstrated that another bacteriophage, MS-2, was not adsorbed by the quartz sand matrix in the column under the same experimental conditions, thereby demonstrating the different degrees of viral attenuation which may occur depending on phage type. Similarly, the results of column studies by Dowd and others (1998) indicated that the isoelectric points (pH of zero electrokinetic charge) of various viruses determined the degree of adsorption to an alluvial deposit in the column matrix.

Lyklema (1991) defined colloids as particles having one or more dimension within the nanometre (10^{-9}m) to micron (10^{-6}) range. This size range incorporates viruses (Harvey, 1991) In a review of colloid mobilisation and transport in groundwater, Ryan and Elimelech (1996) noted that whether colloidal adsorption occurs depends largely on hydrophobic and electrostatic forces operating between a colloid and a surface. In the absence of organic matter, adsorption will be dominated by electrostatic forces.

Stumm (1992) observed that natural solids tend to develop a surface charge when immersed in water, due to complexation/ionisation of surface functional groups, ion adsorption and/or ionic substitution in the crystal framework. Similarly, Elimelech and others (1995) noted that the polarity and magnitude of the charge is pH dependant, and that the point at which there is no net charge on the surface is called the point of zero charge (PZC). In a review of viral attenuation in a number of soil types, Gerba and Bitton (1984) found that virus adsorption was greater in soils having high PZC values than those having low PZC values, thereby providing an indication of the importance of the surface charge of different materials on viral attenuation.

Data provided by Stumm and Morgan (1996) summarised the isoelectric points of various common minerals, but noted that the actual charges on particular surfaces at the interface with the surrounding solution may depend not only on pH, but also on the presence of other ions. Moreover, studies by Thompson and Pownall (1989) have shown that calcite can have either positive or negative charge, at a given pH, depending on the electrolyte content of the

measuring solution. Despite these complications, column studies such as those by Zhuang and Jin (2003) and Lukasik and others (1999) have shown that negatively charged viruses can be attracted or repelled by solid surfaces depending on mineralogy and aqueous conditions.

In general, theoretical predictions on adsorption of negatively-charged particles to positive surfaces, generally referred to as favourable deposition, are reasonably accurate (Ryan and Elimelech, 1996). In contrast, predictions of rates of adsorption of negatively charged particles to negatively charged surfaces, referred to as unfavourable deposition, are often underestimated by orders of magnitude. Elimelech and others (1995) explain this later discrepancy as a consequence of imperfections on mineral surfaces that produce surficial variations in the density and polarity of electrostatic charge. These imperfections include cracks, lattice defects, chemical impurities and edge effects (Ross and Olivier, 1964). Moreover, Johnson and others (1996) extended this concept beyond individual surfaces to incorporate separate grains using pure quartz sands and iron-oxide coated quartz sands. This type of system approaches conditions found in many aquifers, where a variety of minerals may exist together (Kleinedam and others, 1999). These minerals may have different surface charges at a given pH (Stumm & Morgan, 1996).

Another reason for the failure of theoretical models to predict colloidal adsorption rates relates to deviations from the smooth surfaces assumed in theories, is due to surface roughness (Ryan and Elimelech, 1996). Rough surfaces may alter colloid-fixed surface interaction energies (Bowen and Epstein, 1979). Since both irregular grain shapes and variable compositions occur together in natural deposits, actual interactions between colloids and aquifer materials may result in considerable departures from theoretical predictions (Ginn and others 2002)

This paper investigates virus transport and interactions with natural sands, sampled from a porous aquifer, and attempts to identify compositional and textural influences on viral attenuation processes. The overall investigative approach adopted involved identifying minerals present in natural sand and relating the attenuation capacity of the sand to the minerals and their distribution on grain surfaces, where they are available to interact with viruses. The relative influence of specific minerals was assessed by carrying out experiments using individual minerals, or a more limited number of minerals than present in the natural sands. All sands used had the same grain size and approximately equal grain angularity. A secondary objective of this work was to determine the relative roles of short-term viral inactivation and adsorption on viral attenuation processes in the sand.

To achieve the above objectives, a series of column experiments were carried out in which a pulse of bacteriophages was injected into columns filled with different types of saturated sand, with different mineralogies. By monitoring

phage concentrations in the column effluent, relative to a conservative tracer, the degree of virus attenuation could be established. Adsorbed but still virulent phages were subsequently desorbed by soaking with Tryptone, an amino acid/peptide solution. Mass balance calculations permitted the proportions of viruses that were adsorbed and inactivated to be determined. This was achieved by comparing the quantity of H40/1 injected with that recovered in the column effluent, and those released by desorption.

2.3 Material and Methods

2.3.1 Sand Types Investigated.

The attenuation capacity of samples of the sediments underlying the Kappelen test site (Kappelen), Switzerland (Kennedy and others, 2001b) formed the focal point of this investigation. Visual inspection of the samples showed the deposits to consist of sands and gravels containing a variety of different types of rock fragments and minerals. Application of 1N HCl to selected sediment samples in the field, revealed carbonate to be present on a number of surfaces including siliceous materials such as granite clasts.

Granulometric data for the samples collected from three boreholes suggest, that in all but one case, coarse sand to silt sized grains (ø<1mm) make up no more than 20% of total sample mass (Noseda, 1999; Diomande 2000). Nonetheless, preliminary surface area calculations for these grain size fractions indicate that they constitute over 75% of the total solid surface area, assuming all grains to be spherical, thereby reflecting their relative importance in adsorption processes, where available surface area dictates the degree of reaction (Ross and Olivier, 1964).

Agitated, wet sieving using standard sieve sizes (DIN. ISO 3310/1) separated sand and silt/clay grain size fractions from coarser gravels in the 33 samples (Kappelen Sands) collected from three boreholes. The samples were subsequently rinsed in deionised water. Following washing the sands were oven dried at 40°C under ventilated conditions to remove excess moisture while preventing changes in the structure of constituent minerals which may occur at high temperatures (Lambe, 1951). Microscopic examination of sand samples failed to detect staining associated with the presence of iron or manganese oxides / hydroxides.

A composite sample consisting of medium grained sand fractions (250μm<ø<500μm) from the 33 grab samples of borehole cuttings was mixed and used for subsequent column experiments.

Four sets of experiments were completed, using Kappelen Sands that were subjected to different treatments. The different sand types were as follows:

- Fresh Sands: These were Kappelen Sands that had not been used beforehand. Tracer tests using this material permitted the capacity of fresh sands to attenuate viruses to be investigated.
- Reused Sands: These sands were used repeatedly in a series of successive experiments. The experiments permitted the effects of repeated testing on the sands viral attenuation capacity to be evaluated. At the end of each experiment, sands were washed in deionised water and oven dried at 40°C.
- Washed Sands: These sands were soaked in synthetic freshwater(see below) three times and rinsed in de-ionised water following the same procedure used in the pre-experimental column packing process, and the post-experimental rinsing processes respectively (see below). Investigations using these sands permitted the effects of the column packing/rinsing process on the Kappelen sands attenuation capacity to be distinguished from other effects resulting from the experimental process that may affect the sands ability to adsorb viruses. To determine the relative influence of the later, the results of experiments using the washed sands were compared with those obtained using the reused sands.
- Acid-digested Sands: These sands were Kappelen sands that were digested in an acid bath consisting of a 36% acetic acid solution, buffered with sodium acetate to pH 4.2, over a ten-hour period, before rinsing in deionised water and drying at 40°C. The acid digestion process removed calcium carbonate and thus permitted the influence of calcite on attenuation to be assessed by comparing virus recoveries with those from experiments using the Fresh Sands and the Washed Sands.

Apart from the Kappelen Sands, the following sands were used to investigate the influence of specific minerals on bacteriophage attenuation.

- Quartz Sands: Medium-grained analytical grade quartz sand (Aldrich, Steinheim, Germany).
- Granitic Sands: A medium grained granitic sand dominated by quartz and feldspars. The difference in attenuation capacity between this sand and the quartz sands permitted the influence of feldspars on virus attenuation to be assessed.
- Calcite Sands: Medium-grained calcite sands, prepared by crushing a block of limestone and separating the resulting 250μm<ø<500 μm fraction by agitated wet sieving with de-ionised water. This sand allowed the influence of pure calcite on attenuation to be assessed.
- Quartz-Calcite Mixture: A mixture of the above-mentioned Quartz Sands and Calcite Sands with the same proportion of calcite as that determined to cover grain surfaces of fresh Kappelen sands according to X-ray fluorescence data (See Below). This sand was prepared to act as a model carbonate/silicate system that could be compared with the Kappelen sands.

Experiments using the Quartz Sands and the Calcite Sands employed fresh materials each time. However, experiments using the Quartz-Calcite Mixture used the same material for successive experiments to further investigate the effects of re-use on viral attenuation capacity compared to the Reused Sands.

2.3.2 Compositional Characterisation of Sand

In order to more thoroughly characterise the mineralogical content and organic carbon composition of the Kappelen Sands, a programme of x-ray diffraction (XRD) analysis and pyrolysis was carried out. This programme was complimented by scanning electron microscope and x-ray fluoresence (XRF) studies that permitted the conditions on grain surfaces to be examined in more detail.

XRD analyses using a SCINTAG XRD 2000 diffractometer identified the major minerals constituting the Fresh and Acid-digested Sands. Additional analyses of the silt/clay (ø<63μm) fraction of Kappelen sand and gravel samples, collected during initial sieving to retrieve the Kappelen Sands was also carried out. These analyses investigated whether the mineralogy of the fine-grained material noted on grain surfaces during preliminary examinations of the aquifer material, differed from that of the bulk mineralogy of the sands used in column testing.

Sample preparation and semi-quantitative analyses of the bulk mineralogy of each of the natural polymineralic sands followed the procedure described by Adatte and others (1996). Final composition quantification using external standards generally provides an error varying between 5-10% for the phyllosilicates and 5% for other minerals.

Organic carbon analyses by Rock Eval 6 pyrolysis determined the weight percentage of organic carbon in eight undigested Kappelen sand samples and four acid digested sand samples. This method has a detection limit of 0.1% organic carbon. Further details of this analytical method are contained in Disnar and others (2003).

Scanning electron microscopy of uncoated sand samples using a Philips XL-30 environmental scanning electron microscope (ESEM) at 25KV allowed high resolution visual inspection of surface conditions on the mineral grains of the various polymineralic sands. Additional analyses using the ESEMs EDAX ZAF X-ray fluorescence (XRF) probe allowed a semiquantitative estimation of the proportions of various metals and silicon on a 50μm x 50μm window focused on randomly selected grain surfaces, to be ascertained to ±5%. XRF analyses of the surfaces were compared with model mineral compositions to provide an indication of the relative proportions of various minerals constituting grain surfaces.

2.3.3 Bacteriophage Tracer.

The marine phage H40/1 acted as the viral tracer used to investigate virus interaction with the various sand types used in the column test experiments. H40/1 is a host-specific non-pathogenic B1 type marine bacterial virus (Siphoviridae) hosted by the marine bacterium *Pseudoalteromonas gracilis* (Ackerman and DuBow, 1997). Marine bacteriophages, such as H40/1 and their hosts are naturally absent from groundwater systems (Rossi and Käss, 1997).

Measurements by Rossi (1994) using transmission electron microscopy showed that H40/1 has a capsid (head)measuring 39nm in diameter and a 46nm long tail. Hydrophobicity measurements made using a contact angle goniometer microscope, in the framework of the current research program indicated that the phage was hydrophilic (contact angle: 52°± 1°, n= 6). Similarly, measurements of the electrophoretic mobility of this phage in the synthetic freshwater(SF) used in the experiments indicated that the H40/1 had a strong negative charge at the ambient experimental pH. (ζ-potential H40/1 (pH 7-8)= -23mV ± 1mV, n= 6 for each pH). Moreover, similar measurements made down to pH 5.5 provided the same values, thereby indicating that H40/1s isoelectric point in SF is less than this value.

Prior to starting the experiments, phage production was carried out on Petri dishes using sea water agar (SWA) following the procedure described in Rossi (1994). The surface of double agar layer of petri dishes with confluent lysis was scraped, mixed in a small volume of saline buffer (0.9g/l NaCl, Trishydroxymethylaminomethane (Tris)-HCl, pH 7.5) and centrifuged (15min, 12,000g) so as to remove bacterial cells and agar debris. The supernatant acted as the virus stock (source concentrate) and was stored at 4°C so as to minimize viral inactivation throughout the whole set of experiments.

2.3.4 Synthetic Freshwater/Solute Tracer.

A synthetic freshwater consisting of 8mg/l of KCl, 62mg/l of $MgSO_4.7H_20$, 294 mg/l of $CaCl_2.7H_20$, 21 mg/l of $NaHCO_3$ dissolved in Nanopure© water (Barnsted, Dubuque, IA. Resistivity-18.1MΩ-cm) acted as the tracer solvent/suspending liquid and flushwater for the column experiments. The water was buffered with 1.8mL/L of 1 Molar Tris ($C_4H_{11}NO_3$) (Fluka, Buchs, Switzerland) and adjusted with 1N HCl to pH 8.0 (±0.1). Schijven and others (2001) indicated that concentrations of polyvalent cations can be critical in determining the degree of virus adsorption occurring under unfavourable deposition conditions. Consequently, the bivalent cation concentrations of the synthetic freshwater resembled those of groundwater samples collected from Kappelen, while the pH was approximately 1 unit higher than that observed at the site (Kennedy and others, 2001b).

Saturation calculations made using the hydrochemical model Phreeq (Parkhurst and others, 1980) demonstrated that the water was slightly undersaturated with respect to calcite (Calcite saturation index =-0.4). By using slightly undersaturated water, crystal precipitation, that may change H40/1 transport conditions in the column through virus adsorption to newly precipitated minerals, was avoided. Such facilitated transport has been noted in to occur between viruses and other inorganic minerals in groundwater systems Jin and others (2000).

A 100ppb solution of Uranine, (sodium fluorescein, Fluka, Buchs, Switzerland) acted as the solute tracer. Käss (1997) summarised studies indicating that although Uranine is pH sensitive and photodegrades in strong light, it undergoes little to no interaction with inorganic materials.

Before mixing with H40/1, the SF and tracer reservoirs were agitated with a teflon-coated magnetic stirrer under a vacuum of –70mmHg for 15 min prior to all experiments to remove dissolved gases. At the start of an experiment, phage stock was diluted in saline buffer and 9μL of the solution was added to the 100mL-tracer reservoir containing Uranine. The tracer mixture was homogenised by magnetic stirring to give a stock concentration of 400 plaque-forming units per mL (pfu/mL). Source samples collected from the tracer reservoir immediately after mixing and at half hourly intervals until the end of the experiment. Analyses of these samples permitted virus source concentration variation in the tracer reservoir with time to be determined. Data from the resulting analyses allowed the H40/1 inactivation rates in liquid not interacting with the column matrix to be evaluated. The tracer reservoir was stored at room temperature throughout all experiments (21°C-23°C).

2.3.5 Column Experiment Procedure

Figure 2.1 illustrates the operation of the column apparatus used in the tracer experiments. Prior to each experiment, the 20cm long x 2cm diameter borosilicate glass column was packed with sands in 1cm increments poured into a degassed synthetic freshwater column of 3cm or less. Packing the column matrix using the tap and fill method (Bales and others, 1991) with a 1cm diameter solid glass rod reduced the possibility of grain bridging and the development of preferential flow paths. A notable increase in turbidity was apparent in the water column when packing sands containing calcite. This turbidity quickly disappeared with subsequent flushing. Porosities during all experiments were 43% ± 3.5%.

All column experiments lasted three hours. Triplicate experiments provided an indication of the variation in experiment results. At the end of each experiment, sands were washed in de-ionised water and oven-dried at 40^{o} C in a ventilated atmosphere.

A peristaltic pump (Ismatec IP-15, Glattbrugg, Switzerland), connected to the column by 4mm OD silicone tubing, pumped water/tracer through the column at an approach velocity of 6.9×10^{-4} m/sec, (± 1.1×10^{-4}m/sec between experiments). At least 15 pore volumes of tracer-free synthetic freshwater passed through the column prior to tracer injection to permit chemical equilibration. Tracer test experiments consisted of injecting a short pulse (approximately 0.5 pore volumes) of the H40/1/ Uranine tracer mixture into an actively pumping tracer-free system, followed by an additional eight pore volumes of tracer-free flush water. Kretzschmar and others (1997) used the short pulse technique to minimise the effects due to colloidal ripening/blocking, which respectively prevent or enhance virus adsorption by the presence of existing deposited viruses. These authors found excellent agreement between this technique and the more commonly used step-pulsed technique, where tracers are injected over a prolonged period. Moreover, preliminary column experiments investigating the attenuation capacity of Kappelen sands compared the short pulse method with the step method and found that recoveries using each method varied by ± 3%.

On-line fluorometers monitored solute tracer concentrations in column influent and effluent water at 10 second intervals and could detect Uranine at concentrations as low as 0.1ppb (Schnegg and Bossy, 2001). Regular on-line measurements of pH and conductivity during the experiments confirmed that hydrochemical conditions remained constant during all tracer tests. An automatic sampler continuously collected column effluent samples for bacteriophage analyses at 0.1 pore volume intervals. All experiments were completed at between 21^{o}C and 23^{o}C.

H40/1 concentrations in tracer reservoir samples, and samples collected using the automatic sampler, were assayed using an optimized double agar layer technique (Rossi, 1994) on Sea Water agar (SWA) medium. Rossi (1994) found the detection limit using this method to be less than 1 plaque forming unit per milliliter (Pfu/mL). The results of duplicate analyses for each sample were quantified the day after cultivation, by direct counting.

2.3.6 Miscible Extrusion

Upon completion of experiments, column matrix extrusion was carried out using a 50mL syringe filled with synthetic freshwater. The syringe was connected to the influent side of the inverted sand column and the hydraulic pressure applied by the syringe allowed the column matrix to be extruded and sampled. Sand samples, weighing approximately 1g were collected at three cm intervals along the column length, placed into a 20mL bath of dilute Tryptone (5g/L Fluka, Buchs, Switzerland) and agitated for 15 minutes at 100 rpm using a rotating agitator. Subsequent sampling and viral assays were carried out in an analogous manner to those of column effluent samples. The assays allowed phage

concentrations in the supernatant to be ascertained and related to the dry weight of sand in the sample. Double analyses of duplicate aliquots from each interval allowed sample variability to be assessed.

Figure 2.1: Schematic illustration of column apparatus used during bacteriophage tracer test experiments.

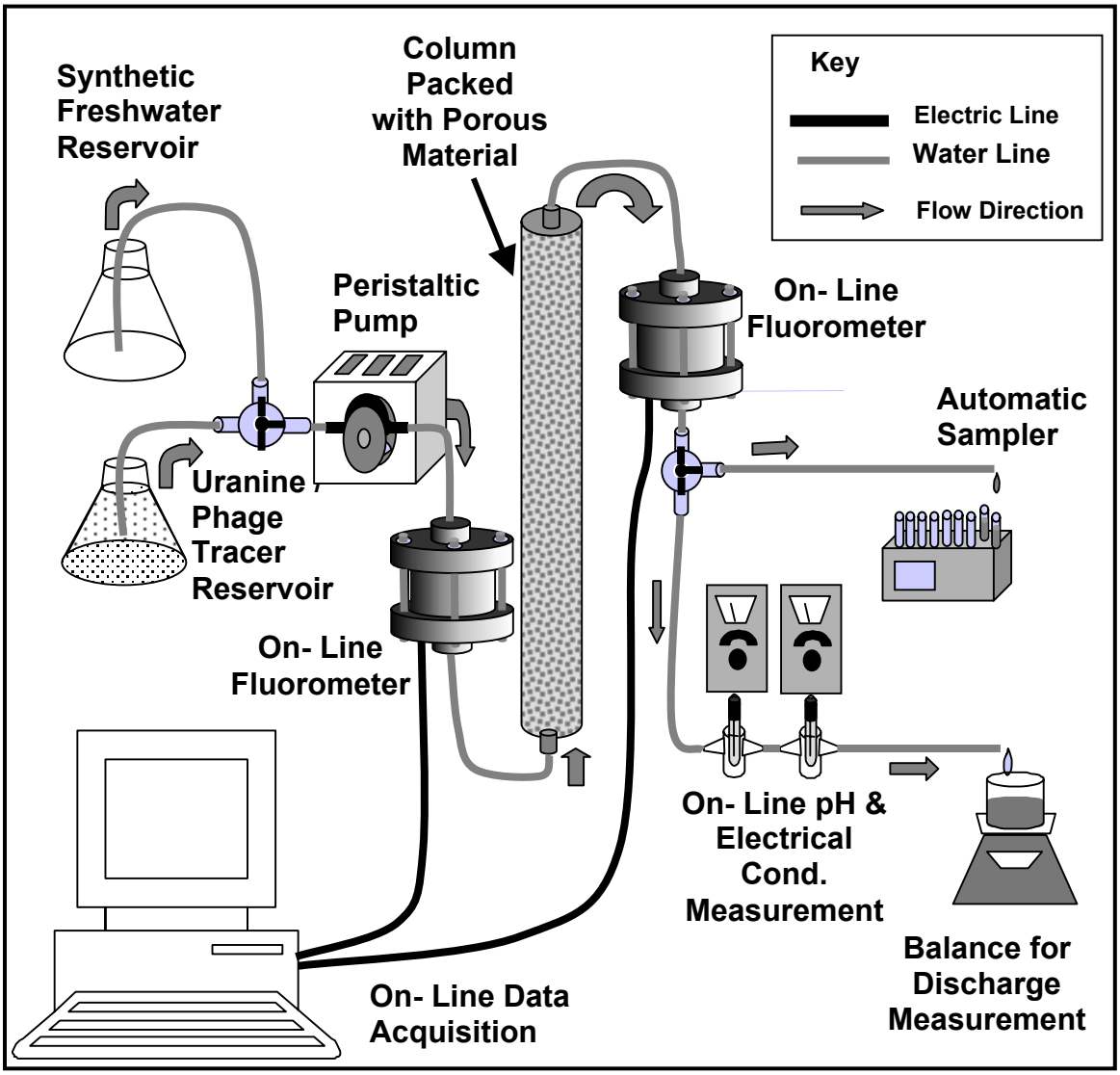

2.4 Data Analysis

Comparison of the mass of H40/1 injected into the column, with that recovered in the column effluent permitted H40/1 recovery (Rec) to be determined for each sand type tested using the following formula:

$$\mathrm{Re}\,c = \frac{Q}{M_0}\int_o^T C dt \qquad (1)$$

where Q is the volumetric flow rate through the column, M_o is the mass injected and the integral term is the temporal integral of the breakthrough curve.

Using the approach of Grolimund and others (1998), the first-order kinetic deposition constant for H40/1 in each sand type, was determined using a one-dimensional solution to the advection- dispersion equation:

$$\frac{\partial C}{\partial t} = \alpha_l v \frac{\partial^2 C}{\partial x^2} - v\frac{\partial C}{\partial x} - kC \qquad (2)$$

where C is the trace concentration(M/L^3), v is the interstitial velocity(L/T), α_l is the dispersivity (L) and k is the first order kinetic H40/1 kinetic deposition constant for each sand type investigated (1/T). α_l and v were determined by solving equation (2) using Uranine breakthrough data under the following boundary conditions:

$C(0,t)=Co \quad 0\le t<\tau$
$C(0,t)=0 \quad t\ge \tau$
$C(\infty,t)=0$
$C(x,0)=0 \quad z\ge 0$

where τ is the duration of the injection pulse. Upon calibration of the Uranine curve, the value of k was adjusted until the relative recovery (H40/1 recovery divided by Uranine recovery) corresponded to that obtained in each experiment. Yao and others (1971) related k to collision efficiency, α (the probability of a particle sticking to a surface upon collision) as follows:

$$k = \frac{3(1-\theta)}{d_c}\alpha\eta v \qquad (3)$$

where θ is the effective porosity, d_c the grain diameter (250μm), η the single collector efficiency. Kretzschmar and others (1999) noted that the value of η is dependant on a systems physical parameters such as flow rate, temperature and matrix size. In contrast, α depends largely on the solution and surface chemistry of the system. The reader is referred to Schijven and Hassanizadeh (2000) for details of the calculation of η. Based on the above equations, the collision efficiencies of the different media investigated could be determined and compared.

2.5 Results

2.5.1 Compositional characterisation of sand

Table 2.1 presents the results of XRD measurements made on the medium sand and the silt/clay sized mineral fractions separated by sieving 33 samples of Kappelen aquifer sand and gravel. The results indicate that both size fractions contain the same major minerals, although the proportion of calcite is higher in the finer-grained fraction, whereas quartz is more abundant in the sand.

The standard deviation of the both minerals ranges between 18% and 29% of the average content, calculated for the two grain size fractions.

Comparative results for XRD and XRF analyses summarising the bulk mineralogy, and mineralogy of grain surfaces, of the Fresh Sands used in column testing are presented in Table 2.2. The results are comparable to the average values obtained for individual samples of Kappelen Sand (Table 2.1 ± one standard deviation), thus indicating that the Fresh Sands were representative of the average mineralogy of the Kappelen aquifer sands. Framework silicates (quartz and feldspars) dominate the Kappelen sands composition (59% of the bulk mineralogy), although calcite is also present in significant quantities (20% of bulk mineralogy). The term “residual minerals” provided by XRD analyses in both Table 2.1 and Table 2.2 refers to minerals present in the samples that could not be identified because they have variable lattice spacings, due to phenomena such as solid solution series. In deposits sampled from the Kappelen area, residual minerals are typically unidentifiable sheet silicates (T.Adatte, pers comm.)

Table 2.1: Summary table of mineralogical analyses of medium sand and silt/clay sized fractions by X-ray diffraction, Kappelen Test Site, Switzerland. Sample size n = 33 for each fraction. (ø=grain diameter). (Details of 63μm<ϕ<250μm fraction contained in Chapter 6.)

Size Fraction	Calcite	Quartz	K-Feldspar	Na-Feldspar	Dolomite	Sheet Silicates	Residual Minerals
ø<63μm							
Mean	40	27	3	6	4	6	15
Standard Deviation	10	5	2	2	4	2	12
250μm<ø<500μm							
Mean	28	39	6	9	1	3	14
Standard Deviation	8	8	4	4	0	1	13

XRF analyses of grain surfaces indicate that the same minerals detected by XRD occur on the sand grain surfaces in similar proportions, although calcite appears to be more abundant to the detriment of sheet silicates. Significantly, analyses of surfaces containing measurable quantities of iron are normally associated with aluminium and silicon in consistent proportions, suggesting that most of the iron present occurs in sheet silicates rather than as iron oxides/hydroxides. This information is consistent with visual observations made in the field, and studies of the sand under the microscope, where no iron or manganese staining was apparent on grain surfaces. Moreover, the

mineralogical interpretation of the results of the XRF analyses corroborates the idea that the residual mineral fraction, quantified by XRD, is dominated by sheet silicates. The results of the mineralogical analyses are consistent with the composition of the source rocks present in the fluvioglacial aquifers catchment (Labhart and Decrouez, 1997).

Table 2.2: Compositions of Granitic Sands, Fresh Sands and Acid-digested Sands determined using semiquantitative XRD and XRF analyses. XRD results provide bulk mineralogical compositions. XRF analyses provide mineralogy of grain surfaces.

Mineral/Sand Type	Fresh Sands (%)		Acid- digested Sands (%)		Granitic Sands (%)	
	XRF	XRD	XRF	XRD	XRF	XRD
Quartz -SiO_2	46	45	50	49	33	37
K Feldspar - $KaAlSi_3O_8$	0	4	7	12	37	14
Albite - $NaAlSi_3O_8$	16	10	23	12	17	27
Calcite- $CaCO_3$	28	20	0	0	0	1
Dolomite - $CaMg(CO_3)_2$	2	0	0	0	0	0
Sheet Silicates*	9	3	20	4	13	5
*Residual minerals**		18		24		15
Percentage of grains partially covered with Iron oxide/ankerite coating	2		1		1	

*X-ray diffraction analyses considers muscovite as the only sheet silicate mineral present in a sample. Other sheet silicates are included as residual minerals. X-ray fluorescence data identifies sheet silicates based on model compositions and potential solid solution series substitutions. These minerals include end members such as Muscovite ($KAl_2(AlSi_3)O_{10}(OH)_2$), Biotite ($K(Mg,Fe)_3(Al,Fe)Si_3O_{10}(OH,F)_2$) and Chlorite ($Mg_5Al(AlSi_3O_{10})(OH)_8$). Limit of resolution of apparatus 1% of surface area.

The images of the grains of Fresh Sands such as that presented in Figure 2.2A demonstrate that the grains have coatings of finer grained material partially covering their surfaces. Similar coatings were apparent on Calcite Sands (Figure 2.2C , Figure 2.2D), but were less abundant on calcite grains in the Quartz-Calcite Mixture, and particularly on Washed Sands. Moreover, the coatings were not apparent on samples of Granitic Sands and Acid-digested Sand studied (Figure 2.2B, Figure 2.2E), although the certain grains in the later material did show signs of corrosion (Figure 2.2F). No corroded grains were apparent in the sample of Fresh Sands investigated.

The SEM images of the Fresh Sands are consistent with the grains being coated in fine calcium carbonate bearing material, as deduced from testing surfaces with 1N HCl in the field. The images suggest that these coatings were removed by repeated soaking and rinsing and/or the acid digestion process.

Organic carbon analyses of both Fresh Sands and Acid-digested Sands failed to detect organic carbon above the analytical detection limit of 0.1% organic carbon.

2.5.2 Column Experiment Results

Figure 2.3 provides representative (median recovery) breakthrough curves for the different sands investigated, showing the average response for the various Kappelen Sands and pure minerals investigated. The response of the Granitic Sands is not presented but resembles that of the Quartz Sands. The results of both of the duplicate analyses for each sample are presented in the figure. It is apparent from the data that the results of individual bacteriophage assays do not vary by more than ± 25% from their average value. This result is also applicable for the results of experiments completed using the Granitic Sands and the Quartz-Calcite Mixture, and for analyses of samples collected during miscible extrusion experiments following selected experiments.

H40/1 recoveries and subsequent derived parameters are presented in Table 2.3 for each sand investigated. Recoveries of up to 98% of H40/1 injected were recovered in column effluent (91%±7%) for the Quartz Sands. Similarly, high recoveries were apparent for the Granitic Sands, where recoveries of up to 98% were observed (average, 92%±6%, n=3). The results contrast strongly with recoveries obtained in experiments using Calcite Sands, where no phages were observed in the column effluent. Recoveries using Fresh Sands were 39%±1%.

Despite the absence of calcite, the Acid-digested Sands had a significant attenuation capacity, which remained consistent with repeated use of the sand (Recovery 73% ± 2%). The consistent relative recoveries observed with the Acid -digested Sands contrast strongly with the variation in relative recovery observed with the Reused Sands (63% ± 23%). Indeed, relative recoveries observed from the results of the first experiment using these sands are less than half of those observed from the third experiment using the same sands. The relative recoveries from this final experiment using the Reused Sands are comparable to those observed from experiments using the Washed Sands, where recoveries were 86.5% ± 5.5%.

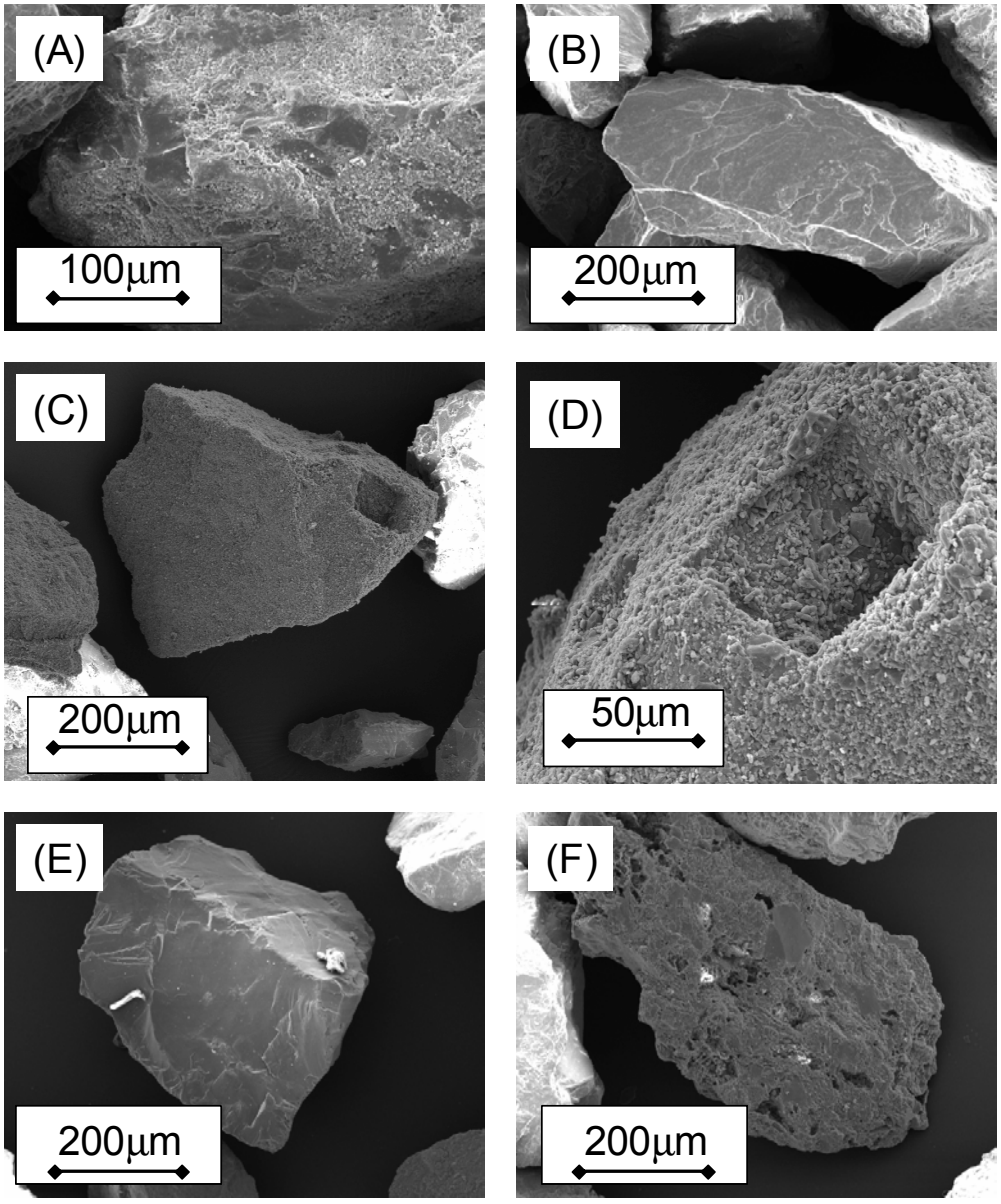

Figure 2.2: Scanning electron microscope photographs of selected granular media investigated. (A) Fresh Sands showing fine-grained material on smooth grain surface.(B) Granitic Sands. Note smooth grain surface. (C) Calcite Sands. (D) Detail of Calcite Sands showing fine-grained sized material on surface. (E) Sand grain from Acid-digested Sands. (F) Corroded sand grain from Acid-digested Sands. Such grains were not observed in undigested sands.

The tendency of increasing recovery with reuse, observed in the Reused Sands, was also apparent in the Quartz-Calcite Mixture. In this case, the increase in recovery is even more dramatic, ranging from 5% recovery in the first

experiment to 60% recovery in the third experiment using the same sand. Clearly there was an additional process operating on both the Reused Sands and Calcite Sands which caused much greater variability in recovery relative to the other sand types.

By accounting for variations in flow velocity and porosity, the collision efficiencies derived from the recovery data using Equation (2) and Equation (3) better reflect the attractive properties of the various sands to colliding H40/1. Despite the slight variations in the flow regime and porosity between experiments, the tendency for the Fresh Sands to act as attractive surfaces for H40/1 deposition is apparent in its higher collision efficiency values relative to the other natural sand types (α-Fresh Sands: 0.032-0.035). Moreover, the increasing recoveries observed in the Reused Sands and in the Quartz-Calcite Mixture are reflected in declining values of collision efficiency by approximately order of magnitude, from 0.032 to 0.0054 in the case of the Reused Sands, and 0.11 to 0.015 in the case of the Quartz-Calcite Mixture. Indeed the α value determined from the final experiment using the Reused Sands resembled that of the Washed Sands (0.0025-0.0068).

No significant decline in the concentration of H40/1 concentration in the tracer source reservoirs over the duration of the experiments was observed. This suggests that inactivation of suspended H40/1 in the tracer reservoir over the duration of the experimental period is insignificant.

2.5.3 Extrusion Experiments

Figure 2.4 summarises the results of the extrusion experiments for each type of sand investigated, apart from the Granite Sands which could not be studied due to insufficient materials. The results confirmed that all sands contained adsorbed, yet still virulent phages at the end of each experiment. The proportion of adsorbed yet still virulent phages detected in the extrusion process ranged from less than two percent for the quartz sand to 100% for the pure calcite sand. Moreover, when the numbers of viruses recovered in the extrusion were considered in conjunction with those collected in the column effluent, it is apparent that the number of viruses recovered is equal to the number injected within the range of experimental error. (±5%).

Figure 2.3: Representative Uranine and H40/1 bacteriophage breakthrough curves for the sand types investigated (Quartz/Calcite Mixture & Granite Sands omitted). Circles connected by lines represent Uranine injection/breakthrough curves (Solid circles-Injection signal; Hollow circles-Effluent signal). Triangles represent H40/1 bacteriophage concentrations (Duplicate analyses). All concentrations are relative to those in the tracer reservoir.

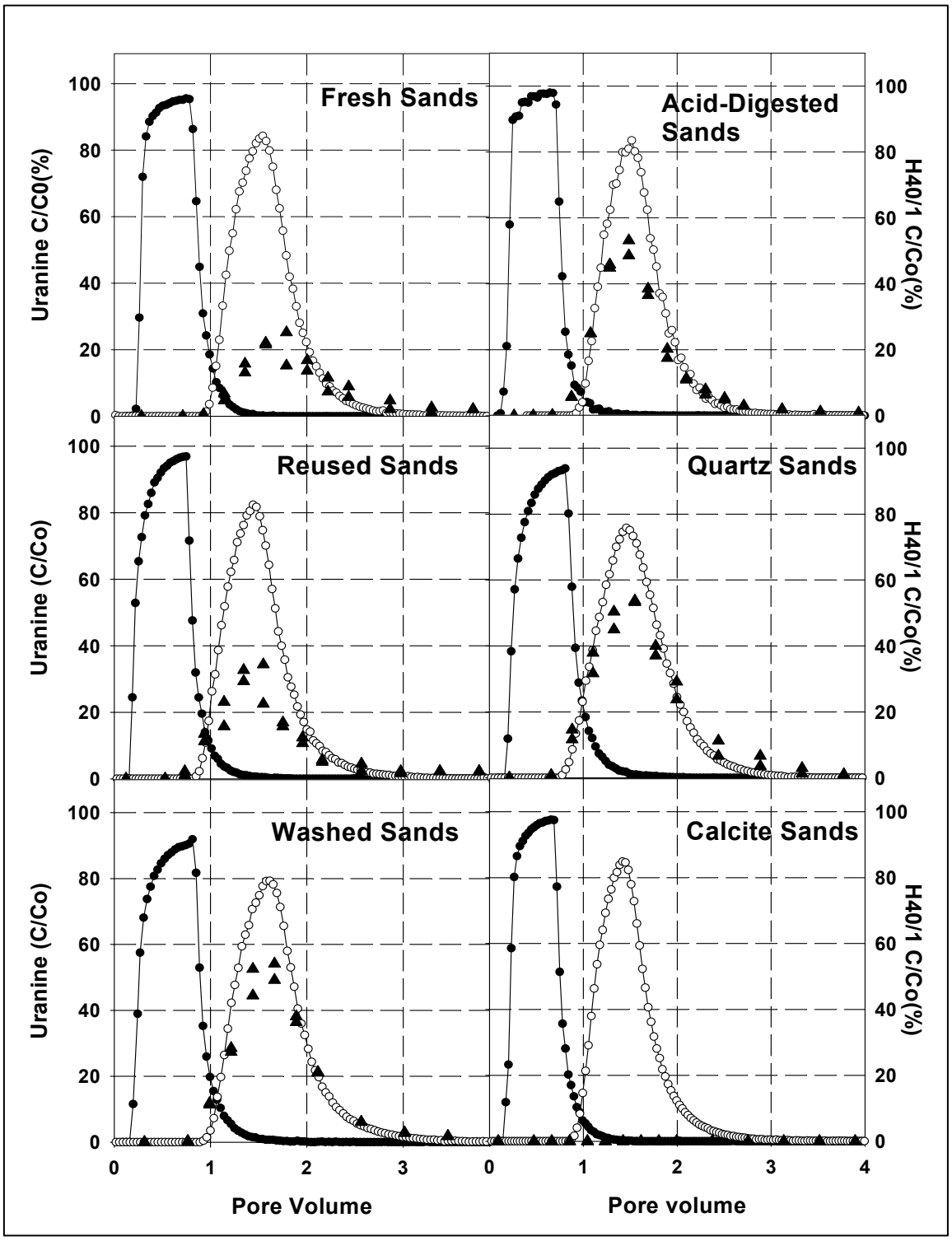

Table 2.3: Summary table of tracer test results for various porous media investigated

Matrix	Expt No.	H40/1 Recovery (%)	Effective Porosity (%)	k (1/sec)	Vel (m/sec)	Collision Efficiency
Fresh Sands	1	38	41	3.4E-03	6.8E-04	3.5E-02
	2	38	43	2.8E-03	7.3E-04	3.2E-02
	3**	40	40	3.3E-03	7.0E-04	3.2E-02
Reused Sands*	1a**	40	40	3.3E-03	7.0E-04	3.2E-02
	1b	53	41	2.3E-03	7.0E-04	2.3E-02
	1c	60	36	2.0E-03	7.8E-04	1.5E-02
	1d	86	42	5.0E-04	6.7E-04	5.4E-03
Washed Sands	1	81	38	8.2E-04	7.7E-04	6.8E-03
	2	92	37	3.2E-04	7.7E-04	2.5E-03
	3	89	36	3.8E-04	7.7E-04	2.9E-03
Acid-Digested Sands*	1a	75	37	8.7E-04	6.0E-04	1.3E-02
	1b	75	38	8.5E-04	5.9E-04	1.3E-02
	1c	72	42	1.1E-03	6.8E-04	1.2E-02
Quartz Sands	1	93	41	2.1E-04	5.8E-04	2.3E-03
	2	84	42	6.0E-04	7.0E-04	6.3E-03
	3	98	40	7.3E-05	7.1E-04	7.0E-04
Calcite Sands	1	0	41	n/a	7.2E-04	n/a
	2	0	43	n/a	6.7E-04	n/a
	3	0	41	n/a	7.2E-04	n/a
Quartz-Calcite Mixture*	1a	5	40	1.1E-02	4.8E-04	1.1E-01
	1b	11	40	8.1E-03	4.7E-04	7.6E-02
	1c	60	35	2.1E-03	5.0E-04	1.5E-02
Granitic Sands	1	93	43	2.4E-04	6.6E-04	2.8E-03
	2	86	44	5.0E-04	6.5E-04	6.1E-03
	3	98	43	6.7E-05	6.7E-04	7.5E-04

*. Sand reused in successive experiments

**. Sample #3 reused as sample number #1a for experiments with Reused Sands .

2.6 Discussion

The results of the x-ray analyses demonstrate that framework silicates and calcite dominate the mineralogy of both the medium-sand fraction and fine-grained (silt/clay) sized fraction that coats the Kappelen sands, although significant proportions of sheet silicates are present in both materials. On the other hand, the results of the x-ray analyses suggest that the minerals frequently cited to explain bacteriophage adsorption, namely iron oxides and hydroxides, (Lukasic and others, 1999; Ryan and others 2002) are unlikely to be present on no more than 2% of total surface area investigated. Consequently, these minerals are not suspected to be responsible for the high levels of viral attenuation observed in the Kappelen sands.

Miscible extrusion test data for the various sand types investigated indicate that the Tryptone solution was capable of desorbing H40/1 from the sand types investigated. The total recovery of the H40/1 injected indicates that none of the minerals present in the Kappelen sands have caused viral inactivation due to adsorption over the three hour duration of the experiment. Consequently, all phages on mineral surfaces maintain their virulence over this period, despite being adsorbed.

Recoveries of H40/1 observed in the column effluent in tests using individual minerals, or using a subset of the minerals present in the Kappelen sands, provide an insight into the roles of various surfaces in the attenuation process. The high recoveries observed in experiments using quartz sand indicate that this mineral has a low H40/1 adsorption capacity. Similar responses were found by Schulze-Makuch and others (2002) in studies of the migration of the bacteriophage MS-2 through a quartz and feldspar sand, where the authors noted that quartz had a very low adsorption capacity for the negatively charged phage at slightly acidic pHs. In contrast, the authors found that the feldspar in the sand had a greater bacteriophage adsorption capacity. The high virus relative recoveries obtained using the granite sands in our experiments indicate that the additional minerals in this material, notably feldspars (over 51%, according to XRF analyses) and sheet silicates (13% - XRF data) did not have a H40/1 attenuation capacity significantly greater than quartz under ambient conditions.

In contrast to the silicate minerals, the absence of H40/1 in the effluent of columns filled with calcite suggest that this mineral is responsible for the high degrees of H40/1 attenuation observed in the Fresh Sands. However, the successively greater H40/1 relative recoveries and associated declining collision efficiencies in experiments using the Quartz-Calcite Mixture suggest that the attenuation capacity of the calcite is more limited than the results of the experiments carried out using Calcite Sands would initially suggest. The consistent increase in recovery occurs, despite rinsing of sands in de-ionised water at the end of each experiment, which should detach adsorbed phages from

zones of unfavourable attachment, due to reductions in ionic strength (Bales and others, 1991).

Figure 2.4: Relative Proportions of H40/1 Adsorbed on Column Matrix (Dark Grey) and Recovered in Column Effluent (White) for Experiments Using Natural Sands. (Figures represent percentages of H40/1 injected present in adsorbed and effluent fractions)

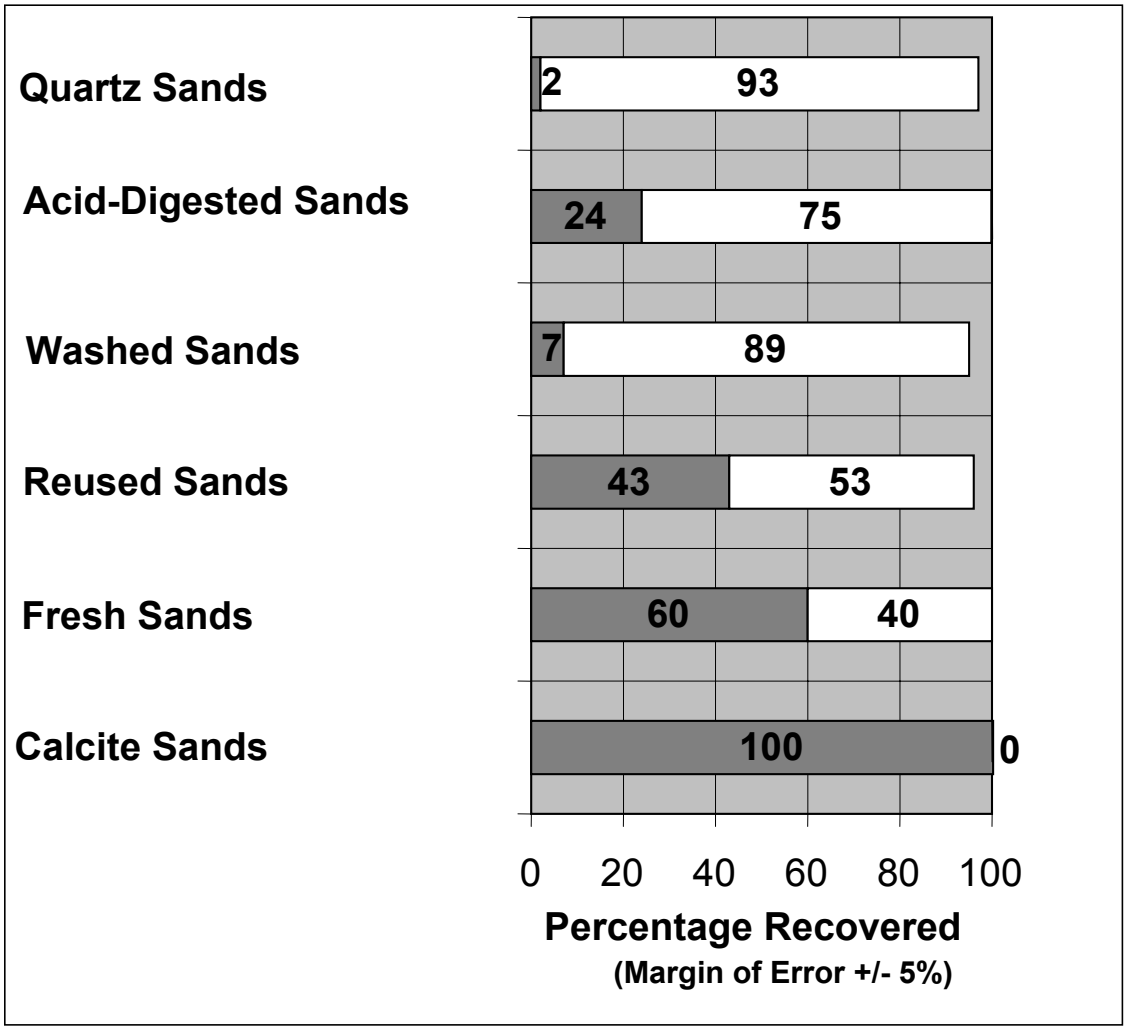

A comparable increase in relative recovery and decline in collision efficiency in successive experiments was also noted with the Reused Sands, suggesting that a similar process was operating. A consistent rise in recovery is often observed where deposition sites are limited and colloidal blocking occurs (Jin and others, 1997). However, the recovery observed in the final experiment with the Reused Sand is comparable to recoveries noted with the Washed Sands, which had not been exposed to H40/1 prior to experimentation. This suggests that blocking may not be responsible for the declining attenuation capacity of the Reused Sands with reuse. Indeed, were blocking responsible, a low recovery/high collision efficiency would be anticipated in the Washed Sands.

The fact that this is not observed suggests that the sand soaking/rinsing process is responsible for the decline in the Reused Sands H40/1 attenuation capacity.

The relative recoveries of the Washed Sands resemble those observed in Quartz Sands and Granitic Sands, despite their differing calcite contents. (A calcite content of 25% wt/wt in the Washed Sands was confirmed by XRD at the end of the experimentation program.) Indeed, recoveries obtained using Washed Sands, suggest that calcite has a negligible attenuation capacity under ambient experimental conditions.

The apparently contradictory results obtained from the column experiments using Washed Sands, compared to those of the Calcite Sands can be explained by considering conditions on the surfaces of the sand grains. Investigations made using scanning electron microscopy revealed that presence of fine-grained silt and clay sized particles on the surface of Fresh Sands and Calcite Sands. These fine-grained coatings were subsequently removed during either the acid digestion and/or washing processes. This conclusion corroborates with observations made while packing columns, where silt and clay sized material was removed in suspension. The silt/clay-sized coating on the surface of the Fresh Sand has similar bulk mineralogy to the sand itself. These observations, coupled with low H40/1 recoveries calculated from column experiment results using coated sands, and the very low organic matter contents, suggest that the coatings on the sand surfaces can adsorb H40/1 better than the uncoated sands, despite having equivalent mineralogies.

Elimelech and O'Melia (1990) demonstrated that protrusions on otherwise smooth grain surfaces can significantly reduce repulsive forces between colloidal particles and collector surfaces, under unfavourable deposition conditions. Similarly, Ross and Olivier (1964) noted that edge effects are one of the principal causes of charge heterogeneity that may reduce, if not reverse, the polarity of surface charge. Such conditions could permit the negatively charged bacteriophages to approach otherwise repulsive surfaces and permit adsorption, especially if the edges of the crystals should be differently charged or have a different surface charge density. Indeed, Jin and others (1997) explained the adsorption of ϕX174 to negatively charged quartz sand through the adsorption onto positively charged edges of medium grained quartz sand. Moreover, work by Bickmore and others (2002) using atomic force microscopy to showed that edge surface area may occupy up to 30% of the total surface area in a clay sized sample, thus reflecting the potential importance of crystal edges in fine-grained materials. Depending on the charges on the edges of the crystals and irregular grain surface due to coatings, significant difference in overall surface charge could be anticipated for a surface covered in a fine-grained material, relative to one covered by coarser material with the equivalent composition, but where a lower proportion of crystal edges are exposed.

The results of column experiments using Fresh Sands, and of experiments using Calcite Sands, suggest that the the fine-grained coatings on the sand surfaces reduce the overall repulsive charge of the surfaces of sand grains sufficiently to permit adsorption of negatively charged H40/1 particles to surfaces that would otherwise be repulsive. The removal of these coatings, by washing, results in less crystal edges present on grain surfaces thus making the surfaces smoother and more repulsive to approaching viruses, thereby reducing the degree of H40/1 adsorption. The net result of this change in surface conditions is that an increased recovery of H40/1 is observed in the column effluent.

A more quantitative indication of the influence of the coatings on H40/1 attenuation capacity can be obtained using a linear mixing model, such as that presented by Ryan and others (1999) which permits the fraction of attractive coverage on grain surfaces to be ascertained as follows:

$$f = \frac{\alpha_{app} - \alpha_o}{\alpha_{patch} - \alpha_o} \qquad (4)$$

where f is the fraction covered by favourable deposition sites, while α_{patch} and α_o are the collision efficiencies for the favourable and unfavourable deposition sites. α_{app} is the apparent collision efficiency determined from the column recovery. If the collision efficiency of favourable deposition sites is assumed to be unity, and the collision efficiency of the unfavourable deposition sites is determined from the Washed Sands, the fractions covered with favourable deposition sites on the Reused Sands are calculated as 3%, 2%, 1% and 0% for experiments #1,#2,#3 and #4 respectively. These data indicate that fraction of grain surfaces covered with favourable deposition sites in the Kappelen sands declines with reuse.

A similar phenomenon is apparent for the calcite sands where the fraction of the sand surface covered in favourable deposition sites declines from 10% to 1% between experiment #1 and experiment#3, according to Equation (4). In the case of both the Calcite Sands, and the Fresh Sands, SEM photographs suggest that the proportion of grains covered with coatings is greater than that calculated. This suggests that the assumption that the grain coatings have a collision efficiency of unity, may be an overestimation and that a lower α value may be more appropriate to express the influence of the crystal edges on H40/1 attenuation.

Textural effects are also believed to be responsible for the greater bacteriophage adsorption observed in Acid-digested Sands, compared to Washed Sands, despite the absence of silt/clay coatings on the sand surfaces. The results of column tests using the Washed Sands indicate that sand grains containing sheet silicates do not attract H40/1. However, the acid digestion process is believed to have removed calcium carbonate and possibly trace amounts (less than 0.1%) of organic matter, that may be present between the layers of sheet silicate minerals (Kübler, 1987), exposed on grain surfaces. Relative recovery data from Washed Sands indicate that neither calcium carbonate nor possible trace organic matter appear to have provided an

attractive deposition sites for the negatively charged hydrophilic bacteriophage such as H40/1. However, removal of these surfaces by acid digestion is suspected to have exposed a number of additional adsorption sites, which permit greater H40/1 adsorption to the column matrix and thus increasing the bacteriophage attenuation capacity of the Acid-digested Sand, relative to the Washed Sands. Consequently, the attenuation capacity of the acid digested sand is believed to be an artefact generated by the acid-digestion process, and is not applicable to attenuation mechanisms operating in the field.

The results of this study further highlight the influence of surface charge heterogeneities in colloid/virus transport noted by other authors (Elimelech and others, 1995; Ryan and Elimelech, 1996; Johnson and others, 1996 Jin and others, 1997;) by emphasising the importance of grain roughness/crystal edge effects on virus adsorption. Indeed, the results indicate that significant differences in the prediction of attenuation capacity in aquifers may arise by using idealized surfaces, including smooth mineral grains that may have the same mineralogy as the aquifer matrix, and that the collision efficiency of a system may also incorporate matrix textural aspects, should surface roughness/edge effects become important in particle deposition. Failure to consider such phenomena may partially explain discrepancies observed between field-based results and those observed in laboratory studies investigating bacteriophage migration, as observed by Schijven and Hassanizadeh (2000). Nonetheless, the importance of laboratory techniques has been demonstrated in this study, both in demonstrating the importance of grain texture in viral attenuation as well as showing that, despite the significant adsorption of H40/1 occurring on the Kappelen sands, the adsorbed bacteriophages retain their infective capacity over the duration of the experiment.

Chapter 3 : Virus Transport in a Fining-Upwards Sedimentary Sequence: Laboratory Experiments and Simulation

3.1 Abstract

A column containing four concentric layers of progressively finer-grained beads (Graded column) was used to model the transport of the bacteriophage T7 in groundwater flowing through a fining-upwards (FU) sedimentary structure. Deposition constants for T7 were determined for each bead size fraction, based on the results of column test packed with a single bead size (uniform columns). Conservative solute and bacteriophage tracer concentrations were modelled during these uniform column experiments using an analytical solution to the advection-dispersion equation. First order deposition was used to simulate bacteriophage attenuation. Resulting deposition constants for different flow velocities indicated that bacteriophage removal could be predicted by filtration theory. Solute and bacteriophage tracer responses in graded column experiments could not be reproduced with a single analytical solution. However, a flux-weighted summation of four one-dimensional advective-dispersive analytical terms could approximate solute breakthrough curves. Moreover, bacteriophage deposition terms, determined from filtration theory, reproduced the T7 breakthrough curve once bacteriophage desorption and inactivation on grain surfaces were incorporated. To evaluate the effect FU sequences on bacteriophage transport in more detail, T7 transport was simulated in sequences similar to those observed in fluvioglacial deposits sampled from a FU bed in a gravel pit, using the same analytical approach. Simulations used hydraulic conductivities determined from granulometric analyses of samples. Calculated breakthrough curve characteristics resemble those observed in field-based experiments. Comparisons with the results of simulations using averaged hydraulic conductivities show that simulations using averaged parameters overestimate mean virus travel times and underestimate recovered masses and peak virus concentrations.

3.2 Introduction

Groundwater is the principal source of drinking water in many parts of the world (van der Leeden and others, 1990). In order to better understand and protect the quality of this resource, an understanding of the processes controlling contaminant occurrence and migration is necessary. Microbiological contaminants (viruses, bacteria and protozoa) form an important category of pollutants that pose a significant threat to public health due to their occurrence in drinking water. Macler and Merkle (2000) indicate that a significant proportion of the 750,000 to 5.9 million cases of water-borne microbial illness that occur in the United States each year are associated with groundwater. The same authors note that, despite recent research, our understanding of how such contamination occurs in groundwater is far from complete and needs additional investigation. A critical aspect of microbiological contamination of groundwater relates to how micro organisms manage to reach water sources. Robertson and Edberg (1999) noted that many micro organisms have been shown to migrate considerable distances in various groundwater environments thus demonstrating that the problem of their occurrence in aquifers may not necessarily be restricted to the zone immediately surrounding water supply wells.

Comparative tracer testing provides a means of studying microbial transport in water by comparing microbial responses to those of a simultaneously injected conservative solute tracer. In recent years a large number of studies have investigated the transport and attenuation of microbes in this way. These studies have included investigations into transport and attenuation of the major microbial groups that pose significant threat to public health, including protozoa, e.g. Harter and others (2000), bacteria, e.g. Bolster and others(1999) and viruses, e.g. Redman and others (2001).

Investigations may be laboratory -based studies that can be carried out even down to the level of individual pores (e.g. Lawerence and Hendry, 1996). Laboratory-based studies have the benefit of permitting conditions to be closely controlled and the fundamental processes influencing micro organism transport and attenuation may thus be identified (Harvey and Garabedian, 1991).

At the other end of the investigation scale, field-based experiments allow in-situ studies of microbial transport and attenuation to be carried out, and the relative importance of mechanisms identified in the laboratory to be assessed in aquifers. Such studies have been carried out in a variety of deposits ranging from fine to medium sands (Schijven and others 1999) to very coarse montane alluvial gravels (Woessner and DeBorde, 1998).

Recent field-based comparative tracer tests carried out at the Kappelen porous medium test site (Kennedy and others, 2001a), Canton Bern, Switzerland have demonstrated striking differences in bacteriophage (bacterial virus) and solute tracer responses in a fluvioglacial sand and gravel aquifer (Figure 3.1). The

breakthrough curves in Figure 3.1 show that as the solute and bacteriophage tracers arrive at an observation well, the rising limb of the bacteriophage breakthrough curve follows that of the conservative solute before truncating and rapidly declining, while the solute concentration continues to rise. Following a steep decline a point of inflection on the bacteriophage breakthrough curve is reached, after which concentrations decline much more gradually. The net result of this process is that peak virus concentrations are observed earlier than peak solute concentrations. Furthermore, total bacteriophage recovery is less than that of the conservative solute tracer. Although laboratory-based uniform column studies using samples of the deposits collected from the site also demonstrated lower virus recoveries, the pattern of breakthrough was significantly different to that observed in the field. In the lab-based studies, bacteriophage and solute tracer breakthrough curves more strongly resembled one another, although phage peak concentration and recovery were lower.

The above example of a microbial/solute tracer investigation carried out at different scales that yield different relative responses has also been observed in other studies carried out at other sites (Harvey and Garabedian, 1991; Bales and others, 1995; Schijven and others, 2002). These differences are often attributed to heterogeneity.

From a geological perspective, the influence of heterogeneity on colloid transport can be compositional, due to variations in the surface composition, as shown for example in laboratory-based studies completed by Johnson and others (1996). However, heterogeneity may also be textural, due to differences in grain size, grain shape etc. (Ryan and Elimelech, 1996). Moreover, Sun and others (2001) demonstrated that the combined effect of compositional and textural heterogeneities can further complicate colloidal (and thus bacteriophage) migration in porous media.

Although the overall importance of aquifer heterogeneity has been widely recognised, its characterisation in hydrogeological investigations has proved more problematic. This is largely a result of the limited size of samples of aquifer material available for scrutiny during such studies. Anderson and others (1999) noted that less than 1% of a 9900m^3 sand and gravel aquifer would be directly investigated, were seventy 3.3m deep boreholes to be drilled. Moreover, associated hydrogeological investigative techniques, such as pumping tests, may investigate aquifers at scales that are appropriate for water resource investigations, but these scales are inadequate for studying contaminant transport (Aspiron and Aigner, 1999). For example, Essaid and others (1993) showed that fine details of aquifer heterogeneity, which could not be adequately characterised using such techniques, were crucial in reproducing the shape of a crude oil plume in computer simulations.

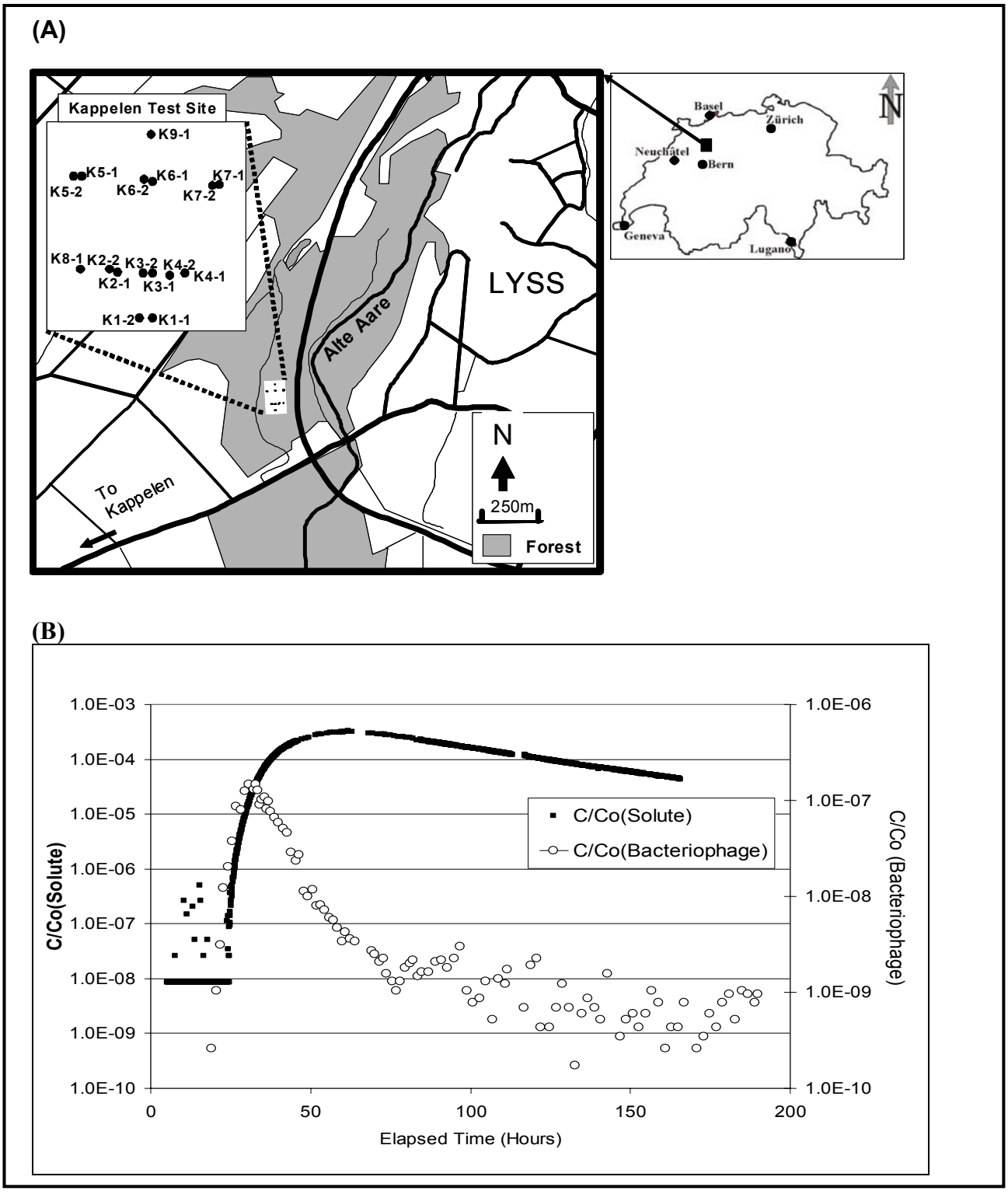

Figure 3.1: (A) Location map of Kappelen Test Site, Canton Bern, Switzerland with inlay showing monitoring well locations. (B) Solute/bacteriophage breakthrough curves at monitoring well K3-2 for tracer test completed July 2001. (Injection in K1-2.) (Note solute and particle curves plotted on different scales to highlight difference in tracer response.)

Geostatistical methods have been developed as a means of assessing variability in groundwater systems (Gelhar, 1993; LaBolle and others, 1996). In relatively homogeneous deposits, where abundant data are available, such techniques can be of considerable use. However, many geostatistical approaches assume that the spatial variability of the property of interest is small and that trends vary slowly (Wheatcroft and Taylor, 1988). In many hydrogeological systems, the spatial heterogeneity of many properties is high and varies rapidly. Consequently, the above geostatistical assumptions may not apply (Huggenberger and Aiger, 1999).

Under such conditions, alternative approaches, such as outcrop analogies of aquifer systems, may be more appropriate in advancing our understanding of the influence of heterogeneity in hydrogeological processes(Klingbeil and others, 1999; Bersezio and others, 1999). The principal of this approach involves developing an understanding of aquifer heterogeneity by using direct geological observations of similar deposits exposed at the ground surface. These observations may be coupled with geophysical methods such as seismic refraction or ground-penetrating radar to gain a fuller appreciation of the compositional and/or textural variations present in an aquifer (Huggenberger, 1993). Studies, such as those by Bersezio and others (1999) demonstrated that this technique can be combined with hydrogeological numerical modelling methods to be used to provide an indication of the influence of aquifer conditions on contaminant transport in strongly heterogeneous conditions. Nonetheless, the authors noted that although the simulations appeared to provide qualitatively convincing results, predictions made using such an approach would be far from confident. Such uncertainties are largely a result of a lack of data concerning the structure of the various sedimentary units in the aquifer and their inter-relationship.

Dreyer (1993) noted that sedimentary structures may be systematically characterised and quantified into a hierarchy. Huggenberger and Aiger (1999) suggested the approach should be applied to aquifers using a classification that regards subdivisions as both genetic sedimentological units and hydrostratigraphic units, as follows:

- Giga-scale features: e.g. hydrostratigraphy related to an entire basin.
- Mega-scale features: e.g. facies associations related to a depositional systems.
- Macro-scale features: e.g features related to facies dynamics
- Meso-scale structures: e.g.sedimentary structures related to sediment dynamics.
- Microscale differences: e.g. pore-scale features.

Field-based microbiological contaminant transport studies are typically carried out at the scale of metres to 10s of metres (e.g. Bales and others, 1995). This scale corresponds to that of many exposures where macro-scale architectural

elements may also be characterised. In contrast, laboratory based studies tend to focus on homogeneous media and pore scale processes (Lawrence and Hendry, 1996). To date investigations have tended to focus on the laboratory scale or the field scale, while studies incorporating a range of scales remain rare (e.g. Ryan and others 2002). Moreover, studies at these scales often neglect features which may occur on an intermediate scale, e.g. the meso scale. Indeed, this lack of continuum is believed to be responsible, at least to some degree, for the discrepancies in solute/particle relative response between investigations carried out at the laboratory and field scales, which have been explained to date as a result of “heterogeneity”.

This study aimed to investigate microbial tracer response relative to a conservative solute in a simulated meso-scale feature, namely a fining-upwards sedimentary sequence, i.e. a structure within a bed whose grain size varies gradually from coarse material at its base to finer material at the top. Such structures may occur in many sedimentary environments, including alluvial deposits, where they may develop at various stages of a rivers maturity (Reading, 1986). The investigation of virus transport through a fining-upward sequence involved two phases. An experimental phase consisted of laboratory-scale investigations of the transport of a mixture of bacteriophage and conservative solute tracers injected into columns. Glass beads were employed as the porous medium for the investigations to avoid complications that may be associated with edge effects / grain angularity (Ryan and Elimelech, 1996).

The columns were packed either with a single bead size or with four internally uniform concentric cylinders of beads that became progressively finer moving toward the centre of the column (Graded Column). This later structure was used to approximate the flow regime in a bed with depth-dependant grain size distribution. The second phase of this study involved simulation of the tracer breakthrough patterns observed during the experimentation phase. Granulometric analyses of samples collected from a natural fining-upwards sequence allowed the hydraulic characteristics within the bed containing the sequence to be investigated. These data were used to simulate virus and solute flow and transport using an analogous approach to that used for the laboratory experimental data. The data generated by these simulations were compared to solute and virus breakthrough patterns observed in the field.

3.3 Materials and Methods

3.3.1 Glass beads

All column experiments used spherical soda lime glass beads (Potters Industries, Germany) as the porous matrix for column experiments. The experiments investigated the attenuation capacity of four different bead sizes measuring 63μm, 125μm, 250 μm and 500 μm in diameter. In order to remove impurities from the glass surface before starting the experiments, the beads were

soaked in 0.1N NaOH for 45 min, before rinsing in deionionised water and soaking in 1N HNO_3 for 45min. This process was followed by thoroughly rinsing the beads in deionised water and drying at 60 degrees centigrade (°C). Furthermore, in order to minimise potential cross contamination between experiments, the beads were placed in a sieve with a finer mesh size than their diameter and thoroughly washed in deionised water prior to drying for 20 hours at 60 ° C following each experiment.

3.3.2 Synthetic Freshwater/Solute Tracer

A synthetic freshwater consisting of precise quantities of selected salts dissolved in Nanopure© (Barnsted, Van Nuys, USA) water was prepared according to Moore and others (1982). Two mL per litre of 0.1M Potassium hydrogenophtalate ($C_8H_5KO_4$) (Merck) buffer was added to the water and the pH of the system adjusted to 4.6 with 1N HCl. This pH was necessary to enable bacteriophages to stick to the surfaces of the glass beads.

The resulting synthetic freshwater acted as the tracer solvent/suspending liquid and flush water for the column experiments. A 100ppb solution of Uranine (sodium fluorescene. Fluka, Buchs, Switzerland) acted as the solute tracer. Käss (1997) summarised studies indicating that although Uranine is pH sensitive and degrades in strong light, it undergoes little to no interaction with inorganic materials and was thus assumed to act conservatively during the column tests.

3.3.3 Bacteriophage Tracer:

Bacteriophages (phages) are non-pathogenic colloidal sized particles that infect specific species of bacteria. The phage T7 acted as the microbial tracer for all column test experiments. T7's capsid (head) measures 17nm in diameter while its tail is 43nm long. This phage belongs to the *Podoviridae* family (morphotype C1). T7 is hosted by the bacterium *Escherichia coli B*. Zeta potential measurements made using a Zeta Master (Malvern Instruments, Malvern, UK), within the framework of this study, showed that T7 has a zeta-potential in synthetic freshwater at pH 6.2 of between –8 and –16mV. Measurements made at pH 8.5 determined the phages zeta potential to be –29mV. Similarly, hydrophobicity measurements made using a contact angle microscope showed this phage type to be hydrophobic (Contact angle: 89 to 92 degrees).

Prior to starting the experiments, T7 production was carried out on Petri dishes using Luvia Bertani agar (LB) with a double agar layer technique. The confluent lysis on the surface of the double agar layer of the petri dishes plates was scraped, mixed in a small volume of saline buffer (0.9g/l NaCl) and centrifuged (15min, 12,000g) to remove bacterial cells and agar debris. The supernatant acted as the virus stock (source concentrate) and was stored at 4°C to minimize viral inactivation (loss of virulence) throughout the whole set of experiments.

Mixing of the phage/Uranine mixture and subsequent sampling and enumeration followed the procedure described in the methodology section of Chapter 2.

3.3.4 Column Experiment Procedure.

Two types of column experiment were carried out in order to characterise phage transport in a sedimentary structure. Experiments investigating phage transport through a uniform matrix using a single bead size employed a 25cm long, 1.9cm internal diameter borosilicate glass column (uniform column). An additional series of experiments investigated flow in a concentrically layered column system where multiple grain sizes were used. These later experiments employed a 30cm long, 5.4cm internal diameter perspex column (graded column). In experiments using a single bead size (ϕ=500μm, 250μm, 125μm or 63 μm), the column packing procedure followed that described in Chapter 2.

An analogous packing procedure to that employed for the uniform column studies was followed for the graded column experiments. The four grain-size fractions, used in the uniform column experiments, were emplaced into separate thin-walled (ca 0.2 mm thick) hollow cylinders, set concentrically around one another and resting on a 1cm-thick filter layer of uniform 500μm diameter beads (Figure 3.2). This graded column system set the finest size fraction in the centre of the column, while progressively coarser fractions were placed further towards the column walls. The column was packed in this manner to reproduce a progressively finer-grained structure. The cylinder diameters were arranged in such a way that the cross-sectional area of each grain size fraction in the column was equal. Once the cylinders were packed, the thin cylinder walls were slowly withdrawn from the column. Upon complete withdrawal, an additional 2cm layer of uniform 500μm diameter beads were place on top of the column, prior to sealing the saturated fully-packed column.
Subsequent tracer testing followed the procedure described in Chapter 2 using the same solute and phage sampling apparatus. Figure 3.2 summarises details of the experimental setup and design. Both graded column experiments and uniform column experiments for each grain size fraction were repeated at least twice to provide an indication of the variation in results between experiments due to packing. Following the graded column tests, the various grain size fractions used were separated by wet sieving using standard sieve sizes (DIN. ISO 3310/1), and washing with de-ionised water. The separated fractions were dried at 60°C for 24 hours prior to re-use.

Three pore volumes of solute/phage tracer were injected during uniform column experiments. This approach permitted the principal virus attenuation characteristics to be investigated. The prolonged injection of a constant tracer concentration allowed determination of whether there were a limited number of deposition sites in the column matrix. Were this the case, a gradual rise in phage

concentration would be observed in the column effluent, relative to the solute tracer concentrations. The experiments were carried out at constant flow rates of approximately 4.2mL/min and 1.6mL/min for the three coarsest grain size fractions in order to evaluate the influence of variable flow velocity on T7s attenuation. Experiments in the finest grain-size fraction were only carried out at the lower flow rate since it was feared that the higher flow rate might generate excessive hydraulic gradients resulting in a rupturing of the deposits and the development of preferential flow paths.

Since one of the principal objectives of experiments using the graded column was to attempt to reproduce conditions observed at the field scale, a short pulse, resembling field-based injection conditions (approximately 0.3 pore volumes,) was injected during graded column experiments. Kretzschmar and others (1997) note that short pulse experiments of this type provide an excellent agreement with step pulse experiments, where more than one pore volume is injected, once first order deposition is the dominant attenuation process.

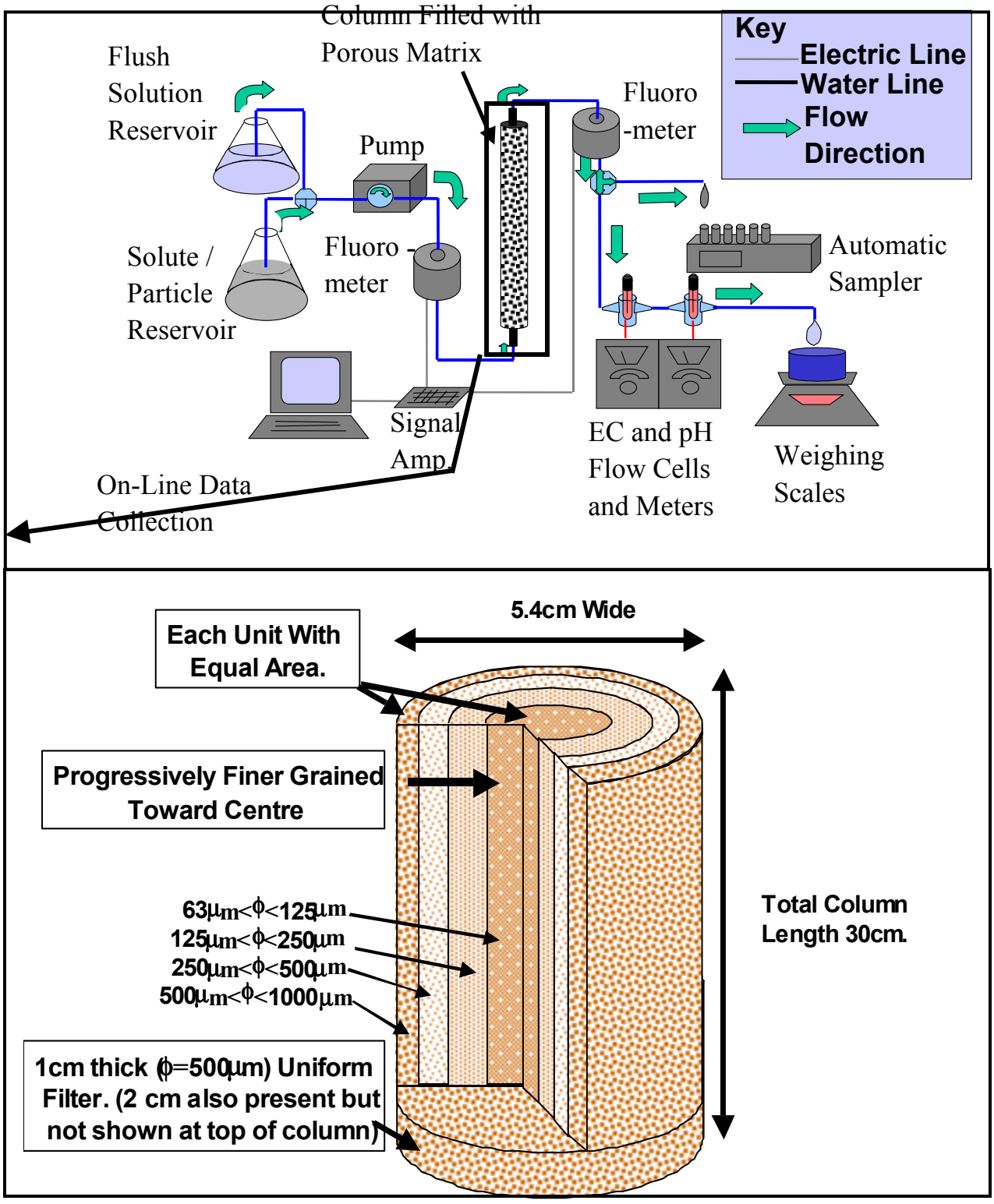

Figure 3.2 : Schematic illustration of column apparatus used during bacteriophage tracer test. Experiments with detail of Graded Column Apparatus. Column used for experiments with single bead size: 25 cm long x 1.9cm in diameter.

3.3.5. Natural Granular Media.

In order to evaluate grain size and subsequent hydraulic conductivity variation in a sedimentary structure, samples were collected from a bed containing a fining-upward sequence of sand and gravel for granulometric analysis. The sampling location was a recently exposed face in the Walperswil fluvioglacial gravel pit (Walperswil, Canton Bern, Switzerland-Figure 3.3a), approximately five km northwest of the Kappelen Test Site. Discrete samples were taken from freshly excavated deposits in 2cm to 5cm thick intervals ranging from the erosive base of the bed to the top of the ca. 30-35cm thick fining-upward sequence. Clean stainless steel plates set above and below each sample interval isolated the deposits to be excavated from adjacent samples, while preventing finer-grain sized fractions from being lost during sampling. In this way a total of 21 samples were collected from three different sections in the bed. All three sections were located within one metre of one another.

Visual examination of field samples revealed them to be dominated by subrounded to well rounded gravel with a subordinate proportion of sand, which became more predominant toward the top of the bed. Furthermore, field-based inspection indicated that carbonates and framework silicates (quartz and feldspars) dominated sample mineralogy.

The sand and gravel samples were subdivided into differing grain size fractions by agitated wet sieving using standard sieve sizes (DIN. ISO 3310/1) and subsequently oven dried at 40 degrees C overnight, before weighing. Figure 3.3b presents the grading curves for six samples collected from one of the sections.

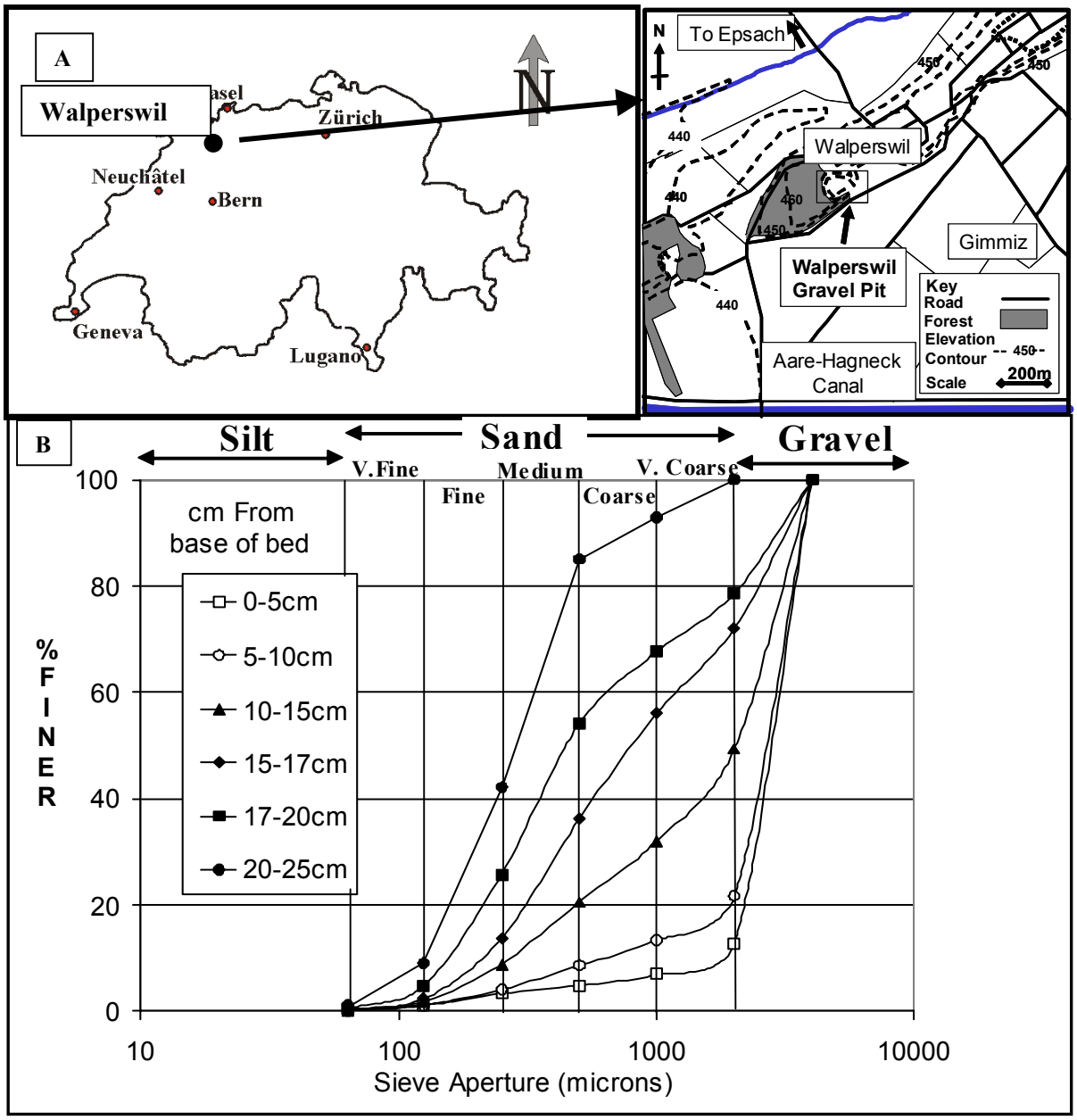

Figure 3.3: (A) Sampling location map for Walperswil gravels. (B) Representative grain size distribution curves for samples collected from a section through a fining-upward sequence.

3.4 Data Analyses

3.4.1 Column Test Analyses.

Virus transport characteristics were evaluated using the advection-dispersion equation, coupled to kinetic parameters derived from classical filtration theory. The fundamental equations governing the transport processes are given

in Bolster and others (1999). These equations have been modified to account for viral inactivation on solid surfaces and suspended in liquid as follows:

$$\frac{\partial C}{\partial t} + \frac{\rho_b}{\theta}\frac{\partial S}{\partial t} + = D_L \frac{\partial^2 C}{\partial x^2} - v\frac{\partial C}{\partial x} - \mu_l C - \mu_s \frac{\rho_b}{\theta} S \quad (3.1)$$

$$\frac{\rho_b}{\theta}\frac{\partial S}{\partial t} = k_c C - k_d \frac{\rho_b}{\theta} S - \mu_s \frac{\rho_b}{\theta} S \quad (3.2)$$

where C is the concentration of T7 in the liquid (M/L^3); S is the adsorbed phage concentration (M/L^3); t is time (T); x is distance from the injection point (L); D_L is the (longitudinal) dispersion (L^2/T); v is the advective water velocity (L/T); ρ_b is the dry bulk density (M/L^3); θ is the porosity (-); $\mu_s$and μ_l are inactivation rates of T7 adsorbed onto solid surfaces and in liquid(1/T); k_d is the detachment rate constant (1/T) and k_c is the deposition constant. Equations (1) and (2) are solved in Laplace space using the procedure provided in the Appendix at the end of the thesis.

According to filtration theory, k_c may be determined as follows (Tien and Payatakes, 1979):

$$k_c = \frac{3(1-\theta)}{2d_c}\eta\alpha v \quad (3.3)$$

where d_c is the matrix diameter, α is the collision efficiency and η is the single collector efficiency. Yao and others (1971) define the collision efficiency as the probability of attachment resulting from a collision between a particle and a solid surface. Kretzschmar and others (1999) note that α reflects the attractive properties resulting from solution and surface chemistry.

In contrast, the single collector efficiency is dependant on physical parameters of the system including surface area accessible for deposition, pore structure, flow velocity, particle density and particle size. Given T7s small size, η can be calculated using Penrod and others (1996) modification of Rajagopalan and Tien's (1976) equation:

$$\eta = 4A_s^{\frac{1}{3}} N_{Pe}^{-\frac{2}{3}} \quad (3.4)$$

where

$$A_s = \frac{2(1-\gamma^5)}{(2-3\gamma+3\gamma^5-2\gamma^6)}, \gamma = (1-\theta)^{\frac{1}{3}} \quad (3.5)$$

$$N_{Pe} = \frac{3\pi\mu d_p d_c q}{kT} \quad (3.6)$$

where d_p is the particle diameter (1.7×10^{-8}m); μ is the fluid viscosity (9.3×10^{-4} Pas^{-1}); q is the specific discharge (m/s); k is the Boltzman constant(1.38048×10^{-23} J/K); T is the temperature (297 K).

In both uniform and graded column experiments, T7s transport characteristics were determined using the solution of Equation (1) and Equation

(2) for a short injection pulse. Maximum and minimum deposition rate constants were determined for each grain size with uniform column data by visually fitting breakthrough curves to the experimental data to provide an upper and lower limit to the potential best fit value. Best-fit deposition constants for each size fraction were then established by determining the minimum of the residuals between observed and simulated concentrations using least-squares method. By applying values of η calculated from the filtration theory, based on known porosities and matrix diameters, and using the values of k_c for T7 derived from the solution to Equations (3.1) and (3.2), α could be calculated using Equation (3.3). This parameter could then be used with hydrodynamic data and grain diameter/porosity data to determine phage deposition constants under differing flow regimes in the graded column experiments.

A numerical solute transport model suggested that little lateral exchange occurs over short distances in the graded system. Consequently it was assumed reasonable to simulate the mass transport regime in the graded column by the superimposition of four one-dimensional analytical terms, using the approach derived by Maloszewski (1992). Advective velocity and dispersion were determined by fitting the Uranine breakthrough curve using the solution equation (3.1), ensuring that the total simulated outflow corresponded to that observed during the experiment. Using the calculated α values, deposition constants could be calculated for each layer in the graded column using Equation (3.3) and Equation (3.4) while accounting for different flow velocities, determined from the Uranine breakthrough curve. Overall bacteriophage breakthrough curves could thus be reconstructed using the flux-weighted average of the four analytical solutions.

3.4.2 Analytical Model – Gravel Deposits.

The hydraulic conductivity of the various intervals sampled in the Walperswil gravels were estimated using the Kozeny-Carman equation (Bear, 1972) with a 5% variation in porosity around a typical value of 30% for gravels (Freeze and Cherry, 1979). The equation relates hydraulic conductivity to grain size as follows:

$$K = (\frac{\rho_f g}{\mu})(\frac{\theta^3}{(1-\theta)^2})(\frac{d_{10}}{180}) \qquad (7)$$

where d_{10} is the finest 10% retained during sieving, and is regarded as the representative grain diameter in controlling hydraulic conductivity. Martin and others (1996) demonstrated that the d_{10} diameter is also most appropriate for describing micro organism transport in porous media. Hydraulic conductivites calculated using equation (7) were plotted with distance from the base of the bed and fitted to a best-fit function to determine magnitude of hydraulic conductivity variation with depth in the fining-upward sequence.

Based on the results of the granulometric analyses, solute and particle transport were simulated through a bed with a similar hydraulic conductivity

profile, i.e. hydraulic conductivity varying over a similar magnitude within a 50cm thick bed. The bed was discretised into eight 6.25-cm thick unimodal grain-size units of uniform hydraulic conductivity, and a uniform hydraulic gradient applied across a 50cm length of the bed. Simulations proceeded in an analogous manner to those in the graded column experiments, i.e. by using the analytical equation summation for simulating breakthrough curves. Deposition constants were calculated using Equation (3) and Equation (4) assuming uniform collision efficiency for the entire sequence. Detachment and inactivation constants were kept at approximately the same ratio as those used in reproducing the graded column breakthrough curves. Dispersion was calculated assuming a constant dispersivity of 1.25 cm.

Simulations were carried out for two different beds with coarser and finer grain sizes to investigate the effect of grain-size on phage breakthrough (ϕ=10mm to ϕ=1.33mm and ϕ=1mm to ϕ=0.133mm respectively). The resulting hydraulic conductivities varied over the same order of magnitude as those observed at the Walperswil Gravel samples. The hydraulic gradient was adjusted in each case to ensure equal flow velocities across both beds.

Collision efficiencies were 0.3 for the coarser grained bed. Preliminary simulations in the fine-grained bed, using α=0.3, demonstrated that over 99.9% of viruses recovered were derived from the coarsest grained bed. Consequently a lower collision efficiency of α=0.1 was selected for this sequence.

The results of these simulations were compared with solute and phage breakthrough curves obtained when averaged grain sizes and hydraulic conductivities were used instead of the coarse-grained fining-upward sequence, assuming equal collision efficiencies.

3.5 Results

3.5.1 Uniform Column Tests.

Figure 3.4 presents representative breakthrough curves for Uranine and T7 obtained from the uniform column tests for each bead size. In each size fraction, substantial attenuation of T7 occurred, with the smallest sized bead having the lowest recovery. In all experiments, T7 concentrations reached a plateau suggesting that deposition sites were not a limiting factor in the attenuation process. Significant tailing in the column injection signal prevented accurate assessment of T7 release constants with the analytical approach employed. This is a result of dispersion associated with a difference in diameter between the injection line and the on-line fluorometer measurement cell , resulting in irregular mixing in the cell, rather than pure piston flow. Despite this complication, the data permit deposition constants to be calculated, if the detachment term is assumed negligible in comparison to the adsorption term.

Experiment	Diameter (μm)	Flow Rate (mL/min)	Dispersion (m^2/day)	Velocity (m/day)	k_c (1/day)	Collision Efficiency (α) (-)	Effective Porosity (-)
500μm#1	500μm	4.4	0.08	60	235	4.1e-2	0.37
500μm#2	500μm	1.6	0.04	21	173	4.7e-2	0.39
500μm#3	500μm	1.6	0.04	21	152	4.1e-2	0.39
500μm#4	500μm	4.15	0.08	55	238	4.5e-2	0.38
250μm#1	250μm	4.12	0.1	60	210	1.0e-2	0.35
250μm#2	250μm	4.45	0.1	60	243	1.4e-2	0.38
250μm#3	250μm	1.6	0.05	21	162	1.4e-2	0.39
125μm#1	125μm	4.4	0.1	60	282	4.9e-3	0.37
125μm#2	125μm	1.6	0.07	23	240	5.1e-3	0.35
63μm#1	63μm	1.56	0.06	24	218	1.3e-3	0.33
63μm#2	63μm	1.61	0.08	22	185	1.4e-3	0.37

Table 3.1: Model parameters used to simulate results of single bead size uniform column experiments.

It is noteworthy that the range of deposition constants varied within each grain size fraction. However, once differences in flow velocity and specific flux were accounted for with Equation (3) through to Equation (6), calculated collision efficiencies for different discharge rates fall into the same range (Table 3.1). This result indicates that the filtration theory is an appropriate means of evaluating T7 deposition constants at different discharge rates in the various media investigated (Table 3.1).

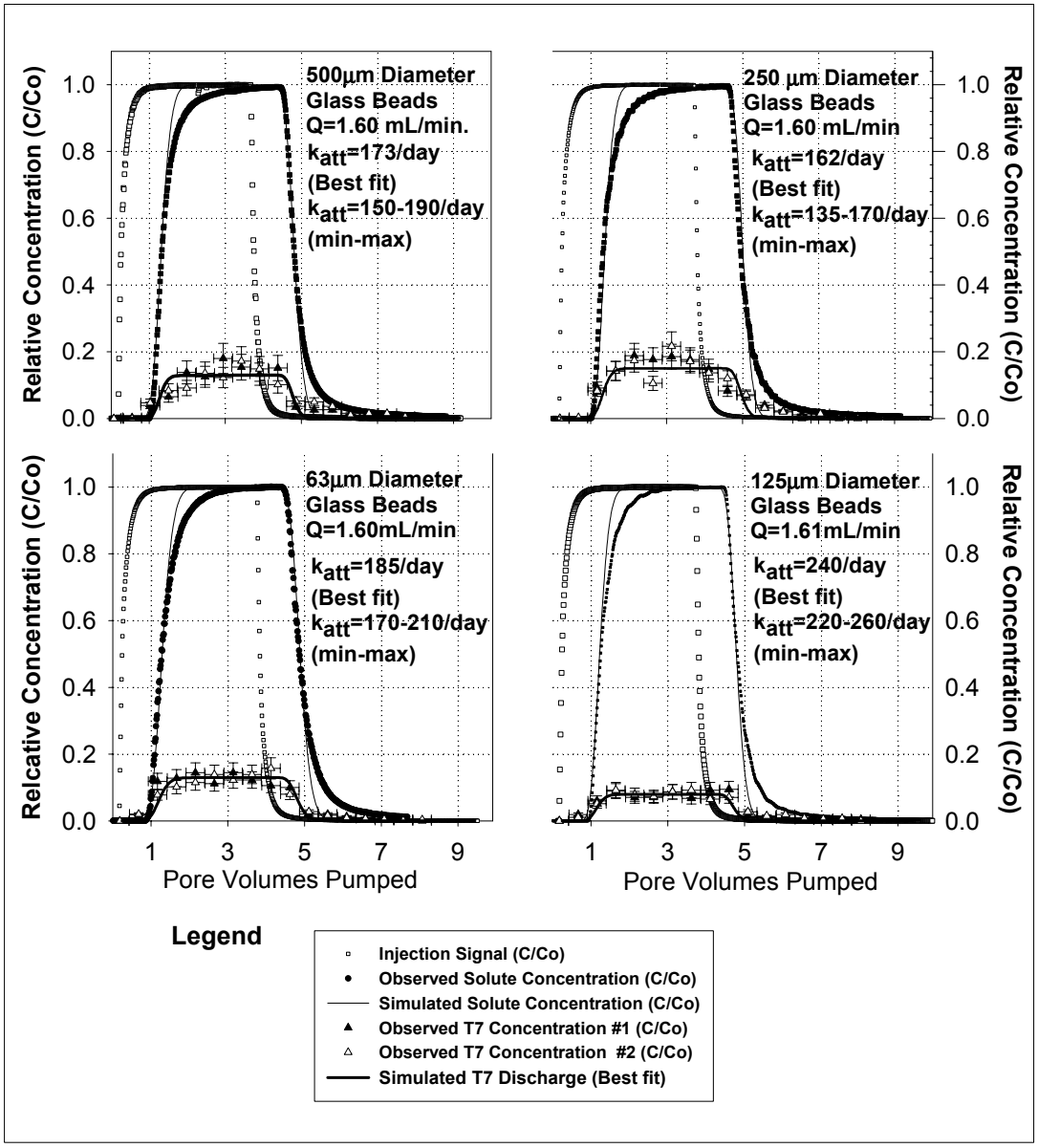

Figure 3.4: Representative breakthrough curves for the four bead sizes investigated. Observed relative concentrations represented as points and simulated breakthrough curves represented as lines. Temporal resolution of T7 data is +/- 0.2 pore volumes. Bacteriophage relative concentration error bars +/- 25% of observed concentration.

3.5.2 Graded Column Tests: Experimental Data

Figure 3.5 presents the results Graded Column Test #2, along with mathematical model simulation results. The results are representative of all three graded column experiments and reflect the significant differences in T7 and

Uranine breakthrough curves. It is nonetheless worth noting that the irregular oscillations in Uranine concentration observed at low concentrations in the later part of the curve vary from one experiment to another and are believed to be associated with irregularities due to column packing.

Both T7 and Uranine breakthrough curves differ from those generated, using uniform single grain size columns, in that both breakthrough curves are considerably more skewed to the left and display significant tailing, despite almost perfect short pulse injection signals. However, even though Uranine and T7 first arrivals and peak concentrations correspond in the graded column tests within the margins of error, peak T7 concentrations are substantially lower than those of the solute. Moreover, the Uranine and T7 tailing parts of respective breakthrough curves differ in their characteristics. That of the bacteriophage curve tends to decline more rapidly before flattening out and declining more slowly than that of the Uranine. These phenomena bear stronger resemblance to breakthrough curves observed in field-based experiments (Figure 3.1) than to those observed laboratory-based homogeneous columns tests.

Using these data the Uranine breakthrough curve can be reproduced with four flux-weighted superimposed analytical solutions, with a total discharge equivalent to that observed (Figure 3.5). Moreover, by using the resulting velocity values, T7s kinetic deposition parameters could be determined for each layer in the graded column based on collision efficiencies determined from uniform column experiments using equations (3) and (4) (Table 3.2).

The resulting parameters permitted T7 breakthrough curves to be generated for all three graded bed simulations. The results of Graded Column test #2, presented in Figure 3.5, demonstrate that the calculated first order deposition parameters provide an excellent fit to the phage breakthrough curve up to approximately three pore volumes, incorporating over 99% of the mass recovered. Nonetheless, despite the fact that adsorption alone could reproduce the curve peak that incorporates most of the mass of phages recovered during the experiment, first order deposition alone was incapable of reproducing the tailing observed. A desorption term was thus necessary. Application of this term improved the correspondence between the observed and simulated curves in the tailing section. However, simple adsorption/desorption alone could not reproduce the sloping tail observed in T7s breakthrough curves following the point of inflection. This gentle sloping phenomenon is attributed to viral inactivation. Since source reservoir concentrations indicated that the rate of T7 inactivation in the liquid was not significant over the duration of any of the experiments, T7 inactivation on the column matrix was concluded to be responsible for the gradual decline in the concentration desorbing bacteriophages. In order to simulate this phenomenon, the rate of desorption was increased and a concomitant inactivation rate on the surface applied using the model. The results of these simulations are also presented in Figure 3.5.

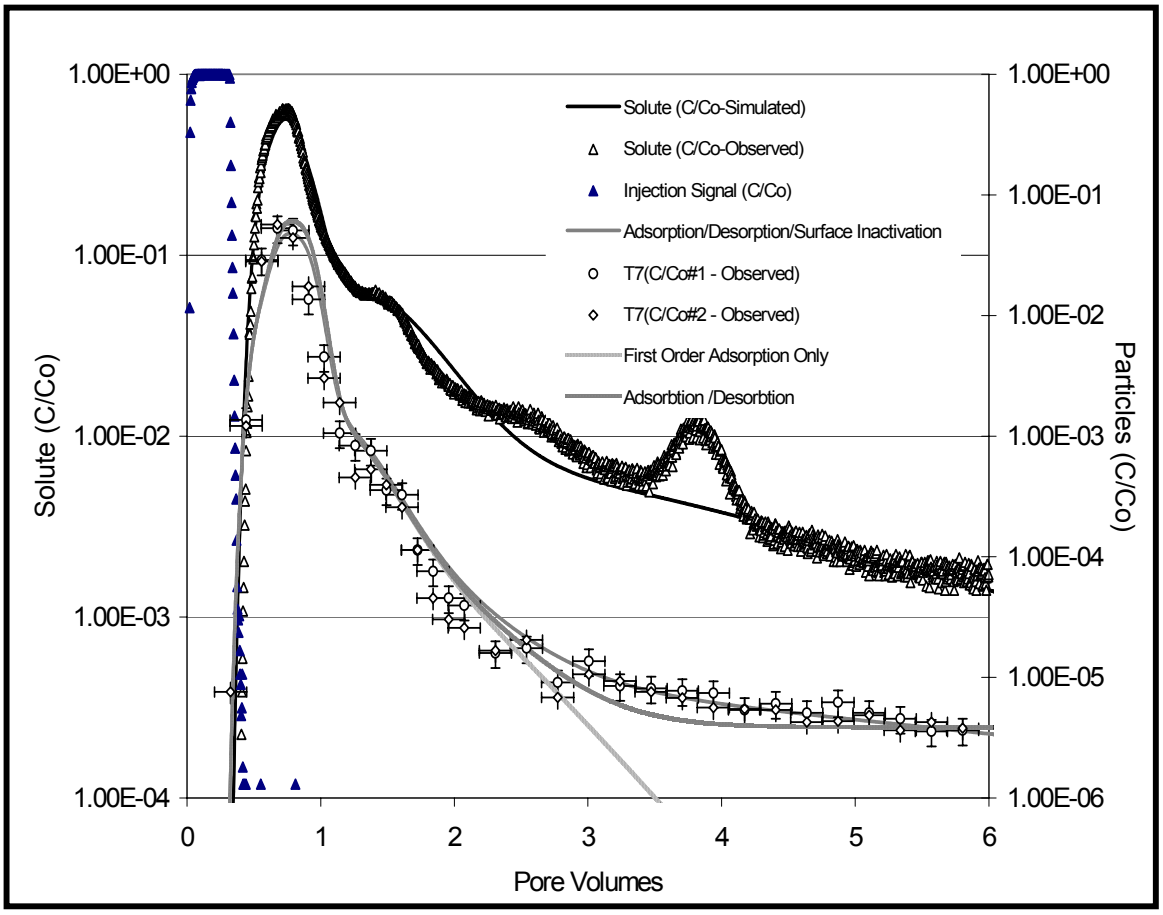

Figure 3.5: Logarithmic plot of observed and simulated Uranine and T7 breakthrough curves for Graded Column Experiment #2. The figure also presents the results of modelling scenarios with first order adsorption and first order adsorption/desorption being considered without surface inactivation of T7.

3.5.3 Natural Gravels – Granulometry and Transport Simulations

The results of granulometric analyses, such as those presented in Figure 3.3, have been used to ascertain the hydraulic conductivity variation with depth in the fining upwards sequence sampled at Walperswil. Figure 3.6 presents the results of the hydraulic conductivity calculations based these granulometric analyses. The data show a statistically significant log-linear variation in hydraulic conductivity from the base of the bed to the top, with values at the top of the bed being approximately an order of magnitude lower than those found at the base. For the 50cm thick bed under consideration in the simulations, hydraulic conductivity was assumed to vary by a similar magnitude between the base and the top of the simulated fining up-ward sequence. The parameters used in these simulations are presented in Table 3.3.

Figure 3.7a and Figure 3.7b presents the results of solute and particle simulations in the fining-upward sequence for both coarser grained and finer

grained beds, assuming equal flow velocities. It is noteworthy that although the solute profiles for both beds are equal, peak particle concentrations and resulting recoveries are significantly lower in the finer-grained unit. Moreover, a significant difference in peak concentration times is apparent between conservative and bacteriophage tracers in the later case. The relative contributions of each subunit in both coarse grained and fine-grained sequences presented in Table 3. The results demonstrate that a much greater relative contribution is made by particles in the coarsest bed of the fine-gained sequence, relative to that in the coarser sequence.

Figure 3.7 and Table 3.3 also present the results of solute and particle simulations assuming averaged hydraulic conductivity and grain size for the coarse-grained bed. Peak solute and particle concentrations in the discretised heterogeneous bed and the averaged simulation differ significantly. The averaged systems peak arrival time is significantly later than that of the heterogeneous system. Moreover, particle peak concentrations are significantly lower in the averaged system. Furthermore, additional simulations have shown that the difference between averaged and discretised simulations increases with increasing contrast in grain size between the base and the top of the bed.

3.6 Discussion

The results of the experiments carried out using uniformly sized beads demonstrate that the all bead sizes have a significant capacity to attenuate T7 under the ambient experimental conditions. Moreover, the similarity of the values for the collision efficiencies, determined at different flow rates using the uniform column test data, suggests that Tien and Payatakes (1979) approach to calculating deposition constants is appropriate for phage filtration. This approach has allowed deposition constants for T7 to be determined for the various layers in the graded column experiments using advective velocity data derived from Uranine breakthrough curves. These constants have successfully permitted T7 concentration peak responses in all graded column experiments to be simulated. However, additional terms simulating desorption and viral inactivation on bead surfaces needed to be incorporated to account for the tailing observed after the T7 peak had passed.

Experimental solute and particle breakthrough curves generated with the graded columns differ substantially from those generated using data from the uniform column experiments. It is noteworthy that analysis of these curves using conventional mass transport solutions is unable to reproduce the breakthrough curves observed with a single advective velocity and dispersion term. This suggests that the distribution of hydraulic conductivities in many aquifers is more complex than often assumed and needs to be accounted for by phenomena such as the internal structure of individual beds.

Experiment	Grain Diameter (μm)	Flow Rate x 1000 (m^3/day)	Advective Velocity (m/day)	Dispersion (m2/day)	Effective Porosity (-)	k_c (1/day)
Graded	500μm	2.117	18.7	0.043	0.19*	537
Bed#1	250μm	3.175	14.4	0.086	0.44	81
k_d=0.008/day	125μm	2.016	8.6	0.086	0.39	130
μ_s=1.0/day	63μm	8.338	3.6	0.086	0.39	84
Graded	500μm	3.110	18.7	0.043	0.26	280
Bed#2	250μm	3.326	14.4	0.050	0.38	104
k_d=0.04/day	125μm	1.786	7.5	0.100	0.40	123
μ_s=9.0/day	63μm	0.634	2.7	0.120	0.40	79
Graded	500μm	3.701	16.0	0.043	0.39	158
Bed#3	250μm	2.736	12.0	0.086	0.39	100
k_d=0.03/day	125μm	1.390	6.0	0.100	0.39	121
μ_s=6.0/day	63μm	0.734	3.2	0.110	0.39	86

Table 3.2: Model parameters used to simulate results of graded bed column experiments

Grain Diameter (μm)	Advective Velocity (m/day)	Dispersion (m^2/day)	Proportion of Solute Recovery	Proportion of Particle Recovery	k_c (1/day)	k_d (1/day)	μ_s (1/day)
Coarse-grained fining-upwards sequence α=0.3.							
10000	34.6	0.432	44.0	68.0	21	0.003	3.0
7499	19.4	0.243	24.8	25.7	27	0.003	3.0
5623	10.9	0.137	13.9	5.8	37	0.003	3.0
4217	6.1	0.077	7.8	0.4	49	0.003	3.0
3162	3.5	0.043	4.4	<0.1	65	0.003	3.0
2371	1.9	0.024	2.5	<0.1	87	0.003	3.0
1778	1.1	0.014	1.4	<0.1	116	0.003	3.0
1334	0.6	0.008	0.8	<0.1	154	0.003	3.0
Peak Solute Conc: 39% at 0.37 Pore Volumes (PV), Peak Particle Conc: 32% at 0.37 PV							
Averaged Value Simulation							
4498	9.8	0.122	100.0	1.0	38.7	0.003	3.0
Peak Solute Conc: 31% at 1.0 Pore Volumes (PV), Peak Particle Conc: 0.5% at 0.96 PV							
Fine-grained fining-upwards sequence α=0.1							
1000	34.6	0.432	44.0	99.5	318	0.03	3.0
750	19.4	0.243	24.8	0.5	425	0.03	3.0
562	10.9	0.137	13.9	<0.1	566	0.03	3.0
422	6.1	0.077	7.8	<0.1	755	0.03	3.0
316	3.5	0.043	4.4	<0.1	467	0.03	3.0
237	1.9	0.024	2.5	<0.1	1342	0.03	3.0
178	1.1	0.014	1.4	<0.1	1790	0.03	3.0
133	0.6	0.008	0.8	<0.1	2387	0.03	3.0
Peak Solute Conc: 39% at 0.37 Pore Volumes (PV), Peak Particle Conc: 0.7% at 0.33 PV							

Table 3.3: Model inputs and relative proportions of solute and particle recovery for solute and virus transport simulations in fining-upward sequence.

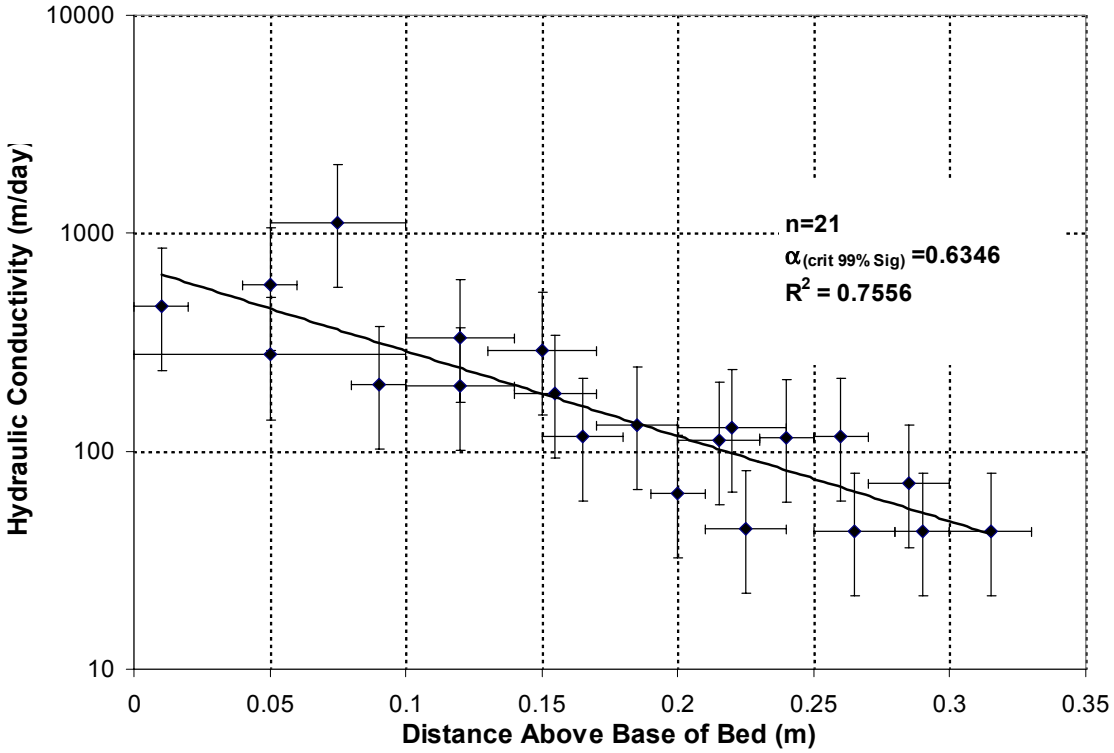

Figure 3.6: Plot of calculated hydraulic conductivity with distance from base of fining-upward sequence. Walperswil gravel. Note: Hydraulic conductivity errors calculated based on plus or minus 5% porosity variation.

The results of grain size analyses of sand and gravel samples collected from the bed containing the fining-upward sequence at the Walperswil gravel pit, indicate a strong log-linear variation in hydraulic conductivity with distance from the base of the bed. Flow and transport processes in this structure were modelled using a series texturally uniform subunits with the same overall degree of grain size/hydraulic conductivity variation as that observed in the fining upward sequence. Resulting conservative tracer breakthrough curves generated by superimposing a series of flux-weighted advective-dispersive terms bear a strong resemblance to solute breakthrough curves observed in tracer tests completed at the nearby Kappelen test site (Figure 3.1). Moreover, by applying a uniform collision efficiency to the discretised structure, the dependency of bacteriophage breakthrough on grain size, and thus deposition constant could be evaluated. Once again responses bear a strong qualitative resemblance to those observed at the Kappelen field site and other porous media sites. The experimental results suggest that features that influence solute and microbial transport at low levels in the hierarchy of sedimentary structures may also manifest themselves at higher levels in the same scheme.

Despite the above similarities, it is noteworthy that the simulation results must be regarded as a simplification of virus transport in natural systems. This

arises largely from the fact that collision efficiency is unlikely to be uniform in natural deposits, but rather will depend strongly on the chemical nature of the aquifer matrix (mineralogy). Mineralogy may vary within individual beds and is dictated by parameters such as the energy of the transporting medium at the time of deposition, grain dimensions and mineral density (Allen, 1985). Consequently, minerals such as clays will be more likely deposited at the end of depositional events when available energy is waning and settling is more probable. Investigations by Rossi and Aragno (1999) demonstrated that clay minerals such as montmorillonite and attapulgite can have significant bacteriophage attenuation capacity. Moreover, these fine grained minerals can also influence the hydraulic conductivity of the sediments thereby controlling the groundwater velocity, and by inference, the residence time of water /tracers in the system. Greater residence time increases the possibility of adsorption of bacteriophages to mineral surfaces. Consequently, greater bacteriophage attenuation would be anticipated in the finer-grained part of a bed due to both higher collision efficiency, resulting from differing mineralogy, and increased residence time, resulting from finer grain size.

Both grain size and mineral distribution are related to depositional environment. Consequently, identification of an appropriate facies model can be of considerable use in considering the potential sedimentary structures and their distribution in an aquifer. This in turn can be of great assistance in evaluating the migration and consequent distribution of microbial contaminants in groundwater.

Overall, the results of the simulations highlight the importance of geological conditions in predicting virus transport in porous aquifer. Both the distribution of grain size and collision efficiency will strongly determine the degree of bacteriophage attenuation in heterogeneous deposits such as those containing fining-upward sedimentary structures. Indeed, if predictions concerning solute and bacteriophage mass transport are simplified, and uniform conditions assumed, as were simulated for the coarse grained fining upwards sequence, the resulting predictions will underestimate the maximum concentration of particles observed. Furthermore, the anticipated mass of bacteriophages recovered at a monitoring point will also be under-estimated.

The results of this study demonstrate the importance of geological heterogeneity in site characterisation when considering viral transport in groundwater, particularly with respect to grain size and mineralogy. In a more general sense the data and associated simulations further underscore the importance of appropriate site characterisation techniques when considering protection of groundwater as a drinking water supply.

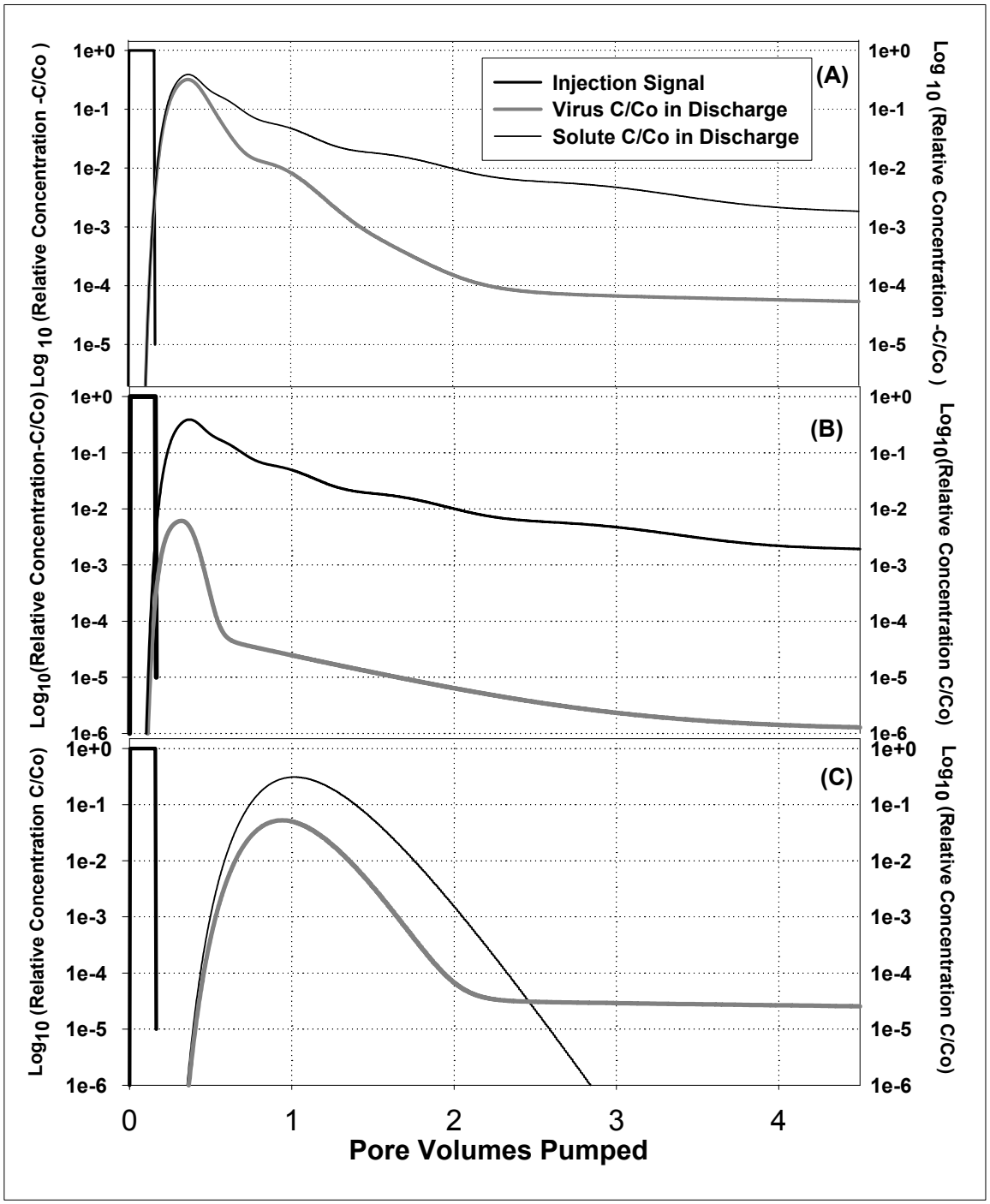

Figure 3.7: Results of analytical simulations of solute and virus transport in graded beds. (a) Bed grain size 10000μm at base, 1000μm at top.; $\alpha = 0.3$. (b) Bed grain size 1000μm at base, 100μm at top; a=0.1. (c) Simulation for coarse-grained bed, assuming averaged grain diameter (4498 μm). α=0.1. Note peak virus concentrations are significantly lower than heterogeneous system with sedimentary structure, despite lower collision efficiency, and arrival times later.

Chapter 4 : Identification of Zones of Preferential Groundwater Tracer Transport Using a Mobile Downhole Fluorometer.

4.1 Abstract:

A mobile downhole fluorometer was used to detect zones of preferential groundwater tracer transport in an observation well. Identification of such zones is not possible if a sample is collected over a wells entire screened interval. Laboratory-based tests using the fluorometer and a purpose-built apparatus demonstrated that the meter could be used with tracers to characterise wellwater flow regimes. During field-based tracer tests in a porous aquifer, the fluorometer monitored Uranine concentrations in an observation well with a 12m long saturated screened interval ten metres down gradient of a fully-penetrating injection well. Test results showed that the tracer occurred in the observation well over a discrete 2.5m thick interval. Single-well dilution tests and vertical flow data indicated that water entered the well at additional depths, but no tracer was detected at these levels. A numerical model reproducing dilution test concentration profiles indicated that water entered the well through other horizons at comparable velocities to those in the tracer-bearing zone. These data suggest that groundwater flow direction varied with depth in the aquifer under investigation. Moreover, simulations of tracer arrival indicated that the tracer distribution in the observation well may be derived from a tracer bearing zone no thicker than 0.5m.

4.2 Introduction

An absence of sufficient geological data and complex wellwater flow dynamics often hinder the accurate assessment of groundwater conditions during hydrogeological investigations using wells with long screened intervals. Rushton and Howard (1982) highlighted the unreliability of open boreholes as groundwater level observation points during pumping tests. Similarly, Price and Williams (1993) noted that open boreholes are not reliable groundwater sampling points. Nonetheless, time and budget restrictions often require field hydrogeologists to use boreholes and/or wells with long screened intervals to determine hydrogeological parameters. This requirement has prompted subsequent investigations into the influence of open holes and wells with long screened intervals on water sampling and hydraulic conductivity determination (Jones and Lerner, 1995, Kaleris and others 1995, Hutchins, and Acree, 2000)

In terms of wellhead protection area delineation, identification of zones of preferential flow frequently constitutes a critical aspect in the contaminant transport assessment. Tracer tests can provide considerable information about the variability of mass transport rates between wells (Käss, 1997). However, sampling techniques as well as injection well and monitoring well construction may be highly variable from one test to another. Typically individual samples are collected over the entire screened interval of the well, e.g. Kennedy and others, 2001a. However when individual monitoring wells are screened against deposits with variable hydraulic conductivities, groundwater flow rates in preferential flow zones can be under-estimated using this monitoring technique. Consequently, as such methods fail to reflect the variation in hydraulic properties of the deposits in contact with the well screen, the groundwater flow velocities necessary for establishing realistic aquifer protection zones around water supply wells may be inaccurately estimated. Tracer monitoring techniques may be modified for wells with long screened intervals using multiple pump systems, such as level-determined groundwater sampling in open wells (Rapp and others ,1998). However, such approaches rely on extracting water from wells and so induce hydraulic gradients. Similarly, Schirmer and others (1995) noted that multi-level packer systems and/or low-flow sampling cannot be confidently used where wells have gravel packs and vertical gradients. Moreover, even when vertical gradients are not present, the small intervals sampled with low-flow sampling techniques imply that it is possible that all preferential flow zones of interest may not be sampled using such an approach.

This paper presents a method for measuring tracer concentration profiles in boreholes using a mobile submersible borehole fluorometer. This system has allowed zones of preferential groundwater flow supplying wells with long screened intervals to be located, even in wells with gravel packs and vertical gradients. The method may be applied to single wells where rates of fluorescent tracer dilution may be related to groundwater flow rates, or as a monitoring tool in

observation wells where it may be used to identify zones of tracer arrival. Integrating both single well and observation well approaches allows insights into the well water flow regime and the behaviour of tracer upon arrival in an observation well to be obtained. These methods, their verification under controlled laboratory conditions, and their application in the field are described below.

4.3 Materials

4.3.1 Fluorometer

All investigations employed a University of Neuchatel Geomagnetism Group (GGUN) downhole fluorometer (also referred to as the sonde). The sonde (74mm in diameter by 200mm in length) is submersible in a water column to a depth of 70m. An optical cell measures fluorescent tracer concentrations of the water passing through a sampling chamber set in the centre of the sonde (Figure 4.1). The sonde is capable of detecting Uranine (Sodium Fluorescene. Excitation wavelength 491nm, Emission wavelength 512nm) to a concentration of 0.02 parts per billion (ppb).

A multicore cable provides the mechanical support to suspend the fluorometer in the borehole, while permitting optical cell signals to be relayed to a data logger at the ground surface. Signal data may be observed directly in the field on a laptop computer that displays fluorometer data using dedicated software. This allows zones of interest in a borehole to be rapidly identified. A more comprehensive description of the GGUN downhole fluorometers operation is contained in Schnegg and Bossy (2001).

4.3.2 Pulley System

Except where otherwise stated, the fluorometer was adapted for use in the tests described below to allow regular measurements to be made while being continuously being raised and lowered over a predetermined interval, using a programmable pulley system. The pulley consisted of a programmable motor and a spool of 0.1mm thick piano wire cable and was set back from the borehole under study by a distance (I). The length of I, equal to the length interval under investigation downhole (Figure 4.2). The pulley cable attached to the fluorometers multicore cable using a connecting clip. To ensure ease of movement in the borehole, the downhole fluorometer was centred over the hole using a tripod with an attached roller. This arrangement allowed the multicore cable to easily slide back and forth. By releasing and withdrawing the pulley cable, the sonde could be raised and lowered in a borehole. Instructions provided to the pulley motor, via a laptop computer, specified the depth of the first

measurement, the distance between the fluorescence measurements (5cm minimum) and number of measurements that the fluorometer must make per cycle.

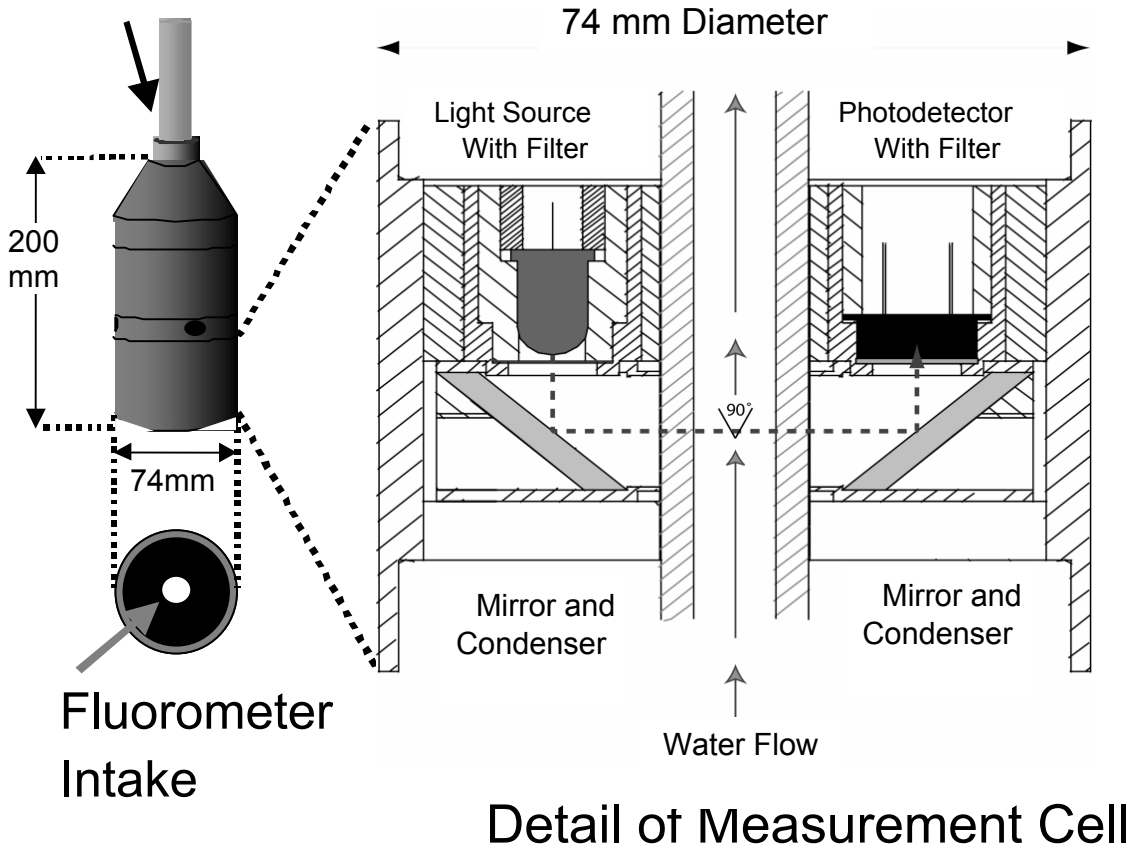

Figure 4.1: Diagram illustrating the dimensions and internal operation of the downhole fluorometer. A mirror reflects filtered light emitted from a source into a sampling cell in the centre of the meter. The filtered light causes target compounds present in the water flowing through the sampling cell to fluoresce. A photodetector set at 90° to the light source detects the fluorescence and generates a signal in proportion to the target compound concentration. This signal is transmitted to the ground surface via a multicore cable.

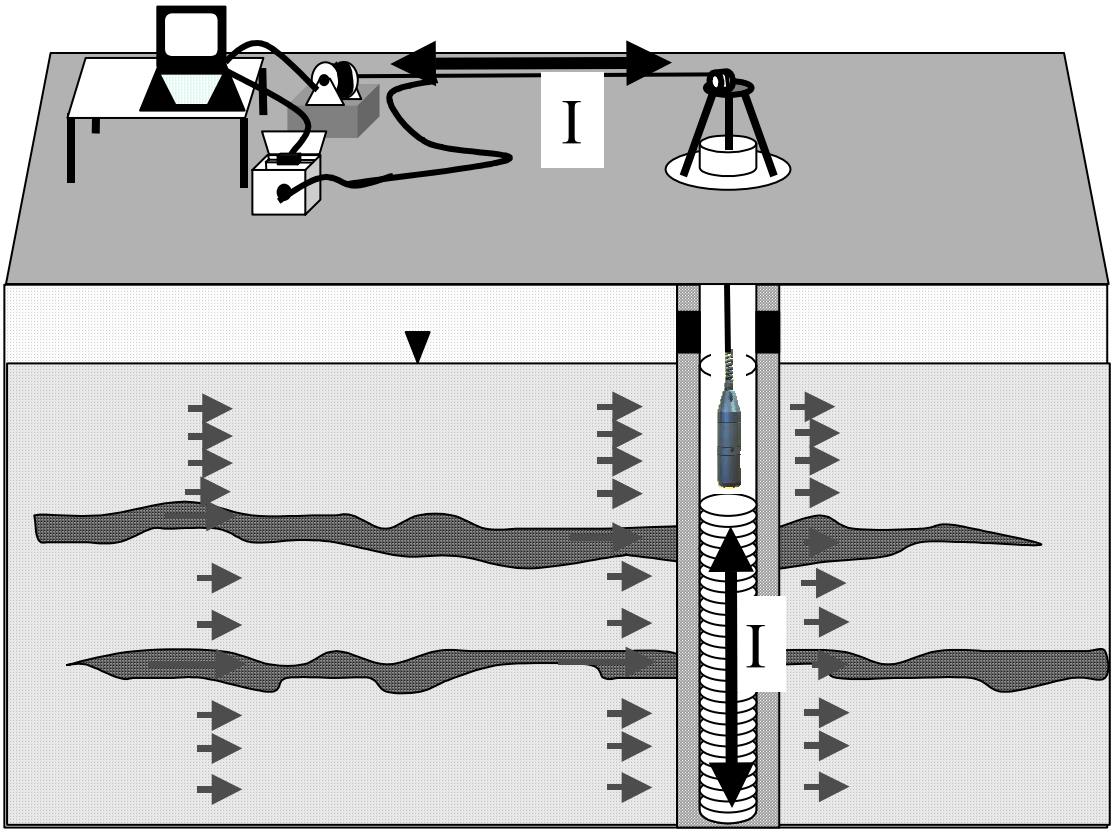

Figure 4.2: Illustration of the operation of the mobile fluorometer in the field. The multicore cable suspending the fluorometer in the borehole is attached to the programmable pulley cable. The pulley continuously releases and withdraws its cable over an interval I, which corresponds to the investigation interval in the well under study.

4.3.3 Laboratory Apparatus.

Prior to initiating field measurements, a series of investigations evaluated the ability of the fluorometer to detect tracer entering or leaving a borehole via preferential flow horizons, using a purpose built Laboratory apparatus (Figure 4.3). The apparatus consisted of a 1.7 metre long 6 inch (15.24cm) internal diameter (ID) Perspex tube (Lab borehole) with a eight holes each drilled at two levels to permit water to flow through the 6 inch tube at a constant flow rate. The downhole fluorometer pulley was placed on top of the borehole and the sonde inverted in the 6-inch tube (due to Laboratory space restrictions). The fluorometer could thus measure tracer concentration profiles in the borehole over time, while the transparent wall of Lab borehole walls permitted the location of tracer and the sonde in the well to be visually compared with on-going measurements.

A three-way valve, connected to the tubing, which supplied the influent side of the Lab borehole, permitted water to enter via either the upper or lower set of holes, or through both. Similarly, another three-way valve on the effluent side of the borehole allowed water to leave at either or both levels. This valve system permitted the flow regime in the borehole to be controlled. Opening both sets of valves at one level ensured a horizontal flow regime. On the other hand, by permitting water to enter and exit at alternate levels, while blocking flow through corresponding tubes on the opposite side of the same level resulted in water flowing vertically, upwards or downwards, in the well, depending on the configuration used. An additional three-way valve placed on the influent line allowed tracer to be injected into water entering the borehole, thus permitting tracer arrival to be simulated.

All circulating water was maintained at room temperature throughout experiments to prevent the formation of thermal convective cells in the borehole. Constant head reservoir temperature was verified at regular intervals using an electronic thermometer (accuracy +/- 0.1°C).

4.4 Experiments

4.4.1 Laboratory experiments

The Laboratory apparatus permitted a series of investigations to be carried out to evaluate the performance of the fluorometer in detecting tracer in a borehole under controlled conditions. Following each experiment, a pump removed all water from the Lab borehole, prior to refilling with fresh, tracer-free water for subsequent experiments.

The following experiments were completed using the Lab borehole:

4.4.1a Identification of depth of tracer occurrence: Prior to initiating experiments in which water flows through the Lab borehole, a series of tests were conducted using a column of still water. A peristaltic pump injected approximately 20ml of concentrated tracer at a known depth directly into the 6-inch (15.24cm) borehole, after which measurements with the mobile downhole fluorometer were initiated. Tracer concentrations were sufficiently high to be visible through the boreholes Perspex walls. A series of measurement cycles generated the tracer concentration profiles in the hole. This permitted an assessment of how accurately the sonde could detect the depth of tracer occurrence. Successive measurement cycles allowed the effects of the meters movement on tracer distribution in a borehole to be established.

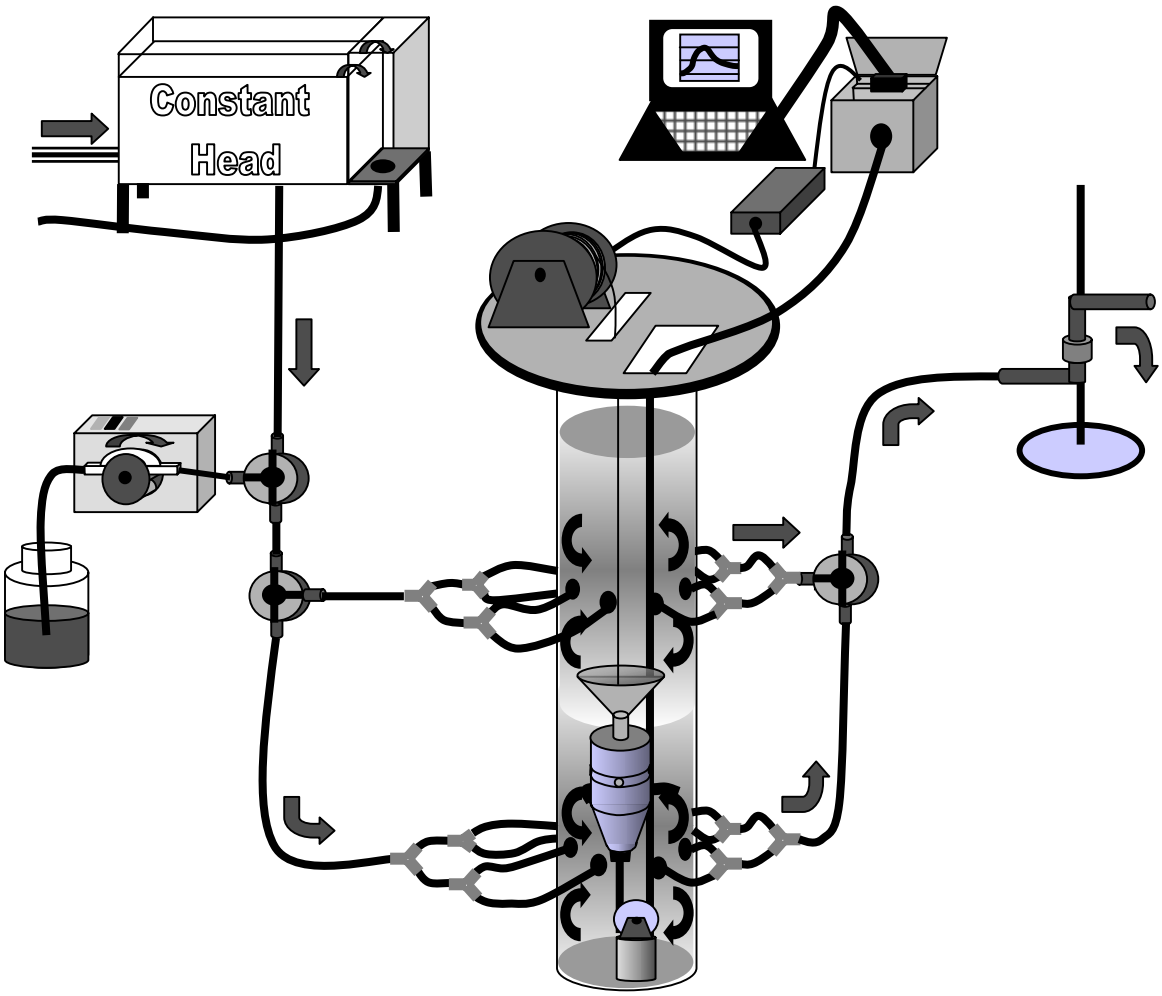

Figure 4.3: Diagram illustrating the functioning of the Laboratory Apparatus. Broad arrows illustrate the directions followed by flowing water. Water from the fixed head reservoir flowed at a constant rate through the central 6 inch (15.24 cm) tube at one or two levels. The fluorometer measured tracer concentration profiles.

4.4.1b Identification of zones of preferential transport by dilution (Single Well Dilution Tests). During this series of experiments the mobile downhole fluorometer measured tracer concentration in the 6-inch borehole as water passed horizontally through the active flow zones at a rate of 2 litres/min. Prior to initiating fluorometer measurements, a small volume of concentrated tracer was injected along the Lab boreholes water column. Water leaving the borehole in the zones of active flow was replaced by tracer free water on the influent side thus diluting the concentration of tracer in the active flow zones. Additional experiments carried from 0.25 to 5 l/min investigated whether the results at 2 l/min. were representative of other flow rates. This series of experiments investigated whether the downhole fluorometer could be used to ascertain the

position of active flow zones in an individual well, based on tracer concentration profiles.

(a) *4.4.1c Identification of zones of tracer arrival*. Injecting tracer into the influent water before it entered the 6-inch tube, while monitoring with the mobile fluorometer allowed the meters efficiency in detecting zones of tracer arrival to be assessed. Tracer-bearing influent water, flowing at 2 litres/min, entered the Lab borehole while the fluorometer monitored for fluorescent tracer in the boreholes water column. The tests permitted the accuracy of the fluorometer to identify the depth and concentration in zones where tracer-bearing water enters the borehole to be determined. Moreover, as with single well dilution tests described above, repeated measurements allowed the consistency of the fluorometer in identifying the depths of tracer arrival to be ascertained, while those carried out at between 0.25 to 5l/min investigated whether similar responses were observed at different flow rates.

4.4.1d Vertical flow rate measurement: A further series of experiments involved injecting tracer into the influent water before it enters the Lab borehole, where water was flowing vertically. During these experiments, the tracer solution entered the borehole at one level, but was forced to leave by flowing upwards to another level, and so the effects of vertical flow on tracer distribution could be investigated.

As an alternative to measuring rates of vertical flow in boreholes using heat flow meters / impeller flow meters, the fluorometer was adapted to measure tracer concentrations in the vertical flow stream of a borehole. In this method, the fluorometer was set at a fixed point in the borehole and a pulse of tracer injected at a fixed separation distance from the meters measurement cell. The fluorometer was set above the injection point (intake facing downwards) to measure upward flow, or set below the injection point (intake facing upwards) to measure downward flow. In the case where the flow direction is not known, individual measurements must be made either side of the injection point, i.e. two separate injections must be made. However, should two fluorometers be available, one can be set at either side of the injection point, thus reducing the necessary number of injections to one.

The fluorometers data logger measured tracer concentration with time and allowed breakthrough curves to be generated. The centroid of the resulting breakthrough curve provided the necessary data to determine the vertical flow velocity, and thus the flow rate, in the well (Drost, and others 1968). The method was investigated using the Laboratory apparatus under known vertical flow rates, and the expected results compared to those obtained.

4.4.2 Field Investigations.

Following Laboratory investigations, the methods developed under controlled conditions were applied in the field at a porous aquifer test site that used wells with long screened intervals to monitor groundwater conditions.

4.4.2a. Site Description : The GSF's Dornach test-site (Dornach) is located on the Munich Gravel Plane near the village of Dornach on the eastern outskirts of Munich, Germany. The site is representative of perialpine gravel aquifers where tracer tests have shown that groundwater flow rates may approach 100m/day. Available well construction diagrams and drilling records for Dornach indicate that it is underlain by approximately 14m of Quaternary sands and gravels. These deposits overlie Tertiary sands and silts (Müller and Seiler, 2001). Seiler (1988) reports the gravels to have hydraulic conducitivities of the order of $5x10^{-1}$ cm/s, with a hydraulic gradient of the order of 0.005 to 0.01 across the site. The test-site consists of seven wells set in a 20m wide semicircular array with an eighth well in the centre, equidistant from the other wells (Figure 4.4). Three of these have been used in the framework of this study, B1, B7 and B8. The wells have 12m long screens that are set against the full saturated thickness of the Quaternary sands and gravels. Groundwater level measurements at the site indicate that water table fluctuates between approximately 1 and 3 metres below ground surface (mBGS).

Previous comparative tracer testing at the Dornach test site using Uranine in conjunction with heavy metals tracers (Muller and Seiler, 2001) and Cadmium and Arsenic (Zahn, and Seiler, 1992), showed that tracers were transported from the two inch (2") internal diameter (ID) injection well, B1 to the observation wells B8 (8" ID) and B7 (2 " ID). During these tests, the whole-well circulation method was employed, whereby water from the bottom of the observation wells was pumped to the surface to flow through on-line meters monitoring for selected parameters. After passing through the monitoring system, the water was reinjected into the well at the water table. The whole well approach maintained a static water level, while permitting high resolution tracer monitoring to be carried out. However, the method failed to permit identification of the depth(s) of tracer arrivals in observation wells.

4.4.2b Field Experiments: During the current study, a series of tests further examined tracer transport between injection well, B1, and observation wells, B8 and B7 with a view to better understanding tracer transport at Dornach. During these tests, Uranine acted as a solute tracer. Käss (1997) summarised the results of a number of previous tracer tests using Uranine carried out at a variety of locations, and concluded that the tracer is not retarded by aquifer materials relative to other conservative tracers, once significant quantities of organic matter are absent. Moreover, comparative tracer tests carried out at the Dornach site

using Uranine and bromide showed no significant difference in arrival time between the two tracers (German Mallén, 2002, pers comm).

A suite of tracer tests carried out at the Dornach test site allowed the applicability of the downhole fluorometer as a tool in tracer testing to be assessed. In all tests, the tracer was circulated across the screened interval of the injection well using the whole well recirculation technique. Prior to carrying out investigations with the downhole fluorometer, two tests were completed in which tracer concentrations were monitored in observation wells B7 and B8 using whole well sampling techniques (circulating at approximately 17 l/min in both wells). These tests were carried out in July 2000 (Whole Well Test #1) and May 2001 (Whole Well Test #2). Subsequent to these tests, a pair of additional investigations carried out using low flow sampling techniques examined the variation in breakthrough curves at different depths in monitoring well B8 in August 2002. One test (Low Flow #1) investigated tracer response at four equally spaced intervals, while the other test (Low Flow#2) sampled zones identified as containing tracer according to downhole fluorometer test results. Complimentary tracer testing using the bacteriophage H40/1 was used to investigate the response of particulate tracers relative to Uranine during Low Flow #2.

Two tracer tests, Downhole#1 and Downhole#2 used the mobile downhole fluorometer to examine tracer concentration profiles with depth in B8 following Uranine injection in B1. Downhole #1 was carried out in July 2001 and a subsequent test, Downhole#2 was carried out in August 2002. Both tests monitored tracer concentrations in the interval from 3 to 14.5mBGS at half-hourly intervals for the first twelve hours after injection and again at 24 hours after injection.

Single well dilution testing, associated with Downhole #2 was carried out at B8 to more fully characterise its wellwater flow regime. Triplicate single well dilution tests initiated at hourly intervals measured Uranine concentrations over the wells screened interval, starting approximately four minutes after the tracer was injected, in the same manner as used in the Laboratory experiments.

Following the single well dilution tests, vertical flow measurements of upward and downward flow component of wellwater flow in B8 were completed at 0.5 to 1m intervals along the screened interval. An injection line set between 25 and 50cm from the fluorometers sampling chamber permitted approximately 200mL of 50mg/l Uranine to be pumped into the water column over a 30-sec interval during each measurement. Tracer monitoring continued for 15 minutes to 50 minutes after each injection pulse.

Figure 4.4: Site Location Map / Geological cross section of the Dornach Test Site. (Modified from Müller and Seiler, 2001)

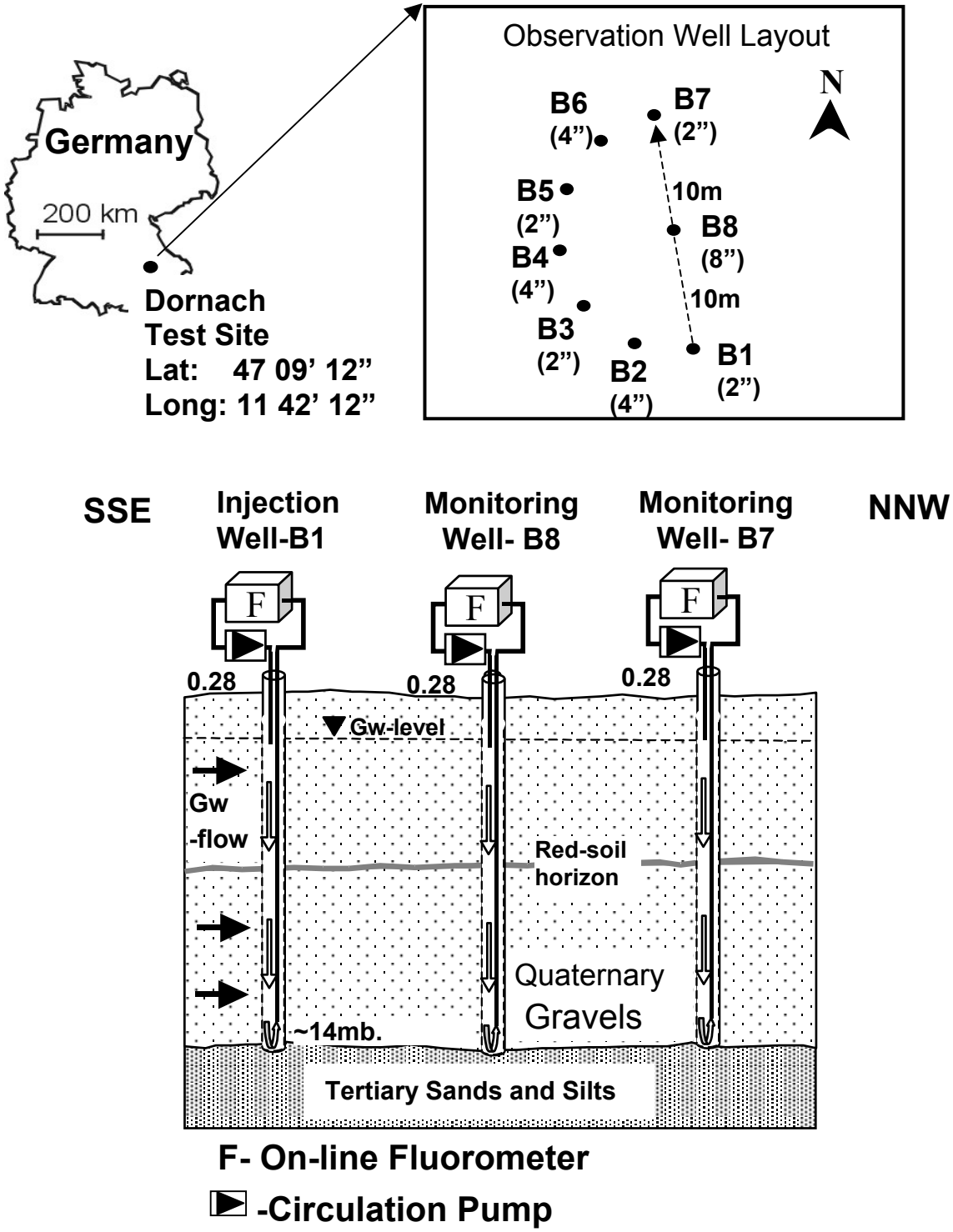

4.5 Modelling

In order to further understand tracer response in well B8 at the Dornach test site, a numerical model incorporating vertical flow test data and single well dilution test data was developed based on a tracer mass balance and the principal of conservation of well volume. The goal of the model was to simulate the concentration profiles observed in B8 during dilution tests and, using the resulting calibration data, investigate whether the breakthrough curves observed during Downhole #2 could be generated.

The fundamental mass balance equation for the model states

$$\frac{\partial M}{\partial t} = V \frac{\partial C}{\partial t} \qquad (4.1)$$

where M is the tracer mass (M).
C is tracer concentration (ML^{-3}).
V is the volume of tracer (L^3).
t is time (T).

This may be expressed in terms of vertical and horizontal fluxes as follows:

$$\frac{\partial C}{\partial t} = -\frac{2q(z)_h}{\pi r_w} C(z) - q(z)_z \frac{\partial C}{\partial z} \qquad (4.2)$$

where $q(z)_h$ is depth-dependant horizontal flux leaving the well (L/T).

z is depth from water table (L); r_w is the well radius (L).

$q(z)_z$ is the depth-dependant vertical flux flowing through the well (L/T).

Moreover, since V for each cell remains constant.

$$\frac{\partial Q_h}{\partial t} + \frac{\partial Q_z}{\partial t} = 0 \qquad (4.3)$$

where Q_h is the horizontal flow rate (L^3T^{-1}).
Q_z is the vertical flow rate (L^3T^{-1})..

Figure 4.5 illustrates the application of this model to a discretised segment of a well displaying vertical and horizontal well specific flux components. Applying the above approach, the water column in B8 was discretised into 0.25m cells. Using equation (4.2), values of $q(z)_h$ and $q(z)_z$ were varied for each cell to reproduce the variation in C(z) observed by coupling flow rates and concentrations in adjacent cells to one another.

Linear interpolation between vertical flow rate measuring points allowed a rate to be assigned to each cell. The observed values of C(z), obtained from downhole fluorometer measurements were averaged over 5 measurement increments of 5 cm each during dilution tests. Model simulations used time steps

that allowed no more than 1/20th of a cell volume to pass through a cell during each step to limit numerical dispersion effects. Finally, all concentrations were expressed relative to those observed at 4.0mBGS. Concentrations at this level remained constant between measurements started 4 minutes after injection and those observed after 30 minutes.

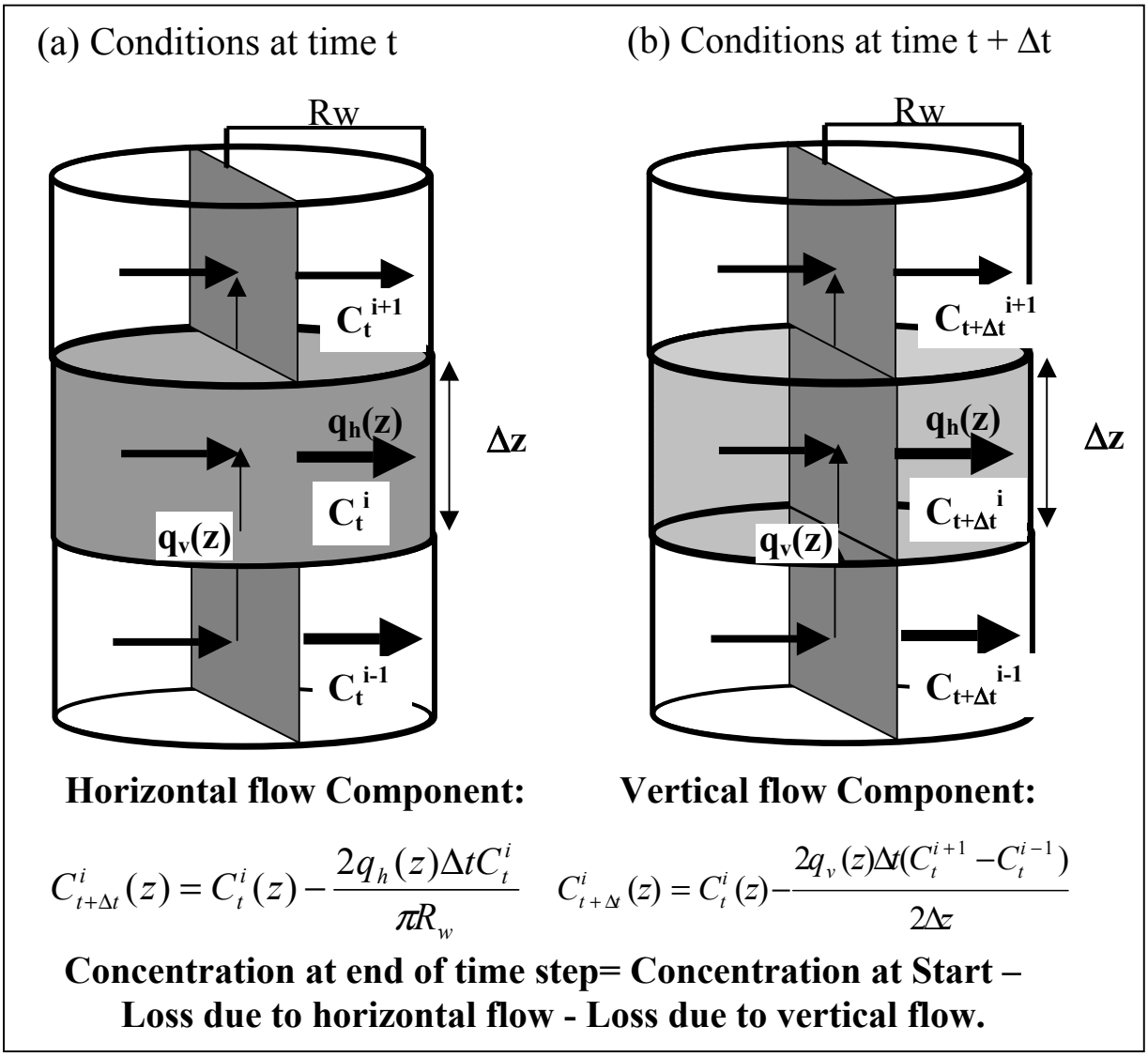

Figure 4.5 : Schematic illustration of mass balance modelling process. Decline in tracer concentration in a cell of thickness Δz during a time step Δt results from removal by vertical flow across the cell $q_v(z)$ and by horizontal flow $q_h(h)$ into the aquifer. No tracer can enters the well from up-gradient, nor can tracer enter from the top or base of the water column. The final analytical version of this derivation reduces to equation 4.2.

4.6 Calibration

Model calibration was carried out in order to determine depth-specific horizontal fluxes across the screen of B8 that could reproduce the tracer concentration profile generated during the single well dilution tests at B8. Since water entering the well from the aquifer was tracer free, the overall concentration in the well could only decline with time. In order to calibrate the well water flow model for B8, vertical flow rates were varied from their calculated value within the proportions calculated based on measurements using the Lab borehole. Moreover, variations in the vertical flow rate needed to be compensated for by changes in horizontal flow rate, as stated in equation (4.3). Zones within the water column, where purely horizontal flow was measured were either classified as convergent flow zones or divergent flow zones. Convergent flow zones received water vertically from adjacent cells, while divergent flow zones discharged water to adjacent cells. Horizontal and vertical flow rates were varied until the tracer profile corresponded to that observed in the field.

Following calibration, the model was used to simulate tracer arrival into B8 and the resulting profile compared to observed data. This procedure acted as a means of verifying that the observed model parameters were sufficiently realistic. Arrival was simulated by maintaining a constant concentration at a zone of tracer arrival, while running the model over the time required to measure a tracer profile in the wells water column. The time period was sufficiently short (10 mins) such that the tracer concentration at the point of arrival could be considered essentially constant, based on existing breakthrough curves. The location and thickness of the horizon supplying tracer to the borehole were selected based on qualitative observations of tracer concentration profiles made during the Laboratory-based experiments.

4.7 Results

4.7.1 Laboratory Testing

The results of the tracer occurrence tests in the Lab borehole demonstrated that the fluorometer could be used to determine the depth of tracer occurrence. Although the fluorometer moves continuously, inefficient flow through the sampling chamber results in water not being fully flushed as the fluorometer advances. This results in liquid being temporarily retained by the meter. This liquid is subsequently released and enters the fluorometer measurement cell during later measurements. Consequently, upon encountering a tracer bearing zone in a well, true tracer concentrations must be regarded as possibly being greater than those measured, since temporarily stored tracer-free water may be

released to dilute the tracer in the sampling chamber. Conversely, tracer entering the fluorometer is incompletely flushed and can be released at a later time which may indicate that low concentrations of tracer occur at in tracer-free zones. Under the hydrodynamic conditions employed, laboratory tests suggest that residual quantities of tracer encountered at a particular level may be released up to 20 cm further in a measurement cycle.

In addition, measurements made during successive cycles during tracer occurrence experiments demonstrated that the action of the sonde in the 6-inch tube tends to result in redistribution of tracer. This process leads to homogenisation of the tracer with tracer-free water, if there is no zone of active flow through the Lab borehole. Moreover, subsequent testing using a prototype of a 50mm diameter downhole fluorometer demonstrated that the degree of mixing generated by this narrower sonde was significantly less than that of the 74mm wide model.

The results of the single well dilution experiments indicate that the downhole fluorometer is capable of identifying zones of preferential flow. Figure 4.6a shows, that when flow is purely horizontal, the lowest tracer concentrations observed during well dilution tests are consistently in the zones of active flow. This occurs despite homogenisation due to the action of the sonde passing through the interval of measurement. Similarly, Figure 4.6b presents the results of a typical tracer arrival test. The figure shows that when measurements are made of tracer entering the Lab borehole, concentrations are greatest in zones of active flow. In contrast to dilution tests, the peak concentrations occur consistently around the zone of tracer arrival.

Identification of preferential flow zones is more complex when a vertical flow regime operates in the borehole. In this case, the tracer is advected vertically by the water entering the borehole. This process results in the tracer spreading out to occupy the thickness across which vertical flow occurs. (Figure 4.6c) Despite this phenomenon, it is noteworthy that the highest tracer concentrations occurred consistently around the inflow zone during tracer arrival experiments. Moreover, the marked concentration decline associated with the outflow zone (within the range of measurement error) shows that the fluorometer is capable of detecting the zone where the tracer leaves the well. Nonetheless, should vertical flow be neglected under these circumstances, concentrations measured by the fluorometer would suggest that the tracer arrives in a thicker zone than it actually does. Consequently, if tracer behaviour in boreholes is to be adequately characterised, the influence of vertical flow on tracer distribution must be assessed.

Experimental breakthrough curves generated during vertical flow tests carried out using the Lab borehole indicate that this measurement method may underestimate vertical flow rates by up to 30%, using the centroid time to calculate velocity. Nonetheless the experimental results show that the downhole fluorometer may be used to characterise both the magnitude and direction (upward or downward) of water flow in a borehole. This approach offers a practical alternative to other methods of vertical flow testing, such as heat pulse or impeller flow meters, in fast flowing systems where tracer is rapidly removed from the borehole.

4.7.2 Field results

The results of the whole-well tracer tests at the Dornach test site demonstrate that Uranine is transported between the injection well B1 and monitoring wells B7 and B8 at different rates. The first arrival times, peak concentration times and peak concentrations for Whole Well #1, provided in Table 4.1, indicate that the average velocity between B1 and B7, 20m away, is significantly greater than between B1 and B8, 10m away. Furthermore, the results of Whole Well #2 demonstrated that the maximum concentration of tracer reaching B7 can be greater than at B8. These data provide an insight into the variability of groundwater flow trajectories in the deposits underlying the site. However, the results provide no information on the vertical variability of tracer arrivals along the screened intervals of the monitoring wells. In contrast, the results of Low Flow #1 and Low Flow #2 clearly demonstrate that, depending on the depth at which samples are collected, differing tracer responses may be obtained from B8 (Table 4.1).

The data from Low Flow #1 display this phenomenon particularly well. The sample pump set at 12m BGS detected that the highest concentrations of Uranine. In contrast, samples collected using the pump set at 14mBGS contained no detectable quantities of tracer. Samples collected from the remaining two sampling points contained Uranine but in lower concentrations. (A breakthrough curve could not be confidently generated using samples collected at 8.65mBGS as concentrations observed were too close to the detection limit of the fluorometer used).

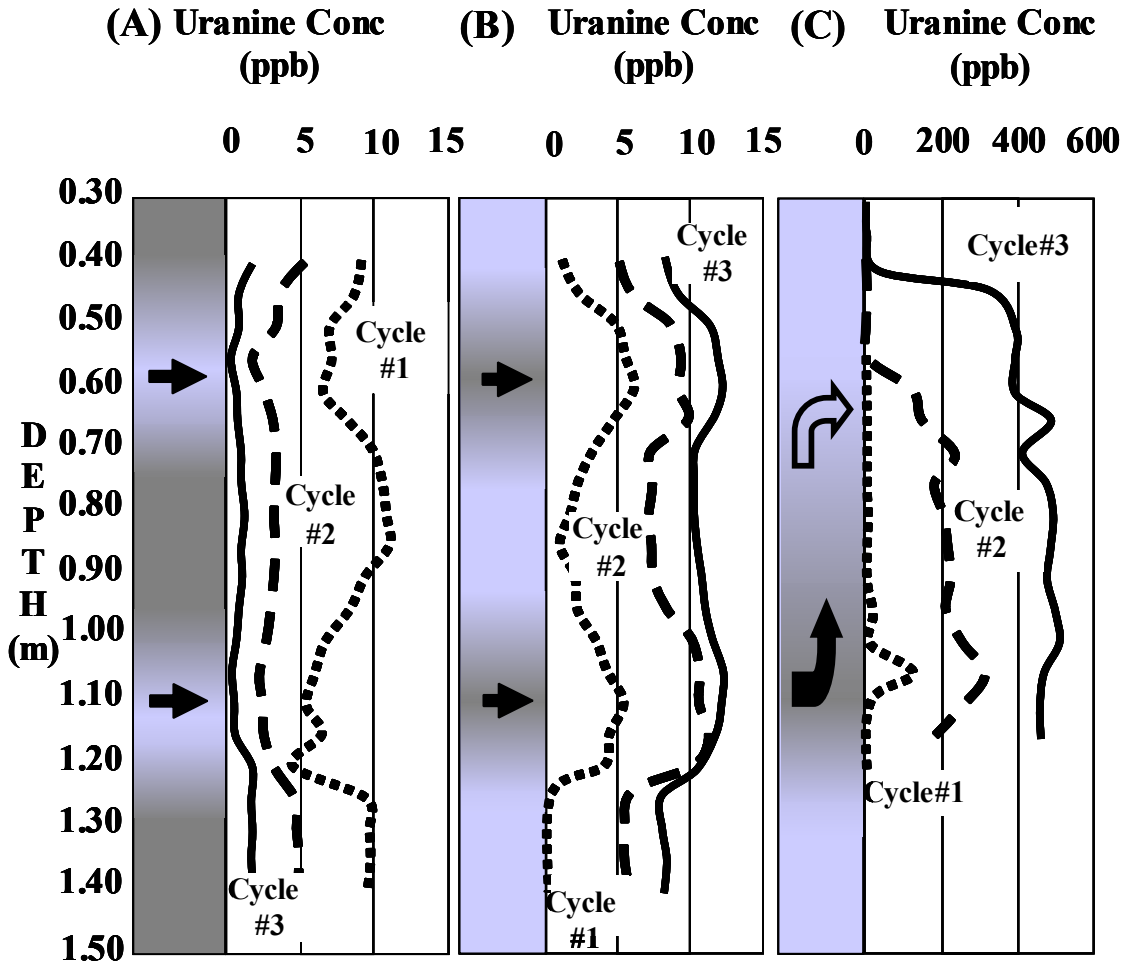

Figure 4.6: Diagram summarising the results of tracer tests using the Laboratory apparatus. Grey figures to the right of each graph indicate the distribution of tracer in the borehole. Dark grey represents zones of more concentrated tracer occurrence. Light grey indicates zones of less concentrated tracer occurrence. Bold arrows indicate flow directions. (a) Tracer dilution test results. (b) Tracer arrival test results. (c) Tracer propagation with vertical flow. (No further propagation after 10 minutes). All Uranine concentrations are in mg/l.

It is notable that tracer first arrival and peak concentration times at 5.5mBGS in Low Flow #1 were earlier than those observed at 12mBGS during Low Flow #1. Moreover, the results from Low Flow #2 at B8 are consistent with those Low Flow #1 and reflect the variation in tracer concentration with depth. Once again, Uranine concentrations at the sampling point set at 5 mBGS are detectable but are over an order of magnitude lower than those sampled in the zone 11 to 13mBGS. In this latter zone, tracer concentrations are highest at 12mBGS while those at 13 mBGS are lowest.

Comparative tracer testing carried out during Low Flow#2 demonstrated that the variability in solute response is also observed for a bacteriophage tracer

(H40/1) (Figure 4.6). Indeed, bacteriophage responses were comparable to those of the solute tracer. Maximum H40/1 concentrations were observed at approximately the same times at all three sampling points in the 11 to 13mBGS sampling zone. Similarly, as observed with Uranine, the H40/1 breakthrough curve generated from data collected at the 5mBGS zone shows that H40/1 peaked at an earlier time, but at a lower concentration that the deeper sampling points. However, the occurrence of H40/1 tracer at 5 mBGS also illustrated that this zone was also capable of transporting bacteriophages. Indeed, the maximum relative concentration ratios of Uranine to H40/1 at all four sampling points are comparable (2±0.5).

Tracer tests completed using the downhole fluorometer show that tracer occurs in discrete zones in B8. Profiles generated using depth and concentration data show a distinct peak of tracer occurrence at approximately 12mBGS during both tests. The distribution of tracer around this zone varies between the two tests. Measurable concentrations of Uranine were noted between 7.5 and 12.0 mBGS during Downhole #1. In contrast, measurable concentrations were notable between 10.5 and 12.5 mBGS during Downhole #2, although the location of the zone of peak concentration remained consistently around 12mBGS during both tests. Figure 4.8 presents images summarising breakthrough curves observed with depth through time for both Downhole#1 and Downhole#2 for the 7 to 14mBGS interval where high tracer concentrations were observed. The images differ in that the results of the earlier test, Downhole#1, indicated that tracer was present over a much larger depth interval and at higher concentrations compared to the data collected during Downhole #2. This is suspected to be a consequence of differing vertical flow dynamics in the well during the two tests.

Table 4.1 also summarises the results of tracer tests Downhole #1 and Downhole#2 for B8. A secondary zone of tracer occurrence at between approximately 4.0 to 5.0mBGS was detected in the profiles during Downhole#2. The first significant concentrations of Uranine are apparent in this shallower zone at approximately the same time (±0.5 hr) as in the deeper zone of tracer occurrence. However, peak concentration time is earlier than that observed at depth, although the peak concentration observed relative to that at 12mBGS is over an order of magnitude lower. The results of Downhole #2 are consistent with those observed during Low Flow #2. Tracer was also noted at this depth interval during Downhole #1, although the time of first arrival was approximately 0.5 hours later than that observed at depth, and occurred at a slightly shallower depth. Similarly peak concentration detection time was significantly later in the shallower zone than that observed at depth.

Table 4.1: Whole Well, Low Flow & Downhole fluorometer tracer test results, Dornach,.

Test/Observation Well	Sampling Depth (mBTOC)[1]	Starting Conc Co[2] (ppb)[3]	First Arrival (Hrs)[4]	Peak Conc Time (Hours)	Peak Relative Conc (C/Co)	Comment
Whole Well #1	Whole Well	4.55 E+03	2.46	5.31	1.76 E-04	Whole well sampled
B7	Whole Well	4.55 E+03	2.09	4.39	3.13 E-04	Whole well sampled
B8						
Whole Well #2	Whole Well	4.16E+03	3.13	6.04	3.04E-04	Whole well sampled
B7	Whole Well	4.16E+03	3.13	5.88	2.15E-04	Whole well sampled
B8						
Low Flow #1	5.5	2.21 E+05	2.58	3.83	2.82E-05	Q[6]=0.78l/min
B8	8.65	2.21 E+05	N/D[5]	N/D[5]	N/D[5]	Q[6]=0.92l/min
	12	2.21 E+05	3.08	5.83	2.46E-04	Q[6]=0.56l/min
	14	2.21 E+05	N/D[5]	N/D[5]	N/D[5]	Q[6]=0.56l/min
Low Flow #2	5	2.15 E+05	1.97	3.97	2.82E-05	Q[6]=0.79l/min
B8	11	2.15 E+05	3.14	6.14	4.07E-04	Q[6]=1.31l/min
	12	2.15 E+05	3.19	5.93	5.55E-04	Q[6]=0.96l/min
	13	2.15 E+05	3.27	6.05	3.45E-04	Q[6]=1.21l/min
Downhole #1	11.75	1.91 E+05	3.12	6.52	1.54 E-03 (11.85)[7]	Main arrival zone.
	4.15	1.91 E+05	3.52	26.54	1.31 E-05 (4.75)[7]	Secondary arrival zone.
Downhole #2	12.09	1.86 E+05	2.53	7.50	5.05 E-04 (11.97)[7]	Main arrival zone.
	4.52	1.86 E+05	3.02	4.01	2.85 E-05 (4-.63)[7]	Secondary arrival zone.

Notes*: **1.*** mBTOC: metres below top of well casing. *2*. Co determined by dividing mass injected by saturated well volume. *3*. ppb: Parts per billion *4*. Estimated from inflection point on breakthrough curve. *5*.N/D: No determined *6***.** Low flow sampling rate (litres /minute). 7. Depth of maximum tracer concentration occurrence.

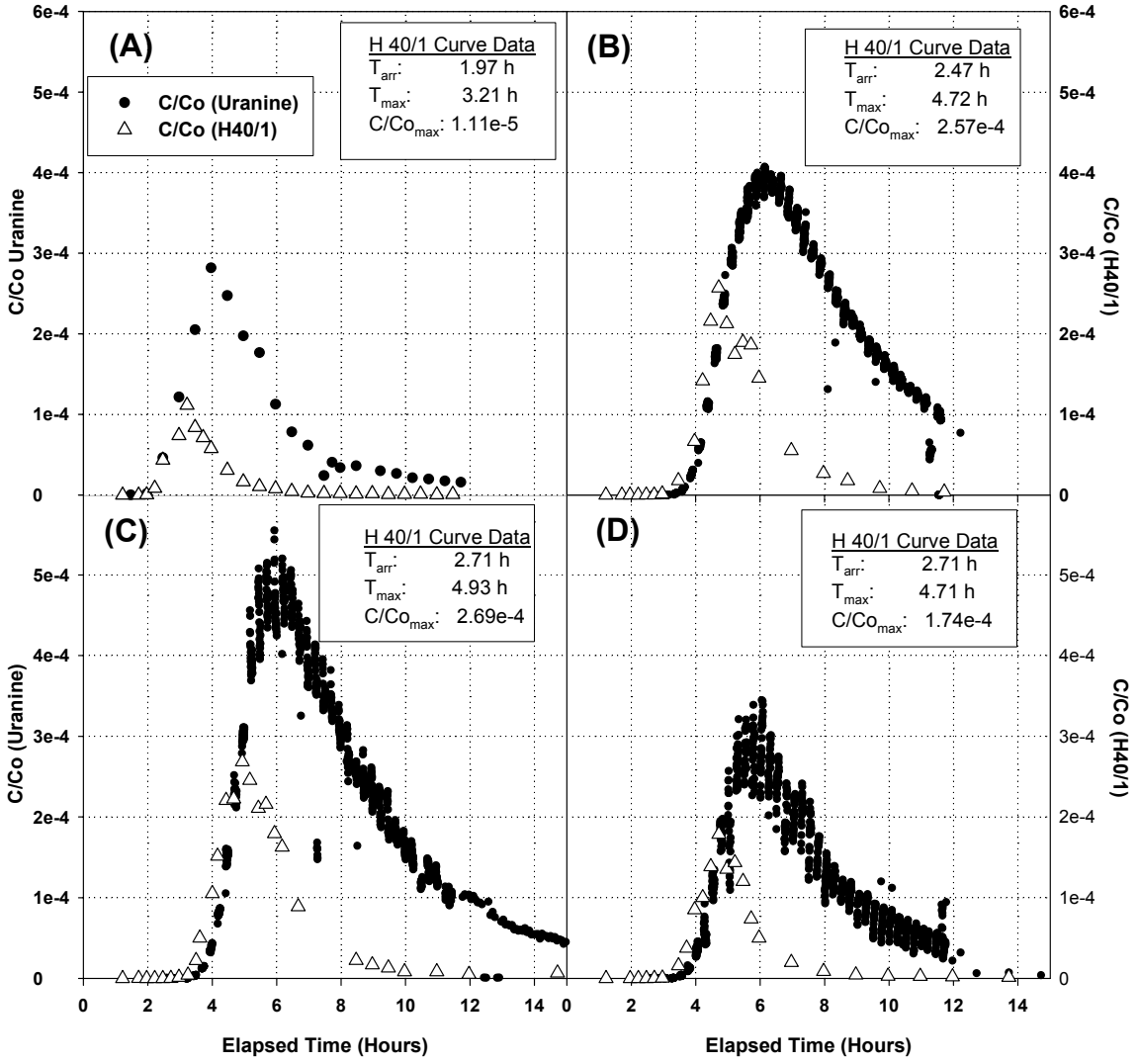

Figure 4.7: Uranine and H40/1 bacteriophage breakthrough curves generated from data collected at B8 during Low Flow #2. (A) 5mBGS (Y-Axis multiplied by 10 to allow scale comparison with other curves). (B) 11mBGS. (C) 12mBGS. (D) 13mBGS. H40/1 first arrival (T_{arr}), peak concentration time (T_{max}) and peak relative concentration (C/Co_{max}) presented in inset for each curve. Curve at 5.5m generated from grab sample analyses. Remaining curves generated from on-line measurements.

It is noteworthy that the Downhole #1 and Downhole #2 tracer concentration profiles, measured over the 7 to 14mBGS interval, display a consistently high tracer concentration at 12mBGS with maximum concentrations occurring approximately at this depth during both tests (Figure 4.7). Furthermore, this phenomenon was apparent during the recession phase of the breakthrough curve, i.e. concentrations remain greatest at approximately 12mBGS even

though whole well concentrations were declining. These observations are consistent with the results of low flow monitoring during Low Flow #2, where maximum tracer concentrations were also observed at 12 mBGS .

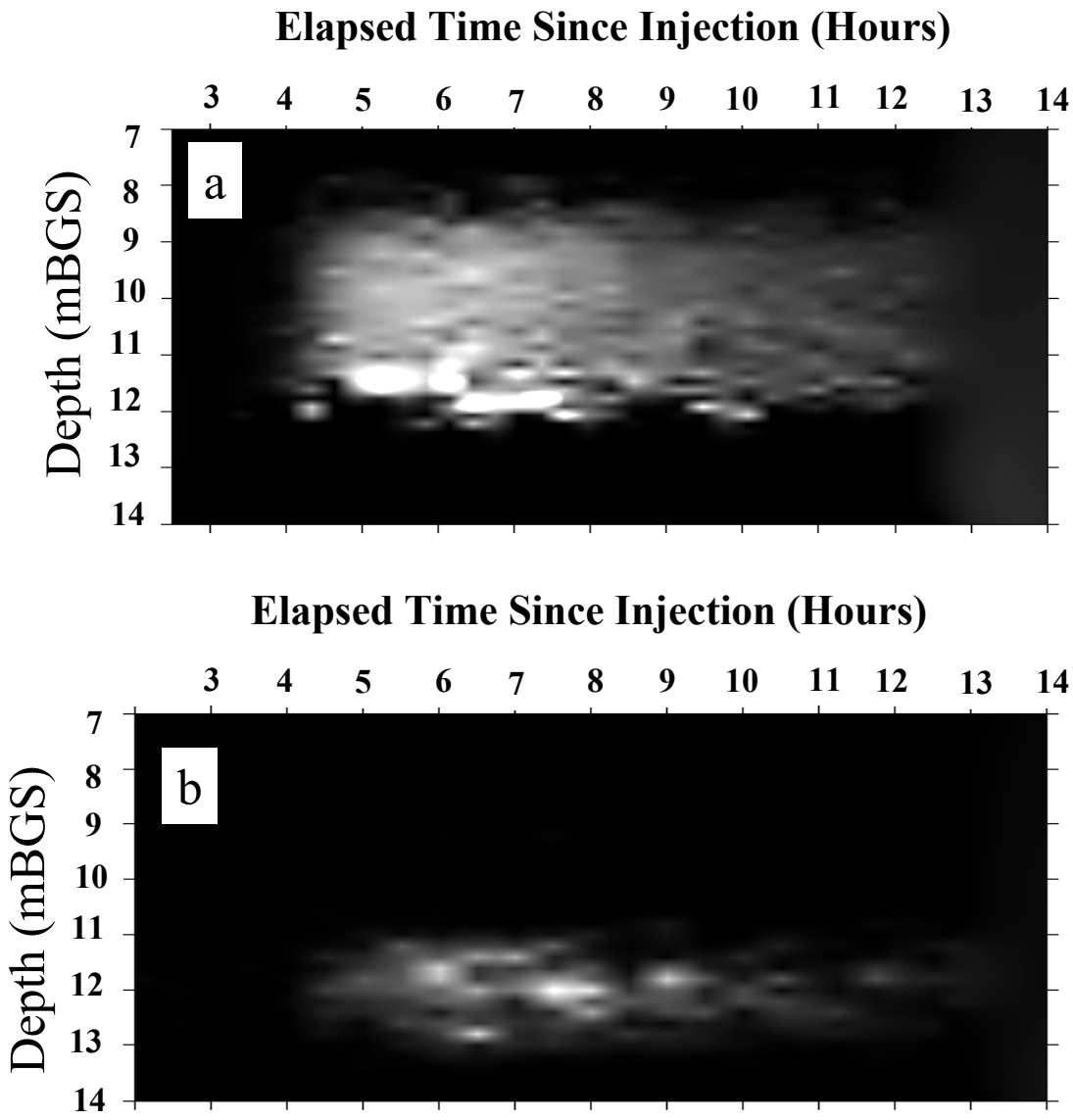

Figure 4.8: Image maps representing tracer relative concentration with depth measured at half hourly intervals at observation well B8, Dornach Test Site. (a) Measured 27-28 June 01 (Max tracer C/Co 1.54 x 10-3) (b) Measured 7-8 August 2002 (Max Tracer C/Co 5.05 x 10-4). Maximum Uranine concentrations represented as white.

Uranine concentration profiles generated from single well dilution test results from B8 are consistent with the results of whole well tracer tests in that they suggest that groundwater flow rates through B8 may exceed 80m/ day.

Approximately seven minutes after tracer injection along the entire screened interval, the tracer has declined to between approximately 80% and 0.05% of its original concentration in the zone between 6 and 14.5 mBGS. The concentration profile observed is provided in Figure 4.9. It is noteworthy that the concentration declines along the entire screened interval, with a notable peak between 8m BGS and 10 mBGS. This pattern is consistent for all test repetitions in B8.

Figure 4.9 also summarises the results of the vertical flow measurements. These measurements indicate that vertical flow gradients vary in magnitude and direction with depth in B8. Notably, vertical flow data show that the peak observed at approximately 9 mBGS during single well dilution tests corresponds to a zone where upwelling and downflowing wellwater converge, and where flow becomes horizontal. These results indicate that water flows into this zone before discharging to the aquifer. This situation contrasts with measurements made in the upper part of the well at approximately 5.5 mBGS which indicate that water enters the well at this level from the aquifer before starting to flow both upwards and downwards in the well.

The vertical flow data from B8 also indicate that the well water flow regime is more complex toward the base of the well. Well water flows upward from near the base of the well at a rate that gradually increases approaching to approximately 12.5 mBGS. Test data indicate that no vertical flow occurs between 12 and 12.5 mBGS suggesting that it is a zone of horizontal flow. Measurements in the water column above this zone suggest that water flows upward once again to the convergent flow zone at 9.5mBGS. The absence of indicators of vertical flow at 12 and 12.5mBGS is unusual since upward flowing water occurs on either side of this zone.

This suggests that a pressure gradient is present across the horizontally flowing zone and vertical flow phenomena should be observed. However, the phenomena are absent. A thin divergent flow zone present in the 12.0 to 12.5 mBGS interval could generate sufficient pressure to act as a hydraulic barrier to prevent upwelling water from crossing the 12 to 12.5 mBGS zone. As the results of the vertical flow tracer testing indicate that none of the injected tracer reached the sondes measurement cell, the downward-flowing water would need to start flowing horizontally once again and leave the well before the tracer could enter into the fluorometers sampling chamber. A thin zone of divergent flow is thus proposed to occur between 12.0 and 12.5 mBGS between the two vertical flow measurement points. The suspected zone was set at 12.3 mBGS in the numerical model of the well water flow regime. This depth corresponds to the zone where sharp declines in Uranine concentration were observed during Downhole #1.

Figure 4.9: Single well dilution test profile of Uranine concentration measured in well B8 at the Dornach Test Site using the downhole fluorometer, 10 August 2002. Measurements were taken between 4 and 11minutes after tracer injection. Arrows on the right-hand side of the plot indicate points of measurement and direction of vertical flow in the well. (Upward flow: Positive. Depth in metres below ground surface.)

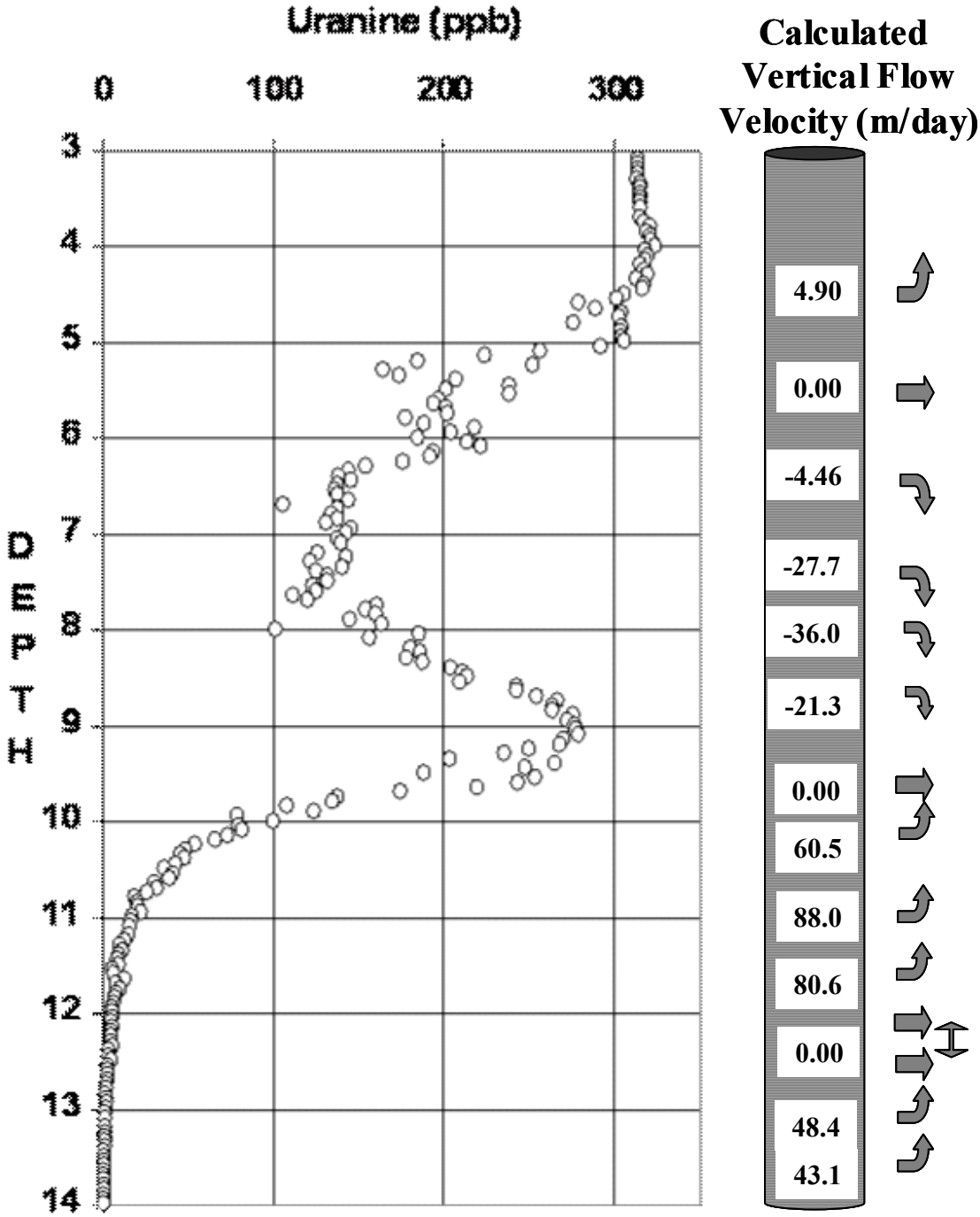

4.7.3 Modelling

Figure 4.10a presents the results of the wellwater flow model produced for B8. The data show that the calibration parameter values used can adequately reproduce the observed data within the constraints specified. The values of $q(z)_h$ selected are presented in Figure 4.10b as a profile with depth. The velocities calculated using the numerical model are the velocities of water leaving the well screen for each depth interval. Using the constraints imposed in equation (4.3), the velocities of the water entering the well can be back calculated when vertical flow rates are known. The entrance velocities are also presented in a depth profile in Figure 4.10b. Figure 4.10c graphically represents the results of the tracer arrival simulation in the well using the hydraulic parameters determined from the model calibration of single well dilution test data.

4.8 Discussion

The results of the Laboratory experiments demonstrate that the fluorometer is capable of detecting fluorescent tracer in a water column with an accuracy of plus or minus 25 cm, despite temporary storage effects and mixing effects in the borehole resulting from sondes movement. The consistent occurrence of low/high concentration points at the zone of active flow during respective well dilution tests/tracer arrival tests indicate the mobile downhole fluorometer is effective at detecting preferential flow zones. However, the process of identifying preferential flow zones is more complicated in wells where water flows vertically, as vertically flowing water spreads the tracer through the water column by advection. Nonetheless, consistent peak concentration measurements at the depth of tracer entry into the borehole still permit these zones to be identified.

Tests employing the downhole fluorometer to measure vertical flow rates have also demonstrated that the meter can determine the magnitude and direction of vertical flow. This method can provide a cost-effective and portable means of determining vertical flow rates in rapidly flowing shallow hydrogeological systems when alternative vertical-flow measurement devices are not available.

The variable tracer breakthrough curves generated from whole-well tracer test data at the Dornach demonstrate that the deposits underlying the site exhibit spatial and temporal variations in mass transport properties. However, the

continuous recirculation method used in Whole Well #1 and Whole Well #2 to monitor for Uranine prevented identification of the contributing horizons along the 12m long screened interval ,set against saturated deposits in B8. Low flow sampling for tracer at different levels in well B8 during Low Flow #1 demonstrated that the tracers arrival in the well was not uniform and that different tracer responses could be observed at different levels in the well. In particular, the contrast between samples collected at 14 and 12mBGS in B8 during Low Flow #1 demonstrates the extreme variability in tracer concentration that can be observed over short distances in wells with long-screened intervals. In contrast, the results of Low Flow #2 demonstrated that consistent solute concentrations occurred in the 11mBGS to 13mBGS zone. Moreover, bacteriophage breakthrough curves generated for the three sampling points within this interval show that similar phenomena were apparent for the virus tracer

Following injection in B1, fluorescent tracer monitoring in B8, using the mobile downhole fluorometer allowed zones of tracer occurrence in the observation well to be identified. The results of both Downhole#1 and Downhole #2 indicated that Uranine was detected in two distinct zones separated from each other by an interval where no significant quantity of tracer was apparent. Concentrations were greatest in the 9mBGS to 12.5mBGS zone, while those in the shallower 4.5 mBGS zone were approximately an order of magnitude lower. The earlier, but lower, peak concentrations observed at the shallower depth during Downhole #2, suggest that the tracer here may be the lateral edge of a more rapidly flowing finger of the tracer plume.

Single well test results and vertical flow test results indicate that groundwater containing no detectable quantity of tracer entered B8 during Downhole#2. Indeed, numerical modelling results simulating the concentrations observed during single-well dilution tests indicate that the velocities of water entering observation well B8 at numerous horizons are comparable to those in the horizon supplying tracer to the well at approximately 12mBGS. These data suggest that the groundwater entering B8 at various levels has not flowed via the injection well B1, but rather arrived at B8 via alternative routes. Otherwise, this water would also contain tracer. Conversely, the breakthrough tracer data obtained from measurements taken at 4-5.5mBGS indicate that some groundwater flowed through B1 and picked up tracer en route. However, the lower tracer concentrations and earlier peak times suggest that this part of the tracer plume did not pass directly through observation well B8. Both lines of evidence suggest that the direction that groundwater flowed in the gravel deposits underlying the Dornach test site was not uniform but varied with depth. This hypothesis is consistent with the greater peak concentrations in observed in B7 compared to those in B8, during Whole Well Test #2.

The forms of the tracer distribution profiles observed in B8 during Downhole#1 and Downhole#2 are similar to those noted during tracer arrival tests generated by the fluorometer using the Lab borehole apparatus, when a vertical flow regime is operating. The consistently high peak concentrations at approximately 12mBGS in B8 suggest that this is the main zone of tracer arrival. Tracer entering the well at this point is subsequently redistributed in the well by vertical flow gradients while being diluted by tracer-free water. These data thus imply that the zone supplying tracer to B8 is thinner than the zone of Uranine occurrence in the well. Indeed model simulations of tracer arrival bear a strong similarity to tracer arrival patterns observed in the field and contain tracer at similar concentrations and at similar depths to those observed (Figure 4.9c). During this simulation, the zone of tracer arrival was set at 0.5m thick. This result emphasises the importance of aquifer heterogeneities in the transport of groundwater tracers to observation wells as well as the potential for long-screened wells and open boreholes to act as conduits for the redistribution of contaminants to other horizons in an aquifer.

4.9 Conclusions

Laboratory-based investigations of the application of a mobile downhole fluorometer demonstrated that the meter can be used to detect zones of preferential groundwater flow and tracer arrival in a well. Moreover, by modifying the fluorometer to allow tracer injection at a fixed separation in a well, the apparatus may be used to determine the direction and magnitude of vertical flow gradients. Applications of these techniques at a sand and gravel aquifer groundwater test site demonstrated that the meter may be used to understand well water flow dynamics and detect zones of tracer arrival. When the results of single well dilution tests, vertical flow testing and tracer arrival tests are considered together, the well water flow regime may be numerically modelled. Modelling results for a fully penetrating observation well indicated that during tracer arrival tests, tracer could have entered B8 in a zone no more than 50cm thick and be spread over a larger screened interval by vertical gradients. Entrance and exit velocities demonstrate that water flowed into the well at comparable velocities from other horizons but did not contain tracer. These data indicate that groundwater flow trajectories in the aquifer varied with depth.

Figure 4.10: Numerical modelling results for well B8, Dornach Test Site.
(a) Observed and simulated single well dilution test results.
(b) Profile of horizontal flow velocities entering and exiting the well.
(c) Observed and simulated tracer arrival concentration profiles. Arrival at 12 to 12.5mBGS.

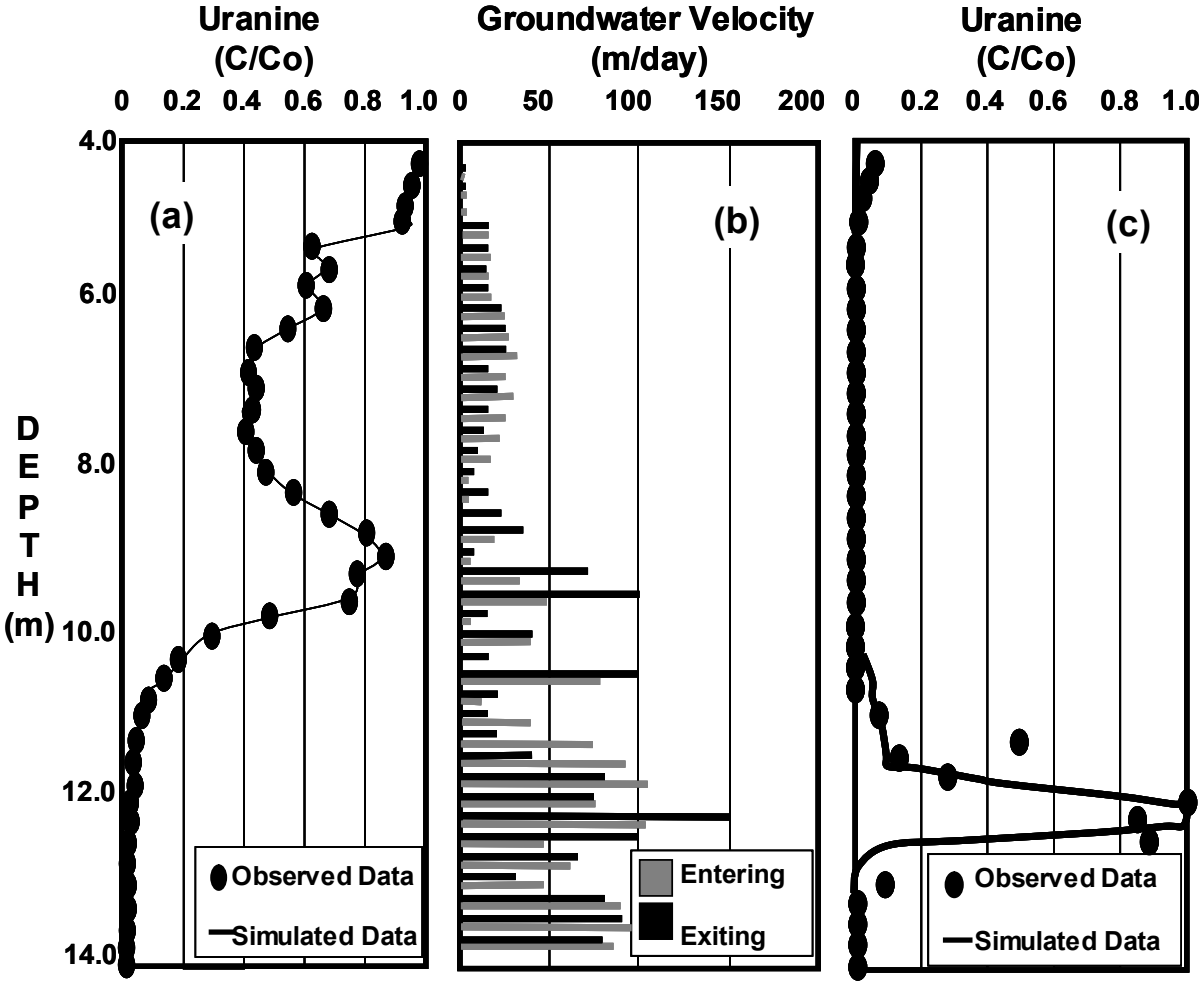

Chapter 5 :Bacterial and Viral Tracer Transport in a Highly Permeable Gravel Aquifer

5.1 Abstract

Comparative tracer testing using the bacteriophage *H40/1* and the bacteria *E.coli* and *P.putida* (biocolloids) with Uranine demonstrated that the capacity of a fluvioglacial gravel aquifer to attenuate biocolloids varied spatially. High *E.coli* relative recoveries suggested biocolloid attenuation was dominated by physio-chemical filtration, and that straining was insignificant. Despite its smaller size and lower collision efficiency, *H40/1* was not significantly more mobile than bacterial tracers. Maximum relative concentrations of bacterial tracers greater than those of solutes indicated size exclusion processes affected biocolloid transport. These processes also resulted in biocolloid breakthrough curves having lower dispersions and higher interstitial velocities than non-reactive solute tracers. Analysis of late time data indicated that all three biocolloids were reversibly adsorbed to some degree. Test results show that in the absence of inactivation on grain surfaces, reversibly adsorbed contaminants had the potential to pose a greater threat to public health than non-reacting contaminants, due the prolonged persistence of low but potentially infectious concentrations of biocolloids in groundwater.

5.2 Introduction

Recent years have seen a considerable increase in concern over drinking water quality in both the developed world and in the developing world. Microbiological contamination, due to the presence of pathogenic viruses, bacteria and protozoa (pathogens) has been an issue of particular concern. In 1999, the World Health Organisation estimated that water related illnesses caused over 2.3 million deaths worldwide (WHO, 1999). Keswick and others (1982) demonstrated that bacteria, viruses and protozoa can migrate considerable distance in aquifers, indicating that a portion of the water-borne illnesses cited are groundwater derived. Indeed, a survey of groundwater supplies in South Africa by Mackintosh & Colvin (2003) indicated that almost all rural groundwater supplies in the Western Cape were microbiologically contaminated. These authors noted that such poor water quality contributes significantly to water-borne illnesses that cause an estimated 43,000 deaths nationwide every year. Similarly, Macler and Merkle (2000) estimated that a significant proportion of the 750,000 to 5.9 million groundwater-related illnesses occurring in the United States (US) every year were a result of microbial contamination, reflecting the threat posed by pathogens to groundwater quality, even in developed nations.

The prevalence of microbiological contamination of groundwater supplies in the US has spurred the United States Environmental Protection Agency (USEPA) to propose a set of regulations known as the Ground Water Rule (GWR) as a means of reducing the threat of pathogen-contaminated groundwater to public health (USEPA 2000). The GWR recognises that certain aquifer types are “hydrogeologically sensitive”. Hydrogeologically sensitive aquifers have a low capacity to attenuate pathogens and include gravel aquifers.

Gravel aquifers constitute an economically important source of groundwater in many parts of Central Europe. Huggenberger (1993) noted that fluvioglacial gravel outwash deposits from braided river systems make up more than two thirds of aquifers in Switzerland, where groundwater constitutes approximately 80% of the total water supply (SAEFL, 2003). These types of aquifers can be highly heterogeneous, both in terms of texture and composition (geochemistry) (Huggenberger & Aigner, 1999). Moreover, because of their heterogeneity, fluvioglacial gravel aquifers often have complex groundwater flow regimes with preferential flow zones that can give rise to contaminant plumes that depart considerably from those generated by numerical modelling under assumed idealised conditions (Anderson and others, 1999). Tracer tests carried out in these types of deposits have demonstrated that the rapidly flowing groundwater may transport contaminants at rates of over 100 meters per day under passive gradient conditions (Rossi and others, 1994). Consequently, contaminants entering these types of aquifers may reach potential receptors in a short period. This has important implications for groundwater contamination by

pathogens where concentrations of microbiological contaminants can decline with the length of time spent in an aquifer.

In a review of particle transport through porous media, Mc.Dowell-Boyer and others (1986) recognised that particles, including pathogens, may be removed by three attenuation mechanisms, caking, straining and physico-chemical filtration. Caking occurs where particles are of comparable size or larger than pores and accumulate at the surface of a porous material. Straining occurs when particles are typically ≥5% of the average pore diameter; this allows particles to enter into a porous medium, where they are mechanically removed in smaller pores. Physico-chemical filtration takes place when particles are very small relative to the porous mediums grain size. During physico-chemical filtration, particles tend to be removed by chemical and physical forces between the particles and porous medium.

In most aquifers, bacteria (ø≤1μm) and protozoa (ø≤10μm) may be removed by physico-chemical filtration, although straining may contribute to overall attenuation. Although the largest viruses are comparable size to the smallest bacteria, viruses as a group are smaller than other micro-organisms. Consequently their removal from porous media tends to be more strongly dominated by physico-chemical filtration forces. Indeed, because of their small size and their suspected enhanced mobility relative to other micro-organisms, viruses have been made the focal point of the GWR (Macler & Merkle, 2000), where they are used to evaluate the natural disinfection capacity of an aquifer. Natural disinfection is defined as “source water treatment via virus attenuation by natural subsurface processes such as virus inactivation (loss of virulence), dispersion (dilution) and irreversible sorption to aquifer framework solids” (USEPA, 1992). However, the determination of the disinfection capacity of aquifers has proven difficult; this is largely because mechanisms controlling pathogen transport and attenuation remain poorly understood (Macler & Merkle, 2000).

In order to further understand pathogen transport and attenuation processes in aquifers, a number of research programs have been undertaken in recent years to investigate these phenomena in detail. Many of these studies have been completed in the laboratory. The controlled conditions imposed in laboratory investigations permit attenuation mechanisms to be more confidently identified (Harvey and others, 1993). However, laboratory systems simulate aquifer pore structure to a limited extent. Indeed, studies by Smith and others (1985) highlighted the importance of natural soil structure in controlling the transport of microbiological contaminants, which may not be observed in repacked soil columns commonly used in laboratory studies.

McDowell-Boyer and others (1986) argued that the results of Smith and others (1985) emphasised the importance of field studies of particle transport to complement laboratory-based investigations. Field-based experiments studying

microorganism transport typically involve injecting solute and particle tracers into an aquifer and monitoring tracer responses at one or more observation points (Harvey and others, 1991; Bales and others, 1995; DeBorde and others, 1999). Particles are generally colloid sized (10^{-6}m to 10^{-9}m along at least 1 axis) and may be of inorganic origin (inorganic colloids), organic but non-biological colloids (e.g. humic acids), or biological particles (biocolloids). Both inorganic colloids and biocolloids have been used in field-scale experiments investigating micro-organism transport (e.g. Bales and others, 1997; Ryan and others , 1999). However, biocolloids have the added benefit that they may undergo similar attenuation processes to the microbiological contaminant of interest, e.g. inactivation (Ryan and others, 2002). Both bacteria and viruses have been used as biocolloid tracers in numerous field studies over the past 15 years (Harvey and others, 1989, Harvey and others, 1991, Bales and others, 1995, DeBorde and others ,1999, Ryan and others, 2002).

In a review of the use of micro-organisms as tracers in groundwater systems, Harvey (1997) noted that in relatively homogeneous media, microbiological tracers that do not become immobilised exhibit similar responses to conservative solute tracers. However, as aquifer physical heterogeneity increases, the dissimilarity between particle and solute tracer responses increases. Ginn and others (2002) reviewed work investigating this phenomenon using bacteria-size tracers and noted that it was believed to be a result of exclusion processes that may prevent colloids from flowing through the slower flowing parts of the effective porosity accessible to solutes. The overall result is that biocolloid tracers may be transported at faster average velocities than solutes, and the resulting particle breakthrough curve may have a lower dispersion. Consequently, biocolloid transport through heterogeneous aquifers where exclusion processes are operational may result in lower biocolloid attenuation due to reduced dilution. This may increase the maximum concentrations observed at a monitoring point. In the case of viral contamination, this diminished attenuation may reduce an aquifers natural disinfection capacity.

Work investigating biocolloid transport in groundwater in rapidly flowing gravel aquifers has tended to focus on virus transport (Rossi and others, 1994, DeBorde and others, 1999, Kennedy and others, 2001b, Woessner and others, 2001). This work has provided important information on the viral attenuation capacity of these types of deposits and, in some cases, highlighted the importance of textural heterogeneities in controlling virus transport (Kennedy and others, 2001b). To date however, comparative studies of bacterial and viral migration in this aquifer type have been largely neglected.

This paper describes tests carried out in a coarse grained fluvioglacial gravel aquifer. These tests compare the transport and attenuation of bacteria and viruses. The behaviour of two different bacteria of similar size but suspected of having different physico-chemical surface properties is compared with that of a bacteriophage (bacterial virus or phage), which had been previously been used

in tracer tests in hydrogeologically similar deposits at other locations. Examination of the results of these studies have been used to ascertain the relative importance of various attenuation processes operating on bacteria and viruses as they flow through fluvioglacial aquifers, and to evaluate their implications in terms of their potential impact on public health.

5.3 Site Description

The Dornach Groundwater Test Site (Dornach-Figure 5.1) was instrumented in 1968 and forms part of the Munich Gravel Plain Aquifer, Germany (Seiler, 1970). Tracer testing at Dornach has previously been used to study the migration of various contaminants in groundwater, including arsenic and cadmium (Zahn & Seiler, 1992), and dissolved organic carbon (Müller & Seiler, 2001). Moreover, groundwater derived from this aquifer caused an outbreak of dysentery in the nearby village of Ismaning in 1978, thus reflecting the vulnerability of the aquifer to microbiological contamination.

Grain size analyses of 110 samples of borehole cuttings collected during monitoring well installation at Dornach showed that the site was immediately underlain by approximately 14 metres of poorly sorted Quaternary gravels, with the diameter of the finest 10% of grains in each sample (d_{10}) ranging from 60μm to 600μm (Klotz and others, 1980). Analysis of samples of aquifer material indicated the aquifer consisted of approximately 90-98 % limestone and dolomite clasts, 1-2 % quartz fragments, 0.5-3 % crystalline igneous and metamorphic material and 1-8 % sandstone clasts. Fine-grained Tertiary sands and silts underlie the gravel aquifer (Müller & Seiler, 2001).

Dornachs monitoring network consists of seven wells set in a semicircular array and an eighth well bisecting the diameter (Figure 5.1). The wells vary in internal diameter (ID) from 2 to 8 inches ID (5.08 to 20.32 cm). All wells are fully penetrating and screened against the entire saturated thickness of the gravels. Due to low effective porosity (n_e = 11 ± 1 %, at $n_{total} \approx 25\%$) the groundwater table, at about 2 ± 1 metres below ground surface (mBGS), is subjected to substantial precipitation-induced fluctuations, which can affect the groundwater flow velocity between the wells (Männel, 2002). Chemical analyses of water samples carried out during the course of previous studies at the site indicated that the Dornach aquifer contained cold (10° C) aerobic, calcium bicarbonate type groundwaters (Zahn and Seiler, 1992).

5.4 Materials

In order to gain a fuller appreciation of bacterial and viral (Biocolloid) transport and attenuation processes in the Dornach sands and gravels, a series of tracer tests were carried out. The transport of two bacterial tracers and a viral tracer were compared with that of a conservative solute tracer. The bacterial tracers used were *Escherichia coli (E.coli)* and *Pseudomonas putida (P.putida)*.

The bacteriophage (bacterial virus or phage) *H40/1* acted as the viral tracer. In all cases Uranine was employed as the conservative solute tracer. Käss (1997) summarised the results of a series of tracer experiments using Uranine and noted that, except in the case where significant quantities of organic matter are present, Uranine was not retarded or attenuated in the deposits under investigation. Moreover, a comparative tracer test carried out at Dornach in the wider framework of this study using bromide and Uranine showed that both tracers had almost identical breakthrough curves, thus corroborating the assumption that Uranine behaves conservatively.

H40/1 and *P.putida* were not detected in the groundwater prior to tracer testing. *E.coli* was occasionally detected in Dornach groundwater samples at background levels of 1-2 colony forming units per decilitre (Cfu/100mL); these bacteria are derived from organic fertilisers used on the agricultural land surrounding the site.

E.coli, normally originates from the intestinal tract of warm-blooded animals. This bacterium is a peritrich flagellated, rod (0.5μm x 2 μm) (Maki and others., 2000), belonging to the γ-subgroup of *proteobacteria*. *E.coli* DSM 498, the subspecies used in Dornach, belongs to risk class 1 (no risk for health and environment) and has an optimal growth temperature of 37°C. *E.coli* requires a nutritient-rich medium for growth. Zeta potential measurements made by Jucker and others (1999) indicated that the strains *E.coli* 07 & *E.coli* 08 had zeta potentials of -44.8mV and -25.6mV in 0.1M KCl (pH 7.2) solution reflecting not only their net negative surface charge, but the variability of this property between different strains. Similarly, contact angle measurements made for these two strains with water suggested that they were hydrophilic (Contact angles of 29° and 36° for *E.coli* 07 and *E.coli* 08 respectively).

The non pathogenic bacterium *P.putida* is a gram negative rod (1 x 3-4 μm) with polar flagella that belongs to the γ-subgroup of *proteobacteria.* *P.putida* inhabits soil and water (Brock and Madigan, 1991). Jucker and others (1996) noted that, unlike *E.coli*, *P.putida* is hydrophobic and had a negative zeta potential (-25mV) based on measurements made in 0.01mM KNO_3 solution (pH range 7-8). This negative potential reflected *P.putidas* net negative surface charge at ambient groundwater pH.

Both *E.coli* and *P.putida* were grown in liquid Luria broth medium for 15 hours, harvested by centrifugation at 5000 x g for 10 min and washed twice with sterile 0.9 % NaCl solution to remove nutrients. Finally the pellet was suspended in 0.9 % NaCl solution and stored at 4°C until its use in field tests.

Prior to tracer testing, aliquots of water were sampled for to evaluate background levels of bacterial tracer. Analyses, following the same procedures as used on subsequent samples, showed that *E.coli*, derived from organic fertilisers used on the surrounding agricultural land, could occur in water samples

at levels of 1-2 colony forming units per 100 ml (cfu/mL). *P.putida* was not detected in background samples.

For detection and enumeration of both bacterial tracers, water samples of up to 100mL were filtered through 0.45 µm membranes (Millipore). *E.coli* DSM 498 was incubated on Endo Agar (Merck) at 37°C for 24 to 36 hours. The remaining water in each sample was stored in dark conditions at 4°C, to allow further incubation of less concentrated samples in case that bacterial counts were too high. *P.putida* was incubated on mineral salt medium with benzoate as single carbon source at 30°C for 36-48 hours. All groundwater samples collected for bacterial analysis were analysed in duplicate. Concentrations varied around the average analysed value by ± 20%. Information concerning *H40/1*s zeta potential/hydrophobicity are provided in Chapter 2, along with details of how this phage was concentrated and assayed.

Prior to their use in the field, aliquots of each of the biocolloid tracer stocks were mixed with site groundwater and stored at ambient groundwater temperatures, throughout the duration of each tracer test. Regular sampling and analyses of this water permitted the inactivation rates of the biocolloid tracers suspended in site groundwater to be determined.

5.5 Tracer Test Methodology

Figure 5.1 presents the monitoring well array at the Dornach Test Site. Two tests were carried out on consecutive days during two separate investigation periods in July 2000 and May 2001, under natural gradient conditions. *E.coli* acted as the bacterial tracer during the July 2000 study, while *P.putida* was used in May 2001. The response of *H40/1* was studied during both investigation periods. During each period, 100mg of Uranine was injected with a bacterial tracer as a slug, either simultaneously in the case of *E.coli*, or 15 minutes beforehand in the case of *P.putida*. Injection of the bacterial tracer and Uranine was followed 24 hours later by a second test in which slugs of Uranine (100mg) and *H40/1* were simultaneously injected. *H40/1* was injected during both the July 2000 and May 2001 investigation periods to investigate whether the virus attenuation characteristics between the injection well and monitoing wells varied temporally. A second pulse of *H40/1* was injected eight hours after the initial pulse during the May 2001 experiment to verify experimental repeatability and to assess the degree to error associated with analytical noise.

Both the injection well (B1) and the observation wells (B7 and B8) contained tubing connected to suction pumps that drew water from the base of the well to the ground surface at a rate of ca.17 l/min, where it passed through an on-line fluorometer. Measurements made using the fluorometers allowed Uranine concentrations to be determined at intervals as low as one per minute, thus permitting Uranine injection and breakthrough signals to be generated with a high degree of accuracy. After passing through the on-line monitoring system, the

pumped water was re-injected into the injection well at the water table. Times taken for circulation of a single well volume were approximately 1.5 minutes for B1 and B7 and 23 minutes for B8.

Since the water levels in the wells remained static, the hydraulic gradient and thus the velocity of groundwater flowing through the wells is assumed to be unaffected by the on-line monitoring procedure. Rates of tracer concentration decline in the injection well were such that the assumption of instantaneous injection of tracer into the aquifer was practically fulfilled. (1% of the original tracer concentration was observed in groundwater circulating in B1 20 minutes after the start of injection). This assumption was confirmed using a preliminary numerical model in which the injection signal was convoluted with a temporal Dirac transfer function to simulate tracer transport, and compared to the results of simulations using the transfer function alone. The results of the two outputs demonstrated negligible differences.

Previous field-based studies in deposits hydrogeologically similar to those observed at Dornach have shown that bacteriophage first arrivals at monitoring wells can occur at, or slightly before those for the solute tracer (Kennedy, 2001). Consequently the output from the on-line fluorometers was used to modify sampling and analysis strategies for the biocolloid tracers to allow first arrivals to be detected with a high degree of resolution (±15 minutes).

Water samples, collected at the monitoring well reinjection points, were maintained at 4°C to 8°C to inhibit processes that may accelerate biocolloid inactivation due to elevated ambient temperatures. All biocolloid tracer samples were analysed within 48 hours of sampling. Uranine samples collected for laboratory-based spectofluorometric analyses, to calibrate on-line field fluorometer data, were collected and preserved in a similar manner to the biocolloids. Solute and biocolloid tracer monitoring continued over at least a 24 hour period following injection. Monitoring of bacterial tracer concentrations during each investigation period continued until the end of subsequent tracer tests using bacteriophages, i.e. 48-52 hours after bacterial tracer injection.

5.6 Mass Transport Modelling

Numerical modelling of biocolloid tracer mass transport and attenuation in groundwater at Dornach followed the one dimensional approach used by Schijven and others (1999):

$$\frac{\partial C}{\partial t} = D\frac{\partial^2 C}{\partial x^2} - v\frac{\partial C}{\partial x} - kcC - \mu_l C + k_{\det}\frac{\rho_b}{\theta}S \qquad (1)$$

$$\frac{\rho_b}{\theta}\frac{\partial S}{\partial t} = kcC - k_{\det}\frac{\rho_b}{\theta}S - \mu_s\frac{\rho_b}{\theta}S \qquad (2)$$

where C is the tracer concentration in the groundwater (ML^{-3}), S is the concentration of adsorbed biocolloid (ML^{-3}), t is elapsed time since injection (T), x is the distance from the injection point (L), D is the hydrodynamic dispersion (L^2T^-

^{1}), v is the interstitial velocity (LT^{-1}) and kc is the first order rate deposition constant(T^{-1}), k_{det} is the release constant (T^{-1}), ρ_b is the bulk density of the aquifer material (ML^{-3}), θ is the aquifer porosity (-). μ_l and μ_s are the inactivation rates of biocolloids suspended in groundwater and adsorbed on aquifer materials respectively (T^{-1}). Chemotaxis (bacterial movement resulting from chemical gradients), which may affect bacterial transport, was assumed negligible due to the absence of evidence for chemical gradient across the site. Moreover, potential changes in the surface characteristics of viable bacteria were not believed to have a significant influence on breakthrough responses due to the short duration of the experiments.

Equation (1) and Equation (2) were solved numerically using the approach described in the Appendix at the end of this thesis. The conventional approach to modelling uses non-reactive solute tracers to determine transport parameters. Attenuation parameters are subsequently adjusted to fit the reactive tracer breakthrough curve. In simulating virus breakthrough curves using the model described in Equation (1) and Equation (2), Schijven and Hassanizedeh (2000) noted that overall the first order deposition and release terms control the breakthrough curve peak height, while the slope of the residual tracer tail is largely controlled by the inactivation rate of biocolloids adsorbed to aquifer materials. The position of the point of inflection between the breakthrough curve and the start of residual tailing is largely determined by the value of the kinetic release term. The model fitting process thus provides and indication of the attenuation capacity of the aquifer materials along the flow path connecting the injection well and monitoring point to be determined.

Since solute and particle tracers may behave differently in the same medium, should exclusion processes operate, an alternative means of simulating particle responses was developed. Following this approach, biocolloid relative recovery was calculated with respect to Uranine, but particle mass transport parameters were ascertained independently of those of the solute tracer. According to Harvey and others (1991), relative recovery (RR) is calculated as follows:

$$RR = \frac{\int_0^T \frac{Tr(t)}{T_0} dt}{\int_0^T \frac{C(t)}{C_0} dt} \qquad (3)$$

where Tr(t) is the biocolloid concentration at time t, C(t) is the conservative solute at the same time and T is the duration of the experiment. To and Co are the original concentrations of the biocolloid and solute tracers respectively.

Figure 5.1: Monitoring well construction map and geological cross section for Dornach Test Site, Germany (Modified from Müller & Seiler, 2001).

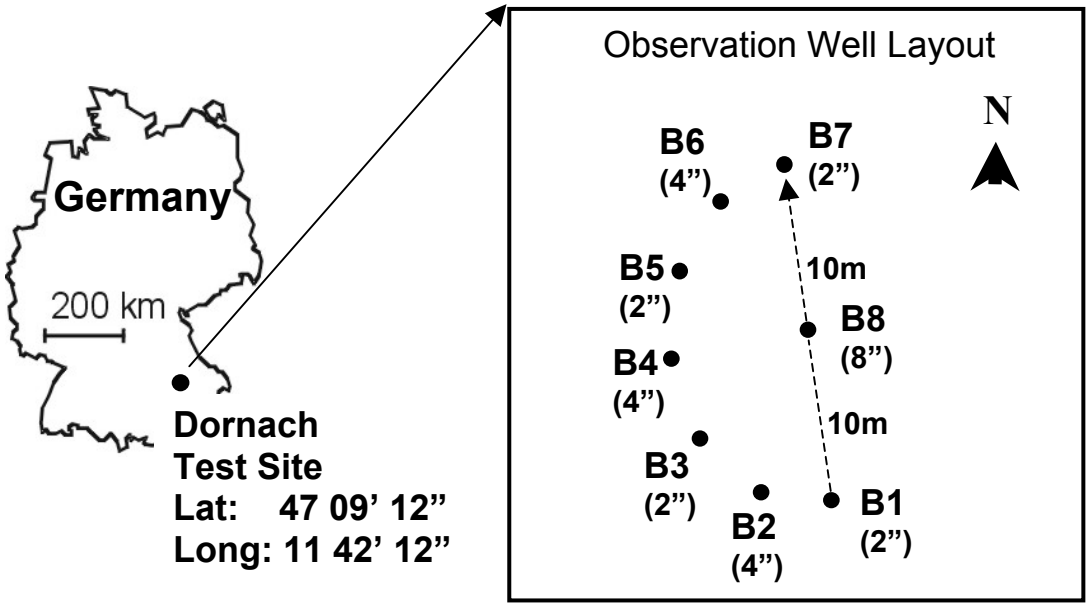

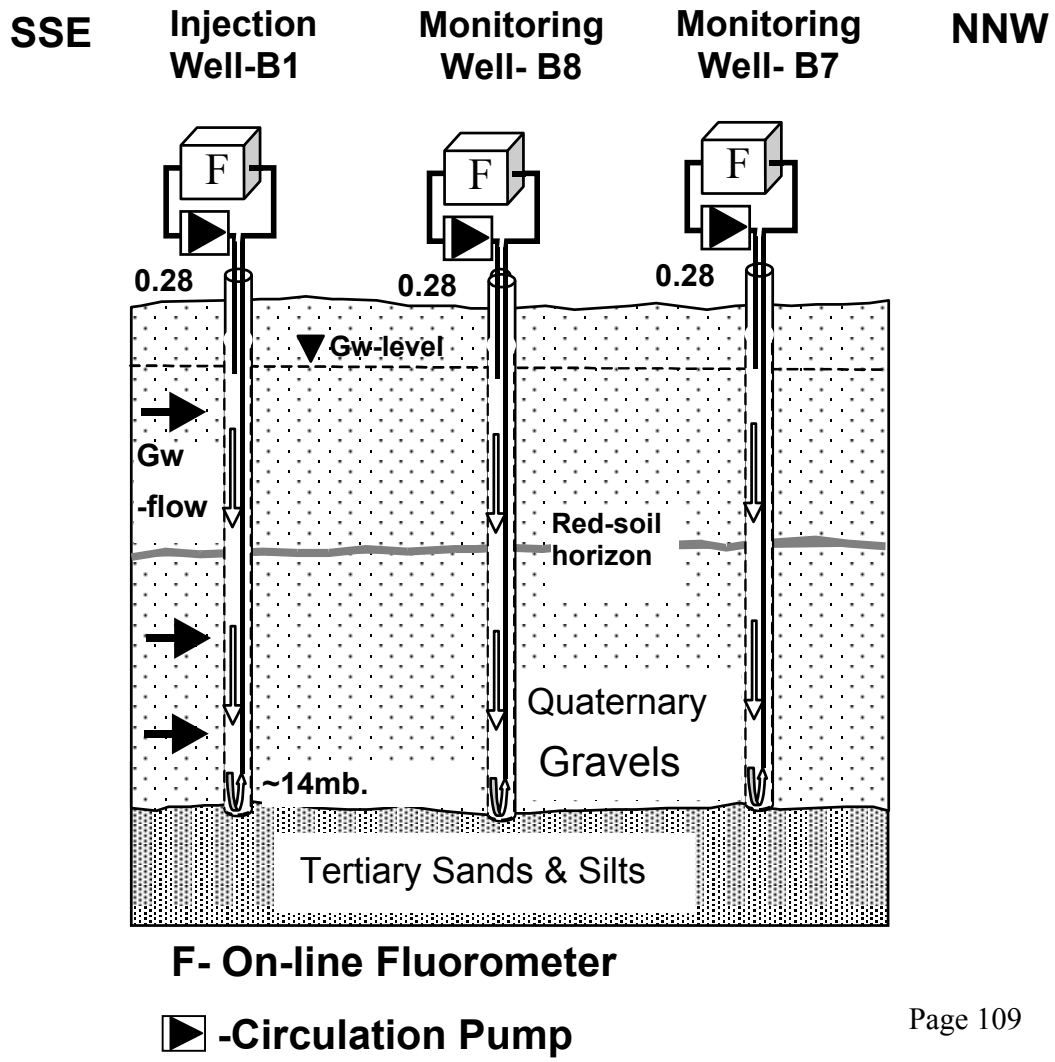

Interstitial velocity and dispersion are determined in this approach by curve fitting to observed biocolloid breakthrough curves. However, since the velocity calculated from the colloidal breakthrough curves overestimates its actual value, due to peak shift towards earlier time resulting from attenuation processes (Zhang and others 2001), an iterative fitting process is necessary to calculate the colloid transport parameters without the influence of attenuation.

The first step in the process involves initially assuming that the observed colloid breakthrough curve response is conservative and that no attenuation occurred. The computer program Traci (Werner, 1997) was used to determine the best-fit interstitial velocity and dispersion values for the one-dimensional biocolloid breakthrough curves obtained. The recovery determined from the resulting best fit breakthrough curve is assumed to be 100%. First order kinetic deposition, release and inactivation constants are subsequently applied, using the solution to Equation (1) and Equation (2), to generate the same biocolloid relative recoveries as observed in the field. Once a RR equivalent to that observed with the field data is obtained, the resulting attenuated curve is normalised relative to the observed colloid breakthrough curve by dividing the attenuated curve data by a correction factor CF, defined as follows:

$$CF = \frac{(Tr\max)_{attenuated}}{(Tr\max)_{nonattenuated}} \qquad (4)$$

where $(Tr\ max)_{attenuated}$ is the peak concentration of the attenuated curve, and $(Tr\ max)_{nonattenuated}$ is the peak concentration of the field curve simulated from the Traci program. Following this correction, velocity and deposition constants are progressively adjusted, while maintaining the same relative recovery, until the normalised attenuated curve corresponds to the biocolloid breakthrough curve observed in the field, thereby providing appropriate transport and attenuation parameters. Preliminary model simulations demonstrated that, unlike groundwater velocity, dispersion was virtually insensitive to the range of first order adsorption constants used, i.e the dispersion value did not change when deposition was simulated. Consequently dispersion values determined using the Traci program were applied in all subsequent calculations.

First order biocolloid deposition constants determined by the above process can be related to interactions between a microbial tracer and the aquifer material under ambient hydrodynamic conditions by the filtration theory of Tien & Payatakes (1979) as follows:

$$kc = \frac{3(1-\theta)}{2d_c}\eta\alpha v \qquad (5)$$

where d_c is the matrix size (L), α is the collision efficiency (-), η is the single collector efficiency (-) and θ is the porosity (-).

Equation (5) reflects a two-stage process. The first part of the process involves transporting particles to the surface, by interception, gravitation and

Brownian motion (Yao and others, 1971) defined by η. The second part of the process involves collisions with fixed surface resulting in the particle sticking or being repelled; this is expressed by α. Kretzschmar and others (1999) noted that α defines the probability of attachment resulting from a collision between a particle and a solid surface and reflects the attractive properties resulting from solution and surface chemistry. The single collector efficiency, is dependant on physical parameters in the system such as particle size, particle density, accessible surface area for deposition, pore structure and flow velocity. Using the Logan and others (1995) modification of Rajagopalan & Tien's (1976) model, η can be calculated as follows:

$$\eta = 4A_s^{\frac{1}{3}} N_{Pe}^{-\frac{2}{3}} + A_s N_{Lo}^{\frac{1}{8}} N_R^{\frac{15}{8}} + 0.00338 A_s N_G^{1.2} N_R^{-0.4} \qquad (6)$$

where

$$A_s = \frac{2(1-\gamma^5)}{(2-3\gamma+3\gamma^5-2\gamma^6)}, \gamma = (1-\theta)^{\frac{1}{3}} \qquad (7)$$

$$N_{Pe} = \frac{3\pi\mu d_p d_c q}{kT} \qquad (8)$$

$$N_{Lo} = \frac{4H}{9\pi d_p^2 q} \qquad (9)$$

$$N_R = \frac{d_p}{d_c} \qquad (10)$$

$$N_G = \frac{g(\rho_p - \rho_f) d_p^2}{18\mu q} \qquad (11)$$

where d_p is the particle diameter (m); μ is the fluid viscosity (9.3×10^{-4} Pas^{-1}); q is the specific discharge (m/s); k is the Boltzman constant(1.38048×10^{-23} J/K); T is the temperature (set at ambient groundwater temperature, 283° K); H is the Hamaker Constant ($1x10^{-20}$J); ρ_f is the fluid density ($998Kgm^{-3}$); ρ_p is the biocolloid density, (assumed to be $1080Kgm^{-3}$) and g is acceleration due to gravity ($9.81ms^{-2}$).

Equations (5) to Equation (11) therefore allow the physical and chemical properties of the aquifer to be related to those of the particle under investigation. Consequently, the filtration theory provides a means of understanding particle breakthrough responses in terms of grain size and compositional variations in an aquifer, once kc has been determined.

If collision efficiencies are determined based on particle responses at one observation point, the resulting values may be used to ascertain effective grain sizes attenuating particles at a second point, assuming geochemical homogeneity. However, should the calculated effective grain sizes determined for differently sized particles suggest unequal effective grain sizes, the data would thus imply that the collision efficiencies of the two particles are not the same as those calculated for the first observation point. Since water chemistry does not

vary significantly in the Dornach aquifer, the difference in collision efficiencies for a particle would thus reflect variations in the composition of aquifer materials.

5.7 Results

5.7.1 Tracer Responses – B7

Tracer test results for monitoring well B7 (Figure 5.2) obtained during both investigation periods show that Uranine breakthrough curves from tests completed on successive days have similar peak relative concentrations (C/Co max) that were observed at similar times (Table 5.1). In contrast curves generated during different investigation periods are more dissimilar. The maximum Uranine relative concentration occurred slightly later during the May 2001 investigation period than in July 2000. Moreover, the maximum relative concentrations were higher in May 2001. Nonetheless breakthrough curves show that during both investigation periods tracer relative concentrations returned to less than 5% of the maximum relative concentration observed 24 hours after injection. (Mechanical problems prevented measurements later than 17 hours after injection on May 16 2001. However, extrapolation, and analogy with the breakthrough curve constructed using data obtained the previous day, suggests that concentrations returned to comparable levels.)

The *H40/1* breakthrough curve for the July 2000 test at B7 (Figure 5.2a) shows that the maximum viral tracer relative concentration were observed slightly earlier than that of Uranine, but at a lower relative concentration (Table 5.1). Moreover, the rising limb of the virus breakthrough curve rose after that of Uranine and declined more rapidly after the peak concentration had been reached. Relative recovery calculated with respect to Uranine recovery, 24 hours after injection, showed that 17% of the virus injected was recovered. Indeed approximately 94 % of the total virus recovery was obtained within 10 hours of injection. However, residual quantities of H40/1 were still being observed at the end of monitoring (24 hours after injection).

The *E.coli* response at B7 during the July 2000 test contrasts notably with that of Uranine (Figure 5.2b). *E.coli* relative concentrations rose slightly earlier than those of Uranine, and peaked at a maximum relative concentration of 2.76×10^{-4} 5.05 hours after injection. After peaking, *E.coli* relative concentrations declined rapidly until approximately 13 hours after injection, where they stabilised at a value of approximately 1×10^{-5} until the end of monitoring (48 hours after injection). In contrast the maximum relative concentration of Uranine (2.06×10^{-4}) observed at B7 during the July 17 test was lower than that of *E.coli*, and was observed over 45 minutes later. Moreover, Uranine concentrations declined more gradually after their maximum concentration had been reached, but continued to do so until the end of the test. Indeed 24 hours after injection *E.coli* relative concentrations once again exceeded those of Uranine and continued to do so until the end of monitoring.

The influence of the low but constant *E.coli* concentrations observed at B7 after the main part of the breakthrough curve has passed resulted in a gradual rise in relative recovery until the end of monitoring. Indeed the *E.coli* cumulative recovery curve, which shows a rapid rise in relative recovery until approximately 9 hours after injection, continued to rise gradually to 63% at 24 hours after injection, increasing to 76% at 48 hours after injection, assuming negligible additional Uranine recovery 24 hours after injection at B7.

B7 breakthrough curves generated from 15 May 2001 data show that the *P.putida* and Uranine breakthrough curves differ significantly from one another (Figure 5.2d). However, the *P.putida* breakthrough curve displayed similar features to that of *E.Coli*, i.e. the rising limb of the bacterial breakthrough curve rose before that of Uranine and reached a higher maximum concentration. The temporal offset between the bacterial and Uranine peaks was larger than for *E.Coli* with a value of about 1.25 hours. *P.putida* relative concentrations decline more rapidly once peak concentrations have been reached. *P.putida* relative recoveries at 10 hours after injection (50.4%) were approximately equal to those observed for *E.coli* at this location at the same time (52%). However, unlike *E.coli*, *P.putida* concentrations did not stabilise at a constant level but continued to decline after the main breakthrough curve peak had passed 10 hours, resulting in a lower relative recovery 24 hours after injection (52%).

The results of repetitive testing with *H40/1* during the May 2001 investigation period, showed that the two bacteriophage pulses had approximately the same relative recovery, (26%±2%. Second pulse not plotted). The shape of the *H40/1* breakthrough curve at B7 in May 2001, although having a similar first arrival time and peak concentration time, had a higher relative recovery than that generated the previous July (Figure 5.2c). Moreover, the response of the virus breakthrough curve relative to that of Uranine differed from that previously observed. The rising limb of the *H40/1* breakthrough curve rose simultaneously with that of Uranine, before peaking at a maximum concentration slightly more than half (57%) of the solute tracer, and then declining more rapidly. Total phage recovery could not be calculated later than 10 hours after injection due to the introduction of the second pulse of *H40/1* into the aquifer at 8 hours after *H40/1*/Uranine injection.

Table 5.1: Summary table of tracer test breakthrough results. Dornach Test Site, Germany.

		B7				B8			
	Tracer	t_{arr}(hr)	t_{max}(hr)	C/Co $_{max}$	Relative Recovery (%)	t_{arr}(hr)	t_{max}(hr)	C/Co $_{max}$	Relative Recovery (%)
July 2000	Uranine	3.20[1]	5.89	2.06 x10^{-4}	-	2.37[1]	4.27	3.67 x10^{-4}	-
	E.Coli	3.05	5.05[2]	2.76 x10^{-4}	63(76)[3]	2.80	4.80[2]	2.98 x10^{-4}	77 (90)[3]
	Uranine	2.46[1]	5.31	1.76 x10^{-4}	-	2.09[1]	4.39	3.13 x10^{-4}	-
	H40/1	3.00	5.00[2]	8.77 x10^{-5}	17	3.00	4.25[2]	1.48 x10^{-4}	32
May 2001	Uranine	3.11[1]	5.94	2.46 x10^{-4}	-	3.13[1] (2.92)[4]	5.88 (6.08)[4]	2.15 x10^{-4} (1.75 x10^{-4})[4]	-
	P.putida	2.25	4.75[2]	2.98 x10^{-4}	52	2.76	5.00[2]	1.29 x10^{-4}	17
	Uranine	3.13[1]	6.04	3.04 x10^{-4}	-	3.13[1]	5.88	2.15 x10^{-4}	-
	H40/1	3.03	4.78[2]	1.74 x10^{-4}	28 (24.4)[5]	2.25	4.51[2]	1.27 x10^{-4}	20 (24.3)[5]

Notes

1. Uranine first arrivals estimated from inflection point on rising limb of breakthrough curve.
2. Minimum measurement interval 0.25 hours.
3. Relative recovery calculated 24 hours after injection. Values in brackets after 48 hours.
4. Uranine breakthrough curve for *H40/1* test used for calculations due to mechanical problems with fluorometer during test with *P.putida*. (Observed values in brackets.)
5. Values in parenthesis: Relative recovery for second *H40/1* pulse.

5.7.2 Tracer Response-B8

As observed at B7, Uranine breakthrough curves generated on successive days of testing at B8 bear strong similarities to each other (Figure 5.3). Indeed, Uranine first arrival times and maximum concentration times observed for tests carried out on successive days correspond within 15 minutes of each other in both the July 2000 and May 2001 (Table 5.1). However, differences between curves generated during different investigation periods were apparent. Overall, maximum Uranine concentrations were observed over 1.5 hours later during the May 2001 test, and at concentrations approximately 60% lower than those noted in July 2000. Moreover, the Uranine concentrations observed at B8 24 hours after injection in July 2000 were approximately 1% of the maximum concentration observed in the breakthrough curve. In contrast, the concentration in May 2001 was 9%, reflecting the greater degree of tailing observed during the more recent test period.

The *H40/1* breakthrough curve generated from the July 2000 data shows that although peak concentrations were observed slightly earlier than those of Uranine, maximum viral tracer relative concentrations ($1.48x10^{-4}$) were approximately half of those observed for Uranine ($3.13x10^{-4}$) (Figure 5.3a). Moreover, the rising limb of the *H40/1* breakthrough curve rose after that of Uranine, and declined more rapidly after peak virus concentrations were reached. *H40/1* relative recoveries at B8 during the July 2000 experiment reached 30% eight hours after injection, but only rose an additional 2% in the subsequent 16 hours. (Relative recovery was calculated based on assumed 100% Uranine recovery 24 hours after injection.)

The *E.coli* response observed at B8 during the July 2000 tracer test resembled that of Uranine until approximately seven hours after injection (Figure 5.3b), although the bacterial tracer breakthrough rises and peaks slightly later than the solute. From approximately seven hours after injection until ten hours after injection, *E.coli* concentrations decline more rapidly than those of Uranine, after which *E.coli* relative concentrations remain constant at between $5x10^{-6}$ and $8x10^{-6}$ until the end of monitoring. In contrast, Uranine relative concentrations decline more slowly, but at a more consistent rate after maximum solute tracer concentrations have been observed. As observed at B7, approximately 24 hours after injection, *E.coli* concentrations exceed those of Uranine. *E.coli* relative recoveries during the July 2000 tracer test were 77% at 24 hours after injection, rising to 90% at 48 hours after injection, assuming that Uranine concentrations arriving at B8 24 hours after injection made an insignificant contribution to total Uranine recovery.

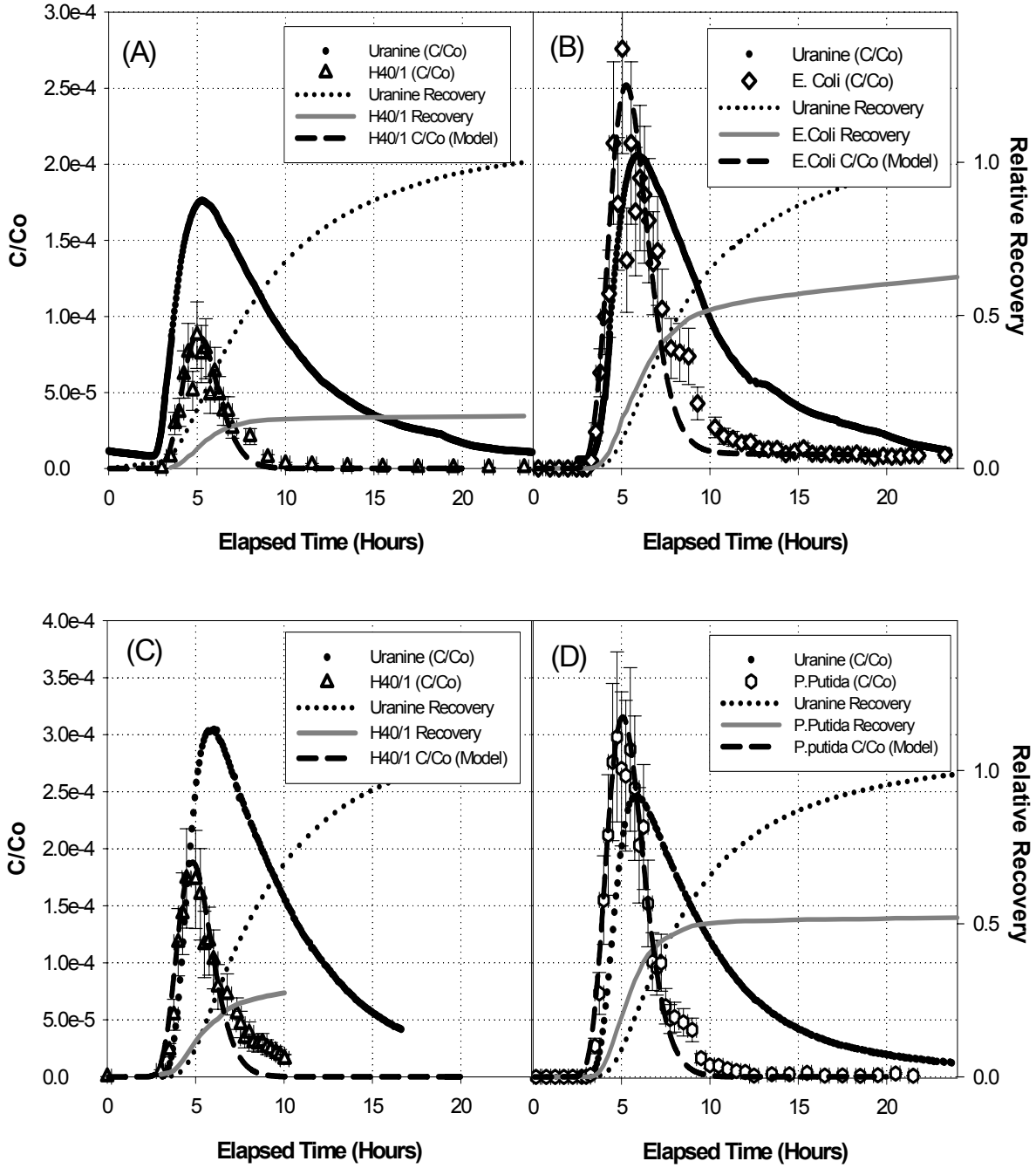

Figure 5.2: Observed solute and biocolloid breakthrough curves and cumulative recovery curves. Monitoring well B7, Dornach Test Site, Dornach, Germany. Solute breakthrough curves digitised from hardcopy print-out.*(A) H40/1* & Uranine, 18 July 2000. (B) *E.coli* & Uranine, 17 July 2000. (*E.Coli* Background Conc.: 2.25×10^{-8}). (C) *H40/1* & Uranine, 16 May 2001. (D) *P.putida* & Uranine, 15 July 2000. Modelled biocolloid breakthrough shown as dashed line. Temporal biocolloid sampling error ±0.25 hours. Analytical biocolloid error ± 25% of measured conc.

The *P.putida* breakthrough curve generated for B8 for the May 2001 investigation period is presented in Figure 5.3c. The curve contrasts with that observed at B7. *P.putida* relative concentrations rise simultaneously with those of Uranine but reach their maximum relative concentration of $1.29x10^{-4}$ at five hours after injection (Table 5.1). In contrast Uranine reaches its maximum concentration of $2.15x10^{-4}$ (estimated-see Figure 5.3) at approximately 6 hours after injection. At 10 hours after injection, *P.putida* relative recovery is 16.5%, rising to 17% in the following 14 hours and to 18% in the subsequent 24 hours.

The *H40/1* breakthrough curve generated at B8 in May 2001 resembles that obtained using data from the experiment completed previous July (Figure 5.3c and 5.3a respectively). Maximum *H40/1* relative concentrations of $1.27x10^{-4}$ were observed 4.51 hours after injection during the May 2001 experiment, compared to a maximum relative concentration of $1.48x10^{-4}$ observed at 4.25 hours after injection observed in July 2000 (Table 5.1). However, the *H40/1* response observed in May 2001 differs from that observed in July, where the rising limb of the *H40/1* breakthrough curve was later than that of the Uranine curve. In contrast, during the May 2001 experiment the relative concentrations of Uranine and *H40/1* increased simultaneously. However, the maximum *H40/1* relative concentration ($1.27x10^{-4}$) was observed over an hour before that of Uranine ($2.15x10^{-4}$). Moreover, *H40/1* relative concentrations declined more rapidly than those of Uranine. Relative recoveries estimated based on the first pulse of *H40/1* up until 10 hours after injection indicate that approximately 20% of the viral tracer was recovered relative to Uranine. Recovery based on the second pulse was 24.3%.

5.8 Discussion

5.8.1 Breakthrough Curve Responses

The results of the solute and biocolloid comparative tracer tests carried out at Dornach provide an important insight into the processes affecting micro-organism transport and attenuation in the Munich Gravel Plain Aquifer. The responses of the tracers investigated varied depending on both the tracer and monitoring well location. Significantly, the degree of attenuation was not necessarily greater with increased distance from the injection well. Moreover the degree of tracer attenuation observed at B7 or B8 for the tracers that were used repeatedly (*H40/1* and Uranine) varied from one investigation period to the next. However, the consistent Uranine breakthrough curves observed at both B7 and B8 during tests carried out on successive days indicate that mass transport processes did not change significantly during the 48 hour duration of each investigation period. Consequently, the responses of different tracers at a given monitoring point, monitored on successive days, may be compared with one another.

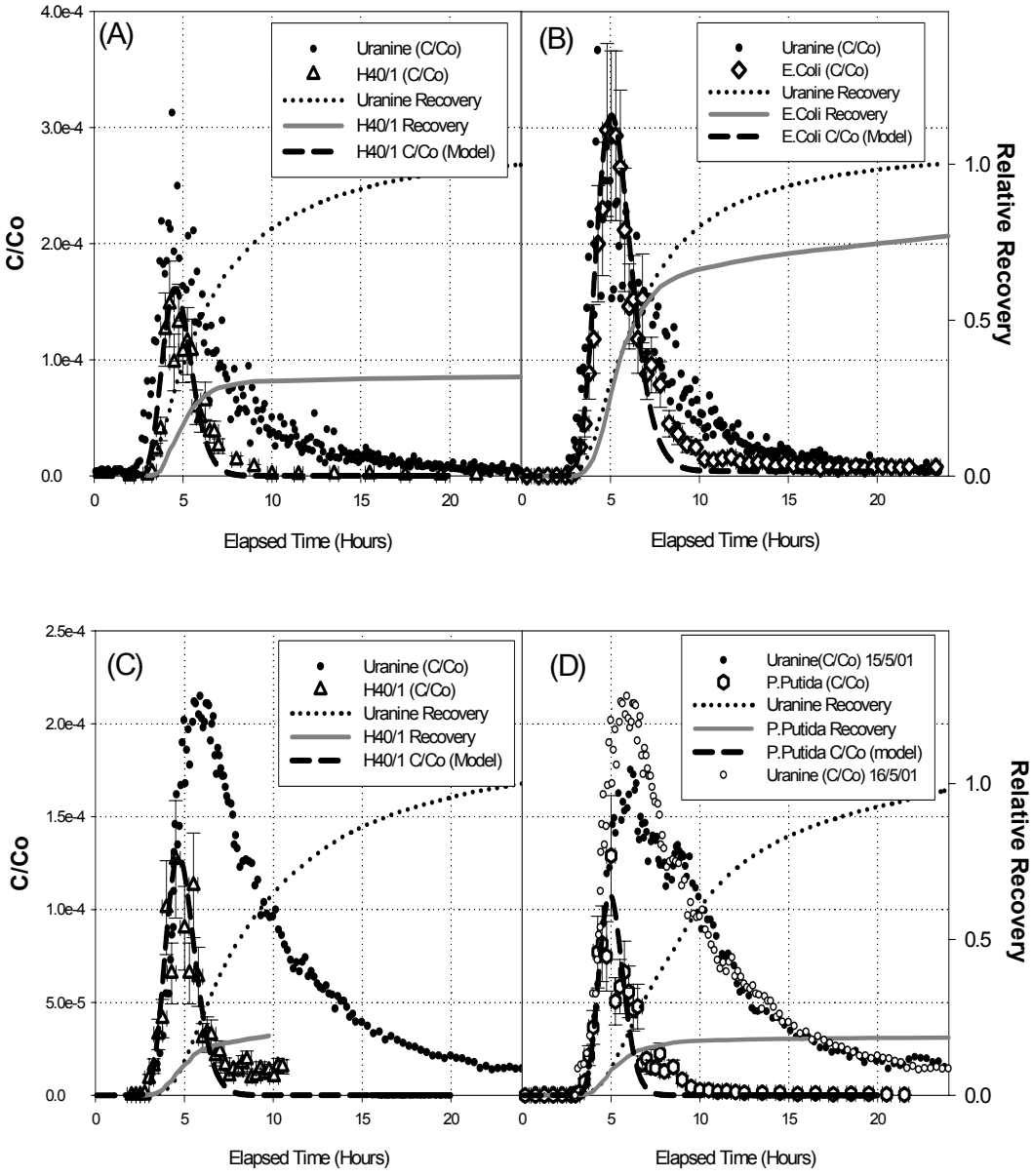

Figure 5.3: Observed solute and biocolloid breakthrough curves and cumulative recovery curves. Monitoring well B8, Dornach Test Site, Dornach, Germany. Solute breakthrough curves downloaded directly from data logger. (A) *H40/1* & Uranine, 18 July 2000. (B) *E.coli* & Uranine, 17 July 2000. (*E.Coli* Background Conc.: 2.25×10^{-8}). (C) *H40/1* & Uranine, 16 May 2001. (D) *P.putida* & Uranine, 15 July 2000. Irregular signal between 5 and 9 hours after injection due to blockage in fluorometer. Uranine response from 16 May 2001 presented for comparative purposes and used in subsequent calculations. Modelled biocolloid breakthrough curves shown as dashed line. Temporal biocolloid sampling error ±0.25 hours. Analytical biocolloid error ± 25% of measured conc.

In all tracer tests, biocolloid relative recoveries at both B7 and B8 were less than unity. This implies that bacterial and viral tracers were attenuated in the aquifer underlying Dornach. Measurements of inactivation rates of biocolloid tracers suspended in site groundwater indicated that no significant change in either bacterial or viral tracer concentration occurred over the period during which the experiments were carried out. This lack of evidence for inactivation of suspended biocolloids thus suggests that microbiological attenuation processes in the aquifer were a result of interactions between bacterial and viral tracers with aquifer surfaces. Consequently, given that the groundwater flow regime remained the same on successive days of an investigation period, variations in the responses of different biocolloid tracers at each well may thus be concluded to be due to differences in particle properties (,e.g. size, surface charge, hydrophobicity).

The high relative recoveries of *E.coli* at B7 and B8 during the July 2000 investigation suggest that straining of bacteria due to their size was not a significant and that physico-chemical filtration was the dominant attenuation mechanism. Similarly, high recoveries observed for *P.putida* and a comparable breakthrough curve to that observed for *E.coli* at B7 until seven hours after injection suggest that physico-chemical filtration also controlled the attenuation along the flow path(s) transporting biocolloids between B1 and B7 during the May 2001 investigation period.

H40/1 relative recoveries were less than or comparable to those of the bacterial tracers during both the July 2000 and May 2001 investigation events. This occurred despite the fact that the length of the short axes of *E.coli* and *P.putida* particles are over 25 and 50 times larger than the diameter of *H40/1* capsid respectively. Consequently, the smaller size of viruses alone does not appear to be a sufficient basis to suspect greater mobility in coarse grained deposits where straining of larger particles is insignificant. This issue is discussed in further detail in section 5.8.3.

5.8.2 Size exclusion Processes in Biocolloid Transport

As noted in section 5.6, the conventional approach to modelling tracer breakthrough curves involves using a conservative solute tracer to determine transport parameters (velocity and dispersion). These parameters are subsequently employed to determine reactive tracer (biocolloid) attenuation rates, assuming that transport parameters are identical for both tracers. This approach has been successfully applied to biocolloid breakthrough curve data generated from tracer tests carried out in relatively uniform porous media (Harvey & Garabedian, 1991; Schijven and others, 2002). However, the approach is not valid should biocolloid and solute tracer transport parameters differ due to phenomena such as exclusion processes.

In studies investigating exclusion processes in groundwater, peak biocolloid concentrations have been noted to occur before those of conservative solute tracers (Ginn and others, 2002). However, Zhang and others (2001) demonstrated that first order kinetic attenuation of colloids, while reducing maximum colloid concentrations also shifts the time that maximum colloid concentrations are observed to the left on a breakthrough curve, i.e. toward earlier time. This occurs even though both tracers have the same dispersion and interstitial velocity. Moreover, Zhang and others' (2001) study noted that as attenuation occurs, the rising limb of the colloid breakthrough curve shifts to the right. Consequently, colloidal tracers with the same velocity and dispersion as a conservative solute tracer, but affected by first order kinetic adsorption, will have a breakthrough curve with a rising limb that occurs after the solute tracer, but which reaches a lower maximum concentration earlier. If peak colloid concentrations are observed before those of the solute tracer, but the breakthrough curve does not have the aforementioned form, colloidal velocity and dispersion must be regarded as different from those of the solute.

Qualitative examination of *E.coli* and *H40/1* responses at B8, and the *H40/1* response at B7 show that biocolloid peak concentrations were lower than those of the solute tracer and were observed at an earlier time. Moreover, the breakthrough curve rising limbs rise after those of Uranine. These criteria suggest that the biocolloids may be transported at the same rate as the solute tracer, based on the Zhang and others (2002) criteria. However, numerical modelling of biocolloid breakthrough curves using velocity and dispersion values derived from Uranine breakthrough curves demonstrated that dispersion values obtained from solute breakthrough curves were too high to adequately reproduce either virus or bacterial tracer responses. This suggests that the biocolloid and solute tracer interstitial velocities and dispersions differ from each other along the flow paths connecting the injection well and the monitoring points.

In a similar manner, maximum relative concentrations of bacterial tracers in excess of those of solute tracers that arrived at earlier times, as observed at B7, cannot be reproduced by assuming that both solute and biocolloid tracers have the same velocity and dispersion. Moreover, the fact that *H40/1* and *P.putida* relative concentrations at B8, and the *H40/1* responses at B7 observed during the May 2001 tracer test rose at the same time as Uranine, despite significant attenuation, indicate that the biocolloids were not transported at the same rates as the solute tracer.

The breakthrough curves generated at B7 and B8 demonstrate that exclusion processes affected the biocolloid tracers transported between the injection well and the observation points. Grolimund and others (1998) present the results of a laboratory based study of colloidal transport where exclusion processes were observed. The authors noted that colloidal tracers arrived earlier than solute tracers due to more rapid transport through large pores. However, this study also showed that colloid relative recoveries were significantly less than

unity. It was argued that this was partially a consequence of particles being excluded from smaller pores through which colloidal particles cannot pass, but through which solutes may flow (pore exclusion). In contrast to the Grolimund and others (1998) study, the high *E.coli* recoveries observed at B7 and B8 during the July 2000 investigation period suggest that pore exclusion was not a significant process in biocolloid transport between B1 and the monitoring wells B7 and B8. Due to their smaller size, it follows that *H40/1* transport was not significantly influenced by pore exclusion during this period either. The lower *P.putida* relative recoveries observed at B8 make it more difficult to categorically rule out the influence of size exclusion on biocolloid transport from the injection well during the May 2001 investigation period. However, high *P.putida* relative recovery observed at B7 suggests that pore exclusion did not play a strong role in influencing bacterial transport to this monitoring well.

In contrast to pore exclusion, size exclusion, offers a plausible means of explaining the differing responses between biocolloid tracers and Uranine observed at Dornach. In size exclusion, biocolloid tracers cannot access the marginal, more slowly flowing parts of pores, which are accessible to solute tracers, due to their size. Rather they are transported in the more rapidly flowing central part of the pore throats. Moreover, because the biocolloids are concentrated in the central parts of pores, they experience a more limited range of groundwater velocities and thus have lower dispersions. The net result of these processes is that non-reactive biocolloids can breakthrough more rapidly than a solute tracer at an observation point, and with higher maximum concentrations. After reaching maximum concentrations, biocolloid tracer concentrations decline rapidly, as biocolloid-free water flushes the system. In contrast, solute breakthrough curves are typically broader and more disperse and have lower maximum concentrations that arrive later compared to biocolloids. After reaching maximum concentrations, solute tracer concentrations decline more slowly as tracer that has flowed through slower moving parts of pore throats arrives at a monitoring point. The influence of molecular diffusion due to concentration gradients on solute tracer response could not be confidently determined at Dornach using the available data, but may play a role in further reducing the maximum concentration and prolonging the tailing in breakthrough curves.

5.8.3 Numerical Modelling Results

Numerical modelling of biocolloid breakthrough curves permitted further study of bacterial and virus transport and attenuation processes operating at Dornach during the July 2000 and May 2001 investigation periods. Given the differences in biocolloid and solute tracer behaviour outlined above, numerical modelling of biocolloid transport used the approach described in Section 5.6, which takes into account differences in transport characteristics compared to solutes. Simulated biocolloid responses for the curves at B7 and B8 are presented in Figure 5.2 and Figure 5.3 respectively and show that the approach generally provides good fits

to the rising limbs, peak concentrations and late time concentration data observed in the field. However, model fits corresponding to the later part of the main breakthrough curve peak are more variable.

Schijven and others (2002) observed similar phenomena in laboratory scale experiments, where they were attributed to a second type of biocolloid deposition site that had different adsorption and release constants. Alternatively, this discrepancy may be due to the particle velocity distribution being non-Gaussian, which could be approximated by a series of superimposed Gaussian breakthrough curves. Harvey and Garabedian (1991) argued that this later approach was appropriate to explain selected biocolloid breakthrough curves observed in the sandy aquifer at Cape Cod. Studies carried out within the wider framework of this study, simulating virus transport in sedimentary structures, demonstrated that such a regime could be possible in sand and gravel deposits. However, insufficient information existed to discriminate between these two hypotheses at Dornach. Nonetheless, the consistency of interstitial velocity and dispersion values obtained from numerical modelling from one tracer test to another at both monitoring wells during an investigation period suggests that the numerical modelling technique employed is an adequate means of simulating biocolloid response, despite the above complications (Table 5.2). This is corroborated by reconstructed conservative response breakthrough curves, with kinetic parameters set to zero generated for each well using test data collected on successive days that bear a strong resemblance to each other.

5.8.3.a Deposition Constants: The deposition and desorption constants necessary to reproduce the biocolloid breakthrough curves are presented in Table 5.2. These constants reflect the degree of adsorption experienced by each biocolloid investigated. Deposition constants calculated for different biocolloids vary from one monitoring location to another, reflecting the spatial variability in adsorption capacity at the site. Moreover, *H40/1* deposition constants calculated for both B7 and B8 vary between investigation periods, reflecting changes in the virus adsorption capacity of the aquifer with the changes in the groundwater flow regime.

By using filtration theory equations (Equation (5) through Equation (11)), biocolloid deposition constants could be used to reconcile attenuation phenomena for different particles under the different groundwater flow regimes. Assuming a typical effective grain size 200μm for aquifer material (data from Klotz and others, 1980) along the flow path connecting the injection well with B8 during the July 2000 investigation period, collision efficiencies were calculated for *H40/1* and *E.coli*. These values are presented in Table 5.2. It is noteworthy that the calculated collision efficiency of *E.coli* is over twice that of *H40/1*, suggesting that the bacterial tracer is twice as likely to stick to a grain upon collision as the virus. Nonetheless, the *H40/1* is attenuated to a much greater degree. This is consistent with simulations carried out by Elimelech and others (1995) who used the filtration theory to show that, all other conditions being equal, particles

between 0.5μm and 1μm in diameter can travel up to 100 times further in an aquifer than particles measuring 40nm in diameter. The greater attenuation of smaller sized particles occurs because smaller particles are influenced to a greater degree by Brownian motion, compared to larger particles, which have greater inertia. This results in smaller particles striking collector surfaces more frequently than larger particles. Consequently, although *H40/1* has lower collision efficiency than *E.coli*, it strikes aquifer grain surfaces more often. This gives rise to a greater number of opportunities for *H40/1* to stick to aquifer grains and ultimately results in a greater degree of virus adsorption.

Numerical modelling of the biocolloid breakthrough curves from B7 and B8 indicated that groundwater flowed at different velocities during the July 2000 and May 2001 investigation periods. The anticipated changes in deposition constant can be related to the variation in groundwater flow regime by considering *H40/1* responses and relative recoveries for both investigation periods as a baseline by which to compare the responses of the two bacterial tracers. According to the filtration theory, increases in groundwater velocity increase biocolloid deposition constants. By using the *H40/1* collision efficiencies determined from the July 2000 deposition constants, the filtration theory was used to predict deposition constants for responses observed at B7 and B8 under the groundwater flow regime operating at the site in May 2001. The predicted rate constants do not correspond to those calculated using the field data, even when a 15% margin of error is incorporated. Indeed, if the *H40/1* collision efficiency is assumed to be constant across the site, effective collector diameters of 232 μm and 169μm are necessary at B7 and B8 respectively to obtain the deposition constants determined from the May 2001 data. In contrast, effective diameters of 187μm and 200μm were used for B7 and B8 in tests carried out in July 2000. This implies that the differences in deposition constant values calculated from the July 2000 and May 2001 breakthrough curves are a consequence not only of changing hydrodynamics, but also due to tracer flowing from the injection well to B7 and B8 along flow paths with different attenuation characteristics.

Using *E.coli* and *H40/1* collision efficiencies calculated for the flow path between B1 and B8 (under an assumed effective grain diameter of 200μm), the effective grain sizes controlling biocolloid attenuation between B1 and B7 during the July 2000 investigation period were calculated as 186μm and 187μm for the bacterial and viral tracers respectively. The consistency of the two values suggest that the collision efficiencies calculated for *E.coli* and *H40/1* along the flow path between B1 and B8 are also applicable to the path connecting the injection well and B7. This result in turn suggests that any variation in aquifer composition between the flow paths connecting the two monitoring wells to the injection well during the July 2000 investigation period did not cause significant variations in the aquifers *H40/1* or *E.coli* attenuation capacity.

Table 5.2. Estimated model parameters determined from one-dimensional colloid transport and attenuation modelling, along with derived collision efficiencies and relative effective grain sizes, as determined using filtration theory. (Footnote references in bold superscript.)

B7

Tracer/ Date[1]	v (m/day)	D (m^2/day)	Tav (day)[2]	kc (1/day)	kdes (1/day)	μ (1/day)	α[3]	d(Effective) (μm)
E.coli	82.08	36.29	0.24	4.22	0.36	0.00	1.36E-04	186
H40/1 July 2000	82.32	34.34	0.24	8.83	0.10	1.44	6.14E-05	187
P.putida	85.68	37.49	0.23	3.53	0.19	2.16	3.35E-04	319
H40/1 May 2001[4]	88.08	38.04	0.23	6.31[5]	Not Calc[5].	Not Calc[5].	6.14E-05	232

B8

Tracer/ Location[1]	v (m/day)	D (m^2/day)	Tav (day)[2]	kc (1/day)	kdes (1/day)	μ (1/day)	α[3]	d(Effective) (μm)
E.coli	43.73	8.40	0.23	2.90	0.48	0.00	1.36E-04	200
H40/1 July 2000	48.12	7.75	0.21	6.60	0.19	2.40	6.14E-05	200
P.putida	45.60	4.32	0.22	9.26	0.19	2.40	3.35E-04	169
H40/1 May 2001[4]	46.32	7.39	0.22	8.62[5]	Not Calc[5].	Not Calc[5].	6.14E-05	169

Notes:

1. Parameters have same meaning as defined in text.

2. Tav- Average Travel time for Tracer.

3. Collision efficiency calculated with assumed 11% porosity and 10 °C.

Values of other parameters used in calculation provided in text.

4. Desorption and inactivation constants not calculated for H40/1 during May 2001 test due to addition of second pulse of H40/1 to verify experimental repeatability

5. Injection of a second pulse of *H40/1* prevented release constants from being determined for the virus breakthrough curves. However, sensitivity analysis of the bacterial breakthrough curves and the *H40/1* curves from the previous July indicated that the omission of the release constant increased the value of the deposition constant by no more than 10%.

Collision efficiencies calculated for *P.putida* flowing from the injection well to B8 during the May 2001 investigation period were based on the assumption that collision efficiency remained the same throughout the aquifer, as appeared appropriate for *E.coli* during the July 2000 investigation period. Based on this approach, the collision efficiency for the tracer was calculated using the *P.putida* breakthrough curve from B8. (An effective grain size of 169μm was used in this calculation, based on *H40/1* response in the tracer test carried out the following day.) Once again the collision efficiency of the bacterial tracer was considerably higher than that of *H40/1*(by a factor of 5.45). However, the use of the *H40/1* and *P.putida* collision efficiencies determined for B8 to predict effective grain sizes at B7 failed to yield a consistent diameter for the two biocolloid tracers, even when a 25% margin of error in relative recovery was incorporated into calculations (Table 5.2). These data suggest that the assumption that *P.putida* collision efficiency is identical along flow paths connecting the injection well to B7 and to B8 may not be valid. This in turn implies that different rates of *P.putida* attenuation observed in breakthrough curves from B7 and B8 may be a consequence of compositional variations in the aquifer underlying Dornach.

5.8.3.b Release Constants / inactivation Rates: First order kinetic desorption (release) constants were necessary to reproduce the late time response for all biocolloids investigated. The occurrence of particle desorption implies that the adsorption processes were at least partially reversible for all the biocolloids investigated at Dornach. As was the case with deposition constants, desorption rates vary with particle type and monitoring location. Low deposition constant and higher release constant values obtained for *E.coli* reflect almost total (90%) biocolloid relative recovery at B8, indicating that adsorption of this tracer is almost fully reversible and that it is not strongly adsorbed to aquifer materials (Table 5.2). In contrast, the release constants calculated for *H40/1* are approximately one half to one quarter of those for *E.coli*. This suggests that *H40/1* is more strongly adsorbed to aquifer materials than *E.coli*. Moreover, *P.putida* has similar desorption rates to *H40/1*, suggesting that it too is more strongly bound to the aquifer materials than *E.coli*.

The sustained decline in *H40/1* and *P.putida* relative concentrations in the later parts of their respective breakthrough curves at both B7 and B8 contrast notably with the breakthrough curves for *E.coli*. Schijven and others (1999) claim that the declining slope in the tail of biocolloid breakthrough curves, observed once the main breakthrough peak has passed, is mainly a result of inactivation processes occurring while a biocolloid is adsorbed to aquifer materials. Indeed, inactivation rates of between 1.44/day and 2.40/day for both *P.putida* and *H40/1* suggest that inactivation while adsorbed to aquifer materials is a significant process in the overall attenuation of these biocolloids. In contrast, no significant slope was observed in the late time tails of the *E.coli* breakthrough curves. Consequently, inactivation rates could not be confidently determined for *E.coli*

adsorbed to aquifer materials underlying Dornach. This suggests either that *E.coli* is not inactivated while adsorbed to the aquifer materials or that inactivation does occur but at rates that are significantly lower than those of *P.putida* and *H40/1*.

Overall, numerical modelling of the bacterial and biocolloid breakthrough curves have demonstrated that the capacity of the aquifer materials underlying Dornach to attenuate biocolloids varies both with the biocolloid under study and the location of the monitoring point in the aquifer. Moreover, application of the filtration theory to *H40/1* data indicated that the aquifers attenuation capacity for individual biocolloids may also vary with time as flow paths change.

5.9 Implications for Public Health

The results of the biocolloid tracer tests carried out in the aquifer underlying Dornach demonstrate that both bacteria and viruses may be transported in the groundwater flowing through the aquifer at velocities of up to 88m per day. Although all biocolloids were attenuated, the degree attenuation varied significantly. Significantly, test results indicated viruses are not more mobile due to their smaller size. Indeed, breakthrough curves generated at B7 for both bacterial tracers demonstrated that these larger particles were attenuated to a significantly lower degree than the viral tracer, despite indications that the virus had a lower collision efficiency. This result suggests that bacterial-sized biocolloids of between 1μm and 5μm may pose a greater threat to public health than viruses when present in groundwater flowing through coarse grained aquifers where straining has little influence on attenuation processes. Although not investigated in this research, cysts of protozoa such as Cryptosporidium fall into this category. Moreover, these cysts have considerable potential to impact public health, not only due to their size, but also due to their ability to withstand inactivation more strongly than viruses (Schijven and others, 2003) and their greater capacity to resist standard waste water disinfection procedures (Rose and others, 1996)

Breakthrough curves generated for both B7 and B8 have provided compelling evidence of the influence of exclusion processes on biocolloid transport. Exclusion processes at Dornach have resulted in biocolloids being transported at higher average velocities than solute tracers. Moreover, the dispersion values of resulting breakthrough curves were significantly lower. At B7, this has resulted in the observed maximum bacterial biocolloid concentrations exceeding those of the conservative solute tracer. In terms of public health concerns, this could result pathogens arriving at a groundwater source more quickly and attaining a higher maximum concentration than that predicted using conservative solutes, depending on the degree of biocolloid adsorption/inactivation. Given the association of exclusion processes with heterogeneous deposits (Harvey, 1997), and the highly variable texture of fluvioglacial aquifers (Huggenberger, 1993), it is possible that these processes

operate more widely in this type of aquifer type than previously suspected. The absence of these phenomena in experiments carried out under laboratory conditions during the course of this study further illustrates the continued need for field based studies to identify certain transport phenomena.

Breakthrough curve modelling has also indicated that first order kinetic adsorption decreased maximum biocolloid concentrations observed at both monitoring points relative to an unadsorbed tracer. However, late time data demonstrate that adsorption was at least partially reversible for all biocolloids investigated. Indeed in the case of *E.coli*, the high relative recoveries observed suggest that almost all bacteria adsorbed could be desorbed. The fact that adsorbed contaminants may be released back into groundwater at a later time may prolong the risk of disease from water sources, particularly where low concentrations may be sufficient to cause infection. Westwood and Sattar (1976) demonstrated this to be the case for certain viruses. Consequently, reversible adsorption processes, although reducing maximum pathogen concentrations in a system may prolong the long term risk of infection. In this respect, reversibly adsorbed contaminants may be more detrimental to public health than a contaminant that does not react with aquifer materials. Under these circumstances the importance of inactivation processes that occur while pathogens are adsorbed on aquifer materials becomes critical in reducing contaminant concentrations to acceptable levels.

Chapter 6 : Geochemical Influences on H40/1 Bacteriophage Inactivation in Glaciofluvial Sands.

6.1 Abstract

Geochemical heterogeneities may cause spatial variations in virus inactivation rates resulting from interactions with minerals that can lead to differences in natural disinfection capacity within an aquifer. Column studies investigating the interaction of the bacteriophage H40/1 with natural sands sampled from the Kappelen Test Site (Kappelen), Bern, Switzerland showed that inactivation rates are higher for adsorbed bacteriophages than for those suspended in groundwater. Moreover, breakthrough curves obtained from field-based tracer tests at Kappelen indicated that the adsorbed H40/1 is inactivated in-situ at comparable rates. Statistical analyses of mineralogical data failed to demonstrate significant spatial variations in aquifer composition either across the site or with depth. In contrast hydrochemical analyses of groundwater samples collected at Kappelen demonstrated that iron-reducing groundwater occurs below aerobic waters. Tracer breakthrough curves indicate that H40/1 survival is not affected by variable redox conditions. Investigation results suggest that spatial geochemical variability does not significantly affect H40/1s inactivation rate.

6.2 Introduction

Filtration by aquifer materials has historically been assumed to be an effective means of removing pathogenic microbiological contaminants (viruses, bacteria and protozoa) from groundwater. As a consequence of this assumption, regulations controlling the microbiological quality of groundwaters for human consumption have often been less stringent than those for surface waters. (Macler & Merkle, 2000.). However, Craun (1986) estimated that untreated groundwater has been responsible for one third of water borne disease outbreaks in recent decades in the USA. Groundwater contamination by viruses has been a particular point of concern, in part due to their small size and their suspected greater mobility relative other micro-organisms (Macler & Merkle, 2000). Ryan and others (2002) noted that the fact that approximately 80% of water-borne disease outbreaks in the US where the causative agent was identified, were due to viruses prompted the United States Environmental Protection Agency (USEPA) to make viruses the focal point of the proposed groundwater disinfection rule. According to this rule, suppliers of groundwater destined for public consumption would need to demonstrate natural disinfection if the water was not to be treated (Macler, 1996). The USEPA defines natural disinfection as “Source water treatment via virus attenuation by natural subsurface processes such as virus inactivation, dispersion (dilution) and irreversible adsorption to aquifer framework solids” (USEPA, 1992).

Adsorption to sediments and inactivation are the two main processes by which infective viruses are attenuated in aquifers (Ryan and others, 1999). Adsorption results from viruses interacting with solid surfaces and becoming attached. In an extensive review of viral attenuation processes, Schijven and Hassanizadeh (2000) noted that virus adsorption in groundwater is usually regarded as a kinetic process that results in reductions in virus concentration, relative to conservative tracers. Moreover, the authors noted that this process is strongly influenced by both the nature of the adsorbing surface and the chemistry of the water suspending the virus. However, studies by Bales and others (1991) have shown that adsorption may not necessarily be irreversible and that at least a portion of the viruses adsorbed onto mineral surfaces may be capable of subsequent desorption while remaining virulent. Moreover, Westwood & Suttar (1976) noted that in extreme cases only 1 virus may be sufficient to cause illness, suggesting that reversible adsorption processes, although reducing maximum virus concentrations, could be potentially more detrimental to public health than non-sorbing pathogens.

Inactivation results in the loss of a virus’ infective capacity. This loss is the result of the disruption of protein coating on the virus capsid (head) and associated nucleic acid degradation (Gerba and Bitton, 1984). The inactivation process in aquifers is controlled by both the physical environment (Yates and others, 1987) and virus-specific physiochemical properties (Yamagishi and Ozeli, 1972).

Virus inactivation may occur when viruses are both suspended in liquid and when adsorbed onto surfaces (Sobsey and others, 1980). The enhancement /reduction of viral inactivation rates due to interactions with solids varies from one virus to another and depends on the strength of attachment (Hurst and others, 1980).

Grant and others (1993) listed three alternative states affecting viral inactivation resulting from reversible adsorption onto solid surfaces:

1. Quasi-equilibrium adsorption (QEA): Virus inactivation rates on a surface are equal to those in the liquid.
2. Quasi-equilibrium adsorption reduced inactivation (QEARI): Virus inactivation rates on surfaces are lower than those in the liquid.
3. Quasi-equilibrium adsorption surface sink (QEASS): Virus inactivation rates on a surface are greater than those in a liquid.

Consequently, virus attenuation due to interactions with aquifer surfaces must be regarded as a complex process in which adsorption and inactivation can be inter-related. Furthermore, the dependence of virus adsorption processes on mineralogy and hydrochemistry imply that geochemical parameters may indirectly influence viral inactivation by encouraging or discouraging virus adsorption to surfaces where inactivation rates may be different to those in suspension.

The contribution of viral inactivation due to interactions with aquifer materials is often difficult to determine. Indeed, Pedley & Howard (1997) noted that virus survival in groundwater systems remains poorly understood. Part of the reason for the lack of understanding concerning virus adsorption and inactivation in groundwater systems may relate to the various approaches used by different researchers to study this topic. Much research has been carried out into viral adsorption and inactivation employing a variety of different techniques, particularly at the laboratory scale. These have included batch studies (Gerba & Goyal and others, 1981; Sobsey and others, 1980; Sobsey and others, 1986) and dynamic column experiments (Bales and others, 1991; Loveland and others, 1996; Penrod and others, 1996). Harvey and others (1989) noted laboratory scale experiments allow controlled chemical and physical conditions to be imposed that may allow attenuation mechanisms to be confidently characterised.

More recently, field-scale experiments have investigated in-situ viral inactivation rates of adsorbed viruses in aquifers (Bales and others, 1997, Schijven and others, 2000, Ryan and others, 2002). Investigations by Ryan and others (2002) in particular, have provided considerable insight into viral inactivation processes in natural porous deposits by integrating laboratory scale and field scale investigative techniques. Nonetheless, Harvey (1997) noted that the results of laboratory and field scale experiments investigating microbiological contaminant transport and attenuation often provide inconsistent results, due in part to heterogeneities in the deposits under investigation in the field.

The variable mineralogy and texture often encountered in natural deposits (Tucker, 1980) can be considerably more complex than the compositionally and texturally uniform deposits often employed in many laboratory investigations (e.g. Bales and others, 1991; Loveland and others, 1996; Penrod and others, 1996). The natural deposits making up many aquifers may have different compositions and/or textures that vary in space (Huggenberger & Aigner, 1999; Kleinedam and others, 1999). These different units may have variable virus adsorption characteristics, and thus by inference may inactivate viruses to different degrees. Furthermore, the minerals in contact with the groundwater may influence aquifer hydrochemistry (Stumm & Morgan, 1996). This may result in differences in groundwater chemistry in different parts of an aquifer. Geochemical variations in mineralogy and/or hydrochemistry in aquifers may therefore either directly or indirectly influence virus inactivation rates. This may in turn give rise to variable disinfection rates in different parts on the same aquifer.

This study investigated virus inactivation in sand and gravel deposits at a site that forms part of a regionally important aquifer. Inactivation investigations have been carried out using laboratory-based and field-based methods. Laboratory studies examined viral adsorption and inactivation in the fine sand-sized fraction of samples of aquifer material to ascertain the degree to which suspended viruses are inactivated relative to those adsorbed on aquifer surfaces. Field-scale studies investigated viral transport and attenuation processes in the aquifer by means of tracer testing. These investigations were complimented by a program of geochemical site characterisation which examined the spatial variability of the mineralogy and hydrochemistry of that part of the aquifer underlying the site. The results of these studies were used to assess the potential degree to which virus inactivation may be influenced by compositional and textural aquifer heterogeneity, and the degree to which laboratory-based investigations could be used to further understand virus inactivation processes in the field.

6.3 Field Site Setting and Previous Investigations

The Kappelen test site (Kappelen) is located approximately 15km north west of the city of Bern, Switzerland. The site measures approximately 90m x 60m and is located in relatively flat wooded terrain that is bounded to the west by intensively cultivated agricultural land and to the east by a motorway and the town of Lyss (Figure 6.1). A monitoring well network installed at the site consists of seven 5-inch diameter (125mm) OD shallow/deep HDPE well pairs set in a roughly triangular array, and two additional deep wells, constructed with identical materials, to the north and west of the shallow/deep array.

Wells set in the shallow part of the underlying aquifer (with the suffix –2) have 3 to 4 metre long well screens set approximately from 4 to 8 metres below ground surface (m BGS), while those set in the deep part (with the suffix –1) have a 3 to 5 metre long well screen, screened at between 10 and 16m BGS. Kennedy and others (2001a) provide construction details of the wells. Visual

analysis of borehole cuttings from the nine locations drilled at Kappelen revealed that the site is underlain by approximately 16m of unconsolidated polymineralic gravels containing subordinate quantities of sand and silt. These gravels overlie a unit of fine-grained sands and silt/clay (Oyono, 1996).

Specific capacity hydraulic testing of the monitoring wells by Kennedy and others (2001a) provided estimates of the hydraulic conductivities of the gravels, assuming uniform contributions from all horizons set against the well screen. Using this approach, hydraulic conductivities in the lower part of the aquifer were estimated to be between $5x10^{-4}$m/s and $1x10^{-2}$m/s, while those in the upper part of the aquifer were estimated to be lower, at $1x10^{-4}$m/s. However, grain size analysis of 33 sand and gravel samples collected from three borehole cores at K3-1, K7-1 and K8-1indicated that the Kappelen deposits were highly heterogeneous. (Noseda, 1999; Diomande, 2000). Calculations based on these granulometric data have shown that although the sand and silt sized fractions of the samples investigated typically constitute no more that 20% of the sample mass, these materials contribute over 75% of the total surface area of the samples. Since available surface area controls the degree of adsorption to a surface by materials dissolved /suspended in adjacent liquid (Ross & Olivier, 1964), these finer grained materials are thus believed to play an important role in virus adsorption processes in the saturated deposits underlying the site.

Virus transport at Kappelen was previously studied by Kennedy and others (2001a). The results of these investigations confirmed the groundwater flow direction indicated by hydraulic gradient data with tracing tests in both the shallow and deep parts of the aquifer. Tests involved injecting high concentrations of the bacteriophage (bacterial virus or phage) H40/1 into the groundwater along with the solute tracer, Uranine (Sodium Fluorescein) in either monitoring well K1-1, or monitoring well K1-2, and observing relative tracer responses in downgradient observation wells. Both tracers were absent from the aquifer prior to injection. Tests completed between March 1997 and August 1997 investigated virus mass transport in the deeper part of the aquifer. Similarly, tests carried out between November 1997 and July 1998 studied virus behaviour relative to Uranine in the shallower part of the aquifer.

Figure 6.1: Location Map for the Kappelen Test Site, Canton Bern, Switzerland. Inlay: Details of Monitoring Well Locations.

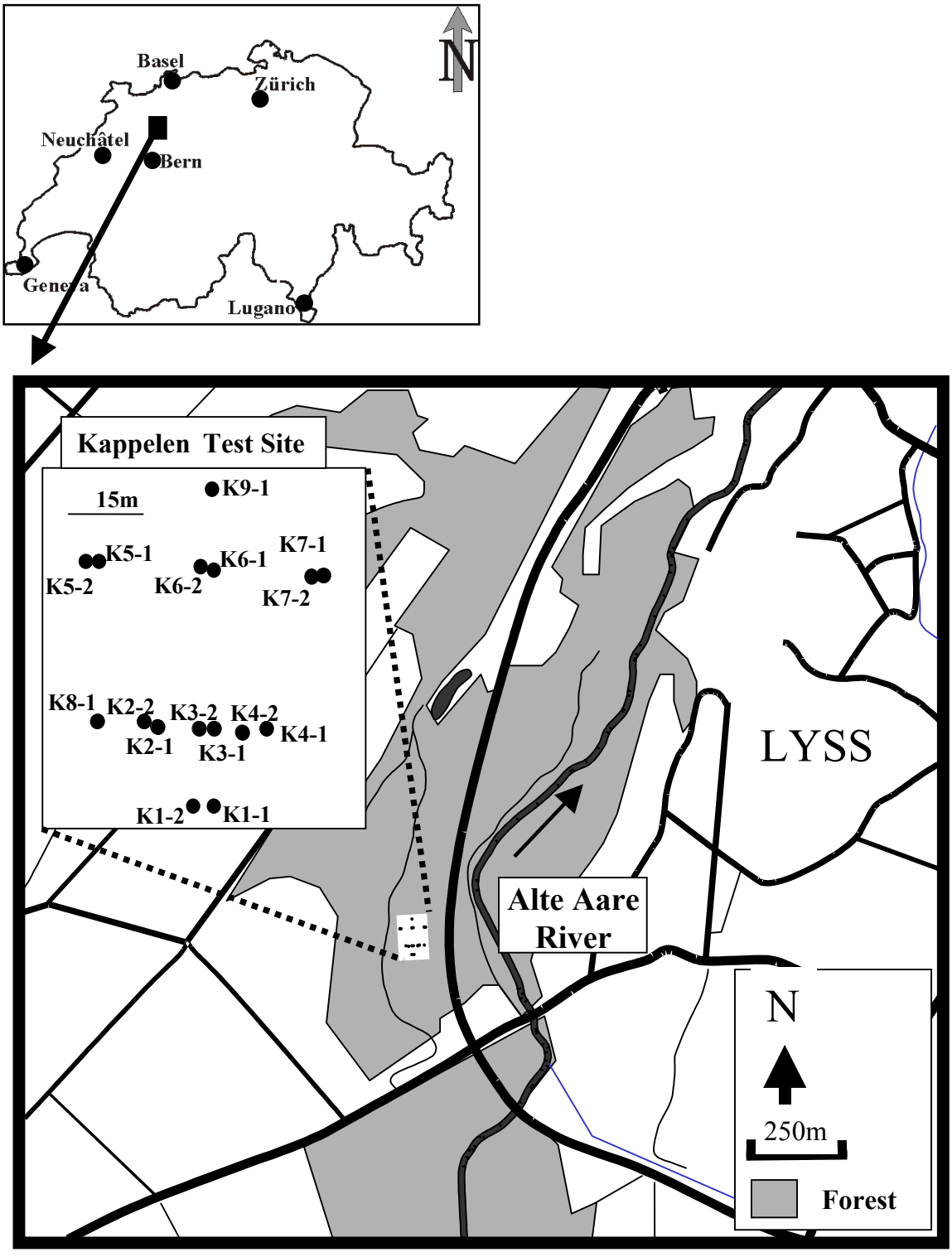

Field hydrochemical sampling carried out in the framework of this earlier research in 1997 recognised that the regionally variable redox conditions, observed in groundwater samples collected from wells in the vicinity of the Kappelen test site (Wersin and others, 2001), also affected the water present in the aquifer below the site (Kennedy and others, 2001a).

6.4 Materials and Methods

6.4.1 Mineralogical Studies

An indication of the mineralogical composition of the Kappelen aquifer and its variability was obtained in a program of X-ray diffraction (XRD) analyses of the four grain fractions of 33 samples of aquifer material. Sand and gravel samples were collected from the cuttings of the three cored boreholes, at K3-1, K7-1 and K8-1 at approximately equal depth intervals. Due to their perceived importance in virus attenuation, processes, investigations focused on the finer-grained fractions (diameter (ø) <4mm) of the aquifer material. Four sand-sized and silt/clay-sized fractions were separated for each sample by passing them through DIN. ISO 3310/1 stainless steel sieves and rinsing in deionised water before drying at 40 °C overnight. The four grain size fractions analysed for each sample were silt and clay (ø<63μm), very fine and fine sand (63μm<ø <250μm), medium and coarse sand (250μm<ø <1000μm) and very coarse sand / granular gravel (1000μm<ø <4000μm). Details of the XRD analytical techniques employed are presented in Chapter 2. The results of these analyses permitted the dominant minerals in the sand and silt/clay sized fractions making up the deposits underlying Kappelen to be identified. Comparisons of results for various samples permitted the degree of spatial variation in mineralogy to be ascertained.

6.4.2 Column Experiments

Virus attenuation processes were investigated using a 25cm long x 1.8cm diameter borosilicate glass column packed with saturated fine-grained (63μm<ø<250μm) Kappelen sands. A Uranine/H40/1 bacteriophage tracer mixture dissolved/suspended in synthetic freshwater (SF) was passed through the column at a flow rate resembling that observed in the field (4.1 ml/min ± 0.2 ml/min between experiments). Following injection of a pore volume of the tracer mixture, an additional six pore volumes of tracer-free SF was passed through the column. The reader is referred to Chapter 2 for further details of the column apparatus and the tracers used in the experiment.

Subsequent to tracer injection/flushing, two pore volumes of 5g/l of protein hydrolysate (Tryptone) mixed in SF with 100μg/l Uranine were passed through the column to release still-virulent viruses that were adsorbed to the aquifer sands. This flushing process was carried out either 30 minutes or 36 hours after the end of bacteriophage injection. Following tryptone injection, the column was

flushed with an additional six pore volumes of tracer-free SF before ending the experiment. Both experiments, where Tryptone was injected 30 minutes after phage injection and 36 hours after phage injection, were repeated in triplicate to ensure experimental reproductability.

Column effluent samples, collected throughout the experiment at 0.3 pore volume intervals, were assayed for H40/1 content using the double layer assay technique (Rossi and others, 1994) within three hours of sampling. Similarly, samples collected at regular intervals from the tracer reservoir were analysed in a similar manner in order to ascertain the H40/1 concentration in the tracer source reservoir, and how it varied over the duration of the experiment. Due to logistical constraints, all experiments were carried out at room temperature (21°C-23°C).

6.4.3 Tracer Testing:

Tracer tests were carried out in the shallow and deep parts of the Kappelen aquifer in July 2001 and August 2001, respectively with a view to investigating virus transport and attenuation processes at the field scale. In both tests, Uranine acted as the solute tracer and the bacteriophage H40/1 was the virus tracer.

The test carried out in the shallow part of the aquifer involved injecting Uranine and H40/1 into K1-2 and monitoring tracer responses in K3-2 and K4-2 down gradient. The injection process involved gradually adding 15 litres of 5g/litre Uranine mixed with 1.65×10^{10} plaque forming units per millilitre(pfu)/ml of H40/1, into an actively circulating system that pumped water from the base of the injection well to the ground surface before being re-injected at the top of the well screen. This approach had the benefit of not disturbing the static water level, and thus permitted tracer to leave the injection well under natural gradient conditions. Tracer injection was carried out over a 34 minute period, and circulated for ten hours thereafter. Regular sampling and analysis of the injection well water permitted temporal Uranine and H40/1 concentration changes in the injection well to be monitored. Samples of the original tracer mixture, kept in the field over the duration of a tracer test, were collected at 12 hour intervals to assess whether suspended H40/1 inactivation was occurring in Kappelen groundwater.

Groundwater monitoring at K3-2 and K4-2 for Uranine and H40/1 content began 5.5 hours after the start of injection and continued until 165 hours after injection. On-line University of Neuchâtel Geomagnetism Group fluorometers (Schnegg & Bossy, 2001) monitored Uranine concentrations at four minute intervals at both locations where well water was circulated using the same system as that employed in K1-2. Peristaltic pumps supplied aliquots of the circulating water to automatic samplers where water samples were collected for bacteriophage analysis over 20 minute intervals (Figure 6.2).

All samples collected for bacteriophage analysis were refrigerated, and assayed within 24 hours of sampling using a two stage process. An initial stage qualitatively determined whether H40/1 was present in a sample or not. A subsequent stage permitted phage concentrations in samples to be accurately quantified using a series of successive dilutions, where necessary, until no more than 150-200 pfu/petri dish were present in each sample. H40/1 assays of all samples were carried out using the double layer technique (Rossi, 1994).

Tracer testing in the deep part of the aquifer involved injecting 75g of Uranine and $6.3x10^{14}$pfu of H40/1 in K1-1 over a one hour period following the same procedure as described for the shallow zone tracer test. Similarly, monitoring of tracer concentrations in groundwater samples was carried out at K2-1 and K3-1 in the same manner as that used at K3-2 and K4-2 during the shallow zone tracer test. Monitoring at both K2-1 and K3-1 continued for 72 hours after the start of injection.

6.4.4 Hydrochemical Sampling

Two campaigns of hydrochemical sampling were carried out at Kappelen in June 2001 and in February 2002. Sampling consisted of pumping monitoring wells at low flow rates (inducing less than 1cm of drawdown) at the top and base of the screened interval of each well, while monitoring hydrochemical conditions of the discharge water at the well head. Well head hydrochemical parameters monitored (with measurement instruments in parenthesis) were temperature/electrical conductivity (WTW LF 318 electrical conductivity meter/thermometer), pH (Orion Research 407 ion analyser/Sentix 60 pH electrode), redox potential (Orion research 407 ion analyser/Metrohm combined redox electrode) and dissolved oxygen (WTW oxi330 dissolved oxygen meter). Once the wellhead parameters stabilised, samples were collected for analyses. Analyses of groundwater samples using a Hanna instruments C-211 ion analyser allowed concentrations of ferrous iron to be immediately determined at well head after sampling, while field-based hydrogen sulphide analysis was carried out during the February 2002 sampling event by degassing samples in the presence of compound sensitive paper (Hach, Ames-IA, USA). Anion and cation water samples were stored in two separate 250mL HDPE bottles and analysed in the laboratory using ion chromatography (DIONEX).

Acidification of samples for major cation analyses using 1M HNO_3 ensured that no changes in ammonium concentrations occurred prior to analyses. Total organic carbon and dissolved organic carbon samples collected during the February 2002 campaign were stored in zero headspace 40mL glass vials with 2mL of 1 M H_2SO_4 prior to analysis by combustion. All samples were refrigerated to 5°C immediately upon collection.

6.5 Results

6.5.1 Mineralogical Analyses

Table 6.1 summarises the results of the XRD analyses of the sand and silt/clay size fractions of the 33 samples collected from borehole cuttings at K3, K7 and K8. All samples are dominated by framework silicates (quartz, K feldspar & Na feldspar), carbonates (calcite & dolomite) and sheet silicates. The residual minerals presented in the table represent additional sheet silicates whose exact mineralogy could not be confidently identified by XRD (T. Adatte, pers comm). Significantly, iron-oxide minerals commonly associated with virus attenuation (Ryan and others, 1999, Lukasik and others, 2000) were not detected, except in one sample of silt/clay material, where it made up approximately 2% of constituent minerals. This is consistent with microscopic observations of the aquifer material, where staining associated with these mineral types was not observed.

Figure 6.3 graphically presents the relative compositions of the major minerals identified in each grain size fraction and the compares mineralogy of each grain size fraction in samples collected in the shallower part of the aquifer with that of samples obtained at depth. Similarly, Figure 6.4 illustrates the variation in mineralogy for grain-size each fraction by borehole.

Overall the XRD data for each mineral identified show that, although all grain size fractions contain the same minerals, the relative proportions of each mineral can vary from one fraction to the other. However, Mann-Whitney statistical comparisons of the mineralogy of each fraction in the upper and lower parts of the aquifer failed to find significant differences in the aquifer mineralogy between the two zones (at the α= 1% confidence level). Similarly, Kuskall-Wallis analysis of variations in mineralogy from one borehole to another failed to reveal significant lateral variations in mineralogy.

Despite the similarity in mineralogy between sampling locations and with depth, it is possible that difference in the residual mineral fraction between samples collected from different parts of the aquifer existed. However, the lack of significant difference in the composition of identifiable minerals suggests that the source material was the same throughout the period in which the aquifer was deposited. Consequently, the composition of the residual mineral fraction is not anticipated to change either.

6.5.2 Column tests

The results of H40/1 assays of column effluent samples plotted relative to source concentrations in the tracer reservoir (relative concentration) permitted variations in bacteriophage concentration with time (breakthrough curve) to be generated for each experiment. Integration of the bacteriophage breakthrough curves generated prior to Tryptone flushing allowed the proportion of H40/1 that

managed to flow through the column to be determined. Based on this figure the H40/1 attenuation capacity of the Kappelen sands in the column could be determined. Integration of the H40/1 breakthrough curve generated by subsequent flushing using the Tryptone solution allowed the proportion of still virulent H40/1 that could be desorbed from the Kapelen sands by the solution to be determined.

Measurements of H40/1 concentration variation with time in the source tracer reservoir permitted inactivation rates of H40/1 suspended in SF at ambient experimental temperatures to be determined. These rates were used to correct virus recoveries calculated from column effluent assays, where inactivation rates of H40/1 suspended in liquid were shown to be significant.

Figure 6.2: Schematic diagram illustrating the operation of the sampling apparatus used for tracer testing. A submersible pump pumped well water through an on-line fluorometer at the well head, permitting Uranine concentrations to be measured. The circulating water (indicated by dark grey arrows) passed through a flowmeter before reaching a three-way valve. A portion of the water at the three way valve was pumped to an automatic sampler to permit bacteriophage sample collection. Remaining water was returned to the well.

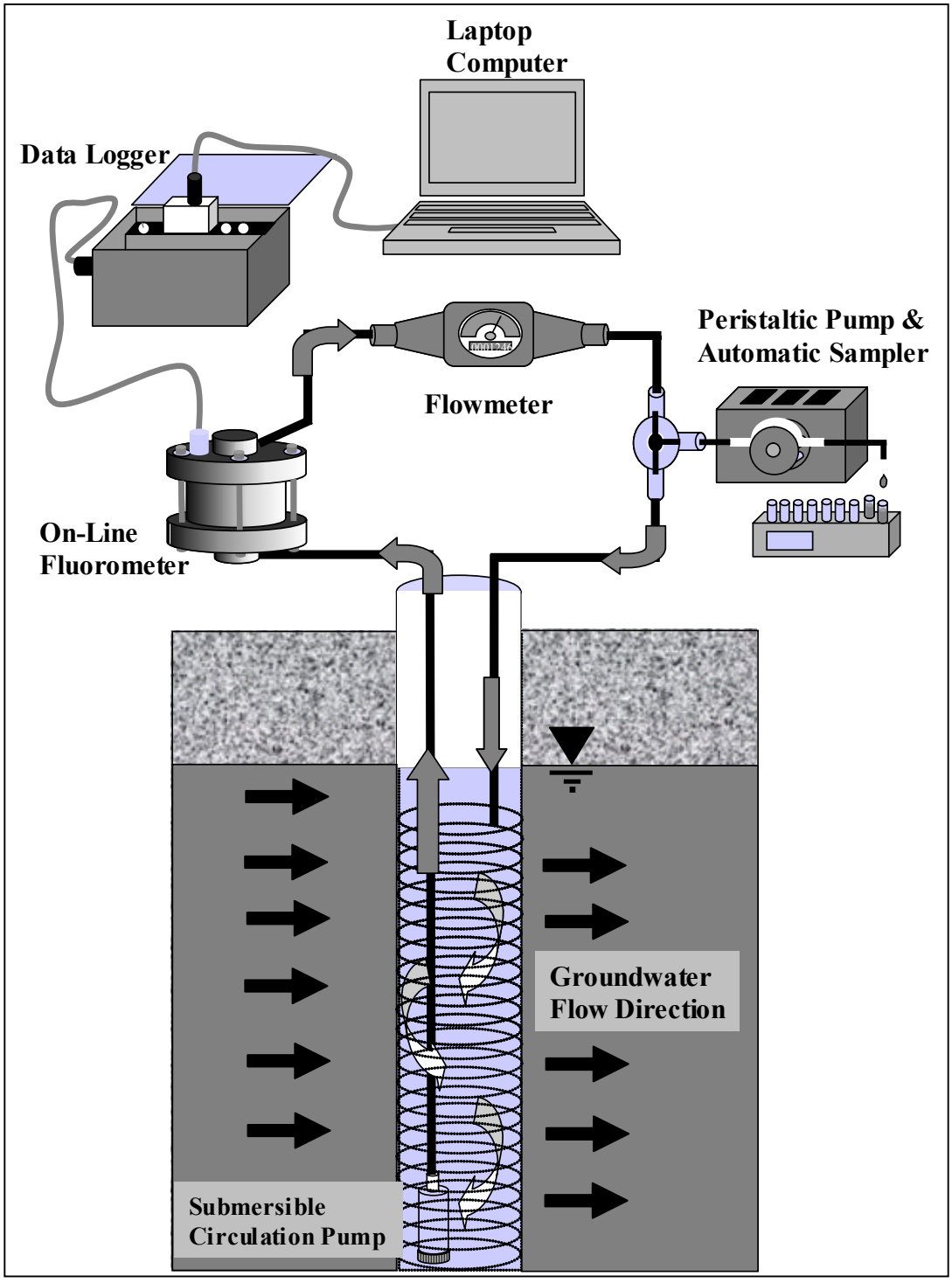

Table 6.1: Summary of results of XRD mineralogical analyses.

Size Fraction	Calcite (%Vol)	Quartz (%Vol)	K-Feldspar (%Vol)	Na Feldspar (%Vol)	Dolomite (%Vol)	Sheet Silicates (%Vol)	Ankerite (%Vol)	Residual Minerals* (%Vol)
ø<63µm								
Mean	40.36	26.63	2.65	6.02	4.39	5.71	0.05	14.53
Maximum	54.43	35.87	12.47	12.12	16.20	9.82	1.29	48.02
Minimum	16.45	13.71	0.00	2.32	0.00	2.97	0.00	0.36
Std. Deviation	9.72	5.33	2.14	2.24	4.02	1.68	0.24	12.03
No. Samples	33	33	33	33	33	33	32	32
63µm<ø<250µm								
Mean	26.07	38.52	4.53	9.11	0.93	3.49	0.01	17.35
Maximum	37.24	47.50	10.53	18.43	5.89	5.94	0.17	62.64
Minimum	6.71	18.49	1.41	3.33	0.00	1.34	0.00	0.72
Std. Dev.	6.76	6.38	2.33	3.51	1.20	1.17	0.03	13.30
No Samples	33	33	33	33	33	33	33	33
250µm<ø<1000µm								
Mean	27.58	39.08	6.18	9.27	0.55	3.40	0.01	13.93
Maximum	51.74	53.51	15.52	21.80	2.02	6.01	0.22	63.57
Minimum	13.70	15.23	1.05	2.04	0.00	1.50	0.00	0.20
Std. Dev.	8.01	8.36	4.49	4.31	0.49	1.09	0.04	13.23
No Samples	33	33	33	33	33	33	33	33
1000µm<ø<4000µm								
Mean	41.14	32.86	2.06	4.67	0.32	3.28	0.00	15.71
Maximum	60.31	43.88	19.46	12.88	1.99	6.74	0.00	59.95
Minimum	13.98	15.90	0.00	0.74	0.00	0.00	0.00	0.12
Std. Dev.	10.14	6.55	3.25	2.77	0.47	1.56	0.00	15.35
No Samples	34	34	34	34	34	34	34	34

Notes: Residual Minerals are those not identified by XRD analyses and are regarded as unidentified sheet silicates.
Goethite only detected in one sample of silt/clay material. Data not presented in table.

Figure 6.3: Trilinear Plots of Variation of Mineralogy with Grain Size Fraction Kappelen Test Site. (A) ø<63µm, (B) 63µm<ø<250µm, (C) 250µm<ø<1000µm, (D) 1000µm<ø<4000µm. Note: Hollow diamonds denote samples from 8.5 to 16 metres below ground surface (mBGS). Black squares denote samples from 3 to 8.5 mBGS.

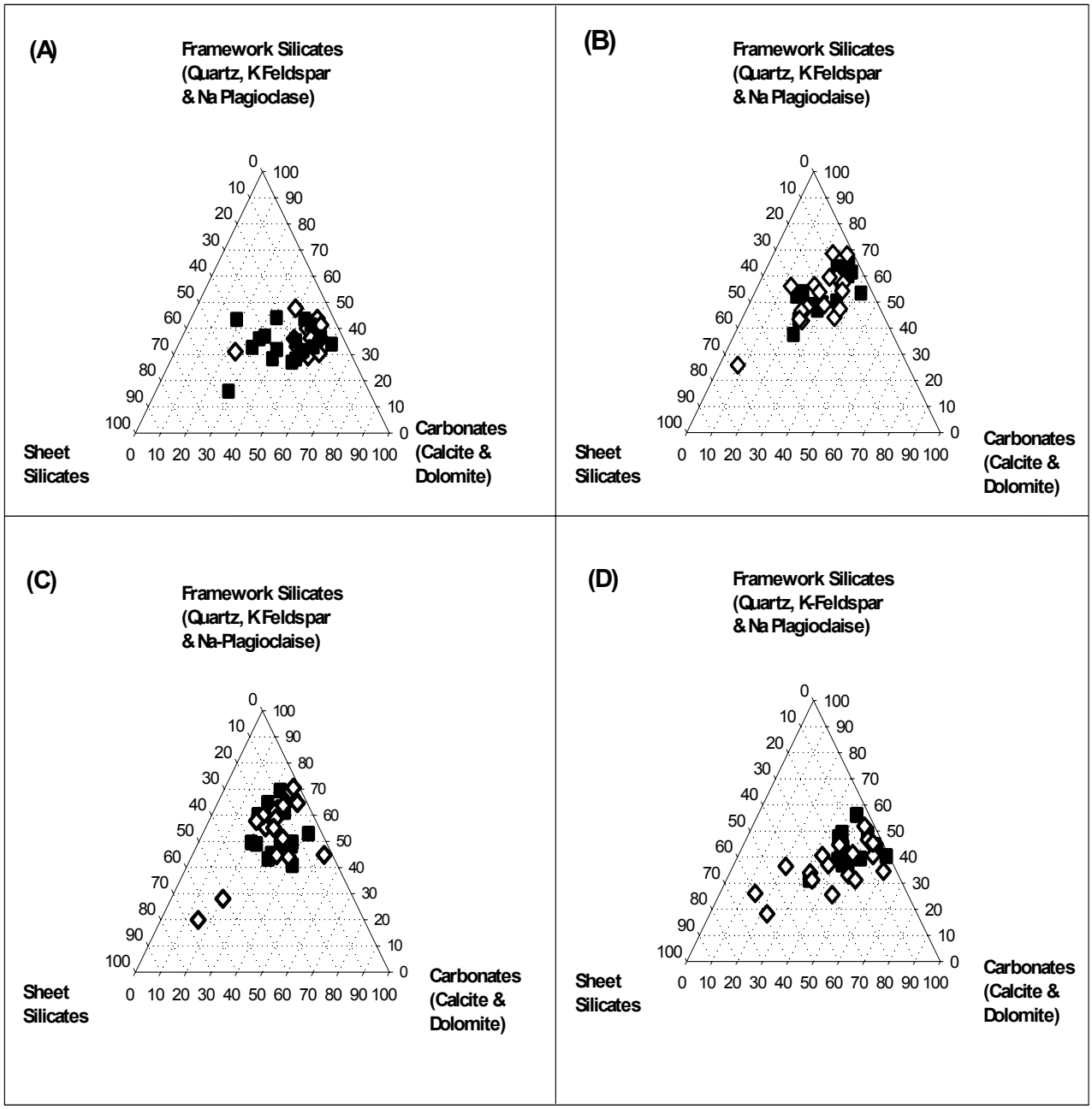

Figure 6.4: Trilinear plots of variation of mineralogy with sampling location and grain size.(a) ø<63µm, (b) 63µm<ø<250µm, (c) 250µm<ø<1000µm, (d) 1000µm<ø <4000µm. Note: Solid circles denote samples collected at K3-1; Hollow circles denote samples collected at K7-1; Inverted triangles denote samples collected at K8-1.

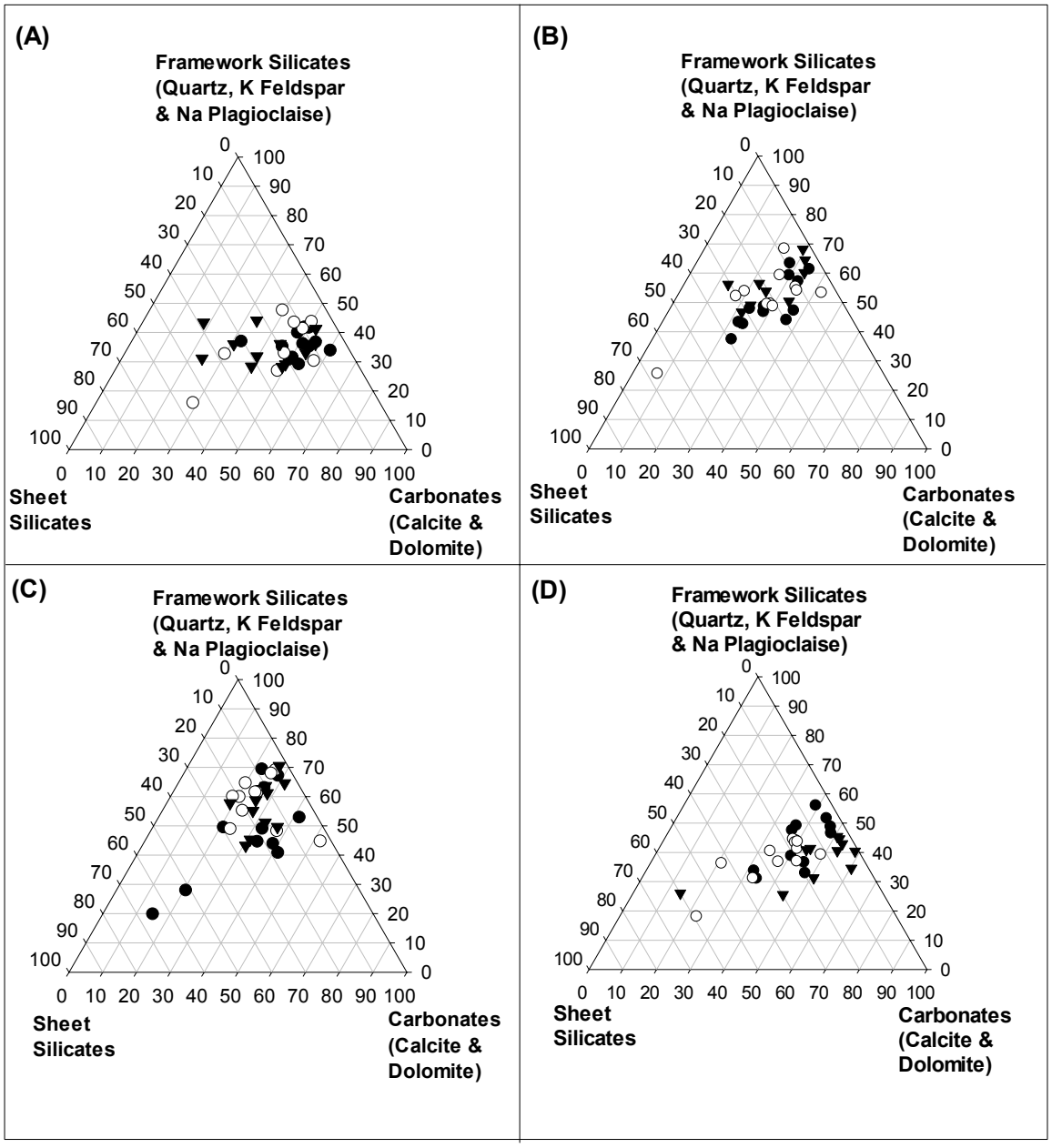

Table 6.2 summarises the results of the column testing. The results of viral assays indicated that H40/1 contents in both source and effluent samples individual analyses varied by ± 25% of the average value measured. Data noise associated with this variability meant that inactivation rates of suspended H40/1 could not be calculated for short term experiments where Tryptone flushing was

carried out 30 minutes after bacteriophage injection. In contrast H40/1 contents in the tracer source reservoir had declined sufficiently after 36 hours to permit inactivation rates of between 0.27/day and 0.34/day to be determined for phages suspended in liquid.

H40/1 recoveries calculated from the analysis of column effluent samples prior to Tryptone flushing ranged from 0.0% to 3.1% of the original mass injected. These data indicate that the Kappelen sands used in the column tests have a high capacity to attenuate H40/1. Nonetheless, despite the low recoveries observed almost all H40/1 injected were released (within a 20% margin of error) in subsequent flushing with the Tryptone half an hour after injection. Since assays of samples collected from the source reservoir indicated that suspended H40/1 concentrations did not decline significantly over the duration of these experiments, masses recovered based on effluent concentrations therefore indicate that adsorption was the dominant attenuation process removing virulent viruses and that neither inactivation of suspended nor adsorbed phages was significant during the time frame of these experiments.

In contrast to the short term experiments, the masses of adsorbed viruses eluted by soaking the Kappelen sands in Tryptone after 36 hours range from 55.4% to 66.5% of the original mass injected, after suspended H40/1 inactivation rates are incorporated into the recovery calculations. Loveland and others (1996) demonstrated that virus adsorption to a solid surface can be reversible or irreversible but not both. This implies that the mechanisms of virus adsorption onto surfaces do not change. Consequently, all viruses adsorbed to Kappelen sands, which could be released by Tryptone flushing during short term experiments, should be released by the same process after longer time periods. This is not observed and thus suggests that another process, namely inactivation, is occurring on the surfaces of the Kappelen sands.

Calculated inactivation rates of H40/1 adsorbed on the Kappelen sands used in the column experiments ranged from 0.42/day to 0.63/day, once the inactivation rate of suspended bacteriophages had been accounted for in calculations. These rates are greater than those determined for suspended H40/1. Consequently, the column experiments indicate that the Kappelen sands can preferentially inactivate H40/1 while it is adsorbed to Kappelen sands, relative to those in suspension (QEASS).

6.5.3 Field-based Tracer Test Results

The results of H40/1 assays and Uranine analyses of groundwater samples collected during the July 2001 and August 2001 field-based tracer tests were used to generate breakthrough curves for observation wells K3-2 and K4-2 by dividing tracer concentrations by their respective injected masses. Table 6.3 summarises the results of tracer tests carried out in July and August 2001 and compares them to results obtained during the previous phase of investigation

carried out by Kennedy and others (2001a). Both H40/1 and Uranine were detected in K3-2 and K4-2 following the shallow zone tracer test, as observed previously. However, differences exist in tracer first arrival times, peak concentration times and peak concentrations to various degrees. Nonetheless, it is noteworthy that relative recoveries of H40/1 with respect to Uranine in both cases are comparable, to within approximately an order of magnitude.

Figure 6.5a and Figure 6.5c present the breakthrough curves for H40/1 and Uranine observed in K3-2 during the July 2001 tracer test, along with the injection signal based on solute and particle concentrations in samples collected during tracer circulation. Figure 6.5b presents the results of analyses of bacteriophage samples collected from the tracer reservoir at regular intervals throughout the duration of the July test. No apparent decline in concentration is apparent from the data suggesting that viral inactivation due to reactions with the Kappelen groundwater was not a significant process throughout the duration of this test.

Table 6.2: Summary Table of Results for Column Tests Investigating H40/1 Inactivation.

Experiment	Recovery (%)	Recovery after Tryptone flush (%)	Inactivation rate in liquid (1/day)	Inactivation rate due to interaction with sand (1/day)	Comment
Kappelen Sand #1	0.4	91.1	n/c	n/c	Tryptone Flush after 30 min.
Kappelen Sand #2	0.4	79.2	n/c	n/c	Tryptone Flush after 30 min.
Kappelen Sand #3	3.1	80.9	n/c	n/c	Tryptone Flush after 30 min.
Kappelen Sand #4	0.0	66.5	0.28	0.56	Tryptone Flush after 36 hours.
Kappelen Sand #5	0.4	55.4	0.34	0.63	Tryptone Flush after 36 hours.
Kappelen Sand #6	0.1	55.5	0.27	0.42	Tryptone Flush after 36 hours.

Notes: Recovery is the mass of H40/1 recovered relative to the mass injected.
n/c: Could not be calculated due to data noise.
Inactivation rates assume first order decay.
Recovery Calculations using Tryptone flushing data incorporate inactivation rates in liquid. Margin of error in recovery calculations ±25%.

Table 6.3: Summary table of Uranine and H40/1 tracer responses observed in K3-2 and K4-2 during shallow zone tracer testing in July 1998 and July 2001. Kappelen, Switzerland.

		Uranine			**H40/1**			
Well	Date	First Arrival (Hours)[1]	Peak Conc. Time (Hours)[1]	Peak C/Co	First Arrival (Hours)[1]	Peak Conc. Time (Hours)[1]	Peak C/Co	Relative Recovery[2] (%)
K3-2	July 2001	24.5	61.9	$3.3x10^{-4}$	19.2	30.8	$1.5x10^{-7}$	$1.46x10^{-2}$
	July 1998[3]	13	83	$1.0x10^{-3}$	12	27	$2.0x10^{-6}$	$2.96x10^{-2}$
K4-2	July 2001	13.8	41.8	$5.9\ x10^{-5}$	10.8	16.8	$2.7x10^{-7}$	$6.30\ x10^{-3}$
	July 1998[3]	14	89	$1.0x10^{-5}$	11	17	$6.0x10^{-8}$	$7.61x10^{-2}$

Notes:1. Time since end of tracer injection.
2. Calculated according to Harvey et al (1989) at 160 hours after injection.
3. Determined using data from Kennedy (2002)

In contrast to tracer tests carried out in the shallow part of the aquifer, neither the solute or bacteriophage tracer was detected in either K2-1 or K3-1 during the tracer test in the deep zone. This result is consistent with observations made by Kennedy and others (2001a) who noted that tracer tests carried out during mid to late summer failed to demonstrate a connection between K1-1 and the observation wells K2-1 and K3-1. In contrast tests made by these authors in May 1997 detected the tracer at K2-1, suggesting that the groundwater flow direction in the aquifer may vary temporally.

Since no solute or particle tracers were detected in the deep well tests during the August 2000 tracer test, Figure 6.5d presents the breakthrough curve generated from K2-1 from samples collected during the May 1997 tracer test to facilitate comparison of tracer responses in the shallow and deep parts of the aquifer (Data from Kennedy, 2001). The breakthrough curve generated from data collected at K2-1 and that from K3-2 have a number of features in common. Concentrations of H40/1 in both curves peak before those of Uranine, but at substantially lower relative concentrations. H40/1 concentrations initially decline more sharply than Uranine after peaking, until they reach a point of inflection, after which bacteriophage levels decline much more gradually. Despite the noise observed in both cases, regression analysis shows the decline in H40/1 relative

concentrations in both K2-1 and K3-2 for the last 100 hours of testing is statistically significant.

Field-based investigations of virus transport in dune sands carried out by Schijven and others (1999), using the bacteriophages MS-2 and PRD-1, obtained similarly shaped breakthrough curves to those obtained at Kappelen. These authors attributed the differences between solute and bacteriophage breakthrough curves to three processes, adsorption, desorption and inactivation. Significantly, the authors noted that the slope of the later part of the tail of the breakthrough curve mainly reflects the inactivation of adsorbed bacteriophages. More specifically, the authors stated that the rate of surface inactivation could be determined from the slope of a plot of the log of relative concentration with time. Applying this approach to the slopes of the tails of temporal C/Co breakthrough curves obtained from the Kappelen tracer test data, surface inactivation rates of 0.3264/day, 0.168/day and 0.365/day were calculated from best fit lines of the tailing parts of the breakthrough curves from K3-2., K4-2 and K2-1 respectively. These data thus indicate that inactivation of adsorbed H40/1 occurs in both the shallow and deep parts of the aquifer.

6.5.4 Chemical and Analyses

Table 6.3 and Table 6.4 summarise the results of hydrochemical analyses of organic carbon content in addition to well head and redox sensitive parameters in groundwater samples collected at Kappelen in June 2001 and January/February 2002 respectively. The data demonstrate that there is not a significant difference in groundwater temperature or pH between wells screened in the upper part of the aquifer and those screened at depth. Moreover, the results of major ion analyses of samples collected in June 2001 differ little from those collected in January/February 2002.

Overall, calcium and bicarbonate dominate the major ion hydrochemistry, and vary little between sampling events (Figure 6.6a). Similarly, little difference is apparent in total and dissolved organic carbon contents (DOC/TOC) in water samples collected from the various wells across the site.

In contrast to the major-ion hydrochemistry, the redox conditions in the various monitoring wells at Kappelen differ substantially with depth. Generally speaking, shallow wells have lower concentrations of species indicating reduced conditions, such as ammonium and ferrous iron, while concentrations of dissolved oxygen and nitrate are higher than those in samples collected from deep wells. Superimposed on this depth-variable pattern is a trend towards more reducing conditions on the western side of the site compared to those on the eastern side. The hydrochemical section presented in Figure 6.6b summarises these phenomena for the two sampling events, using dissolved oxygen, ammonium and ferrous iron concentrations to illustrate the differences in redox conditions in different parts of the aquifer.

Temporally, the overall hydrochemical conditions at the site were slightly more reductive during the February 2002 sampling event. However, the results of the analyses of water samples collected by Kennedy and others (2001a) in spring 1997 indicate,little difference in the concentration of redox sensitive species to those observed during the two more recent sampling events. Consequently the variations are suspected to be a result of seasonal variations rather than forming part of a longer-term temporal trend.

It is noteworthy that testing of groundwater samples during the February 2002 water sampling event failed to detect hydrogen sulphide, despite the presence of sulphur in the water (as sulphate). This indicates that redox conditions at the site were insufficiently reductive to cause changes in the oxidation state of the inorganic sulphur present in the groundwater.

6.6 Discussion

The results of field-based and laboratory-based investigations have provided an insight into H40/1 inactivation processes in the deposits underlying Kappelen. Short-term column tests indicate that the Kappelen sand used in this study had a high H40/1 attenuation capacity. By flushing this sand with Tryptone, following the passage of the bacteriophage, still-virulent H40/1 adsorbed to the sand could be released. Flushing 30 minutes after virus injection indicated that all adsorbed phages (with a 25% margin of error) were recovered in the column effluent. This result indicated that, in the short term, adsorption was the dominant attenuation mechanism removing H40/1 from suspension, and that inactivation was not significant.

Flushing of the Kappelen sands with Tryptone 36 hours after bacteriophage injection demonstrated that H40/1 could be released from aquifer surfaces after prolonged periods. However, mass balance calculations indicated a deficit in the number of bacteriophages recovered, even when inactivation rates of suspended H40/1 were taken into account. These data suggest that H40/1s inactivation rate, while adsorbed to the Kappelen sands, was greater than in suspension.

The results of the study are consistent with those of Blanc & Nassar (1996) who reported accelerated inactivation of the bacteriophage MS-2 when it was adsorbed to loamy sand. In contrast, studies by Grant and others (1993) indicated that inactivation rates of the bacteriophage λ, were lower when suspended in liquid than while adsorbed to Ottawa sand. Rossi (1994) studied the inactivation of six different bacteriophages on three different clay minerals and observed that relative inactivation rates for suspended and adsorbed bacteriophages depended both on the bacteriophage type and the adsorbing mineral surface.

Figure 6.5: Plots of Uranine & H40/1 relative concentrations (C/Co) with time. Solute concentrations are represented by a solid line. H40/1 Concentrations are represented by hollow circles. (A) K1-2 Injection Well. July 2001 Tracer Test. (B) H40/1 variation in source reservoir. (C)Breakthrough curves observed at K3-2. July 2001. The origin of daily fluctuations in phage concentration remains undetermined. (D) Breakthrough curves observed at K2-1, May 1998 (Data from Kennedy, 2001). H40/1 errors: +/- 25% of observed value. Uranine errors incorporated into thickness of breakthrough curve line.

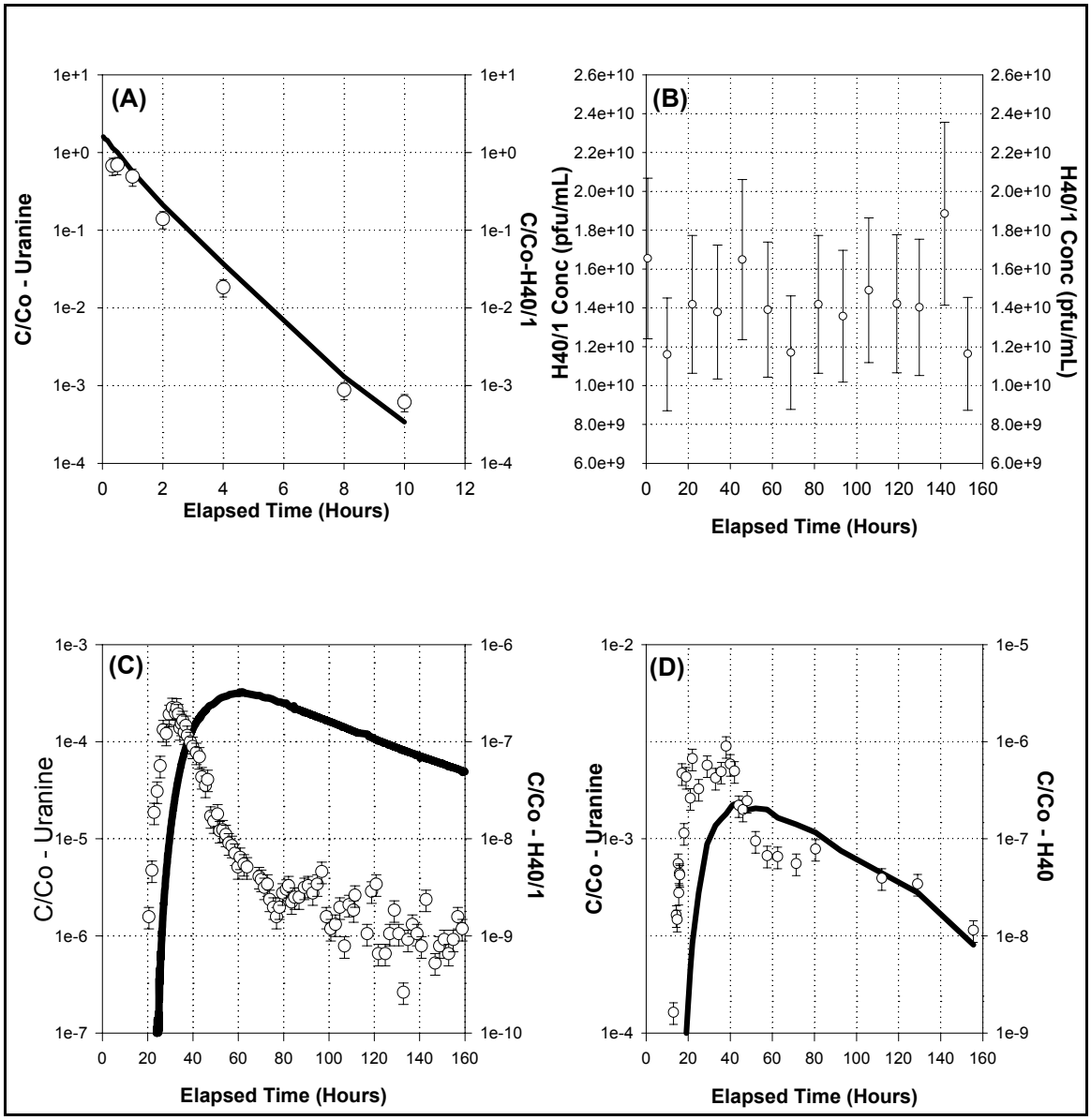

Location	Depth (mBGS)	pH	Temp [°C]	O_2 (mg/l)	Fe^{2+} (mg/l)	NH_4^+ (mg/l)	NO_3 (mg/l)	TOC (mg/l)	SO_4 (mg/l)
K1-1	10	7	10.7	0.06	0.93	0.28	0.67	1.33	38.44
K1-1	13	7.1	10.7	0.16	1.02	0.28	0.45	1.19	38.62
K1-2	5	7.25	12.7	3.38	0.04	0.02	6.22	0.94	35.25
K1-2	8	7.1	10.7	3.54	0.02	0.00	6.71	1.17	35.35
K2-1	10	6.85	10.6	0.05	0.79	0.08	0.22	1.12	40.97
K2-1	15	6.9	10.6	0.06	0.61	0.08	0.28	1.15	41.59
K2-2	5	7.2	10.7	1.80	0.02	0.00	10.10	1.03	34.67
K2-2	8	7.15	10.5	0.56	0.20	0.00	10.33	1.02	34.99
K3-1	10	7.25	10.8	0.06	0.63	0.19	0.52	1.12	39.02
K3-1	15	7.4	10.7	0.13	0.29	0.24	0.36	1.23	39.24
K3-2	5	7	10.7	3.90	0.00	0.00	7.55	1.15	33.79
K3-2	8	7.2	10.7	2.96	0.00	0.03	5.47	0.97	34.46
K4-1	15	7.3	10.6	0.11	0.01	0.06	0.96	0.97	37.35
K4-1	10	7.35	10.7	0.07	0.12	0.03	0.78	1.09	36.86
K4-2	4	7.15	10.7	2.04	0.03	0.02	6.00	0.91	34.98
K4-2	8	7.15	10.4	2.64	0.01	0.03	8.19	1.01	32.61
K5-1	10	6.75	11.1	0.11	1.71	0.64	0.40	0.82	38.66
K5-1	15	7.1	11	0.11	1.71	0.63	0.19	0.80	38.54
K5-2	5	6.9	11	0.33	0.30	0.02	0.17	0.91	39.06
K5-2	8	7	11	0.15	0.27	0.02	0.45	0.97	39.27
K6-1	15	6.7	11	0.11	1.22	0.58	0.61	0.82	38.22
K6-1	10	7	10.9	0.11	1.47	0.53	0.33	0.81	38.41
K6-2	5	7.2	10.4	2.78	0.28	0.00	12.03	0.96	30.37
K6-2	8	7.2	10.2	2.86	0.00	0.00	11.78	0.94	30.31
K7-1	15	7.2	10.9	0.11	0.84	0.58	0.20	0.84	37.83
K7-1	10	7.1	11	0.11	1.19	0.52	0.16	0.90	38.26
K7-2	5	7.3	10	3.14	0.00	0.00	10.07	0.96	32.11
K7-2	8	7.25	10.5	2.55	0.01	0.00	9.82	1.06	34.49
K9-1	12	7.15	11.2	0.11	1.48	0.68	0.37	0.84	37.35
K9-1	16	7.2	11	0.00	1.30	0.67	0.28	0.87	37.59

Table 6.3: Results of well head, redox indicator and total organic carbon analyses for groundwater samples collected during the June 2001 sampling campaign.

Table 6.4: Results of well head, redox indicator and organic carbon analyses for groundwater samples collected during the January/February 2002 sampling campaign.

Location	Depth (mBGS)-1	EC (uS/cm)	pH	Temp [°C]	O2 (mg/l)	Fe2+ (mg/l)	NH4+ (mg/l)	NO3 (mg/l)	TOC (mg/l)	DOC-2 (mg/l)	H2S (mg/l)	SO4 (mg/l)
K1-1	10	446	7.17	11.8	0.50	0.53	0.52	0.03	0.84	0.68	<0.1	35.32
K1-1	13	449	7.22	12	0.40	0.84	1.68	0.03	0.68	0.52	<0.1	35.61
K1-2	5	448	7.2	11.5	0.60	0.31	0.30	0.07	0.86	0.70	<0.1	35.46
K1-2	8	452	7.33	11.8	0.40	0.23	0.29	0.03	0.79	0.63	<0.1	36.03
K2-1	10	454	7.17	11.7	0.46	0.53	0.42	0.00	n/m	n/m	<0.1	38.15
K2-1	15	449	7.24	11.7	0.26	n/m	0.00	n/m	n/m	n/m	n/m	n/m
K2-2	5	460	7.09	10.7	1.67	0.06	0.00	0.74	0.61	0.45	<0.1	36.63
K2-2	8	456	7.15	11.4	0.40	0.22	0.03	0.11	0.67	0.51	<0.1	36.74
K4-1	10	506	7.16	11.8	0.54	0.82	0.32	0.05	0.69	0.53	<0.1	31.87
K4-1	15	491	7.21	12.5	0.36	1.23	3.94	0.02	0.60	0.44	<0.1	35.36
K4-2	4	490	6.99	10.9	4.35	0.01	0.00	0.59	0.59	0.43	<0.1	31.37
K4-2	8	502	7.19	11.6	1.81	0.00	0.03	0.47	0.63	0.47	<0.1	33.48
K5-1	10	501	7.24	11.4	0.60	1.33	0.69	0.00	0.77	0.61	<0.1	38.81
K5-1	15	500	7.15	12.2	0.40	1.45	0.75	0.00	0.82	0.66	<0.1	38.88
K5-2	5	510	7.08	10.8	2.80	0.16	0.00	2.04	0.95	0.79	<0.1	35.85
K5-2	8	520	7.09	11.3	0.50	0.44	0.00	1.20	0.80	0.64	<0.1	35.37
K6-1	10	457	7.45	11.4	0.50	0.23	0.12	0.05	0.53	0.37	<0.1	37.65
K6-1	15	472	7.14	11.4	0.30	0.51	0.39	0.03	0.57	0.41	<0.1	37.05
K6-2	5	502	7.08	10.8	3.80	0.04	0.00	1.28	0.61	0.45	<0.1	32.16
K6-2	8	505	7.3	11.8	1.60	0.01	0.00	0.71	0.59	0.43	<0.1	34.70
K7-1	10	507	6.9	11.3	0.30	0.84	0.32	0.10	0.71	0.55	<0.1	34.37
K7-1	15	502	7.17	11.5	0.26	0.79	0.82	0.01	0.61	0.45	<0.1	34.70
K7-2	5	515	7.07	11	3.07	0.00	0.00	0.65	0.62	0.46	<0.1	31.61
K7-2	8	493	7.17	11.9	1.54	n/a	0.00	0.55	0.55	0.39	<0.1	34.36
K9-1	12	495	7.3	11	0.40	1.39	0.84	0.00	0.81	0.65	<0.1	39.31
K9-1	16	507	7.42	11.3	0.40	0.40	1.34	0.02	0.79	0.63	<0.1	39.30
Alte Aare	n/a	385	8	7.1	10.70	n/m	0.83	6.12	1.83	1.67	<0.1	36.03

Note : 1. mBGS - Metres below ground surface.
2. DOC Corrected for filter effect
3. n/m - Not Measured

The results of statistical analyses of the mineralogy of the different grain size fractions of the samples collected from boreholes drilled at Kappelen suggest that although the relative abundance of different mineral types varies between samples, there was no evidence to suggest statistically significant differences in aquifer composition between boreholes, or between the shallower and deeper parts of the underlying aquifer.

Similarly, hydrochemical analyses of water samples collected from across the site failed to reveal differences in major-ion hydrochemistry, pH or organic carbon content in the groundwater either with depth or between sampling locations. In contrast, these analyses did display notable differences in redox potential between the shallower and deeper parts of the aquifer, and between the eastern and western sides of the site to a lesser degree.

The results of bacteriophage tracer testing in the shallower and deeper parts of the aquifer indicate that H40/1 inactivation is occurring while adsorbed to mineral surfaces in both parts of the aquifer. Inactivation rates at both levels are comparable, but are approximately twice those calculated in laboratory based column tests. Yates and others (1987) demonstrated the importance of temperature in accelerating virus inactivation processes. These differences are thus suspected to be a result of the higher temperature at which the laboratory experiments were carried out (21°C-24°C) relative to the ambient temperature of groundwater in the aquifer underlying Kappelen.

The comparable inactivation rates of adsorbed H40/1 in the upper and lower parts of the aquifer underlying Kappelen, coupled with the absence of mineralogical differences in the aquifer suggest that the differences in redox potential observed with depth did not significantly influence H40/1 inactivation rates.

The results of this study demonstrate the potential benefits of employing multiple-scale investigative techniques in order to understand virus inactivation processes. Laboratory based column studies have been used to identify the importance of virus adsorption and inactivation of adsorbed viruses in the disinfection capacity of the deposits underlying Kappelen. Moreover, field-based studies have indicated similar processes operate in situ in the aquifer, albeit at lower rates. Mineralogical analyses have proved useful in removing potential ambiguities concerning the influence of spatial mineralogical variability in the aquifer on H40/1s inactivation rate. Similarly, hydrochemical analyses coupled with the results of the tracer tests have demonstrated that despite differences in redox potential of the water in the shallower and deeper parts of the aquifer underlying Kappelen, hydrochemical variations at the site do not appear to influence H40/1s inactivation rate.

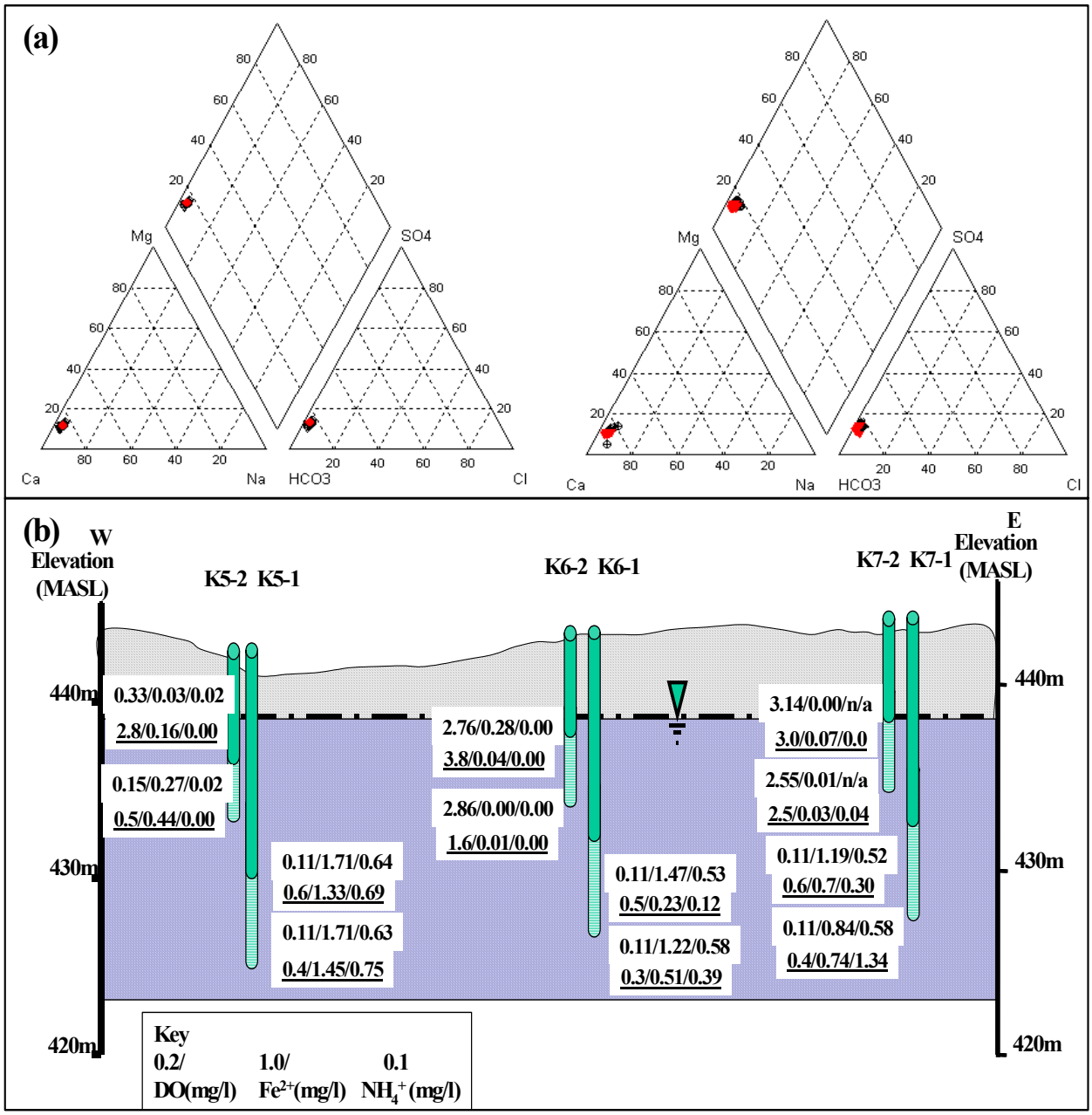

Figure 6.6: (a) Piper plots of major ion chemistry in Groundwater Samples from Kappelen June 2001 - Left, January/ February 2002 - Right. The similarity of analyses from shallow and deep parts of the aquifer means that water samples cannot be distinguished on the basis of major ion hydrochemistry. (b) East-west hydrochemical cross-section with representative redox indicators. June 2001 (not underlined), January/February 2002 - underlined.

Chapter 7 Conclusions & Outlook

7.1 Background

Worldwide epidemiological statistics demonstrate that pathogenic contamination of groundwater remains a significant public health issue in both the developing world and the developed world. This information has recently prompted a substantial increase in investigations in the fields of both colloid and micro-organism transport in aquifers. Within the overall framework of this research, virus transport has received particular attention, with a number of transport and attenuation studies being carried out both at the laboratory scale and at the field scale. However, despite the advances in our understanding of virus behaviour in aquifers resulting from these studies, viral transport and attenuation remains poorly understood, with the results of studies at different scales of investigation often being difficult to reconcile with one other.

Part of the reason for the lack of understanding concerning viral transport and attenuation is due to the natural complexity of many of the aquifers through which viruses are transported. Studies of aquifer outcrop analogies have shown that economically important fluvioglacial gravel deposits that form aquifers in many parts of Central Europe, can be highly heterogeneous in both compositional and textural terms on scales ranging from individual grains to entire basins. Moreover, numerical simulations of the groundwater flow regime in these deposits have demonstrated that such heterogeneities can have a considerable influence on the form that contaminant plumes may take.

Due to the potential importance of these heterogeneities in influencing virus transport, the investigation rationale followed in this thesis involved investigating transport and attenuation processes on a range of scales. Phenomena studied extended from processes that occurred on individual grains (microscale), through processes operating in sedimentary structures (mesoscale) to field studies that operated over 10s of metres (macro-scale). Employing this continuum approach has provided an indication of the role of heterogeneities may play in virus transport, and their appropriate level of operation to be identified / distinguished from processes that may operate over longer or shorter distances.

7.2 Virus Transport Processes

Since virus attenuation is believed to be a (first order) kinetic process, groundwater residence times and the rates of virus transport are critical in determining the degree of attenuation that occurs in an aquifer. In this respect, the results of both meso-scale laboratory investigations and field studies highlighted the importance of preferential flow paths in transport processes operating in heterogeneous porous media. Field-scale tracer tests carried out at

Dornach using a mobile downhole fluorometer, and associated low flow sampling demonstrated that approximately 95% of both solute and bacteriophage tracers observed in a monitoring well were derived from a zone no thicker than 50cm within a 12 metre thick column of saturated sands and gravels. The results of these tests coupled with responses from a second observation well demonstrated significant spatial variation in the groundwater velocity field within the aquifer. Similarly, experiments and resulting simulations in meso-scale simulated sedimentary structures in the laboratory further highlighted the potential importance of preferential flow paths in transporting viruses through porous media. Moreover, simulations of transport in a sedimentary structure demonstrated that the use of averaged grain sizes to evaluate transport and attenuation rates significantly overestimated both the average residence time of the water flowing through the system and the degree of viral attenuation. On a field scale this could have significant implications for estimating transport rates for viruses and other biocolloids, should averaged hydraulic conductivities be used in calculations. By following this later approach and failing to account for system heterogeneity, the size of adequate protection zones around supplies may be underestimated. This may partially explain why some protection schemes fail to adequately protect groundwater and suggests that if appropriate protection zones are to be implemented, an understanding of the role and extent of preferential flow zones in groundwater flow and contaminant transport is necessary. As field studies at Dornach and meso-scale laboratory tests have demonstrated, the use of groundwater tracers can be of considerable use in further investigating this issue.

Studies at Dornach have illustrated the importance of appropriate tracer selection for identifying and quantifying virus transport and attenuation processes. Comparison of solute and bacteriophage/bacterial breakthrough curves demonstrated that size exclusion processes were operating in the underlying aquifer. These processes restricted virus transport to the more rapidly flowing parts of the effective porosity available to solute tracers in a preferential flow zone. The fact that water flows more quickly in this part of the porosity, and that viruses are not transported in the slower flowing pore margins means that microbiological tracers may travel at faster average velocities and have reduced dispersions, relative to solutes. The net result of these processes is that virus transport velocities in aquifers may be underestimated based solute tracer breakthrough data. Moreover, because virus dispersion is reduced due to exclusion processes, the maximum virus concentration anticipated at a point may also be underestimated, depending on the degree of attenuation.

The absence of indications that size exclusion was operating during the meso-scale and micro-scale laboratory experiments further highlights the importance of field studies in evaluating virus transport mechanisms, which may not be apparent on smaller scales. Both exclusion processes and the presence of preferential flow zones are believed to occur more frequently in more heterogeneous systems. Consequently, in order to assess the degree of

influence these aspects exert on virus transport and attenuation, accurate site characterisation is essential. Indeed, the characterisation carried out at Dornach with solute and bacteriophage tracers suggested that although size exclusion processes may result in viruses being transported more rapidly, and with lower dispersion than solute tracers, the overall influence of exclusion processes on groundwater transport rates is subordinate to the effects of preferential flow zones in determining the concentrations of viruses that may be encountered at an observation point. Overall however, adequate assessment of the threat of viral contamination to groundwater quality must involve not only an understanding of mass transport, but also characterisation of attenuation processes operating in an aquifer.

7.3 Factors Controlling Biocolloid Attachment

The factors controlling virus attenuation processes in porous media are, as yet not fully understood. Despite significant research efforts in recent years, a comprehensive theoretical basis does not yet exist to predict rates of adsorption and desorption, particularly with respect to the influence of chemical parameters such as water chemistry and particle / collector surface characteristics. On the other hand, investigations using the filtration theory, including studies carried out in the framework of this thesis suggest that the physical influences controlling viral adsorption can be more confidently evaluated. However, it is worth noting that this theory has been developed to simulate spherical particle filtration through geometrically regular sand-sized material where the high number of collisions between particles and collector surfaces permit statistical theories to be applied as a means of representing particle responses (Thilo Hoffman, pers. Comm.). These assumptions may not apply in coarser grained materials where the number of particle-collector collisions may be below the minimum necessary for theoretical assumptions to be valid. Nonetheless, the filtration theory provides some indication of the effect of collector size on particle attenuation, as shown in simulations carried out by Elimelech et al (1995) using finer grained materials highlighted the strong dependence of deposition rates on collector size. These calculations have shown that a three-fold increase in collector diameter may result in a three to six order of magnitude decline in bed attenuation capacity for particles in the ø=200nm to 2µm size range. Furthermore, additional simulations suggested that virus-sized particles may be even more sensitive to collector diameter size. These results are consistent with the results of studies at Dornach that have yielded high biocolloid tracer relative recoveries of between 20% and 90% in zones of high groundwater flow velocity, presumably due to coarser grain size. This suggests that the attenuation capacity of the preferential flow zones supplying tracer to the observation well B8 is limited and that microbiological contaminants may travel large distances in these units should groundwater flow paths fail to intersect finer-grained beds.

Despite its potential shortcomings, data to date suggest that the filtration theory is an adequate means of simulating colloid attenuation in porous media,

particularly in sand-sized materials. The theory allows some important conclusions to be drawn regarding transport through zones where mass transport is predominantly through more coarsely grained deposits. Due to the elevated hydraulic conductivities of these units, groundwater will flow more quickly through them, than through finer materials under equivalent hydraulic gradients. Assuming the filtration theory to be valid, increases in groundwater flow velocity can be expected to result in increases in the first order deposition constant. On the other hand, since water flows more rapidly in preferential flow zones, it takes less time to flow between injection and observation points. This results in lower exposure of contaminants in these beds to potentially adsorbing surfaces and thus less potential attenuation.

Both theoretical and practical studies have shown that the actual degree of attenuation experienced by viruses depends not only on the physical characteristics of the system but also upon the chemical conditions on the collector and virus surfaces, as well as the chemistry of the suspending solution. Interactions between the particle and collector, as expressed by the collision efficiency, have been shown to vary for a given particle from one mineral to another. Since mineralogy may vary within an aquifer and may give rise to compositional heterogeneity that may occur on a range of scales, collision efficiency may vary within an aquifer. Identification of the role of such compositional heterogeneities on virus attenuation is often difficult to achieve on the field scale, where the influence of various minerals may not be differentiated, and a single collision efficiency values are typically used to characterise attenuation processes operating between injection and observation points. Under these circumstances laboratory based techniques provide an alternative means of evaluating the role of specific minerals in virus attenuation operating at the field scale, although as studies at using the Kappelen sands demonstrated, precautions may need to be taken to ensure that features responsible for attenuation, such as grain coatings are not removed during sampling or preparation processes.

Due to uncertainties associated with the DLVO theory for prediction of adsorption rates, laboratory experiments carried out within the framework of this study were completed in conditions resembling those observed in fluvioglacial aquifers. The resulting studies demonstrated that the silicates and carbonates commonly present in aquifers had low virus adsorption capacities, and that adsorption was dominated by surface heterogeneities in the case of the Kappelen sands.

Since the mineralogy and hydrochemistry of the aquifer at Dornach resembled that at Kappelen, it was not surprising that the Dornach gravels also had a low virus attenuation capacity. Significantly, simultaneous tracer tests carried out at the site using bacteria demonstrated that larger biocolloids were attenuated less than viruses despite their significantly greater size and higher collision efficiencies. The higher collector efficiency suggested that they had a

higher affinity for sticking to aquifer materials. Nonetheless the results are once again consistent with the filtration theory which predicts that larger particles such as bacteria will collide less with aquifer surfaces than smaller viruses that are more strongly influenced by Brownian motion giving rise to a more collisions. This suggests that concerns over greater mobility of viruses in aquifer due to their smaller size may be ill-founded.

7.4 Desorption & Inactivation

Field based tracer testing at both the Dornach and Kappelen test sites have demonstrated that attachment to surfaces can be critical in reducing maximum virus concentrations. However, as the *E.coli* breakthrough curves collected from Dornach suggested, the fact that biocolloids are adsorbed is not necessarily of benefit from a public health perspective. Indeed, the *E.coli* data demonstrated that biocolloids may persist for longer than conservative solutes, albeit at low concentrations. Nonetheless, studies by Westwood and Sattar (1975) have demonstrated that such concentrations may be sufficient to cause an outbreak of disease.

Consequently, if biocolloid, and more specifically viral attenuation processes are to be effective viruses must either be permanently adsorbed to aquifer surfaces or inactivated while adsorbed on reversible deposition sites. Once again laboratory-based studies have been shown to offer considerable potential as a means for identifying which surfaces have the capacity to most strongly adsorb viruses and whether adsorption mechanisms on specific surfaces are reversible or irreversible. Laboratory-based and field-based investigations studying inactivation rates at the Kappelen test site demonstrated that for the case of the bacteriophage H40/1 inactivation occurred preferentially on grain surfaces, but was not significantly influenced by geochemical heterogeneity. Moreover, field inactivation rates and those observed in the laboratory were similar, suggesting that this process was not significantly influenced by larger scale heterogeneities at the site.

It is not as yet clear to what degree these results may translate to other viruses, although field breakthrough curves generated in comparative studies by Kennedy (2001) suggest that other phage types are also inactivated while adsorbed on mineral surfaces. However, in such circumstances sufficient late time breakthrough curve data is necessary if inactivation rates are to be confidently predicted.

7.5 Upscaling

As the studies carried out in this thesis have demonstrated the interactions between viruses and natural mineral surfaces can be complex. In order to understand the potential impact of viral contamination on groundwater quality, the mechanisms of viral transport need to be understood. In this respect

numerical modelling becomes a useful tool both for further understanding the influence of various parameters on viral transport and as a predictive tool to evaluate the risk of viral contamination in a groundwater system.

Studies carried out within the framework of this thesis suggest that the filtration theory provides a useful tool for understanding the influence of physical parameters on virus transport. Application of the theory in studies investigating virus transport through a simulated sedimentary structure demonstrated it could be used to predict virus deposition constants for differing flow velocities not only in texturally uniform columns, but also through more complex structured media. This in turn has helped further understand irregular non-Gaussian breakthrough curves often observed. Unfortunately, it is not yet clear to what degree this approach may be applied in the field largely due to uncertainties associated with possible diffusive effects associated with solute breakthrough, as well the possible influence of different deposition sites having different collision efficiencies occurring in the same aquifer. Nonetheless, the results of the studies contained in this thesis clearly highlight the importance of preferential flow zones in microbiological contaminant transport in perialpine gravel aquifers.Indeed, consideration of aquifer heterogeneity may in part help explain phenomena such as variations in biocolloid attenuation rate often noted to vary with distance from an injection point during field-based tracer tests. Studies by authors such as Schijven and others (1999) noted that attenuation rates along the initial parts of tracer flow paths from an injection point are considerably higher than those observed at over greater distances. As simulations of virus transport in fining upwards sequences has shown, attenuation in fine-grained units is significantly greater than in equivalent coarse-grained deposits. On the other hand, as data from the Dornach test site show, attenuation rates in preferential flow zones (presumably coarser-grained beds) can be substantially lower and thus permit pathogens to travel greater distances than may be anticipated based on rates determined from monitoring points closer to the injection point. Detailed site characterisation coupled with appropriate numerical modelling could help shed additional light on this issue. Unfortunately, high data resolution makes deterministic modelling prohibitive when dealing with heterogeneous deposits such as perialpine gravels.

Recent studies completed by Regli and others (2003) suggest a possible alternative means of addressing this issue using modified geostatistical methods. By assigning properties to specific geological units and then estimating the frequency at which each unit occurs in an aquifer based on data sources such as borehole logs and ground penetrating radar profiles, stochastic methods have been used to develop well head protection areas in the fluvioglacial gravels supplying wells adjacent to the Weisse River, Switzerland. Results achieved to date appear promising, although it must be emphasised that data requirements for the implementation such an approach are high. This may necessitate a cost benefit analysis to be carried out to determine the degree of risk of microbiological contamination a water supplier is prepared to take compared to

the amount of information needed to appropriately characterise the aquifer supplying a groundwater source.

7.6 Outlook

The number of publications that have addressed various aspects of pathogen transport in groundwater in recent years reflect the increasing interest and importance that this issue is taking within the scientific community. One of the reasons why research in this area has only become important relatively recently may relate to the subject matter. The study of pathogen transport in aquifers is a multidisciplinary subject requiring inputs from fields as diverse as microbiology, colloid chemistry, hydrogeology and geochemistry. Such a combination of disciplines is not widely encountered. Consequently, many investigations studying pathogen transport have tended to focus on specific issues requiring inputs from a subset of these disciplines. In some cases investigations by researchers studying related aspects of this problem have used diverse methodologies, derived from their backgrounds to address very similar issues. Results from these studies can be incomparable, or possibly contradictory. Standardised methodologies for investigating this topic could assist considerably in resolving this issue.

Investigations into the issue of virus transport in groundwater have been carried out at a range of scales. Numerous laboratory scale studies have investigated this topic over the past 25-20 years. In contrast, field-scale investigations of pathogen transport have historically received less attention, despite their capacity to demonstrate migration processes in situ. This negligence has, in part been a result of the considerable logistical and financial commitments necessary to carry out field investigations. Moreover, the results of these investigations were often inconclusive because of a lack of appropriate data and/or due to uncertainty associated with hydrogeological conditions in the aquifer of interest. Nonetheless, it is an inescapable fact that field-scale investigations are of great relevance when studying pathogenic contamination of aquifers, since it is from these types of deposits that groundwater containing contaminants impacting public health are derived. Recent technological developments have resulted in the availability of materials and equipment that have made more accurate site characterisation and the implementation of field scale tracer programs easier and more cost effective. The prospect of completing mass transport investigations has thus become considerably less prohibitive and is anticipated to result in an increasing number of field studies of microbiological tracer transport in the subsurface in future. This is expected to result in an improved understanding of the relationship between pathogen migration and aquifer structure. Moreover, the availability of new technology can permit testing to continue for more prolonged periods in which the late time responses of virus tracers may be investigated in more detail. This could allow attenuation phenomena such as inactivation processes to be characterised in greater detail.

Given the wide variety of possible geological conditions encountered in aquifers the scope for further hydrogeological research into pathogen transport in groundwater remains considerable. This study has demonstrated the importance of considering aquifer heterogeneity when trying to understand pathogen transport and attenuation. Due to the complexity of highly heterogeneous aquifers, the limited number of points sampled by drilling during site investigation/characterisation are often insufficient to gain an adequate appreciation of the nature of the underlying deposits. The application of surface geophysical methods such as ground penetrating radar and seismic refraction offer a means to enhance our knowledge of subsurface. However, the resolution of these methods can decline with depth and may fail detect phenomena such as preferential flow zones as distance from the ground surface increases. More recently developed downhole geophysical methods such as cross hole radar tomography offer some potential in this area, but may, once again be limited by the number of available sampling points available and the quality of existing site investigation data, particularly if the separation between sampling points is large (H.Paasche, pers comm.)

Further studies using aquifer outcrop analogies may provide a means to better understand heterogeneous aquifer complexity and variability while simultaneously permitting micro and meso scale features pertinent to virus transport to be studied in greater detail. Generation of synthetic groundwater plumes using the outcrop analogy approach have highlighted the potential complexity of contaminant distribution in fluvioglacial deposits and the potential use of the method in understanding deviations from idealised conditions in highly heterogeneous aquifers. Moreover, the potential further study of contaminant migration in meso-scale features such as sedimentary structures, coupled with detailed sampling of outcrop materials shows considerable potential as a means of reconciling microscale laboratory features with macroscale phenomena observed in the field, and thus providing further indications of the relative importance of preferential flow paths in pathogen transport.

Finally, further field-scale investigations need to be coupled with on-going development of theoretical models that may provide an appropriate basis by which virus transport and attenuation processes in different environments may be further understood and compared. This applies particularly to the extension of the filtration theory to gravel-sized deposits and to further development of colloid/collector interaction theories. This later aspect could be used to develop a theoretical basis for predicting the collision efficiencies of microbiological particles with aquifer materials based on a given mineralogy. Ideally both filtration theory and collision theory models could ultimately be used on a predictive basis to protect groundwater supplies. At the time of writing, existing models were capable of predicting filtration rates in sand-sized collectors and deposition rates under favourable deposition conditions and idealised geometries. These theories need to be extended to incorporate the non-idealised conditions of the natural world if virus transport and attenuation processes are to be predicted with any

degree of confidence, and this serious public health issue tackled with a greater degree of confidence.

8. Bibliography

Abu-Ashour, J., Joy, D. M, Lee, H., Whiteley, H. R., and Zelin, S. (1994). Transport of microorganisms through soil. Water, Air and Soil Pollution 75, 141-158.

Ackerman, H. W. and DuBow, M. S. (1987). Virus of procaryotes. [Vol II], pp 242. CRC Press. Boca Raton, Florida.

Adatte, T., Stinnesbeck, W., and Keller, G. (1996). Lithostratigraphic and mineralogic correlations of near K-T boundary clastic sediments in northeastern Mexico: Implications for origin and nature of deposition. Geological Society of America, Special Paper. 307, 211-226.

Allen-King, R. M. (1997). Characterizing the heterogeneity and correlation of perchloroethene sorbtion and hydraulic conductivity using a facies-based approach. Water Resources Research 34[3], 385-396.

Allen, J. R. L. (1985). Principles of physical sedimentology. Pp 272. Allen & Unwin. Herts., UK.

Anderson, M., Aiken, J. S., Webb, E. K., and Mickelson, D. M. (1999). Sedimentology and hydrogeology of two braided stream deposits. Sedimentary Geology 129, 187-199.

Appelo, C. A. J and Postma, D. (1993). Geochemistry, groundwater and pollution. Pp536. Balkema, Rotterdam.

Ashmore, P. E. and Ferguson, R. I. (1986). Interrelationships of channel processes, changes and sediments in a proglacial braided river. Geografiska Annaler 68[A], 361-371.

Aspiron, U. and Aiger, T. (1999). Towards realistic aquifer models: Three-dimensional georadar surveys of quaternary gravel deltas (Singen Basin, SW Germany). Sedimentary Geology 129, 281-297.

Bales, R. C, Gerba, C. P., Grondin, G. H., and Jensen, S. L. (1989). Bacteriophage transport in sandy soil and fractured tuff. Applied and Environmental Microbiology 55, 2061-2067.

Bales, R. C, Hinkle, S. R., Kroeger, T. W., Stocking, K., and Gerba, C. P. (1991). Bacteriophage adsorption during transport through porous media: Chemical perturbations and reversibility. Environmental Science & Technology 25, 2088-2095.

Bales, R. C, Shimin, L., Maguire, K. M., Yahya, M. T., Gerba, C. P., and Harvey, C. (1995). Virus and bacteria transport in a sandy aquifer, Cape Cod, MA. Groundwater 33[4], 653-661.

Bales, R. C, Shimin, L., Yeh, J., Lenczewski, M., and Gerba, C. P. (1997). Bacteriophage and microsphere transport in saturated porous media: Forced gradient experiment at Borden, Ontario. Water Resources Research 33[4], 639-648.

Bear, J. (1972). Dynamics of fluids in porous media. Pp764. American Elsevier Publishing Group. New York,

Behrens, H., Borkovec, M., and Schurtenberger, P. (1998). Aggregation in charge-stabilised suspensions revisited. Langmuir 14, 1951-1954.

Bersezio, R., Bini, A., and Giudici, M. (1999). Effects of sedimentary heterogeneity on groundwater flow in a Quaternary pro-glacial delta environment: Joining facies analysis and numerical modelling. Sedimentary Geology 129, 327-344.

Bickmore, B. R., Nagy, K. L., Sandlin, P. E., and Crater, T. S. (2002). Quantifying surface areas of clays by atomic force microscopy. American Mineralogist 87[5-6], 780-783.

Blanc, R. and Nasser, A. (1996). Effect of effluent quality and temperature on the persistence of viruses in soil. Water Science and Technology 33, 237-242.

Bolster, C. H., Mills, A. L., Hornberger, G. M., and Herman, J. S. (1999). Spatial distribution of deposited bacteria following miscible displacement experiments in intact cores. Water Resources Research 35[6], 1797-1807.

Bowen, B. D. and Epstein, M. (1979). Fine particle deposition on smooth parallel plate channels. Journal of colloid and interface science 72, 81-97.

Brock, T. D. and Madigan, M. T. (1991). Biology of microorganisms. Sixth Edition. Prentice Hall, New York.

Campbell-Rehmann, L., Welty, C., Harvey, R.W., (1999) Stochastic analysis of virus transport in aquifers. Water Resources Res. 35 (7), 1987-2006.

Carvalho Dill, A. (1993). Spatial variability in porous aquifer properties. Synthetical approach by geophysics, tracer techniques and groundwater flow parameters. PhD Thesis. Hydrogeology Centre, University of Neuchâtel.

Craun, G. F. (1986). Statistics of waterborne disease outbreaks (1920-1980). Craun, G. F. Water Diseases in the United States, pp 73, CRC Press. Boca Raton, Florida.

Crump, K. S. (1976). Numerical invesion of Laplace transforms using fourrier series approximation. Journal of Associated Computational Mechanics 23[1], 89-96.

DeBorde, D., Woessner, W., Quinn, T. K., and Ball, P. (1999). Rapid transport of viruses in a floodplain aquifer. Water Research 33[10], 2229-2238.

Degueldre C., Pfeiffer, H.R., Alexander, W., Wernli, B., Bruetsch, R. (1996) Colloid properties in granitic groundwater systems .1. Sampling and characterisation. Applied Geochemistry 11 (5): 677-678

DeHoog, F. R., Knight, J. H., and Stokes, A. N. (1982). An improved method for numerical inversion of Laplace transforms. Journal of Scientific and Statistical Computing 3, 357-366.

Dieulin, A. (1980). Pollutant propagation in an alluvial aquifer: The effect of flow paths. PhD Thesis. Pp 207. Pierre and Marie Curie University, ParisVI.

Diomande, A. K. (2000). A hydrogeological investigation of the Kappelen Aquifer in the Bernese Seeland. Contributions from electrical tomography and the use of artificial tracers. (In French). Masters Thesis, pp 41. Hydrogeology Centre, University of Neuchâtel.

Disnar, J. R., Guillet, B., Keravis, D., Massif, R., and Di-Giovanni, C. (2003). Soil organic matter (SOM) characterization by Rock-eval pyrolysis: Scope and limitations. Organic Geochemistry 34, in press.

Domenico, P. A. and Schwartz, F. W. (1990). Physical and chemical hydrogeology. Pp 824. Wiley, New York.

Dreyer, T. (1993). Geometry and facies of large-scale flow units in fluvial dominated fan-delta front sequences. Advances in reservoir geology. 135-174. Geological Society Spec. Publ. 69, London.

Drost, W., Klotz, D., Koch, A., Moser, H., Neumaier, F., and Rauert, W. (1968). Point dilution methods of investigating groundwater flow by means of radioisotopes. Water Resources Research 4[1], 125-146.

Elimelech, M., Gregory, J., Jia, X., and Williams, R. (1995). Particle deposition and aggredation. Measurement, modelling and simulation. Pp. 441. Butterworth-Heinemann, Oxford.

Elimelech, M. and O'Melia, C. (1990). Kinetics of deposition of colloidal particles in packed beds under attractive double layer interactions. Environmental Science & Technology 24, 1528-1536.

Essaid, H. I., Herkelrath, W. N., and Hess, K. M. (1993). Simulations of fluid distributions observed at a crude oil spill site incorporating hysteresis, oil entrapment and spatial variability of hydraulic properties. Water Resources Research 29[6], 673-684.

European Commission. (1995). Cost Action 65. Hydrogeological aspects of groundwater pollution in karstic areas-Final Report. EUR 16547EN, pp 446. Luxembourg.

Fetter, C. W. (1999). Contaiminant hydrogeology. Second Edition, pp500. Upper, Prentice-Hall, Saddle River, New Jersey.

Freeze, R. A. and Cherry, J. A. (1979). Groundwater. Pp 604, Prentice-Hall, New York.

Garabedian, S., LeBlanc, D. R., Gelhar, L., and Celia, M. A. (1991). Large-scale natural gradient tracer test in sand and gravel, Cape Cod, Massachussetts, 2, Analysis of spatial moments. Water Resources Research 27[911], 924.

Gelhar, L. (1993). Stochastic subsurface hydrology. Prentice-Hall, Englewood Cliffs, NJ.

Gerba, C. P. and Bitton, G. (1984). Microbial pollutants: Their survival and transport pattern to groundwater. In Gerba, C. P. and Bitton, G.(Eds) Groundwater pollution microbiology. 66-68. John Wiley & Sons, New York.

Gerba, C. P., Goyal, S. M., Cech, I., and Bogdan, I. (1981). Quantitative assessment of the adsorptive behaviour of viruses to soils. Environmental Science & Technology 15, 940-944.

Ginn, T. (2000) Comment on "Stochastic analysis of virus transport in aquifers", by Linda L. Campbell Rehmann, Claire Welty and Ronald W. Harvey, Water Resources Research, 36 (7) 1981-1982.

Ginn, T., Wood, B. D., Nelson, K. E., Scheibe, T. D., Murphy, E., and Prabhakar, C. (2002). Processes in microbial transport in the natural subsurface. Advances in Water Resources 25, 1017-1042.

Gleick, P. H. (2002). Dirty water: Estimate deaths from water-related diseases 2000-2020. Pacific Institute Report 1, pp12. Pacific Institute for Studies in Development, Environment and Security.

Grahame, D. C. (1947). The electric double layer theory of electrocapilliarity. Chemical Reviews 41, 441-501.

Grant, S. B. (1994). Virus coagulation in aqueous environments. Environmental Science & Technology 28, 928-933.

Grant, S. B., List, E. J., and Linsttom, M. E. (1993). Kinetic analysis of virus adsorption and inactivation in batch experiments. Water Resources Research 29, 2067-2085.

Grindrod, P. (1993). The impact of colloids on the migration and dispersal of radionuclides within fractured rock. Journal of Contaminant Hydrology 13, 167-181.

Grolimund, D., Elimelech, M., Borkovec, M., Barmettler, K., Kretzschmar, R., and Sticher, H. (1998). Transport of in situ mobilized colloidal particles in packed soil columns. Environmental Science & Technology 32, 3562-3569.

Harter, T., Wagner, S., and Atwill, E. R. (2000). Colloid transport and filtration of Cryptosporidium parvum in sandy soils and aquifer sediments. Environmental Science & Technology 34[1], 62-70.

Harvey, R. W. (1997). Microorganisms as tracers in groundwater injection and recovery experiments: A review. FEMS Microbiology Reviews 20, 461-472.

Harvey, R. W and Garabedian, S. (1991). Use of colloid filtration theory in modeling movement of bacteria through a contaminated sandy aquifer. Environmental Science & Technology 25[1], 178-185.

Harvey, R. W, George, L. H., Smith, R. L., and LeBlanc, D. R. (1989). Transport of microspheres and indigenous bacteria through a sandy aquifer: Results of natural and forced-gradient tracer experiments. Environmental Science & Technology 23, 51-56.

Harvey, R. W, Kinner, N. E., MacDonald, D., Metge, D., and Bunn, A. (1993). Role of physical heterogeneity in the interpretation of small scale laboratory and field observations of bacteria, microbial sized microsphere and bromide transport through aquifer sediments. Water Resources Research 29[8], 2713-2721.

Huggenberger, P. (1993). Radar Facies: Recognition of facies patterns and heterogeneities within Pleistocene Rhine gravels, NE Switzerland. In Best, J. L. and Bristow, C. S. (Eds) Braided Rivers. 163-176. Geological Society Special Publication No. 75. London.

Huggenberger, P. and Aiger, T. (1999). Introduction to the special issue on aquifer sedimentology: Problems, perspectives and modern approaches. Sedimentary Geology 129, 179-186.

Hurst, C. J., Gerba, C. P., and Cech, I. (1980). Effects of environmental variables and soils characteristics on virus survival in soil. Applied and Environmental Microbiology 40[1067], 1079.

Hutchins, S. R. and Acree, S. D. (2000). Groundwater sampling bias observed in shallow, conventional wells. Groundwater Monitoring and Remediation 20[1], 86-83.

Israelachvili, J. N. (1992). Intermolecular and surface forces. Second Edition. Academic Press, London.

Jin, Y., Yates, M. V., Thompson, S. S., and Jury, W. A. (1997). Sorption of viruses during flow through saturated sand columns. Environmental Science & Technology 31, 548-551.

Jin, Y., Pratt, E., Yates, M.V. (2000) Effect of mineral colloids on virus transport through saturated sand columns. Journal of environmental quality 29 (2), 532-539.

Johnson, P. R., Ning, S., and Elimelech, M. (1996). Colloid transport in geochemically heterogenous porous media: Modeling and measurements. Environmental Science & Technology 30, 3284-3293.

Jones, I. and Lerner, D. (1995). Level-determined sampling in an uncased borehole. Journal of Hydrology 17, 291-317.

Jucker, B. (1999). Polymer interactions and bacterial adhesion. PhD Thesis pp.147. EAWAG, Dubbendorf, Switzerland.

Jucker, B., Harms, H., and Zehnder, A. (1996). Adhesion of the positively charged bacterium Stenotrophomonas (Xanthomonas) maltophilia 70401 to glass and Teflon. Journal of Bacteriology , 5472-5479.

Kaleris, V., Hadjitheodorou, C., and Demertracopoulos, A. C. (1995). Numerical simulation of field methods for estimating hydraulic conductivity and concentration profiles. Journal of Hydrology 71[319], 353.

Kass, W. (1997). Tracing technique in geohydrology. Pp. 581. Rotterdam, A.A.Balkema.

Kennedy, K. (2000). Bacteriophages as particle migration indicators in subsurface environments. In Dessargues, A. (Ed) Tracers and modelling in hydrogeology [IAHS Publ no. 262], 151-158. Liége.

Kennedy, K. (2001). Bacteriophage response characterisation in highly permeable porous media aquifers (Switzerland). PhD Thesis. Hydrogeology Centre, University of Neuchatel.

Kennedy, K., Muller, I., Schnegg, P., Rossi, P., and Koezel, R. (2001a). Characterisation of the Kappelen groundwater research site (BE), Switzerland, and preliminary bacteriophage and solute tracer component responses. Beitraege Zur Hydrogeologie. 52[Special Issue for 8th international symposium on water tracing.], 158-180.

Kennedy, K., Niehren, S., Rossi, P., Schnegg, P., Muller, I., and Kinzelbach, W. (2001b). Results of bacteriophage, microsphere and solute tracer migration comparison at Wilerwald Test Field, Switzerland. Beitraege Zur Hydrogeologie. 52[Special Issue for 8th international symposium on water tracing.], 180-210.

Kennedy, K., Schuerch, M., Muller, I., and Vautaz, F. (2001c). Biocolloid and solute tracer transport in gravel aquifers - a groundwater protection perspective. In Seiler, K. P. and Wohnlich, S. (Eds) New approaches to characterizing groundwater flow. Volume 1, 125-128., Balkema, Lisse.

Keswick, B. H., Wang, D., and Gerba, C. P. (1982). The use of micro organisms as groundwater tracers: A review. Groundwater 20[2], 142-149.

Kleineidam, S., Ruegner, H., and Grathwohl, P. (1999). Influence of petrographic composition/ organic matter distribution of fluvial aquifer sediments on the sorption of hydrophobic contaminants. Sedimentary Geology 129, 311-325.

Klingbeil, R., Kleineidam, S., Asprion, U., Aiger, T., and Teutsch, G. (1999). Relating lithofacies to hydrofacies: outcrop-based hydrogeological characterisation of Quaternary gravel deposits. Sedimentary Geology 129, 299-310.

Klotz, D., Seiler, K. P., Moser, H., and Neumaier, F. (1980). Dispersivity and velocity relationship from laboratory and field experiments. Journal of Hydrology 45, 619-641.

Kretzschmar, R., Barmettler, K., Grolimund, D., Yao-de, Y., Borkovec, M., and Sticher, H. (1997). Experimental determination of colloid deposition rates and collision efficiencies in natural porous media. Water Resources Research 33[5], 1129-1137.

Kretzschmar, R., Borkovec, M., Grolimund, D., and Elimelech M. (1999). Mobile subsurface colloids and their role in contaminant transport. Advances in Agronomy, Vol. 66. p.121-193. Academic Press, San Diego.

Kuebler, B. (1987). Illite crystalinity: Normalised preparation and measurement methods. (In French). Cahiers Institut Géologie de Neuchâtel . University of Neuchatel.

Kuo, R. J. and Matijevic, E. (1980). Particle adhesion and removal in model systems. Journal of Colloid Interface Science 78, 407-421.

Labhart, T. and Decrouez, D. (1997). Geology of Switzerland (In French). Third Edition, pp 211., Delachaux-Nestle, Lausanne-Paris.

Lambe, T. W. (1951). Capillary phenomena in cohesionless soils. Transactions of ASCE 116[4], 401-423.

Lawrence, J. R. and Hendry, M. J. (1996). Transport of bacteria through geologic media. Canadian Journal of Microbiology 42, 410-422.

Litton, G. M. and Olsen, T. M. (1993). Colloid deposition rates on silica bed media and artefacts related to collector surface preparation methods. Environmental Science & Technology 27, 185-193.

Lloyd, J. W. L. and Heathcote, J. A. A. (1985). Natural inorganic hydrochemistry in relation to groundwater. Pp 418. Clarendon Press Oxford, UK.

Logan, B. E., Jewett, D. G., Arnold, R. G., Bower, E. J., and O'Melia, C. R. (1995). Clarification of clean bed filtration models. Journal of Environmental Engineering 121[869], 873.

Loveland, J. P., Ryan, J. N., Amy, G. L., and Harevy, R. W. (1996). The reversibility of virus attachment to mineral surfaces. Colloids & Surfaces A - Physiochemical & Engineering Aspects. 107, 205-221.

Lukasic , J., Cheng, Y. F., Lu, F. H., Tamplin, M., and Farrah, S. R. (1999). Removal of microorganisms from water by columns containing sand coated with ferric and aluminium hydroxides. Water Research 33[3], 769-777.

Lyklema, J. (1991). Fundamentals of interface and colloid science. Vol 1. Academic Press, London.

Mackintosh, G. and Colvin, C. (2003). Failure of rural schemes in South Africa to provide potable water. Environmental Geology 44, 101-105.

Macler, B. (1996). Developing the groundwater disinfection rule. Journal American Water Works Association 88, 47-55.

Macler, B. and Merkle, J. C. (2000). Current knowledge on groundwater microbial pathogens and their control. Hydrogeology Journal 8, 29-40.

Maennel, T. (2002). Die Bedeutung von Suffosion und Sedimentation fur die Wasserfuehrung in quartaeren Kiesen der Muencher Schotterbene-Eine Interpretation der Ergebnisse langjaehriger Untersuchungen auf dem Grundwasserversuchsfeld Dornach. Dept of Geography, University of Augsburg.

Maier, R. W. and Pepper, I. L. (2000). Terrestrial environments. Maier, R. W., Pepper, I. L., and Gerba, C. P. Environmental Microbiology. [Chapter 4], 61-91. Academic Press, San Diego.

Maki, N., Gestwicki, J. E., Lake, E. M., Kiessling, L. L., and Adler, J. (2000). Mobility and chemotaxis of filamentous cells of *Escherichia coli***.** Journal of Bacteriology 182[15], 4337-4342.

Maloszewski, P. (1992). Mathematical modelling of tracer transport in different aquifers: Results from ATH test fields. 25-30. In Proc. 6th Int. Symp. Water tracing, Karlsruhe. Hoetzl, H. and Werner, A.(Eds) Balkema, Rotterdam.

Martin, M. J., Logan , B. E., Johnson, W. P., Jewett, D. G., and Arnold, R. G. (1996). Scaling bacterial filtration rates in different sized porous media. Journal of Environmental Engineering May, 407-415.

Martin, R. E., Bower, E. J., and Hanna, L. M. (1992). Application of clean bed filtration theory to bacterial deposition in porous media. Environmental Science & Technology 26, 1053-1058.

Matthess, G., Foster, S. S. D., and Skinner, A. C. (1985). Theoretical background, hydrology and practice of groundwater protection zones. [Volume Six], Pp 204. Hannover, Heise. International Contributions to Hydrogeology.

Maurer, A. M. and Sturchler, D. (1998). A waterborne outbreak of small round structured virus, campylobacter and shingella co-infections in La Neuveville, Switzerland. Epidemiology and Infection 125[2], 325-332.

McDowell-Boyer, L. M., Hunt, J. R., and Sitar, N. (1986). Particle transport through porous media. Water Resources Research 22[13], 1901-1921.

Moore, R. S., Taylor, D. H., Reddy, M. M. M., and Sturman, L. S. (1982). Adsorbtion of reovirus by minerals and soils. Applied and Environmental Microbiology 44, 852-859.

Muller, J. and Seiler, K. P. (2001). The role of DOC and EDTA on the remobilisation of heavy metals in carbonate groundwater. In Seiler, K. P. and Wohnlich, S. (Eds) New approaches to characterising groundwater flow Volume 1, 149-152. Balkema, Lisse..

National Small Flows Clearing House. (1996). Wastewater treatment protects small community life, health. Pipeline 7[3], 1-8.

Niehren, S. and Kinzelbach, W. (1998). Artificial colloid tracer tests: development of a compact on-line microsphere counter and application to soil column experiments. Journal of Hydrology 35, 249-259.

Noseda, N. (1999). Analytical modelling of uranine tracing tests in the unconfined aquifer at the CHYN experimental test site at Kappelen, (BE): An evaluation of sedimentological heterogeneity using multidirectional geophysical methods.(In French). Masters Thesis, Hydrogeology Centre, Universtiy of Neuchâtel.

O'Melia, C. R. (1989). Particle-particle interactions in aquatic systems. Colloids & Surfaces A - Physiochemical & Engineering Aspects. 39, 255-271.

O'Melia, C. R. and Tiler, C. L. (1993). Natural organic matter and colloidal stability: models and measurements. Colloids & Surfaces A - Physiochemical & Engineering Aspects. 73, 89-102.

Oyono, E. (1996). Geophysical and hydraulic study of the hydrogeology of the Kappelen experimental site, (Bern, Switzerland).(In French). Masters Thesis, Hydrogeology Centre, University of Neuchatel.

Pedley, S. and Howard, G. (1997). The public health implications of microbiological contamination of groundwater. Quarterly Journal of Engineering Geology and Hydrogeology 30[2], 179-188.

Penrod, S. L., Olsen, T. M., and Grant, S. B. (1996). Deposition kinetics of two viruses in packed beds of quartz granular media. Langmuir 12, 5576-5587.

Pieper, A. P., Ryan, J. N., Harvey, R. W, Amy, G. L., Illangsekare, T. H., and Metge, D. W. (1997). Transport and recovery of bacteriophage PRD1 in a sand and gravel aquifer. The effect of sewage derived organic matter. Environmental Science & Technology 31, 1163-1170.

Powell, K. L., Cronin, A. A., Pedley, S., and Barrett, M. H. (2002). Microbiological quality of groundwater in UK urban aquifers: Do we know enough? Groundwater quality: Natural and enhanced restoration of groundwater pollution. IAHS Pulb. No. 275, 91-96. Sheffield.

Price, M. and Williams, A. (1993). The influence of unlined boreholes on groundwater chemistry- A comparative study using pore-water extraction and packer sampling. Journal of the Institution of Water and Environmental Management 7[6], 651-659.

Rajagopalan, R. and Tien, C. (1976). Trajectory analysis of deep-bed filtration with the sphere-in-a-cell porous media model. American Institute for Chemical Engineering Journal 28, 523-533.

Rapp, M. C., Fulda, C., Schaefer, W., and Kinzelbach, W. (1998). The dual pumping technique (DPT) for level-determined sampling in fully screened groundwater wells. Journal of Hydrology 207, 220-235.

Reading, H. G. (1986). Sedimentary facies and environments. Second Edition, -pp 615. Blackwell Scientific Publications, Oxford.

Redman, J. A., Estes, M. K., and Grant, S. B. (2001). Resolving macroscale and microscale heterogeneity in virus filtration. Colloids & Surfaces A - Physiochemical & Engineering Aspects. 191[1-2], 57-70.

Redman, J. A., Grant, S. B., Olsen, T. M., Adkins, J. M., Jackson, J. L., Castillo, M. S., and Yanko, W. A. (1999). Physio-chemcial mechanisms responsible for the filtration and mobilization of a filamentous bacteriophage in quartz sand. Water Research 33[1], 43-52.

Regli, C., Rauber, M. and Huggenberger, P. (2003) Analysis of aquifer heterogeneity within a well capture zone, comparison of model data with field experiments: A case study from the river Wiese, Switzerland. Aquatic Sci. 65, 111-128.

Robertson, J. B. and Edberg, S. C. (1997). Natural protection of spring and well drinking water against surface microbial contamination. 1. Hydrogeological parameters. Critical Reviews in Microbiology 23[2], 143-178.

Rodier, E. and Dodds, J. (1995). An experimental study of the transport and capture of colloids in a porous medium subjected to step increases in concentration. Colloids & Surfaces A - Physiochemical & Engineering Aspects. 105[2-3], 221-231.

Rose, J.B., Dickson, L.J., Farrah, S.R., Carnaham, R.P., (1996) Removal of pathogenic indicator microorganisms by a full-scale water reclaimation facility. Water Research 30(11) 2785-2797.

Ross, S. and Olivier, J. P. (1964). On physical adsorption, Wiley Interscience, New York.

Rossi, P. (1994). Advances in biological tracer techniques for hydrology and hydrogeology using bacteriophages. Pp. 197. PhD Thesis, Microbiology Thesis, University of Neuchâtel.

Rossi, P. and Aragno, M. (1999). Analysis of bacteriophage inactivation and its attenuation by adsorption onto colloidal particles by batch agitation techniques. Canadian Journal of Microbiology 45, 9-17.

Rossi, P., Carvalho Dill, A., Muller, I., and Aragno, M. (1994). Comparative tracing experiments in a porous aquifer using bacteriophages and fluorescent dye on a test field

located at Wilerwald (Switzerland) and simultaneously surveyed in detail on a local scale by radio-magneto-tellury (12-240 kHz). Environmental Geology 23, 192-200.

Rossi, P. and Kass, W. (1997). Phages. In Kass, W.(Ed) Tracing technique in Geohydrology. Chapter [2.8], 244-271. A.A.Balkema, Rotterdam.

Rushton, K. R. and Howard, K. W. F. (1982). The unreliability of open observation boreholes in unconfined pumping tests. Groundwater 20, 546-550.

Rutter, P. R. and Vincent, B. (1980). The adhesion of microorganisms to surfaces: physico-chemical aspects. Berkley, R. C. W., Lynch, R. M., Melling, J., Rutter, P. R., and Vincent, B. eds. Microbial adhesion to surfaces. 79-93. E.Horwood Ltd.

Ryan, J. N. and Elimelech, M. (1996). Colloid mobilization and generation in groundwater. Colloids & Surfaces A - Physiochemical & Engineering Aspects. 107, 1-56.

Ryan, J. N., Elimelech, M., Ard, R, Harvey, R. W, and Johnson, P. R. (1999). Bacteriophage PRD1 and silica colloid transport and recovery in an iron oxide coated sand aquifer. Environmental Science & Technology 33, 63-73.

Ryan, J. N., Harvey, R. W, Metge, D., Elimelech, M., Navigato, T., and Pieper, A. P. (2002). Field and laboratory investigations of inactivation of viruses (PRD1 and MS2) attached to iron oxide-coated quartz sand. Environmental Science & Technology 36, 2403-2413.

Saiers, J. E. and Hornberger, G. M. (1996). The role of colloidal kaolinite in the transport of caesium through laboratory sand columns. Water Resources Research 32[1], 33-41.

Saiers, J. E. and Hornberger, G. M. (1999). The influence of ionic strength on the facilitated transport of cesium by kaolinite colloids. Water Resources Research 35[6], 1713-1727.

Schijven, J. F., Hassanizadeh, S., and de Bruin, HAM. (2002). Column experiments to study nonlinear removal of bacteriophages by passage through saturated dune sand. Jounal of Contaminant Hydrology 58[3-4], 243-259.

Schijven, J. F., Hassanizadeh, S., and de Bruin, RHAM. (8-8-2002). Two-site kinetic modelling of bacteriophages transport through columns of saturated dune sand. Journal of Contaminant Hydrology 57[3-4], 259-279.

Schijven, J. F. and Hassanizadel, S. M. (2000). Removal of viruses by soil passage: Overview of modelling, processes and parameters. Critical Reviews in Environmental Science and Technology 30[1], 49-127.

Schijven, J. F., Hoogenboezem, W., and Hassanizadeh, S. (1999). Modelling removal of bacteriophages MS-2 and PRD-1 by dune recharge at Castricum, Netherlands. Water Resources Research 35[4], 1101-1111.

Schijven, J. F., Medema, G., Vogelaar, A., and Hassanizadeh, S. (2000). Removal of microorganisms by deep well injection. Journal of Contaminant Hydrology 44, 301-327.

Schijven, J. F. and Simunek, J. (2002). Kinetic modeling of virus transport at the field scale. Journal of Contaminant Hydrology 55[1-2], 113-135.

Schijven JF, de Bruin HAM, Hassanizadeh SM, Husman AMD (2003) Bacteriophages and clostridium spores as indicator organisms for removal of pathogens by passage through saturated dune sand, WATER RESEARCH 37 (9): 2186-2194.

Schirmer, M., Jones, I., Teutsch, G., and Lerner, D. (1995). Development and testing of multiport sock samplers for groundwater. Journal of Hydrology 171, 239-287.

Schnegg, P. and Bossy, F. (2001). Sonde for downhole measurement of water turbidity and dye tracer concentration. In Seiler, K. P. and Wohnlich, S.(Eds) New Approaches Characterizing Groundwater Flow, Vol.2., 795-799. Swets & Zeitlinger Lisse.

Schultze-Makuch, D., Guan, H., and Pillai, S. D. (2003). Effects of pH and geological medium on bacteriophage MS2 transport in a model aquifer. Geomicrobiology Journal 20, 73-84.

Seiler, K. P. (1970). Vergleichende Untersuchungen zur Bestimmung hydraulischer Parameter auf einem versuchfeld in fluvioglazialen Kiessand-Ablagerungen des bayerischen Alpenvorlandes. Ne 64/2-7. IHD-Wasserforschung, Unpublished Final Report.

Shaw, D. J. (1998). Colloid and surface chemistry. Fourth Edition, -pp 306. Butterworth Heinemann, Oxford.

Silliman, S. E. (2000). Particle transport through two-dimensional, saturated porous media: influence of physical structure of the medium. Journal of Hydrology 167, 79-98.

Sinreich, M., Koezel, R., and Mudry, J. (2003). Principles of specific vulnerability assessment. Zwahlen, F. Vulnerability and risk mapping for the protection of carbonate (Karst) aquifers. Luxemburg, European Commission, Directorate General XII. Science. Final Report (COST Action 620).

Smith, M. S., Thomas, G. W., White, R. E., and Ritonga, D. (1985). Transport of Escherichia coli through intact and disturbed soil columns. Journal of Environmental Quality 14[1], 87-91.

Snow, J. (1854). On the mode of communication of cholera. John Churchill, London.

Sobsey, M. D., Dean, C. H., Knuckles, M. E., and Wagner, R. A. (1980). Interactions and survival of enteric viruses in soil materials. Applied and Environmental Microbiology 40[1], 92-101.

Sobsey, M. D., Shields, P. A., Hauchman, F. H., Hazard, R. L., and Caton, L. (1986). Survival and transport of hepatitis A virus in soils, groundwater and waste water. Water Science and Technology 18, 97-106.

Spielman, L. A. and Friedlander, S. K. (1973). Role of electric double layer in particle deposition by convective diffusion. Journal of Colloid Interface Science 46, 22-31.

Stumm, W. (1992). Chemistry of the solid-water interface. Pp 428. Wiley, New York.

Stumm, W. and Morgan, J. J. (1996). Aquatic chemistry. 3rd Edition, Pp 1022. Wiley, New York.

Sun, N., Sun, N. Z., Elimelech, M., and Ryan, J. N. (2-1-2001). Sensitivity analysis and parameter identifiability for colloid transport in geochemically heterogeneous porous media. Water Resources Research 37[2], 209-222.

Swiss Agency for the Environment, Forests and Landscape (SAEFL) (2003). Groundwater. (in French). Pp31. SAEFL, Berne.

Thompson, D. W. and Pownall, P. G. (1989). Surface electrical properties of calcite. Journal of colloid and interface science 131[1], 74-82.

Tien, C. and Payatakes, J. (1979). Advances in deep bed filtration. American Institute for Chemical Engineering Journal 25, 737-759.

Tucker, M. E. (1981). Sedimentary petrology: An introduction. Pp 252. Blackwells, Oxford.

United States Environmental Protection Agency. (1992). The proposed groundwater disinfection rule. Federal Registrar 52. 33960. Available Notice.

United States Environmental Protection Agency. (2000). National primary drinking water regulations: Groundwater rule; proposed rules. 40 CFR Parts 141 and 142. 30194-30274.

van der Leeden, F., Troise, F. L., and Todd, D. K. (1990). The water encyclopaedia. First Edition, pp 808. Lewis Publishers, Chelsea, MI.

vanOss, C. J. (1995). Hydrophobicity of biosurfaces-origin, quantitative determination and interaction energies. Colloids and Surfaces B: Biointerfaces. 5[91], 110.

Verwey, E. J. W. and Overbeek, J. T. G. (1948). Theory of stability of lyophilic colloids. Elsevier, Amsterdam.

Werner, A. (1997). Traci 95: A computer program for Windows 95 (Versin 4.05B). In Kass, W. Tracing Technique in Geohydrology. Balkema, Rotterdam.

Wersin, P., Abrecht, J., and Hoehner, P. (2002). Large-scale redox plume in glaciofluvial deposits due to sugar-factory wastes and wastewater at Aarberg, Switzerland. Hydrogeology Journal 9, 282-296.

Westwood, J. C. N. and Satter, S. A. (1976). The minimal infective dose. Berg, Bodily Lenete Melnick & Metcalf. Viruses in water. 61-69. American Public Health Association, Washington D.C.

Wheatcroft, S. W. and Taylor , S. W. (1988). An explaination of scale-dependant dispersivity in heterogeneous aquifers using concepts of fractal geometry. Water Resources Research 24, 566-578.

Woessner, W., Ball, P., DeBorde, D., and Troy, T. (2001). Virus transport in a sand and gravel aquifer under field pumping conditions. Groundwater 39[6], 886-894.

Woessner, W. and DeBorde, D. (1998). Virus transport in the floodplain of a headwater stream, western Montana, USA. In Haigh, M. J., Kreck, J., Rajwar, G. S., and Kilmartin, M. P. (Eds) Headwaters: Water resources and soil conservation. 197-207. Balkema, Rotterdam.

World Health Organisation. (1999). World health report- Statistical Annex. WHO . http://www.who.int/whr/1999/en/pdf/Statistical Annex.pdf.

World Health Organisation, UN. (1986). Statistics quarterly. WHO. 39.

Yao, K. M., Habibian, M. T., and O'Melia, C. R. (1971). Water and waste water filtration. Concepts and applications. Environmental Science & Technology 5, 1105-1112.

Yates, M. V., Yates, S. R., Wagner, J., and Gerba, C. P. (1987). Modeling virus survival and transport in the subsurface. Journal of Contaminant Hydrology 1, 329-345.

Zahn, M. T. and Seiler, K. P. (1992). Field studies on the migration of arsenic and cadmium in a carbonate gravel aquifer near Munich (Germany). Journal of Hydrology 133, 201-214.

Zhang, P. F., Johnson, W. P., Piana, M. J., Fuller, C. C., and Naftz, D. L. (2001). Potential artefacts in interpretation of differential breakthrough of colloids and dissolved tracers in the context of transport in a zero valent iron permeable reactive barrier. Groundwater 39[6], 831-840.

Zhuang, J. and Jin, Y. (2003). Virus retention and transport through Al-oxide coated sand columns: Effects of ionic strength and composition. Journal of Contaminant Hydrology 60, 193-209.

9. Appendix

Solution to the advection-dispersion equation with first-order adsorption/desorption and viral inactivation in liquid and on matrix surfaces – Developed by F. Cornaton – CHYN , 2003.

1) The basis of the temporal 1-D equations as expressed in the text is as follows:

$$\frac{\partial C}{\partial t} + \frac{\rho}{\phi}\frac{\partial S}{\partial t} = D\frac{\partial^2 C}{\partial x^2} - v\frac{\partial C}{\partial x} - \mu_w C - \mu_S \frac{\rho}{\phi} S \quad (1)$$

$$\frac{\rho}{\phi}\frac{\partial S}{\partial t} = k_c C - k_d \frac{\rho}{\phi} S - \mu_S \frac{\rho}{\phi} S \quad (2)$$

with $C = C(x,t)$.

All symbols have the same meaning as defined in the text.

2) Laplace transforms of Eqs. (1) and (2)

The equations (1) and (2) may be solved by Laplace transform. The *p*-transformed equations read as follows:

$$p\hat{C}(p) + p\frac{\rho}{\phi}\hat{S}(p) + \mu_w \hat{C}(p) + \mu_S \frac{\rho}{\phi}\hat{S}(p) = D\frac{\partial^2 \hat{C}(p)}{\partial x^2} - v\frac{\partial \hat{C}(p)}{\partial x} \quad (3)$$

$$\hat{S}(p) = \frac{\phi}{\rho}\frac{k_c}{p + k_d + \mu_S}\hat{C}(p) \quad (4)$$

Substituting (4) into (3) and re-arranging yields the following continuity equation:

$$\beta p\hat{C}(p) = D\frac{\partial^2 \hat{C}(p)}{\partial x^2} - v\frac{\partial \hat{C}(p)}{\partial x} \quad (5)$$

with

$$\beta = 1 + \frac{\mu_w}{p} + \frac{k_c(p + \mu_s)}{p(p + k_d + \mu_s)} \quad (6)$$

3) Resolution

Equation (5) may be solved for a time-dependent Dirichlet-type boundary condition at $x = 0$, denoted by the function BC(t), and with zero initial condition on $x \in [0;\infty]$.

Time boundary conditions

$$C(0,t) = \mathrm{BC}(t) \quad (7)$$

$$\left.\frac{\partial C}{\partial x}\right|_{x\to\infty} = 0 \tag{8}$$

p-transformed boundary conditions

$$C(0,p) = \hat{\mathrm{BC}}(p) \tag{9}$$

$$\left.\frac{\partial \hat{C}}{\partial x}\right|_{x\to\infty} = 0 \tag{10}$$

General solution

The general solution of Eq. (5) for the boundary conditions (9) and (10) is:

$$\hat{C}(x,p) = \hat{\mathrm{BC}}(p)\exp\left(\frac{x}{2D}\left(v - \sqrt{v^2 + 4\beta D p}\right)\right) \tag{11}$$

The function BC(*t*) is arbitrary. For a unit pulse boundary condition $C(0,t) = \delta(t)$, the transformed function BC(*t*) is 1. For a step-input of relative concentration during time *T*, the *p*-transformed boundary condition function is

$$\hat{\mathrm{BC}}(p) = \frac{1 - e^{-Tp}}{p} \tag{12}$$

Equation (11) can be viewed as a convolution procedure of the function

$$\hat{C}(x,p) = \exp\left(\frac{x}{2D}\left(v - \sqrt{v^2 + 4\beta D p}\right)\right) \tag{13}$$

with the arbitrary boundary condition function BC(t). Note that Eq. (13) is the solution for the Dirac input (unit response function).

To return into the time-domain, the numerical inversion of the Laplace-transformed solution (11) is performed via the Crump's algorithm (Crump, 1976) with quotient-difference accelerator (De Hoog et al, 1982)